International Journal of Polymer Science

Polymeric Scaffolds for Tissue Engineering

Guest Editors: Xiaoming Li, Tsukasa Akasaka, and Nicholas Dunne

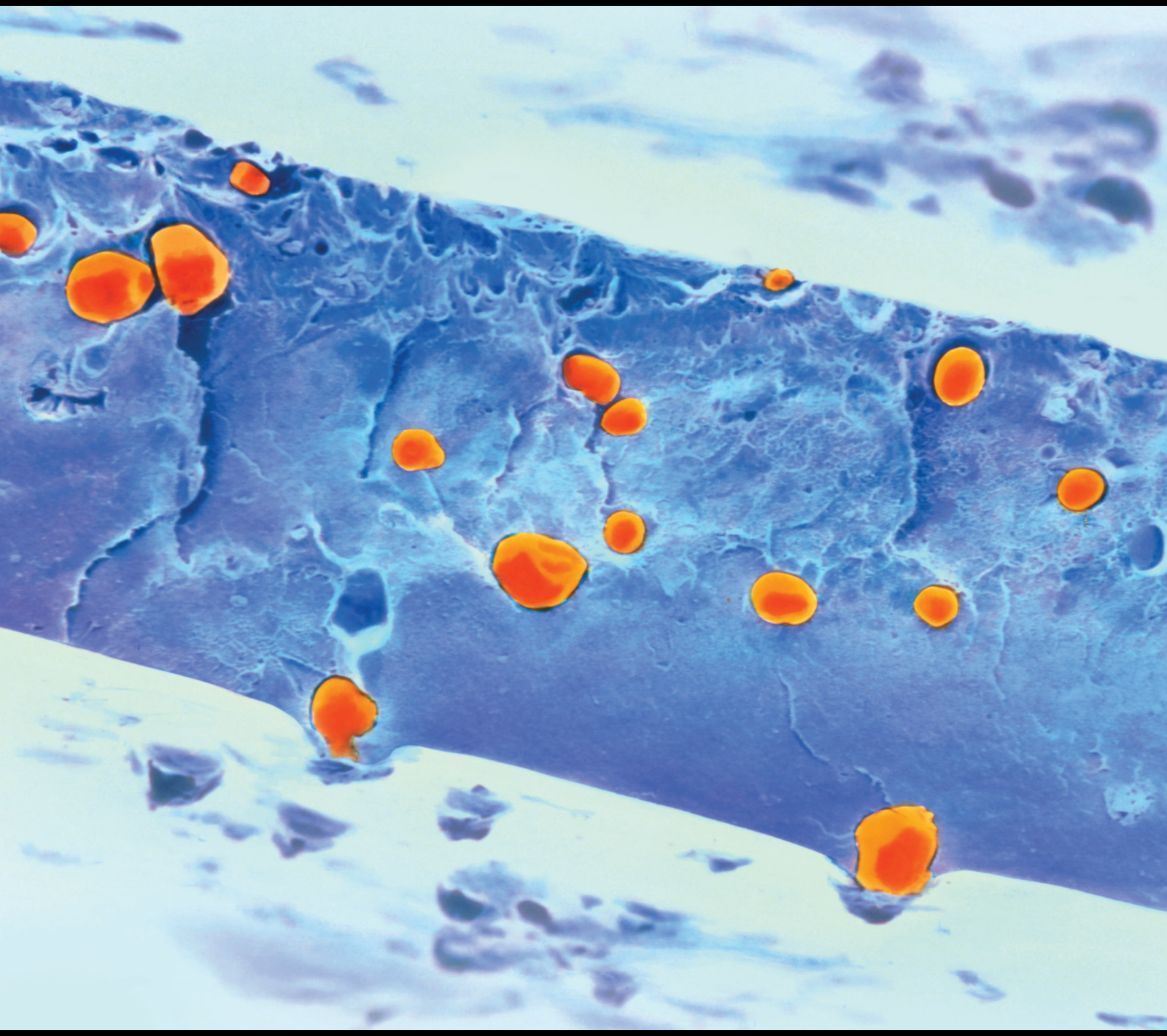

Polymeric Scaffolds for Tissue Engineering

International Journal of Polymer Science

Polymeric Scaffolds for Tissue Engineering

Guest Editors: Xiaoming Li, Tsukasa Akasaka,
and Nicholas Dunne

Editorial Board

Contents

Hindawi Publishing Corporation
International Journal of Polymer Science
Volume 2014, Article ID 917070, 2 pages
http://dx.doi.org/10.1155/2014/917070

Editorial

Polymeric Scaffolds for Tissue Engineering

Xiaoming Li,[1] Tsukasa Akasaka,[2] and Nicholas Dunne[3]

[1] *Key Laboratory for Biomechanics and Mechanobiology of Ministry of Education, School of Biological Science and Medical Engineering, Beihang University, Beijing 100191, China*
[2] *Department of Biomedical Materials and Engineering, Graduate School of Dental Medicine, Hokkaido University, Sapporo 060-8586, Japan*
[3] *School of Mechanical & Aerospace Engineering, Queen's University of Belfast, Belfast BT9 5AH, UK*

Correspondence should be addressed to Xiaoming Li; x.m.li@hotmail.com

Received 6 August 2014; Accepted 6 August 2014; Published 20 August 2014

A fundamental problem that affects all fields of surgery is the paucity of autologous tissue available for surgical reconstructive procedures. When a surgeon removes a tissue that is diseased or damaged, or when a surgeon replaces a tissue that is congenitally absent, the best results are obtained when an individual's own tissues are used for the surgical repair. When it is not possible, the surgeon is forced to use alternative biomaterials and usually selects from either prosthetic, man-made synthetic materials or from biologic materials derived typically from allografts or xenografts [1]. Tissue engineering is a multidisciplinary science that attempts to create living biomaterials from a patient's own cells, which has been an area of immense research in recent years because of its vast potential in the repair or replacement of damaged tissues and organs [2–4]. Scaffold is one of the three most important factors in tissue engineering.

According to Hutmacher [5] a scaffold should have the following main characteristics: it should (1) be bioresorbable and biocompatible with a controllable degradation and resorption rate to match cell/tissue growth in vitro/vivo; (2) have a suitable surface chemistry for cell attachment, proliferation, and differentiation; (3) be three-dimensional and highly porous with an interconnected porous network for cell growth, flow transport of nutrients, and metabolic waste; and (4) have proper mechanical properties to match the tissues at the site of implantation [6].

Scaffolds lie at the heart of all the new tissue engineering approaches because they not only provide mechanical support for embedded cells but also regulate various cellular behaviors by recruiting specific biomolecules or growth factors. Polymeric scaffolds are one of the most widely used scaffold types because of their satisfactory formability, mechanical properties, biocompatibility, and controllable biodegradability [7–9]. To date, polymeric scaffolds have been largely applied to repair hard and soft tissues. However, there are still many challenges that need to be addressed, such as the development of satisfactory processing techniques so as to achieve homogeneous structure and composition throughout the scaffolds and to obtain well-defined internal structures with interconnected porosity to host most cell types. Moreover, additional studies are desired to figure out how to create desirable polymeric scaffolds that serve various functions, including immobilization of transplanted cells, formation of a protective space to prevent unwanted tissue growth into the wound bed while allowing healing with differentiated tissue, and directing migration or growth of cells via scaffold surface properties or via release of soluble bioactive molecules such as growth factors, hormones, and/or cytokines.

Currently, many novel issues on polymeric scaffolds for tissue engineering have been supported. Scaffolds fabricated by using materials such as nanoparticles, nanofibers, nanotubes, and other materials in nanoscale have been tried in tissue engineering. Besides, new technologies which can be available for tissue engineering have been studied.

According to the researches that have been done, kinds of fibers or tubes alternatives have been employed to reinforce the scaffolds for repairing specific tissues, such as ceramic

fibers/tubes, and polymer fibers/tubes [10–13]. The nanomaterials reinforced composites can not only enhance the mechanical property but also improve the biocompatibility and bioactivity of scaffold. In this special issue, several articles are mainly focused on the some specific applications of scaffolds reinforced by nanofibers or nanoparticles. A few novel materials systems are demonstrated, such as nanohydroxyapatite/polyamide 66 composite and HA/collagen/PLA composites. Numerous research programs regarding the material systems which are available for scaffold used for tissue engineering, as well as the new technology, are developed. 3D printing technology has recently gained substantial interest for potential applications in tissue engineering due to the ability to make a three-dimensional object of virtually any shape from a digital model. 3D-printed biopolymers, which combine the 3D printing technology and biopolymers, have shown great potential in tissue engineering application and are receiving significant attention [14–16].

All in all, the issue will give a presentation about scaffolds fabricated using novel system or technology, and, most importantly, it will provide a general guide for the fabrication of more desirable scaffolds for tissue engineering.

Xiaoming Li
Tsukasa Akasaka
Nicholas Dunne

References

[1] A. Y. Lee, N. Mahiler, C. Best, Y. U. Lee, and C. K. Breuer, "Regenerative implants for cardiovascular tissue engineering," *Translational Research*, vol. 163, no. 4, pp. 321–341, 2014.

[2] X. M. Li, L. Wang, Y. B. Fan, Q. L. Feng, F. Z. Cui, and F. Watari, "Nanostructured scaffolds for bone tissue engineering," *Journal of Biomedical Materials Research A*, vol. 101, no. 8, pp. 2424–2435, 2013.

[3] S. P. Nukavarapu and D. L. Dorcemus, "Osteochondral tissue engineering: current strategies and challenges," *Biotechnology Advances*, vol. 31, no. 5, pp. 706–721, 2013.

[4] X. H. Liu, X. M. Li, Y. B. Fan et al., "Repairing goat tibia segmental bone defect using scaffold cultured with mesenchymal stem cells," *Journal of Biomedical Materials Research B*, vol. 94, no. 1, pp. 44–52, 2010.

[5] D. W. Hutmacher, "Scaffolds in tissue engineering bone and cartilage," *Biomaterials*, vol. 21, no. 24, pp. 2529–2543, 2000.

[6] X. Li, Y. Huang, L. Zheng et al., "Effect of substrate stiffness on the functions of rat bone marrow and adipose tissue derived mesenchymal stem cells *in vitro*," *Journal of Biomedical Materials Research A*, vol. 102, no. 4, pp. 1092–1101, 2014.

[7] D. O. Fauza, "Tissue engineering in congenital diaphragmatic hernia," *Seminars in Pediatric Surgery*, vol. 23, pp. 135–140, 2014.

[8] Y. Naito, K. Rocco, H. Kurobe, M. Maxfield, C. Breuer, and T. Shinoka, "Tissue engineering in the vasculature," *The Anatomical Record*, vol. 297, no. 1, pp. 83–97, 2014.

[9] T. J. Keane and S. F. Badylak, "Biomaterials for tissue engineering applications," *Seminars in Pediatric Surgery*, vol. 23, pp. 112–118, 2014.

[10] X. M. Li, H. F. Liu, X. F. Niu et al., "The use of carbon nanotubes to induce osteogenic differentiation of human adipose-derived MSCs in vitro and ectopic bone formation in vivo," *Biomaterials*, vol. 33, no. 19, pp. 4818–4827, 2012.

[11] X. Li, Q. Feng, and F. Cui, "In vitro degradation of porous nanohydroxyapatite/collagen/PLLA scaffold reinforced by chitin fibres," *Materials Science and Engineering C*, vol. 26, no. 4, pp. 716–720, 2006.

[12] X. M. Li, Y. B. Fan, and F. Watari, "Current investigations into carbon nanotubes for biomedical application," *Biomedical Materials*, vol. 5, no. 2, Article ID 022001, 2010.

[13] X. M. Li, R. R. Cui, W. Liu et al., "The use of nano-scaled fibers or tubes to improve biocompatibility and bioactivity of biomedical materials," *Journal of Nanomaterials*, vol. 2013, Article ID 728130, 16 pages, 2013.

[14] T. Serra, M. A. Mateos-Timoneda, J. A. Planell, and M. Navarro, "3D printed PLA-based scaffolds: a versatile tool in regenerative medicine," *Organogenesis*, vol. 9, no. 4, pp. 239–244, 2013.

[15] S. Bose, S. Vahabzadeh, and A. Bandyopadhyay, "Bone tissue engineering using 3D printing," *Materials Today*, vol. 16, pp. 496–504, 2013.

[16] F. Pati, J.-H. Shim, J.-S. Lee et al., "3D printing of cell-laden constructs for heterogeneous tissue regeneration," *Manufacturing Letters*, vol. 1, pp. 49–53, 2013.

Hindawi Publishing Corporation
International Journal of Polymer Science
Volume 2014, Article ID 689390, 9 pages
http://dx.doi.org/10.1155/2014/689390

Review Article

Using Polymeric Scaffolds for Vascular Tissue Engineering

Alida Abruzzo,[1,2] Calogero Fiorica,[3] Vincenzo Davide Palumbo,[1,2,4] Roberta Altomare,[1,2] Giuseppe Damiano,[4] Maria Concetta Gioviale,[4] Giovanni Tomasello,[2,4] Mariano Licciardi,[3] Fabio Salvatore Palumbo,[3] Gaetano Giammona,[3] and Attilio Ignazio Lo Monte[1,2,4]

[1] *PhD Course in Surgical Biotechnology and Regenerative Medicine, University of Palermo, Via Del Vespro, 129 90127 Palermo, Italy*
[2] *Dichirons Department, University of Palermo, Via Del Vespro, 129 90127 Palermo, Italy*
[3] *Department of Biological, Chemical, Pharmaceutical Sciences and Technologies, University of Palermo, Viale delle Scienze, 16 90128 Palermo, Italy*
[4] *"P. Giaccone" Universitary Hospital, School of Medicine, School of Biotechnology, University of Palermo, Via Del Vespro, 129 90127 Palermo, Italy*

Correspondence should be addressed to Attilio Ignazio Lo Monte; attilioignazio.lomonte@unipa.it

Received 6 February 2014; Accepted 9 June 2014; Published 21 July 2014

Academic Editor: Xiaoming Li

With the high occurrence of cardiovascular disease and increasing numbers of patients requiring vascular access, there is a significant need for small-diameter (<6 mm inner diameter) vascular graft that can provide long-term patency. Despite the technological improvements, restenosis and graft thrombosis continue to hamper the success of the implants. Vascular tissue engineering is a new field that has undergone enormous growth over the last decade and has proposed valid solutions for blood vessels repair. The goal of vascular tissue engineering is to produce neovessels and neoorgan tissue from autologous cells using a biodegradable polymer as a scaffold. The most important advantage of tissue-engineered implants is that these tissues can grow, remodel, rebuild, and respond to injury. This review describes the development of polymeric materials over the years and current tissue engineering strategies for the improvement of vascular conduits.

1. Introduction

Each year there is a strong demand for vascular grafts due to arteriosclerosis and other cardiovascular diseases that are the main cause of mortality in the western countries [1–4]. Nowadays, autotransplantation of blood vessels is usually performed; however, the possible presence of vein diseases and a limited availability of autologous blood vessels make this procedure often impracticable [5, 6]. This necessity has led to the use of nonbiodegradable synthetic prostheses and, more recently, to the approach of tissue engineering. Vascular tissue engineering has been described as "an interdisciplinary field that applies the principles and methods of engineering and the life sciences towards the development of biological substitutes that restore, maintain, and improve tissue function" [7]. Its aim is to develop biocompatible scaffolds that mimic the mechanical properties of autogenous conduits, while providing a framework for guided cell repopulation creating a functional cardiovascular conduit [8]. The tissue engineering approach starts from the isolation of specific cells, their growth on a three-dimensional biomimetic scaffold under controlled culture conditions, the delivery of the construct to the desired site, and the direction of new tissue formation into the scaffold while it is degraded [9]. Thus, tissue engineering usually uses three components to achieve its outcomes: (a) cells, (b) scaffolds or matrices to provide a template for tissue ingrowth, and often with the addition of (c) environmental factors (such as compression, shear stresses, and a pulsatile flow in the case of arterial tissue engineering) and/or growth factors or morphogens (physical or chemical factors inducing tissue healing and cell differentiation) [10, 11].

Clearly, the scaffold must be produced on the basis of morphological, physiologic, and mechanical properties of the tissue that need to be regenerated which has to be studied from the anatomical point of view [12]. The wall of a blood

vessel is constituted by three main layers called tunica adventitia, tunica media, and tunica intima. The outermost layer is the tunica adventitia which is mainly composed by fibroblast and elastin and supply mechanical strength and integrity.

Tunica media is composed mainly by smooth muscle cells and elastin and is responsible for the viscoelastic behavior of the vessel. Tunica intima is the inner part of the vessel in contact with the circulating blood and is composed of a single layer of endothelial cells mounted on a basement membrane [2, 13]. Synthetic scaffolds which are intended to mimic the structure of a blood vessel must promote the correct orientation of the different cell types as well as the maintenance of the structural integrity and the long-term patency [14]. In this review, the developments made in the field of replacement of damaged blood vessels from the early surgical approaches to the innovative approach of tissue engineering will be discussed. Particular attention will be given to the use of polymeric materials and to the techniques of production of biomaterials that allow to mimic the morphological characteristics of the blood vessels.

2. From the Early Surgical Approaches to the Nonbiodegradable Grafts

The gold standard material for blood vessels replacement, because of the complex histological structure of this particular tissue, is represented by blood vessels themselves. For this reason the first surgical approaches were oriented to the autologous vessels transplantation [15]. The first approach to the problem of replacing a damaged vascular tract was dated in 1906, when for the first time a venous autograft was used as replacement of a section of an artery. It was José Goyanes who, on the occasion of a popliteal aneurysm, removed the damaged part of the artery and connected the cut ends using a section of the autologous popliteal vein. The patient showed an infection after the operation, but this must be probably caused by the injection of gelatin in the popliteal cavity before the operation, rather than implanting the graft. The subject was hospitalized and did not revealcirculation problems [16, 17]. In 1915, Bernheim provided another approach to repair popliteal aneurysm. The patient in this case had to undergo the removal of about 15 cm popliteal artery, replaced by 12 cm of the saphenous vein [18].

Other case studies were followed, but the two previous cases had considerable importance, as it was from here that came the idea of reconstructing a damaged tissue [19]. The major example of autologous implant is the saphenous vein, which consists of one of the two larger ducts venous lower limb together with the femoral vein and has a diameter generally between 4 and 6 mm. The clear advantage of using this vessel is that it evokes no rejection and shows mechanical characteristics comparable to arteries [20]. In 1948 Kunlin created a femoropopliteal bypass with a system consisting of the reversed saphenous vein, laying the foundation for a practice that is still to be established. In the same year early arterial systems began to spread consisting of foreign tissue but deriving from subjects of the same species [21]. Unfortunately, this approach is burdened by high failure rates, as in the case of saphenous vein graft, due to atherosclerosis and intimal hyperplasia of the transplanted vessels [22]. Furthermore, it was showed that almost 30–40% of patients lack an appropriate saphenous vein [23, 24] due to previous phlebitis, vessel removal, varicosities, hypoplasia, or anatomical unsuitability [25]. There has been also an experimentation of homologous saphenous vein grafts (homograft), but there were no encouraging results in terms of physical and mechanical characteristics. In addition, there were frequent phenomena of rejection and deterioration, and it is supposed that the patency of the conduit remains unaltered only for vessels of diameter greater than 5 mm. For these reasons, in 1960 the homograft was abandoned [26]. Autologous arteries (internal and external iliac, superficial femoral, and internal mammary) were ideal artery bypass in the cardiac and the peripheral arteries but both had a limited availability of sites donors [27]. Because of the excellent long-term patency, the internal mammary artery was considered to be the best choice for coronary artery bypass graft in younger patients. For other patients, when the internal mammary was not available or not indicated, the alternative was represented by the right gastric or intercostal arteries [28]. The possible presence of vein diseases and a limited availability of autologous blood vessels represent the major limitation to the autologous transplantation that has led to the necessity to develop artificial blood vessels [29].

Currently expanded polytetrafluoroethylene (ePTFE) and Dacron (polyethylene terephthalate fibre) have been the most widely used synthetic materials for realizing grafts [30]. Dacron is one of the trade names of PET (polyethylene terephthalate) polymer belonging to the family of thermoplastic polyesters. The Dacron is resistant, deformable, and biostable and is present in different forms. It is used in cardiovascular surgery to achieve large-diameter vascular prostheses, for arterial sutures and for the construction of the valve rings. The highly crystalline and hydrophobic natures of Dacron both prevent hydrolysis of a graft, leading to a potential of residing inside the human body for decades. PET is usually transformed fibers, from its linear macromolecules with an average weight of about 20000 Da. Each wire that constitutes the prosthesis is composed by the association of monofilaments obtained by passage of polymers fused of PET in a supply chain. These wires are then elongated by heat treatment capable of conferring aspect ring. Subsequently, the individual filaments are gathered (spiral or helix) in a single fiber. The fact of being multifilament makes the fiber elastic and manageable. The wire weaved is used to fabricate woven or knitted prosthesis [31]. Teflon is a polymer of tetrafluoroethylene and is identified also as polytetrafluoroethylene (PTFE). It is the most important and used between polymers composed of fluorine and carbon. In the 60's, deriving from Teflon technolgy, PTFE foam (ePTFE), also known as Gore-tex,was developed. It has found application in vascular prostheses in the second half of the 70's. Again, just like in Dacron, the highly crystalline and hydrophobic nature yields a stable product by preventing hydrolysis. Tubular grafts made from ePTFE are produced by an extrusion, drawing, and sintering process and consist of fibrils and nodules, controllable to different pore sizes. The

Gore-Tex is therefore a nondegradable porous polymer with a surface electronegative, which limits the reaction with the components of the blood. It is biostable and in fact has a lesser tendency, for example, to deteriorate in a biological environment compared to PTFE. In general, however, the behavior that it has in a biological environment is influenced by the type of processing to which it is subjected.

In previous experiments it was found that the larger the porosity of the material, the better is its integration with the physiological environment. However, it was found that an implant characterized by high porosity resulted to be also fragile and therefore cannot be used clinically. In a significant study conducted by Isaka et al. [32] a highly porous graft was achieved but it was biocompatible and with the ability to integrate in host tissues. The graft was inserted in the abdominal aorta of eleven purebred dogs of both sexes with a weight between 10 and 12 kg. In the graft used the average internodal distance was 60 m and the structure showed tortuous channels formed by the nodes and fibrils of PTFE. The implant was 30–40 mm long; its inside diameter measured 6 mm and was reinforced by a filament fluoroethylene propylene. The eleven grafts were then inserted into the animals and extracted at intervals of 2 weeks (4 grafts), 4 weeks (4 other grafts), and 80 weeks (3 graft). On the implants removed an evaluation of the resistance to radial tension, longitudinal tension, the retention force of the suture, and the rate of deformation was performed. The results showed that there was no sign of any problems or occlusion at the level of anastomosis. The rate of deformation demonstrates a certain stability of the two properties considered. Furthermore, as regards the retention force of the suture, there was no substantial difference between before and after graftings. Additional experiments demonstrated that ePTFE and Dacron were successful in large-diameter (>5 mm) high-flow vessels, but in low flow or smaller diameter sites they are compromised by thrombogenicity and compliance mismatch [33]. In the 80's and 90's, however, the performance of grafts was evaluated with porosity gradually higher, starting from the assumption that large pores permit a fast growth of tissue from the outside of the graft up within its interstices, allowing a large integration of the prosthesis with the biological environment. Another category of polymers with large diffusion is represented by polyurethanes. Polyurethanes were originally developed commercially in Germany in the 1930s as surface coatings, foams, and adhesives. Segmented PUs are copolymers comprising 3 different monomers, a hard domain derived from a diisocyanate, a chain extender, and a soft domain, most commonly polyol. The soft domain is mainly responsible for flexibility, whereas the hard domain imparts strength. Polyether urethane was relatively insensitive to hydrolysis but susceptible to oxidative degradation.

Polyurethane grafts which have been available for the last 40 years have characteristics that would be ideal for use in bypass procedures, namely, similar compliance to native arteries with a surface that is conducive for seeding [34–37]. Unfortunately, polyurethane grafts have had variable results clinically with a tendency to degrade causing aneurysm formation [38]. Data obtained showed that when compared with ePTFE grafts, the PU graft overall showed no appreciable difference in interval patency in canine aortic model. Furthermore, in a small study, the grafts were implanted in aortoiliac arteries of 4 dogs for 6 months evidencing that luminal thrombus affected 59% of polyurethane graft surfaces compared to 22% of ePTFE graft [39]. Anyhow, tissue reactions to PU grafts are discrepant in the literature because factors such as different compositions of polymers, graft fabrication, porosity, and surface modifications all affect the results. On the basis of these evidences no conclusion can be made as to whether PU grafts may be functionally superior to ePTFE or Dacron grafts until more data become available.

3. Synthetic Prosthetic Grafts Disadvantages and Diffusion of Tissue Engineering

It has been tested that currently available vascular grafts show satisfactory long-term patency rates only in large-caliber arteries (>8 mm), where a massive blood flow may overcome the risk of thrombogenicity. In medium-caliber replacements (6–8 mm), for example, in carotid or common femoral arteries [40], a little difference between prosthetic and autogenous material has been reported.

However, in small-caliber vessels (<6 mm), such as coronary arteries, infrainguinal arteries (below the inguinal ligament), and particularly in low-flow infrageniculate arteries, the outcomes of vascular prostheses are unsatisfactory.

Several methods have been developed to enhance the patency rates. The major example is the linking of heparin to graft surfaces in order to obtain a reduction of the thrombogenic activity [37, 41]. Nevertheless this strategy is associated with the problem of the duration of heparin activity due to premature release of the compound or the presence of a physical barrier, created by adherent blood components. Other modifications are the coating of the luminal surface with carbon so that electronegativity is improved and thus thrombus formation reduced [42]. Another widely used coating material is fibrin glue, which is able to improve endothelialization and other physical and chemical variations [43, 44]. Additionally, synthetic grafts are usually rejected within few months by the immune system of the body if the diameter of the vessel is smaller than 6 mm. This rejection arises from the consequent reocclusion caused by thrombosis, aneurysm, and intimal hyperplasia due to mismatch of compliance (compliance is the opposite of stiffness, measured as the strain/expansion or contraction of the graft with force) [45–50]. Thrombogenicity could be associated with the deposition of fibrin and platelets on the surface of an implanted material or with the proliferation of smooth muscle cells, which migrate from native vessel, invade the intima by growing instead of endothelial cells, and produce extracellular matrix [51]. Intimal hyperplasia (IH) is located at distal anastomosis of prosthetic grafts and generally developed 2–24 months after implantation and includes a variety of factors: a compliance mismatch between a relatively rigid prosthesis and the more elastic native artery [52], graft/artery diameter mismatch, lack of endothelial cells, surgical trauma and flow disturbances resulting in adaptive changes in the subendothelial tissue, characterized by proliferation and migration of vascular smooth muscle

cells from media to intima, and synthesis of extracellular matrix (ECM) proteins. To overcome these issues, novel biomaterials research [53] and particularly tissue engineering modalities are increasingly being adopted [54]. Tissue engineering opened the way to the creation of devices with an adequate mechanical strength and compliance in order to withstand long-term hemodynamic stresses; furthermore, these devices should be nontoxic, nonimmunogenic, biocompatible, available in various sizes for emergency care, resistant to *in vivo* thrombosis, and able to withstand infection and to incorporate into the host tissue with satisfactory graft healing [55], related with reasonable manufacturing costs [27].

It is thought that tissue engineering would be particularly valuable in the production of vascular grafts because of the massive need and precarious supply of natural graft material for clinical use.

The challenges faced by the approach of tissue engineering for replacing blood vessels are substantial. They include providing an elastic vessel wall that can withstand cyclic loading, matching the compliance of the graft with the adjacent host vessel, and a lining for the lumen that is antithrombotic [56]. From the first production of completely biological tissue-engineered blood vessels, composed of intima, media, and an adventitia, using cultured mature smooth muscle cells and endothelial cells in bovine collagen gels by Weinberg and Bell [57], there have been many attempts for successful blood vessel construction through tissue engineering approach.

Various strategies including *in vitro* endothelization of the graft have been used to overcome these problems but few *in vivo* results have been obtained [58, 59]. It is now clear that an intact luminal EC monolayer imparts resistance to thrombus formation and reduces the extent of intimal hyperplasia [60].

Several studies revealed that when blood comes into contact with another surface than the endothelium, there is an elevated risk of thrombosis. These conditions can be related also with loosely attached ECs that can detach right after implantation due to blood flow related shear stress [61]. The EC layer is also able to inhibit actively thrombosis. This is achieved by thrombomodulin receptors, heparin sulfate, proteoglycans, and the secretion of NO, prostacyclin, protein S, and t-PA, all of which inhibit the clotting process. Aside from these features, the endothelium has a primary role in blood pressure regulation, angiogenesis, and adhesion and transmigration of inflammatory cells. It is therefore considered a vital component for maintaining good long-term patency. ECs, however, have limited capacity for regeneration and exhaust their renewal after approximately 70 cell cycles, leading to the hypothesis that endothelialization of vascular grafts occurs via one of four mechanisms: (i) by seeding ECs, (ii) via EC migration from adjacent native vessel, (iii) through deposition of circulating endothelial progenitor cells onto the luminal surface, or (iv) via ingrowth of capillaries through porous grafts [62]. Since Herring proposed a method of seeding ECs onto the luminal surface of synthetic conduits back in 1978 [63, 64], many studies have attempted to improve clinical rates of patency by optimizing EC attachment. Parallel to this, in scaffold-based blood vessel engineering, bioreactors and pulsatile flow systems, designed by many scientists, have been found to progress the mechanical property of the engineered blood vessels by augmenting the deposition and remodeling of extracellular matrix as well as the maturation and differentiation of self-assembled microtissues [65–68].

4. Tissue-Engineered Vascular Grafts

According to the tissue engineering approach a bioengineered tissue should be able to act as a temporary prosthesis that replace a particular damaged tissue for the time necessary to the cells, seeded in it or coming from the sites proximal to the implant, to synthesize a new extracellular matrix contributing to the production of a new tissue. The choice of the starting biomaterial is crucial as it influences the rate of degradation *in vivo*, the structural and functional integrity of the bio engineered tissue, and its gradual elimination from the body. The starting biomaterial also influences the mechanical properties of bioengineered tissue as well as its ability to be recognized as "self" by the body. This last feature is particularly important and can be completed only if the biomaterial carries biological signals that represent a stimulus for the adhesion and proliferation of the cells as well as for the production of new extracellular matrix. In other words, the physical-chemical characteristics of the biomaterial are able to influence the biochemical gap between living tissue and bioengineered ones. In some cases the biomaterial itself can represent a stimulus for the cellular functions (especially when natural components of the extracellular matrix are employed), while in most cases molecules such as growth factors, adhesion moieties, or even drugs of various nature have to be incorporated into bioengineered tissue by physical mixing or covalent bond. In this last case the biomaterial must have free functional groups to be exploited for the functionalization with one or more bioactive molecules. In blood vessels tissue engineering heparin and vascular endothelial growth factor (VEGF) are widely used. Both are in fact able to avoid the formation of thrombotic phenomena due to blood clotting. Heparin has anticoagulant activity and is crucial in the early stages after implantation, whereas VEGF, promoting endothelial cell proliferation, permits the formation of an intact endothelium on the surface of the scaffold in contact with the circulating blood avoiding the creation of turbulent motions responsible of the formation of thrombi. Moreover the presence of a confluent monolayer of endothelial cells prevents the development of pseudointimal hyperplasia by inhibition of bioactive substances responsible for SMC migration, proliferation, and production of ECM [69]. Since the early vascular tissue engineering has spreading, natural or synthetic polymers (or combination of the two classes) have been used as starting materials. Polyesters are a class of synthetic macromolecules widely used in tissue engineering because of their optimal mechanical properties, biocompatibility, and biodegradability.

These polymers have been used as sutures [70] plates and fixtures for fracture fixation devices [71] and scaffolds for cell transplantation [72, 73].

Polyesters such as poly(ε-caprolactone) (PCL), polylactic acid (PLA), and polyglycolic acid have been approved by FDA and extensively employed in experimental trials.

Figure 1: Tubular PHEA-PLA-PCL scaffold.

Concerning the vascular tissue engineering polyesters have been chosen as starting material very often thanks also to their good processability. Among the manipulation techniques electrospinning has gained great attention because it offers the possibility to obtain scaffolds with a defined shape and a complex porous architecture that can mimic the three-dimensional structure of extracellular matrix offering a good support for cell attachment and proliferation [74, 75]. Through electrospinning it is possible to prepare nonwoven mats of polymer fibers with diameters ranging from several microns down to less than 100 nm [76, 77]. Spun mats show amazing characteristics such as very large surface area to volume ratio, flexibility in surface functionalities, and superior mechanical performance (e.g., stiffness and tensile strength) compared with any other known form of the material [78]. These outstanding properties make the polymer fibers be optimal candidates in tissue engineering as substitutes of several tissues [79]. Nottelet et al. [80] developed a PCL-based vascular graft with an internal diameter of 2 or 4 mm. They implanted the cell-free scaffolds to Sprague-Dawley rats in substitution of an infrarenal abdominal aorta portion to evaluate the resistance and the patency of the implanted scaffolds over a period of 12 weeks. Scaffolds showed good surgical handling and suture retention properties and led to successful implantations without thrombosis or aneurysm formation at the three different time points. Authors observed also an almost complete endothelial coverage to the endoluminal graft surface after 6 weeks of implantation but some intima hyperplasia formation was observed in all grafts after 12 weeks.

Infiltration of fibroblast and macrophages was observed through all the scheduled times indicating the presence of an inflammation process even if no chronic lymphocytic reaction was observed.

The *in vivo* result of this study was even encouraging and has outlined the outstanding properties of PCL even if it is clear that some drawbacks are still present to be solved. As mentioned above, an ideal bioengineered tissue should optimally integrate with native tissues exploiting the possibility to be functionalized with bioactive molecules. The lack of functional groups in the starting biomaterial able to promote this type of functionalization could represent a major limitation. The small number of functional groups in the chemical structure of the polyesters limits the possibility to bind significant amounts of most of the bioactive agents and only molecules able to perform their biological function even at very low concentrations could be used.

Zheng et al. [81] produce a nanofibrous vascular graft by electrospinning of PCL functionalized with an arginine-glycine-aspartic acid-(RGD-) containing molecule named Nap-FFGRGD.

They also produce RGD free PCL grafts and compared results obtained from the implantation of the obtained vascular scaffolds in rabbit. Both grafts implanted in rabbit carotid arteries for 2 and 4 weeks showed endothelial cell adhesion in the lumen of the scaffold even if on the RGD-PCL cells were confluent and highly aligned, whereas those on the RGD free PCL graft were randomly aligned.

The endothelialization rates for RGD-PCL grafts were faster than those of the PCL grafts demonstrating the importance to incorporate the active molecule in the vascular graft.

Polyesters could be employed also in combination with bioactive macromolecules (mostly of natural origin) having a direct effect on the cells or with polymers having functional groups exploitable for the binding with the molecules of interest.

Pitarresi et al. [82] electrospun a mixture of PCL and α,β-poly(N-2-hydroxyethyl) (2-aminoethylcarbamate)-D,L-aspartamide-graft-polylactic acid (PHEA-EDA-g-PLA), a synthetic graft copolymer having in its chemical structure several free primary hydroxyl and amino groups coming from the hydrophilic backbone of PHEA-EDA, a biocompatible polymer derived from PHEA which is widely employed for several biomedical application [83–88] (Figures 1 and 2).

PHEA-EDA-g-PLA functional groups were exploited to covalently link a significant amount of heparin (36 μg per mg of scaffold) which has been employed to control the release of fibroblast growth factor. Authors demonstrate that the presence of both heparin and growth factor influences the ability of endothelial cells cultured *in vitro* upon the scaffold to produce an intact endothelial layer. Jia et al. [89] electrospun poly(L-lactic acid) (PLLA) in combination with collagen in order to obtain a scaffold with the optimal mechanical characteristic, due to the presence of the polyester, and able to represent an optimum substratum for cell adhesion and spreading thanks to the presence of collagen. They seeded bone marrow derived mesenchymal stem cells (MSCs) on the obtained nanofibers to investigate the capability of these cells to differentiate into vascular endothelial cells when cultivated with differentiating medium. Authors demonstrated that cells grown on PLLA/Coll nanofibrous scaffolds differentiated in endothelial cells showing cobblestone phenotype with expression of vascular specific proteins such as the platelet endothelial cell adhesion molecule-1 and Von Willebrand factor. The use of stem cells in tissue engineering is becoming increasingly popular because these cells can be extracted from various sources and can proliferate *in vitro* and differentiate into a series of mesodermal lineages, including osteoblasts, chondrocytes, adipocytes, myocytes, and vascular cells [90–93].

Among the polymers of natural origin, silk fibroin has certainly attracted a lot of attention in the field of vascular tissue engineering. Silk fibroin of silkworms is a commonly available natural polypeptidic biopolymer with a long history

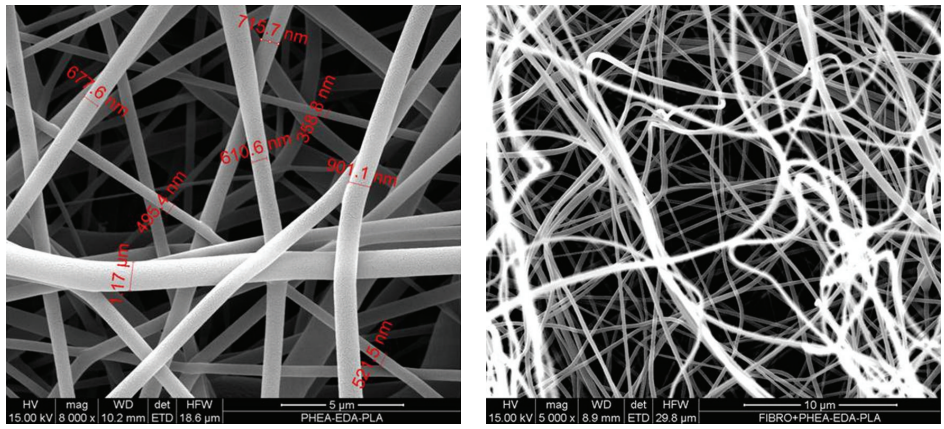

(a) (b)

Figure 2: PHEA-PLA-PCL scaffold. (a) SEM, 8000x, (b) SEM, 5000x.

of applications in the human body as sutures. Increasingly, silk fibroin is exploited in other areas of biomedical science, as a result of new knowledge of its processing and properties like mechanical strength, elasticity, biocompatibility, and controllable biodegradability [94]. Silk based regenerated vascular tissues are clinically used as flow diverting devices and stents and in general [95, 96] the properties of silk fibroin are particularly useful for tissue engineering [97]. The implantation of vascular graft of silk fibroin composites of B. mori and transgenic silkworm into rat abdominal aorta results in excellent patency (about 85%) after a year [98]. Wang et al. produced a fibroin scaffold consisting of silk braided tubes coated (on both inside and outside surfaces) by a film of fibroin cross-linked with poly(ethylene glycol) diglycidyl ether (PEG-DE). Through freeze drying technique authors were able to obtain micro- and nanoscale pores distributed throughout the inner surface of the scaffold.

They tested the biocompatibility *in vitro* on fibroblasts and human umbilical vein endothelial cells demonstrating that the biomaterial causes no inhibitory effect on DNA replication, cell adhesion, or proliferative activity. Cells in fact were able to fully spread on the internal surface and formed an interconnected network [99]. Liu et al. produced sulfated silk fibroin (S-silk) by reaction with chlorosulphonic acid in pyridine and used the obtained biomaterial to form a scaffold by electrospinning technique. They found that the anticoagulant activity of S-silk scaffolds was significantly enhanced compared with silk fibroin nanofibrous scaffolds. Also they demonstrated that both endothelial cells and smooth muscle cells strongly attached to S-silk scaffolds and proliferated well expressing some phenotype-related marker genes and proteins [100].

Several other studies have been conducted by employing natural derived polymers (also in combination with synthetic polymers) for the development of tissue-engineered blood vessels.

Zhu et al. developed a 3D scaffold for vascular tissue engineering by employing hyaluronic acid (HA) and human like collagen (HLC). A tubular structure was obtained by cross-linking the polymers with glutaraldehyde and then by freeze drying the obtained product previously placed in a tubular mold. Authors demonstrated that the presence of HA promotes endothelial cell proliferation and maintains their viability. Furthermore, HA enhances the mechanical properties of vascular hybrid scaffold [101].

5. Conclusions

Despite numerous *in vitro* and *in vivo* results obtained by different research groups in the production of bioengineered blood vessels, to the best of our knowledge, there are no clinical applications of any of these devices.

This denotes a real difficulty of the transposition of the implant from the animal model to humans and thus there is still a need to develop devices able to recreate entirely the functional properties of native blood vessels following the principles of tissue engineering.

There are still many aspects to be explained before a real clinical translation of vascular implants.

Further studies can help to clarify the mechanisms of regeneration and may address towards the choice of a more efficient strategy for scaffold production and cells seeding.

Understanding the role of inflammatory cells in blood vessel regeneration, for example, could be of great importance for the future development of innovative grafts.

It is also desirable to overcome the problem of thrombogenicity in humans, finding a new approach that can retain endothelial cells on grafts for a sufficient period of time under flow conditions *in vivo*.

Conflict of Interests

The authors declare that there is no conflict of interests regarding the publication of this paper.

References

[1] *Heart Disease and Stroke Statistics—2004 Update*, American Heart Association, Dallas, Tex, USA, 2004.

[2] J. G. Nemeno-Guanzon, S. Lee, J. R. Berg et al., "Trends in tissue engineering for blood vessels," *Journal of Biomedicine and Biotechnology*, vol. 2012, Article ID 956345, 14 pages, 2012.

[3] S. A. Hassantash, B. Bikdeli, S. Kalantarian, M. Sadeghian, and H. Afhar, "Pathophysiology of aortocoronary saphenous vein bypass graft disease," *Asian Cardiovascular and Thoracic Annals*, vol. 16, no. 4, pp. 331–336, 2008.

[4] A. Nieponice, L. Soletti, J. Guan et al., "Development of a tissue-engineered vascular graft combining a biodegradable scaffold, muscle-derived stem cells and a rotational vacuum seeding technique," *Biomaterials*, vol. 29, no. 7, pp. 825–833, 2008.

[5] R. A. Guyton, "Coronary artery bypass is superior to drug-eluting stents in multivessel coronary artery disease," *Annals of Thoracic Surgery*, vol. 81, no. 6, pp. 1949–1957, 2006.

[6] L. Norgren, W. R. Hiatt, J. A. Dormandy, M. R. Nehler, K. A. Harris, and F. G. R. Fowkes, "Inter-society consensus for the management of peripheral arterial disease (TASC II)," *Journal of Vascular Surgery*, vol. 45, no. 1, pp. S5–S67, 2007.

[7] R. Langer and J. P. Vacanti, "Tissue engineering," *Science*, vol. 260, no. 5110, pp. 920–926, 1993.

[8] X. Zhang, M. R. Reagan, and D. L. Kaplan, "Electrospun silk biomaterial scaffolds for regenerative medicine," *Advanced Drug Delivery Reviews*, vol. 61, no. 12, pp. 988–1006, 2009.

[9] M. Singh, C. Berkland, and M. S. Detamore, "Strategies and applications for incorporating physical and chemical signal gradients in tissue engineering," *Tissue Engineering B: Reviews*, vol. 14, no. 4, pp. 341–366, 2008.

[10] P. Buijtenhuijs, L. Buttafoco, A. A. Poot et al., "Tissue engineering of blood vessels: characterization of smooth- muscle cells for culturing on collagen and elastin based scaffolds," *Biotechnology and Applied Biochemistry*, vol. 39, no. 2, pp. 141–149, 2004.

[11] K. H. Yow, J. Ingram, S. A. Korossis, E. Ingham, and S. Homer-Vanniasinkam, "Tissue engineering of vascular conduits," *British Journal of Surgery*, vol. 93, no. 6, pp. 652–661, 2006.

[12] K. C. Rustad, M. Sorkin, B. Levi, M. T. Longaker, and G. C. Gurtner, "Strategies for organ level tissue engineering," *Organogenesis*, vol. 6, no. 3, pp. 151–157, 2010.

[13] R. E. Shadwick, "Mechanical design in arteries," *The Journal of Experimental Biology*, vol. 202, no. 23, pp. 3305–3313, 1999.

[14] A. Ratcliffe, "Tissue engineering of vascular grafts," *Matrix Biology*, vol. 19, no. 4, pp. 353–357, 2000.

[15] L. H. Harrison Jr., "Historical aspects in the development of venous autografts," *Annals of Surgery*, vol. 183, no. 2, pp. 101–106, 1976.

[16] D. J. Goyanes, "Substitution plastica de las arterias por las venas,6 arterioplastia venosa, aplicada, como nuevo metodo, al tratamiento de los aneurismas," *El Siglo Medico*, p. 346, 1906.

[17] E. Criado and F. Giron, "José Goyanes Capdevila, unsung pioneer of vascular surgery," *Annals of Vascular Surgery*, vol. 20, no. 3, pp. 422–425, 2006.

[18] B. M. Bernheim, "The ideal operation for aneurysm of the extremity. Report of a case," *Bulletin of Johns Hopkins Hospital*, vol. 27, p. 93, 1916.

[19] G. M. Williams, "Bertram M. Bernheim: a southern vascular surgeon," *Journal of Vascular Surgery*, vol. 16, no. 3, pp. 311–318, 1992.

[20] S. Ravi, Z. Qu, and E. L. Chaikof, "Polymeric materials for tissue engineering of arterial substitutes," *Vascular*, vol. 17, supplement 1, pp. S45–S54, 2009.

[21] J. M. Fichelle, F. Cormier, G. Franco, and F. Luizy, "What are the guidelines for using a venous segment for an arterial bypass ? General review," *Journal des Maladies Vasculaires*, vol. 35, no. 3, pp. 155–161, 2010.

[22] J. M. Sarjeant and M. Rabinovitch, "Understanding and treating vein graft atherosclerosis," *Cardiovascular Pathology*, vol. 11, no. 5, pp. 263–271, 2002.

[23] P. L. Faries, F. W. LoGerfo, S. Arora et al., "A comparative study of alternative conduits for lower extremity revascularization: all-autogenous conduit versus prosthetic grafts," *Journal of Vascular Surgery*, vol. 32, no. 6, pp. 1080–1090, 2000.

[24] P. L. Faries, F. W. Logerfo, S. Arora et al., "Arm vein conduit is superior to composite prosthetic-autogenous grafts in lower extremity revascularization," *Journal of Vascular Surgery*, vol. 31, no. 6, pp. 1119–1127, 2000.

[25] M. C. Donaldson, J. A. Mannick, and A. D. Whittemore, "Causes of primary graft failure after in situ saphenous vein bypass grafting," *Journal of Vascular Surgery*, vol. 15, no. 1, pp. 113–118, 1992.

[26] V. Piccone, "Alternative techniques in coronary artery reconstruction," in *Modern Vascular Grafts*, P. N. Sawyer, Ed., pp. 253–260, McGraw-Hill, New York, NY, USA, 1987.

[27] J. Chlupác, E. Filová, and L. Bacáková, "Blood vessel replacement: 50 years of development and tissue engineering paradigms in vascular surgery," *Physiological Research*, vol. 58, supplement 2, pp. S119–S139, 2009.

[28] G. W. He, "Arterial grafts: clinical classification and pharmacological management," *Annals of Cardiothoracic Surgery*, vol. 2, no. 4, pp. 507–518, 2013.

[29] J. E. McBane, S. Sharifpoor, R. S. Labow, M. Ruel, E. J. Suuronen, and J. P. Santerre, "Tissue engineering a small diameter vessel substitute: engineering constructs with select biomaterials and cells," *Current Vascular Pharmacology*, vol. 10, no. 3, pp. 347–360, 2012.

[30] R. Y. Kannan, H. J. Salacinski, P. E. Butler, G. Hamilton, and A. M. Seifalian, "Current status of prosthetic bypass grafts: a review," *Journal of Biomedical Materials Research B: Applied Biomaterials*, vol. 74, no. 1, pp. 570–581, 2005.

[31] L. Xue and H. P. Greisler, "Biomaterials in the development and future of vascular grafts," *Journal of Vascular Surgery*, vol. 37, no. 2, pp. 472–480, 2003.

[32] M. Isaka, T. Nishibe, Y. Okuda et al., "Experimental study on stability of a high-porosity expanded polytetrafluoroethylene graft in dogs," *Annals of Thoracic and Cardiovascular Surgery*, vol. 12, no. 1, pp. 37–41, 2006.

[33] N. R. Tai, H. J. Salacinski, A. Edwards, and G. Hamilton, "Seifalian AM Compliance of conduits used in vascular reconstruction," *British Journal of Surgery*, vol. 87, no. 11, pp. 1516–1524, 2000.

[34] M. G. Jeschke, V. Hermanutz, S. E. Wolf, and G. B. Koveker, "Polyurethane vascular prostheses decreases neointimal formation compared with expanded polytetrafluoroethylene," *Journal of Vascular Surgery*, vol. 29, no. 1, pp. 168–176, 1999.

[35] H. J. Salacinski, N. R. Tai, G. Punshon, A. Giudiceandrea, G. Hamilton, and A. M. Seifalian, "Optimal endothelialisation of a new compliant poly(carbonate-urea)urethane vascular graft with effect of physiological shear stress," *European Journal of Vascular and Endovascular Surgery*, vol. 20, no. 4, pp. 342–352, 2000.

[36] H. J. Salacinski, G. Punshon, B. Krijgsman, G. Hamilton, and A. M. Seifalian, "A hybrid compliant vascular graft seeded with

microvascular endothelial cells extracted from human omentum," *Artificial Organs*, vol. 25, no. 12, pp. 974–982, 2001.

[37] A. Tiwari, H. Salacinski, A. M. Seifalian, and G. Hamilton, "New prostheses for use in bypass grafts with special emphasis on polyurethanes," *Cardiovascular Surgery*, vol. 10, no. 3, pp. 191–197, 2002.

[38] M. Szycher, "Surface fissuring of polyurethanes following in vivo exposure," in *ASTM STP 859*, A. C. Fraker and D. G. Griffin, Eds., pp. 308–321, American Society of Testing and Materials, Philadelphia, Pa, USA, 1983.

[39] T. E. Brothers, J. C. Stanley, W. E. Burkel, and L. M. Graham, "Graham LM Small-caliber polytetrafluoroethylene grafts: a comparative study in a canine," *Journal of Biomedical Materials Research*, vol. 24, no. 6, pp. 761–771, 1990.

[40] J. J. Ricotta, "Vascular conduits: an overview," in *Vascular Surgery*, R. B. Rutherford, Ed., pp. 688–695, Elsevier-Saunders, Philadelphia, Pa, USA, 2005.

[41] P. C. Begovac, R. C. Thomson, J. L. Fisher, A. Hughson, and A. Gällhagen, "Improvements in GORE-TEX vascular graft performance by Carmeda BioActive surface heparin immobilization," *European Journal of Vascular and Endovascular Surgery*, vol. 25, no. 5, pp. 432–437, 2003.

[42] D. L. Akers, Y. H. Du, and R. F. Kempczinski, "The effect of carbon coating and porosity on early patency of expanded polytetrafluoroethylene grafts: an experimental study," *Journal of Vascular Surgery*, vol. 18, no. 1, pp. 10–15, 1993.

[43] C. Gosselin, D. Ren, and J. Ellinger, "Greisler HP In vivo platelet deposition on polytetrafluoroethylene coated with glue containing fibroblast growth factor 1 and heparin in a canine model," *The American Journal of Surgery*, vol. 170, no. 2, pp. 126–130, 1995.

[44] J. I. Zarge, V. Husak, and P. Huang, "Greisler HP Fibrin glue fibroblast growth factor type 1 and heparin decreases platelet deposition," *The American Journal of Surgery*, vol. 174, no. 2, pp. 188–192, 1997.

[45] W. M. Abbott, J. Megerman, J. E. Hasson, G. L'Italien, and D. F. Warnock, "Effect of compliance mismatch on vascular graft patency," *Journal of Vascular Surgery*, vol. 5, no. 2, pp. 376–382, 1987.

[46] S. G. Wise, M. J. Byrom, A. Waterhouse, P. G. Bannon, M. K. C. Ng, and A. S. Weiss, "A multilayered synthetic human elastin/polycaprolactone hybrid vascular graft with tailored mechanical properties," *Acta Biomaterialia*, vol. 7, no. 1, pp. 295–303, 2011.

[47] K. A. McKenna, M. T. Hinds, R. C. Sarao et al., "Mechanical property characterization of electrospun recombinant human tropoelastin for vascular graft biomaterials," *Acta Biomaterialia*, vol. 8, no. 1, pp. 225–233, 2012.

[48] P. Klinkert, P. N. Post, P. J. Breslau, and J. H. van Bockel, "Saphenous vein versus PTFE for above-knee femoropopliteal bypass. A review of the literature," *European Journal of Vascular and Endovascular Surgery*, vol. 27, no. 4, pp. 357–362, 2004.

[49] S. E. Greenwald and C. L. Berry, "Improving vascular grafts: the importance of mechanical and haemodynamic properties," *The Journal of Pathology*, vol. 190, pp. 292–299, 2000.

[50] A. Hasan, A. Memic, N. Annabi et al., "Electrospun scaffolds for tissue engineering of vascular grafts," *Acta Biomaterialia*, vol. 10, no. 1, pp. 11–25, 2014.

[51] H. Haruguchi and S. Teraoka, "Intimal hyperplasia and hemodynamic factors in arterial bypass and arteriovenous grafts: a review," *Journal of Artificial Organs*, vol. 6, no. 4, pp. 227–235, 2003.

[52] S. Sarkar, H. J. Salacinski, G. Hamilton, and A. M. Seifalian, "The mechanical properties of infrainguinal vascular bypass grafts: their role in influencing patency," *European Journal of Vascular and Endovascular Surgery*, vol. 31, no. 6, pp. 627–636, 2006.

[53] H. Shin, S. Jo, and A. G. Mikos, "Biomimetic materials for tissue engineering," *Biomaterials*, vol. 24, no. 24, pp. 4353–4364, 2003.

[54] B. C. Isenberg, C. Williams, and Tranquillo R. T., "Small-diameter artificial arteries engineered in vitro," *Circulation Research*, vol. 98, no. 1, pp. 25–35, 2006.

[55] J. D. Kakisis, C. D. Liapis, C. Breuer, and B. E. Sumpio, "Artificial blood vessel: the Holy Grail of peripheral vascular surgery," *Journal of Vascular Surgery*, vol. 41, no. 2, pp. 349–354, 2005.

[56] X. Wang, P. Lin, Q. Yao, and C. Chen, "Development of small-diameter vascular grafts," *World Journal of Surgery*, vol. 31, no. 4, pp. 682–689, 2007.

[57] C. B. Weinberg and E. Bell, "A blood vessel model constructed from collagen and cultured vascular cells," *Science*, vol. 231, no. 4736, pp. 397–400, 1986.

[58] T. Liu, S. Liu, K. Zhang, J. Chen, and N. Huang, "Endothelialization of implanted cardiovascular biomaterial surfaces: the development from *in vitro* to *in vivo*," *Journal of Biomedical Materials Research A*, 2013.

[59] P. P. Zilla and H. P. Greisler, Eds., *Tissue Engineering of Vascular Prosthetic Grafts*, RG Landes, Austin, Tex, USA, 1999.

[60] S. Hsu, S. Sun, and D. C. Chen, "Improved retention of endothelial cells seeded on polyurethane small-diameter vascular grafts modified by a recombinant RGD-containing protein," *Artificial Organs*, vol. 27, no. 12, pp. 1068–1078, 2003.

[61] A. W. Clowes, T. R. Kirkman, and M. A. Reidy, "Mechanisms of arterial graft healing. Rapid transmural capillary ingrowth provides a source of intimal endothelium and smooth muscle in porous PTFE prostheses," *The American Journal of Pathology*, vol. 123, no. 2, pp. 220–230, 1986.

[62] M. Herring, A. Gardner, and J. Glover, "A single staged technique for seeding vascular grafts with autogenous endothelium," *Surgery*, vol. 84, no. 4, pp. 498–504, 1978.

[63] M. A. Cleary, E. Geiger, C. Grady, C. Best, Y. Naito, and C. Breuer, "Vascular tissue engineering: the next generation," *Trends in Molecular Medicine*, vol. 18, no. 7, pp. 394–404, 2012.

[64] M. Poh, M. Boyer, A. Solan et al., "Blood vessels engineered from human cells," *The Lancet*, vol. 365, no. 9477, pp. 2122–2124, 2005.

[65] J. M. Kelm, V. Lorber, J. G. Snedeker et al., "A novel concept for scaffold-free vessel tissue engineering: self-assembly of microtissue building blocks," *Journal of Biotechnology*, vol. 148, no. 1, pp. 46–55, 2010.

[66] L. E. Niklason, J. Gao, W. M. Abbott et al., "Functional arteries grown in vitro," *Science*, vol. 284, no. 5413, pp. 489–493, 1999.

[67] L. Buttafoco, P. Engbers-Buijtenhuijs, A. A. Poot, P. J. Dijkstra, I. Vermes, and J. Feijen, "Physical characterization of vascular grafts cultured in a bioreactor," *Biomaterials*, vol. 27, no. 11, pp. 2380–2389, 2006.

[68] N. L'Heureux, S. Pâquet, R. Labbè, L. Germain, and F. A. Auger, "A completely biological tissue-engineered human blood vessel," *The FASEB Journal*, vol. 12, no. 1, pp. 47–56, 1998.

[69] Y. Naito, T. Shinoka, D. Duncan et al., "Vascular tissue engineering: towards the next generation vascular grafts," *Advanced Drug Delivery Reviews*, vol. 63, no. 4-5, pp. 312–323, 2011.

[70] D. E. Cutright, J. D. Beasley III, and B. Perez, "Histologic comparison of polylactic and polyglycolic acid sutures," *Oral Surgery, Oral Medicine, Oral Pathology*, vol. 32, no. 1, pp. 165–173, 1971.

[71] M. H. Mayer and J. O. Hollinger, "Biodegradable bone fixation devices," in *Biomedical Applications of Synthetic Biodegradable Polymers*, J. O. Hollinger, Ed., pp. 173–195, CRC Press, Boca Raton, Fla, USA, 1995.

[72] R. C. Thomson, M. J. Yaszemski, J. M. Powers, and A. G. Mikos, "Fabrication of biodegradable polymer scaffolds to engineer trabecular bone," *Journal of Biomaterials Science, Polymer Edition*, vol. 7, no. 1, pp. 23–38, 1995.

[73] P. A. Gunatillake and R. Adhikari, "Biodegradable synthetic polymers for tissue engineering," *European Cells and Materials*, vol. 5, pp. 1–16, 2003.

[74] S. MacNeil, "Biomaterials for tissue engineering of skin," *Materials Today*, vol. 11, no. 5, pp. 26–35, 2008.

[75] G. Pitarresi, F. S. Palumbo, C. Fiorica, F. Calascibetta, and G. Giammona, "Electrospinning of α,β-poly(*N*-2-hydroxyethyl)-DL-aspartamide-*graft*-polylactic acid to produce a fibrillar scaffold," *European Polymer Journal*, vol. 46, no. 2, pp. 181–184, 2010.

[76] D. H. Reneker and I. Chun, "Nanometre diameter fibres of polymer, produced by electrospinning," *Nanotechnology*, vol. 7, no. 3, pp. 216–223, 1996.

[77] X. Xu, L. Yang, X. Wang et al., "Ultrafine medicated fibers electrospun from W/O emulsions," *Journal of Controlled Release*, vol. 108, no. 1, pp. 33–42, 2005.

[78] Z.-M. Huang, Y. Z. Zhang, M. Kotaki, and S. Ramakrishna, "A review on polymer nanofibers by electrospinning and their applications in nanocomposites," *Composites Science and Technology*, vol. 63, no. 15, pp. 2223–2253, 2003.

[79] W. Li, C. T. Laurencin, E. J. Caterson, R. S. Tuan, and F. K. Ko, "Electrospun nanofibrous structure: a novel scaffold for tissue engineering," *Journal of Biomedical Materials Research*, vol. 60, no. 4, pp. 613–621, 2002.

[80] B. Nottelet, E. Pektok, D. Mandracchia et al., "Factorial design optimization and in vivo feasibility of poly(ε-caprolactone)-micro- and nanofiber-based small diameter vascular grafts," *Journal of Biomedical Materials Research A*, vol. 89, no. 4, pp. 865–875, 2009.

[81] W. Zheng, Z. Wang, L. Song et al., "Endothelialization and patency of RGD-functionalized vascular grafts in a rabbit carotid artery model," *Biomaterials*, vol. 33, no. 10, pp. 2880–2891, 2012.

[82] G. Pitarresi, C. Fiorica, F. S. Palumbo, S. Rigogliuso, G. Ghersi, and G. Giammona, "Heparin functionalized polyaspartamide/polyester scaffold for potential blood vessel regeneration," *Journal of Biomedical Materials Research A*, vol. 102, no. 5, pp. 1334–1341, 2014.

[83] A. I. Lo Monte, M. Licciardi, M. Bellavia et al., "Biocompatibility and biodegradability of electrospun phea-pla scaffolds: our preliminary experience in a murine animal model," *Digest Journal of Nanomaterials and Biostructures*, vol. 7, no. 2, pp. 841–851, 2012.

[84] C. Fiorica, S. Rigogliuso, F. S. Palumbo, G. Pitarresi, G. Giammona, and G. Ghersi, "A fibrillar biodegradable scaffold for blood vessels tissue engineering," *Chemical Engineering Transactions*, vol. 27, pp. 403–408, 2012.

[85] G. Pitarresi, C. Fiorica, F. S. Palumbo, F. Calascibetta, and G. Giammona, "Polyaspartamide-polylactide electrospun scaffolds for potential topical release of Ibuprofen," *Journal of Biomedical Materials Research A*, vol. 100, no. 6, pp. 1565–1572, 2012.

[86] M. Licciardi, G. Cavallaro, M. Di Stefano, C. Fiorica, and G. Giammona, "Polyaspartamide-graft-polymethacrylate nanoparticles for doxorubicin delivery," *Macromolecular Bioscience*, vol. 11, no. 3, pp. 445–454, 2011.

[87] G. Pitarresi, F. S. Palumbo, A. Albanese, M. Licciardi, F. Calascibetta, and G. Giammona, "In situ gel forming graft copolymers of a polyaspartamide and polylactic acid: preparation and characterization," *European Polymer Journal*, vol. 44, no. 11, pp. 3764–3775, 2008.

[88] R. Mendichi, A. G. Schieroni, G. Cavallaro, M. Licciardi, and G. Giammona, "Molecular characterization of α,β-poly(*N*-2-hydroxyethyl)-DL-aspartamide derivatives as potential self-assembling copolymers forming polymeric micelles," *Polymer*, vol. 44, no. 17, pp. 4871–4879, 2003.

[89] L. Jia, M. P. Prabhakaran, X. Qin, and S. Ramakrishna, "Stem cell differentiation on electrospun nanofibrous substrates for vascular tissue engineering," *Materials Science and Engineering C*, vol. 33, no. 8, p. 4640, 2013.

[90] C. Toma, M. F. Pittenger, K. S. Cahill, B. J. Byrne, and P. D. Kessler, "Human mesenchymal stem cells differentiate to a cardiomyocyte phenotype in the adult murine heart," *Circulation*, vol. 105, no. 1, pp. 93–98, 2002.

[91] D. Woodbury, E. J. Schwarz, D. J. Prockop, and I. B. Black, "Adult rat and human bone marrow stromal cells differentiate into neurons," *Journal of Neuroscience Research*, vol. 61, no. 4, pp. 364–370, 2000.

[92] G. Jin, M. P. Prabhakaran, and S. Ramakrishna, "Stem cell differentiation to epidermal lineages on electrospun nanofibrous substrates for skin tissue engineering," *Acta Biomaterialia*, vol. 7, no. 8, pp. 3113–3122, 2011.

[93] X. Xin, M. Hussain, and J. J. Mao, "Continuing differentiation of human mesenchymal stem cells and induced chondrogenic and osteogenic lineages in electrospun PLGA nanofiber scaffold," *Biomaterials*, vol. 28, no. 2, pp. 316–325, 2007.

[94] F. G. Omenetto and D. L. Kaplan, "New opportunities for an ancient material," *Science*, vol. 329, no. 5991, pp. 528–531, 2010.

[95] F. Causin, R. Pascarella, G. Pavesi et al., "Acute endovascular treatment (<48 hours) of uncoilable ruptured aneurysms at non-branching sites using silk flow-diverting devices," *Interventional Neuroradiology*, vol. 17, no. 3, pp. 357–364, 2011.

[96] M. Leonardi, L. Cirillo, F. Toni et al., "Treatment of intracranial aneurysms using flow-diverting silk stents (BALT): a single centre experience," *Interventional Neuroradiology*, vol. 17, no. 3, pp. 306–315, 2011.

[97] B. Kundu, R. Rajkhowa, S. C. Kundu, and X. Wang, "Silk fibroin biomaterials for tissue regenerations," *Advanced Drug Delivery Reviews*, vol. 65, no. 4, pp. 457–470, 2013.

[98] Y. Nakazawa, M. Sato, R. Takahashi et al., "Development of small-diameter vascular grafts based on silk fibroin fibers from bombyx mori for vascular regeneration," *Journal of Biomaterials Science*, vol. 22, no. 1–3, pp. 195–206, 2011.

[99] J. Wang, Y. Wei, H. Yi, Z. Liu, D. Sun, and H. Zhao, "Cytocompatibility of a silk fibroin tubular scaffold," *Materials Science and Engineering C: Materials for Biological Applications*, vol. 34, pp. 429–436, 2014.

[100] H. Liu, X. Li, G. Zhou, H. Fan, and Y. Fan, "Electrospun sulfated silk fibroin nanofibrous scaffolds for vascular tissue engineering," *Biomaterials*, vol. 32, no. 15, pp. 3784–3793, 2011.

[101] C. Zhu, D. Fan, and Y. Wang, "Human-like collagen/hyaluronic acid 3D scaffolds for vascular tissue engineering," *Materials Science & Engineering C: Materials for Biological Applications*, vol. 34, pp. 393–401, 2014.

Hindawi Publishing Corporation
International Journal of Polymer Science
Volume 2014, Article ID 579252, 6 pages
http://dx.doi.org/10.1155/2014/579252

Research Article

The Development of Biomimetic Spherical Hydroxyapatite/Polyamide 66 Biocomposites as Bone Repair Materials

Xuesong Zhang,[1] Ming Lu,[1] Yan Wang,[1] Xiaojing Su,[1] and Xuelian Zhang[2]

[1] *Department of Orthopaedics, Chinese People's Liberation Army General Hospital, Beijing 100853, China*
[2] *Department of Endocrinology, China-Japan Friendship Hospital, Beijing 100029, China*

Correspondence should be addressed to Xuelian Zhang; zhangxuelian66@sina.com

Received 28 February 2014; Accepted 21 May 2014; Published 6 July 2014

Academic Editor: Xiaoming Li

A novel biomedical material composed of spherical hydroxyapatite (s-HA) and polyamide 66 (PA) biocomposite (s-HA/PA) was prepared, and its composition, mechanical properties, and cytocompatibility were characterized and evaluated. The results showed that HA distributed uniformly in the s-HA/PA matrix. Strong molecule interactions and chemical bonds were presented between the s-HA and PA in the composites confirmed by IR and XRD. The composite had excellent compressive strength in the range between 95 and 132 MPa, close to that of natural bone. *In vitro* experiments showed the s-HA/PA composite could improve cell growth, proliferation, and differentiation. Therefore, the developed s-HA/PA composites in this study might be used for tissue engineering and bone repair.

1. Introduction

Hydroxyapatite (HA), with similar composition to natural bone, has been extensively developed for biomedical applications in the past decades because it has good biocompatibility and bioactivity and can bond with host bone directly [1–4]. However, HA ceramics devices, such as filler and porous scaffold, exhibit manifest brittleness, which vastly impedes its clinical applications.

In order to obtain a biomaterial with good bioactivity and good mechanical properties, more and more attention focuses on the researches and medical applications of a composite combining hydroxyapatite with a polymer because such composite possesses both good bioactivity (HA) and good ductility (polymer) [4–10]. Those biocomposites are biocompatible and osteoconductive and hence can bond with host bone directly and thus form a uniquely strong biomaterial-bone interface.

Previous studies have showed that the properties of HA have manifest effects on the properties of the HA/PA composites [11–16]. For example, HA with atom molar Ca/P ratio of 1.67 is very stable and hence shows poor degradability and bioactivity *in vivo* while HA with lower atom molar Ca/P ratio (form 1.5 to 1.67) exhibits higher solubility (degradability) and bioactivity. The size of HA also affects the properties of the obtained composite. A nanoscaled HA shows better bioactivity and enhancement effects on polymer and obtains higher mechanical properties compared to the microsized one because the nanosized HA have obvious surface effect and small size effect [17, 18].

Recently, nanohydroxyapatite (n-HA)/polyamide 66 biocomposites were developed by Sichuan University [1, 17]. The composites were shown to have good mechanical strength similar to natural bone and good compatibility. Furthermore, cage and vertebral plate developed by those composites have been used for spine repair successfully [19]. However, n-HA preparation process is very complex. Moreover, conglomeration of nanoparticles has been deemed to be one of the main obstacles in the preparation of polymer-based nanobiomaterials [20]. Hence, in this study, we prepared HA/PA composite composed of spherical HA with extrusion method, an industrialized method, and the composition, mechanical properties, and preliminary cell responses to the

composites were investigated in order to assess the potential application as bone repair materials.

2. Materials and Method

2.1. Preparation of s-HA/PA. PA (BASF, A3K) and s-HA (provided by Sichuan University) were mixed proportionally and were processed by extrusion method according to the following parameters: extrusion temperature: 230–275°C; main engine speed: 50 HZ; feed rate: 40 HZ.

S-HA/PA composites with 10 w%, 20 w%, 30 w%, and 40 w% s-HA content were prepared and named as 10HA/PA, 20HA/PA, 30HA/PA, and 40HA/PA, respectively.

2.2. IR, XRD, and Mechanical Strength. The composition and structure of the 30HA/PA composite were characterized by Fourier transform infrared spectroscopy (170SX FT-IR Spectrometer; Nicolet, Madison, WI) and X-ray diffraction (X'Pert pro-MPD; Philips, Eindhoven, The Netherlands). To observe the S-HA distribution in PA matrices, the 30HA/PA composite was fractured in liquid nitrogen, and a cross-sectional specimen was observed under a scanning electron microscope (Hitachi S-450). In addition, the effects of the amount of s-HA on the compressive strength of the composite were assessed in the composite samples ($\Phi 10 \times 12$ mm) containing different amounts of s-HA (0 wt%, 10 wt%, 20 wt%, 30 wt%, and 40 wt%) using a mechanical testing machine (REGER 30–50; Shenzhen Reger Co., Ltd., Shenzhen, China) with 50 kN load cells. The cross-head speed was 5 mm/minute, and the load was applied until the specimens were compressed to about 20% of their original height. Five replicates were carried out for each group, and the results are expressed as the mean ± standard deviation.

2.3. Cytocompatibility. Culture cells in a humidified atmosphere with 5% CO_2, MG63 osteoblast-like cells were cultured in Dulbecco's Modified Eagle Medium (DMEM) supplemented with 10% FBS plus 100 U/mL penicillin and 100 μg/mL streptomycin sulfate. Cells were incubated in 25 cm^2 flasks to reach 80% confluence and then detached for further experiments. For all the cell culture experiments, 30HA/PA composite samples with the size of $\Phi 12 \times 2$ mm were used and MAC and tissue culture plate as controls. These samples were sonicated in ethanol and sterilized using ethylene oxide gas.

2.3.1. Cell Proliferation and Morphology. MG-63 osteoblast-like cells were cultured in DMEM supplemented with 10% FBS plus 100 U/mL penicillin and 100 μg/mL streptomycin sulfates at 37°C in a humidified 5% CO_2 atmosphere. Cells were incubated in 25 cm^2 flasks to reach 80% confluence and then detached for further experiments. n-DA/MC composite scaffold samples with the size of $\Phi 6 \times 2$ mm were used for all the cell culture experiments, and tissue culture plate (TCP) was used as a control. These samples were sonicated in ethanol and sterilized using ethylene oxide gas.

The proliferation of MG-63 cells on the scaffold samples was determined by using MTT (3-{4,5-dimethylthiazol-2yl}-2,5-diphenyl-2H-tetrazolium-bromide) assay. MTT measures changes in absorbance at a specific wavelength and is widely used for measuring cell viability. The production of purple formazan in osteoblast cultures with or without the samples was measured after 1, 3, 5, and 7 days of incubation in 24-well culture plates. For this purpose, 100 μL of MTT (MajorBiochem, Shanghai, China) solution (5 mg/mL) was added to each well (containing either cells alone or pellets with adherent cells removed from the original culturing well) and the cells were incubated for 4 hours. Subsequently, the culture medium was aspirated and dimethyl sulfoxide 1000 μL/well was added to dissolve the formazan completely for 10 minutes at 37°C. Then 100 μL of solution was transferred to a 96-well enzyme-linked immunosorbent assay plate and the absorbance was measured at 490 nm using a microplate reader (Multiskan MK3, Thermo Electron Corporation, Waltham, MA). Phase contrast microscopy was used to observe the cell morphology.

2.3.2. ALP Activity. MG-63 cells were seeded on the samples and ALP activity of cells was measured at 1, 3, 5, and 7 days, and the culture medium in 24-well plates was aspirated. 200 μL, 1% Nonidet P-40 (NP-40) solution was added to each well at room temperature (RT) and incubated for 1 hour. The cell lysate was obtained and centrifuged. 50 μL supernatant and 50 μL 2 mg/mL p-nitrophenylphosphate (Sangon, Shanghai, China) substrate solution composed of 0.1 mol/L glycine, 1 mmol/L $MgCl_2 \cdot 6H_2O$ were added to 96-well plates and incubated for 30 min at 37°C. The reaction was quenched by addition of 100 μL, 0.1 N NaOH; the absorbance of ALP was quantified at the wavelength of 405 nm using a microplate reader (SPECTRAmax 384, Molecular Devices, USA). The total protein content in cell lysate was determined using the bicinchoninic acid (BCA) method in aliquots of the same samples with the Pierce protein assay kit (Pierce Biotechnology Inc., Rockford, IL), read at 560 nm, and calculated according to a series of albumin (BSA) standards. The ALP levels were normalized to the total protein content at the end of the experiment.

3. Results

3.1. IR and XRD. Figure 1(a) showed the characteristic peaks of the PA. The –CO–NH– peaks could be observed at about 1556 cm^{-1}, 3307 cm^{-1} (N–H stretching), and 1642 cm^{-1} (C=O). Bonds at 2857 and 2925 cm^{-1} were the characteristic peaks of C–H vibration. In Figure 1(b), the PO_4^{3-} peaks were found at about 566, 953, 1033, and 1107 cm^{-1}. The OH– peaks were found at about 3569 and 605 cm^{-1}. Figure 1(c) was the spectra of composite. It can be seen that peaks of both s-HA and PA presented in the composite, and the peaks had shown clear shifts. The peaks of PA shifted from 1556, 1642, and 3307 cm^{-1} to 1552, 1637, and 3301 cm^{-1}. Owing to the existence of hydrogen, it will absorb more energy than before, resulting in the absorption wavelength getting shorter. So,

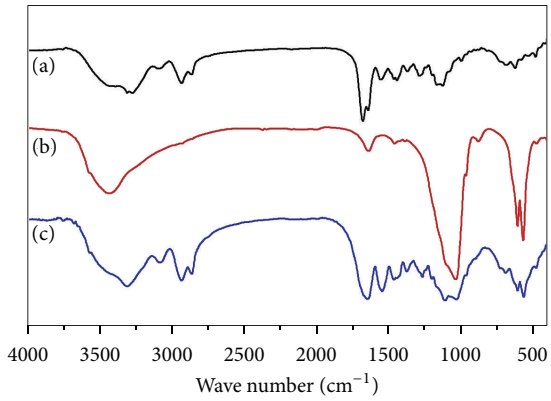

Figure 1: FT-IR spectra of PA (a), s-HA (b), and s-HA/PA composite (c).

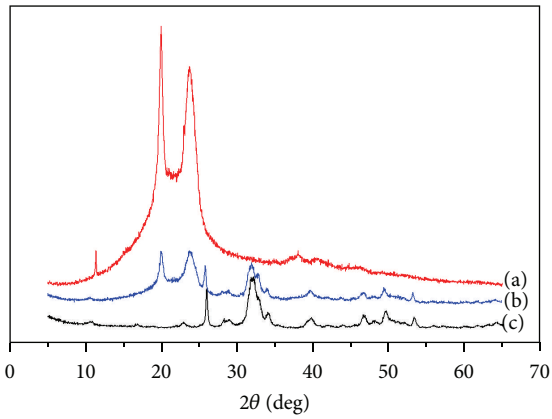

Figure 2: The XRD patterns of PA (a), s-HA/PA composite (b), and s-HA (c).

the peaks of HA shifted from 3569 to 3561 cm^{-1}. Those peaks' shift suggests that hydrogen formed between s-HA and PA.

Figure 2 showed the XRD patterns of PA (a), s-HA/PA composite (b), and s-HA (c). Figure 2(c) indicated that the major characteristic peaks of HA appeared around 25.9°, 32°, 33°, 33.9°, and 39.7°, which were corresponding to the peaks of the bone apatite [5]. Two strong peaks at $2\theta = 19.9°$, 23.5° were attributed to PA in Figure 2(a). Because of the interaction of HA and copolymer, the orderliness of PA was seriously disturbed, which is responsible for the decrease of the intensities of PA peaks in Figure 2(b).

3.2. Compressive Strength of s-HA/PA Composite. The compressive strength of composite with different s-HA is shown in Table 1. It can be seen that the compressive strength increased from 67 MPa to 132 MPa with the increase of s-HA from 0 to 40% in composite.

3.3. SEM Analysis. The SEM photographs of s-HA and s-HA/PA composite are shown in Figure 3. The s-HA was about 20–60 μm (Figure 3(a)) and uniformly distributed in PA matrix (Figure 3(b)). In addition, no cracks between s-HA and PA were observed.

Table 1: Compressive strength of s-HA/PA composite.

Samples	Compression strength (MPa) mean ± SD
PA	67 ± 7
10HA/PA	95 ± 15
20HA/PA	108 ± 9
30HA/PA	126 ± 8
40HA/PA	132 ± 11

3.4. Cytocompatibility

3.4.1. Cell Proliferation. The optical density (OD) values can provide an indicator of cell viability on biomaterials; thus the proliferation of MG63 cells on 30HA/PA composite was evaluated using MTT. As shown in Figure 4, the OD values of the composite and the controls (tissue culture plate, TCP) increased with time, suggesting that MG63 cells were viable on these samples, showing positive cellular responses. No significant difference for OD values was found between the composite and controls at 1, 3, and 5 days. However, the OD value of the composite was higher than those of control at 7 days, indicating that the 30HA/PA composite could promote cell proliferation at 7 days.

3.4.2. ALP Activity. ALP activity of MG63 cells cultured on the 30HA/PA composite was determined at 1, 3, 5, and 7 days. The results are shown in Figure 5. The ALP activity increased with time for both the composite and TCP. No significant difference between the composite and TCP was found at 1 and 3 days. However, the level of ALP activity of cells on the HA/PA composite was obviously higher than those of MAC and tissue culture plate at 5 and 7 days.

3.4.3. Cell Morphology. The phase contrast microscopy images of MG63 cells cultured with the HA/PA composite scaffolds are shown in Figure 6. It can be seen that, after 1 day of culture, the cells had a sheet shape and there were large intercellular spaces. After 3 days, the population of the cells increased and the intercellular spaces reduced manifestly. The cells kept increasing and the gap between cells disappeared after 5 and 7 days, indicating that the HA/PA composite scaffolds had no negative effects on cells growth and maintain normal cell morphology.

4. Discussion

HA has an inorganic component similar to that in human hard tissue. It has a good biocompatibility and can bond to bone tissue in body [1, 21]. The outstanding biological performance of HA biomaterial has been widely proved in the forms of bone filler, coating on titanium alloy, and recently as scaffolds for cell carrier in bone tissue engineering [1, 5, 9, 11]. So, HA is a good candidate for the preparation of ceramic/polymer composites. Previous studies have reported many performances of HA; for example, size and Ca/P ratio exhibited manifest effects on the properties of the resultant

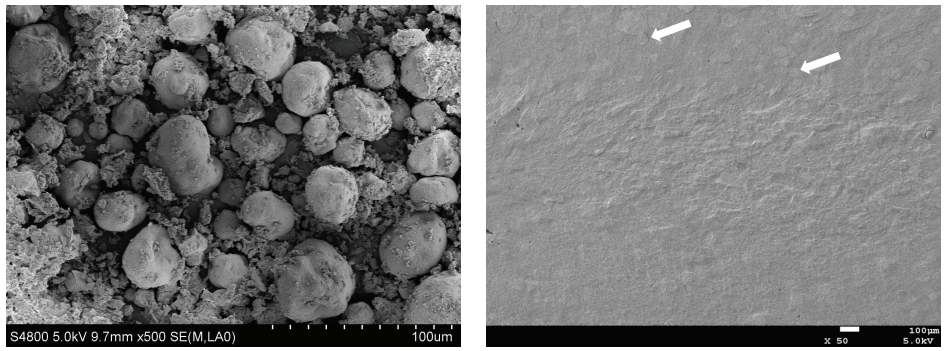

(a) (b)

Figure 3: The morphology of s-HA (a) and s-HA/PA (b).

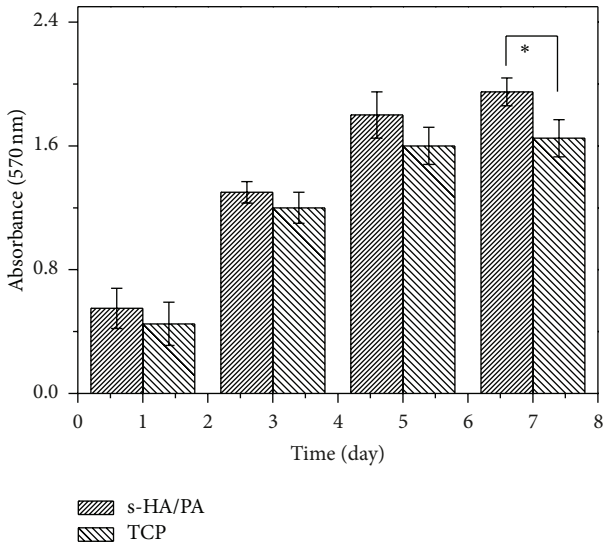

Figure 4: Viability of MG63 cells on s-HA/PA composite by MTT assay, TCP as controls, $^{*}P < 0.05$.

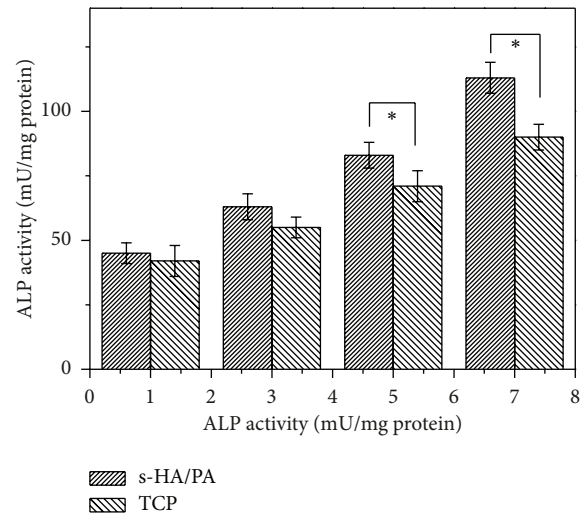

Figure 5: ALP activity of MG63 cells cultured on s-HA/PA composite, TCP as controls, $^{*}P < 0.05$.

composite [22]. Hence, in this study, the spherical HA was used as inorganic phase to enhance polyamide 66 to obtain novel composites, and their properties were characterized. It was shown by IR and XRD that chemical bond was formed between s-HA and PA, which was considered to be a strong interface bond. So when the s-HA are imposed with external pressure, the pressure could be transferred into PA via chemical bond, thus improving the whole mechanical strength. The interface interactions between the polymer and inorganic mineral have been proved to have positive effects on the mechanical properties and the distribution of inorganic particles into the composites [23–25].

In this study, the prepared s-HA/PA composite has a good homogeneity (Figure 3). Furthermore, no obvious interface debonding could be observed in the fracture surface of composite, suggesting that there was a good interface between s-HA and PA, which was consistent with the results of IR and XRD.

The compressive strength of the composites with 10–40 w% s-HA content ranged between 95 and 132 MPa, which was close to that of the natural bone, between 50 and 140 MPa [26]. It has been reported that n-HA/PA composite showed good mechanical strength and could meet the fundamental requirements for supporting after implantation [1]. Compared to that, s-HA/PA composites showed higher compressive strength. Therefore, s-HA/PA should have enough compressive strength for the support requirements *in vivo*.

To evaluate the *in vitro* biocompatibility of biomaterials, the cell culture experiments are useful approaches [27, 28]. In this study, the MG63 cells were used to test the cytocompatibility of the s-HA/PA composite. The results showed that the MG63 cells could proliferate better on the composites, as was demonstrated by the MTT assay, suggesting positive cellular responses to this material. After 7-day culture, the OD values of the composites were significantly higher than those of TCP, indicating that the composites could promote the cell proliferation better and had higher cytocompatibility than TCP. The phase contrast microscopy results exhibited

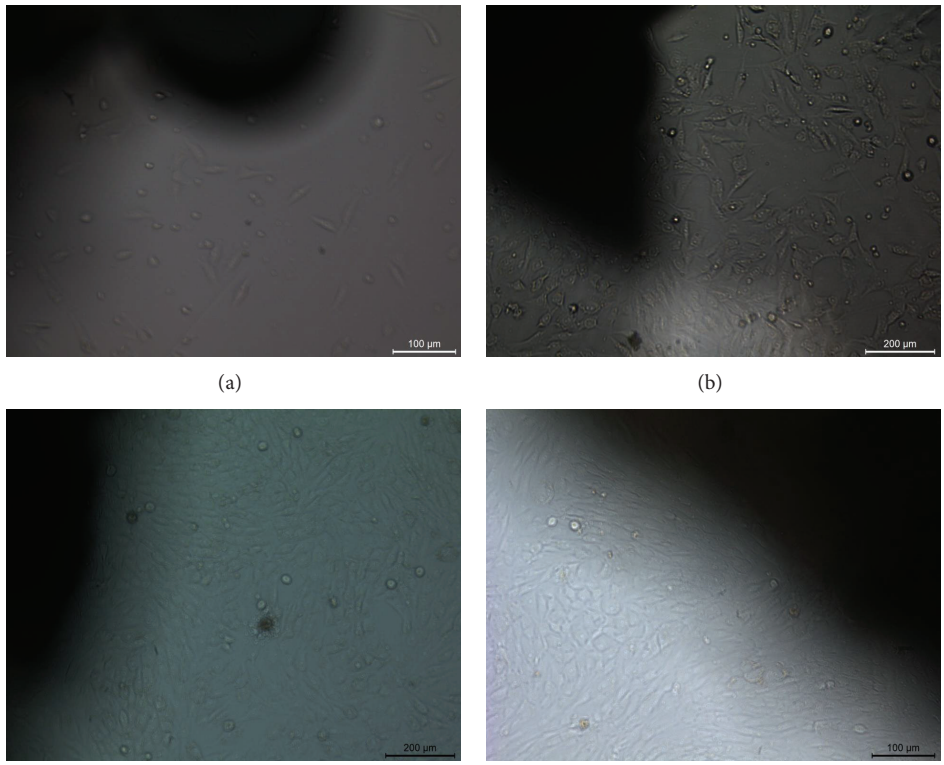

(a) (b)

(c) (d)

Figure 6: Phase contrast microscopy images of MG63 cells cultured on the s-HA/PA composite for 1 day (a), 3 days (b), 5 days (c), and 7 days (d).

that cells population increased with high speed and the spaces among the cells disappeared at 5 days and that the cells maintain normal morphology, suggesting that the s-HA/PA composites had no negative effect on the cell attachment and proliferation. Furthermore, the ALP activity has been used as an early marker for functionality and differentiation of osteoblasts during *in vitro* experiments [29–33]. The results showed that the ALP of the MG63 cells cultured on the s-HA/PA composites exhibited significantly higher levels of expression than that of the cells cultured on TCP at 5 and 7 days, indicating that the composite could induce better the differentiation of the cell into osteogenic cells.

5. Conclusion

Novel s-HA/PA biocomposites were prepared by extrusion method in this study. The s-HA was homogenously distributed into HA/PA matrix and chemical bond was formed at the interface between organic phase and inorganic phase. The compressive strength of composite was close to that of natural bone. Furthermore, the s-HA/PA composites could not only promote cell proliferation but also induce the differentiation of the cell into osteogenic cells. The results indicated that the s-HA/PA biocomposite might be a candidate for bone repair material.

Conflict of Interests

The authors declare that there is no conflict of interests regarding the publication of this paper.

References

[1] H. Wang, Y. Li, Y. Zuo, J. Li, S. Ma, and L. Cheng, "Biocompatibility and osteogenesis of biomimetic nano-hydroxyapatite/polyamide composite scaffolds for bone tissue engineering," *Biomaterials*, vol. 28, no. 22, pp. 3338–3348, 2007.

[2] X. Li, Q. Feng, X. Liu, W. Dong, and F. Cui, "Collagen-based implants reinforced by chitin fibres in a goat shank bone defect model," *Biomaterials*, vol. 27, no. 9, pp. 1917–1923, 2006.

[3] B. Chang, C. K. Lee, K. S. Hong et al., "Osteoconduction at porous hydroxyapatite with various pore configurations," *Biomaterials*, vol. 21, no. 12, pp. 1291–1298, 2000.

[4] A. Hanifi and F. M. Hossein, "Bioresorbability evaluation of hydroxyapatite nanopowders in a stimulated body fluid medium," *Iranian Journal of Pharmaceutical Sciences*, vol. 4, no. 2, pp. 141–148, 2008.

[5] X. Li, L. Wang, Y. Fan, Q. Feng, F. Cui, and F. Watari, "Nanostructured scaffolds for bone tissue engineering," *Journal of Biomedical Materials Research A*, vol. 101A, no. 8, pp. 2424–2435, 2013.

[6] P. Shokrollahi, H. Mirzadeh, O. A. Scherman, and W. T. S. Huck, "Biological and mechanical properties of novel composites based on supramolecular polycaprolactone and functionalized

hydroxyapatite," *Journal of Biomedical Materials Research A*, vol. 95, no. 1, pp. 209–221, 2010.

[7] C. L. Dai, C. S. Liu, J. Wei, H. Hong, and Q. Zhao, "Molecular imprinted macroporous chitosan coated mesoporous silica xerogels for hemorrhage control," *Biomaterials*, vol. 31, no. 30, pp. 7620–7630, 2010.

[8] X. Li, H. Liu, X. Niu et al., "The use of carbon nanotubes to induce osteogenic differentiation of human adipose-derived MSCs *in vitro* and ectopic bone formation *in vivo*," *Biomaterials*, vol. 33, no. 19, pp. 4818–4827, 2012.

[9] I. Armentano, M. Dottori, E. Fortunati, S. Mattioli, and J. M. Kenny, "Biodegradable polymer matrix nanocomposites for tissue engineering: a review," *Polymer Degradation and Stability*, vol. 95, no. 11, pp. 2126–2146, 2010.

[10] K. E. Tanner, "Bioactive composites for bone tissue engineering," *Proceedings of the Institution of Mechanical Engineers H: Journal of Engineering in Medicine*, vol. 224, no. 12, pp. 1359–1372, 2010.

[11] R. Z. Legeros, S. Lin, R. Rohanizadeh, D. Mijares, and J. P. Legeros, "Biphasic calcium phosphate bioceramics: preparation, properties and applications," *Journal of Materials Science: Materials in Medicine*, vol. 14, no. 3, pp. 201–209, 2003.

[12] X. Li, Y. Yang, Y. Fan, Q. Feng, F. Cui, and F. Watari, "Biocomposites reinforced by fibers or tubes as scaffolds for tissue engineering or regenerative medicine," *Journal of Biomedical Materials Research A*, vol. 102, pp. 1580–1594, 2014.

[13] H. Guo, J. C. Su, J. Wei, H. Kong, and C. Liu, "Biocompatibility and osteogenicity of degradable Ca-deficient hydroxyapatite scaffolds from calcium phosphate cement for bone tissue engineering," *Acta Biomaterialia*, vol. 5, no. 1, pp. 268–278, 2009.

[14] J. H. C. Lin, K. H. Kuo, S. J. Ding, and C. P. Ju, "Surface reaction of stoichiometric and calcium-deficient hvdroxyapatite in simulated body fluid," *Journal of Materials Science: Materials in Medicine*, vol. 12, no. 8, pp. 731–741, 2001.

[15] X. Li, C. A. van Blitterswijk, Q. Feng, F. Cui, and F. Watari, "The effect of calcium phosphate microstructure on bone-related cells in vitro," *Biomaterials*, vol. 29, no. 23, pp. 3306–3316, 2008.

[16] Y. E. Greish, "Phase evolution during the low temperature formation of calcium-deficient hydroxyapatite-gypsum composites," *Ceramics International*, vol. 37, no. 5, pp. 1493–1500, 2011.

[17] X. Zhang, Y. B. Li, Z. M. Song, Y. Zuo, and Y. H. Mu, "A study on the mechanical properties of PA66/ HA composites," *China Plastics*, vol. 19, pp. 25–29, 2005.

[18] X. M. Li, H. F. Liu, X. F. Niu et al., "Osteogenic differentiation of human adipose-derived stem cells induced by osteoinductive calcium phosphate ceramics," *Journal of Biomedical Materials Research B: Applied Biomaterials*, vol. 97, no. 1, pp. 10–19, 2011.

[19] X. Yang, Q. Chen, L. Liu et al., "Comparison of anterior cervical fusion by titanium mesh cage versus nano-hydroxyapatite/polyamide cage following single-level corpectomy," *International Orthopaedics*, vol. 37, no. 12, pp. 2421–2427, 2013.

[20] X. Li, H. Gao, M. Uo et al., "Effect of carbon nanotubes on cellular functions in vitro," *Journal of Biomedical Materials Research A*, vol. 91, no. 1, pp. 132–139, 2009.

[21] X. Liu, X. Li, Y. Fan et al., "Repairing goat tibia segmental bone defect using scaffold cultured with mesenchymal stem cells," *Journal of Biomedical Materials Research B: Applied Biomaterials*, vol. 94, no. 1, pp. 44–52, 2010.

[22] X. Wang, Y. Li, J. Wei, and K. De Groot, "Development of biomimetic nano-hydroxyapatite/poly(hexamethylene adipamide) composites," *Biomaterials*, vol. 23, no. 24, pp. 4787–4791, 2002.

[23] W. Jie and L. Yubao, "Tissue engineering scaffold material of nano-apatite crystals and polyamide composite," *European Polymer Journal*, vol. 40, no. 3, pp. 509–515, 2004.

[24] X. Li, L. Wang, Y. Fan, Q. Feng, and F. Cui, "Biocompatibility and toxicity of nanoparticles and nanotubes," *Journal of Nanomaterials*, vol. 2012, Article ID 548389, 19 pages, 2012.

[25] J. Wei, S. J. Heo, D. H. Kim, S. E. Kim, Y. T. Hyun, and J. Shin, "Comparison of physical, chemical and cellular responses to nano- and micro-sized calcium silicate/poly(ε-caprolactone) bioactive composites," *Journal of the Royal Society Interface*, vol. 5, no. 23, pp. 617–630, 2008.

[26] C. C. P. M. Verheyen, J. R. De Wijn, C. A. Van Blitterswijk, and K. De Groot, "Evaluation of hydroxylapatite/poly(L-lactide) composites: mechanical behavior," *Journal of Biomedical Materials Research*, vol. 26, no. 10, pp. 1277–1296, 1992.

[27] K. Leja and G. Lewandowicz, "Polymer biodegradation and biodegradable polymers—a review," *Polish Journal of Environmental Studies*, vol. 19, no. 2, pp. 255–266, 2010.

[28] X. Li, X. Liu, W. Dong et al., "In vitro evaluation of porous poly(L-lactic acid) scaffold reinforced by chitin fibers," *Journal of Biomedical Materials Research B Applied Biomaterials*, vol. 90, no. 2, pp. 503–509, 2009.

[29] L. M. Havill, J. Rogers, L. A. Cox, and M. C. Mahaney, "QTL with pleiotropic effects on serum levels of bone-specific alkaline phosphatase and osteocalcin maps to the baboon ortholog of human chromosome 6p23-21.3," *Journal of Bone and Mineral Research*, vol. 21, no. 12, pp. 1888–1896, 2006.

[30] Q. Li, K. Yu, X. Tian et al., "17beta-Estradiol overcomes human myeloma RPMI8226 cell suppression of growth, ALP activity, and mineralization in rat osteoblasts and improves RANKL/OPG balance in vitro," *Leukemia Research*, vol. 33, no. 9, pp. 1266–1271, 2009.

[31] X. M. Li, Y. Huang, L. S. Zheng et al., "Effect of substrate stiffness on the functions of rat bone marrow and adipose tissue derived mesenchymal stem cells in vitro," *Journal of Biomedical Materials Research A*, vol. 102, no. 4, pp. 1092–1101, 2014.

[32] A. J. Dulgar-Tulloch, R. Bizios, and R. W. Siegel, "Human mesenchymal stem cell adhesion and proliferation in response to ceramic chemistry and nanoscale topography," *Journal of Biomedical Materials Research A*, vol. 90, no. 2, pp. 586–594, 2009.

[33] N. Ribeiro, S. R. Sousa, and F. J. Monteiro, "Influence of crystallite size of nanophased hydroxyapatite on fibronectin and osteonectin adsorption and on MC3T3-E1 osteoblast adhesion and morphology," *Journal of Colloid and Interface Science*, vol. 351, no. 2, pp. 398–406, 2010.

Hindawi Publishing Corporation
International Journal of Polymer Science
Volume 2014, Article ID 439784, 12 pages
http://dx.doi.org/10.1155/2014/439784

Research Article

Surface-Coated Polylactide Fiber Meshes as Tissue Engineering Matrices with Enhanced Cell Integration Properties

Matthias Schnabelrauch,[1] Ralf Wyrwa,[1] Henrike Rebl,[2] Claudia Bergemann,[2] Birgit Finke,[3] Michael Schlosser,[4] Uwe Walschus,[4] Silke Lucke,[4] Klaus-Dieter Weltmann,[3] and J. Barbara Nebe[2]

[1] *Biomaterials Department, INNOVENT e. V., Prüssingstraβe 27B, 07745 Jena, Germany*
[2] *Department of Cell Biology, University Medical Center Rostock, Schillingallee 69, 18057 Rostock, Germany*
[3] *Leibniz-Institute for Plasma Science and Technology e. V. (INP), Felix-Hausdorff-Straβe 2, 17489 Greifswald, Germany*
[4] *Research Group of Predictive Diagnostics, Department of Medical Biochemistry and Molecular Biology, Ernst-Moritz-Arndt University of Greifswald, Greifswalder Straβe 11c, 17495 Karlsburg, Germany*

Correspondence should be addressed to Matthias Schnabelrauch; ms@innovent-jena.de

Received 6 February 2014; Accepted 20 May 2014; Published 15 June 2014

Academic Editor: Nicholas Dunne

Poly(L-lactide-*co*-D/L-lactide)-based fiber meshes resembling structural features of the native extracellular matrix have been prepared by electrospinning. Subsequent coating of the electrospun fibers with an ultrathin plasma-polymerized allylamine (PPAAm) layer after appropriate preactivation with continuous O_2/Ar plasma changed the hydrophobic nature of the polylactide surface into a hydrophilic polymer network and provided positively charged amino groups on the fiber surface able to interact with negatively charged pericellular matrix components. In vitro cell experiments using different human cell types (epithelial origin: gingiva and uroepithelium; bone cells: osteoblasts) revealed that the PPAAm-activated surfaces promoted the occupancy of the meshes by cells accompanied by improved initial cell spreading. This nanolayer is stable in its cell adhesive characteristics also after γ-sterilization. An in vivo study in a rat intramuscular implantation model demonstrated that the local inflammatory tissue response did not differ between PPAAm-coated and untreated polylactide meshes.

1. Introduction

Electrospinning is a long-known polymer processing technique that has received remarkable interest during the last decade for biomedical applications like tissue engineering and drug delivery [1–5]. The technique is applicable to both polymer solutions and melts [6, 7] and enables the fabrication of made-on purpose tissue engineering matrices resembling major structural features of the native extracellular matrix [8, 9]. Polymer meshes resulting from electrospinning are characterized by an interconnective porous network of more or less ordered polymeric fibers with diameters in the range between 3 nm and 2.5 μm. Those artificial matrices are of great interest in tissue reconstruction to act as cell support guiding cell adhesion, proliferation, and differentiation [10, 11]. Both natural polymers like collagen [12, 13], silk [14], or different polysaccharides [15] and synthetic polymers particularly the well-known biodegradable polylactones [16], polyanhydrides [17], or polyurethanes [18] are well suited for processing by this technique.

The principal applicability of electrospun fiber meshes made of artificial polymers like polylactones for cell cultivation purposes has been shown in numerous studies using different cell types including cardiomyocytes [19], smooth muscle cells [20], keratinocytes [21], fibroblasts [22], and osteoblasts [23].

With regard to their use as tissue engineering scaffolds, a drawback of many synthetic polymers is their innate hydrophobicity which often impairs initial protein adsorption and cell adhesion [24]. Different strategies have been proposed to overcome this problem including the synthesis

of block copolymers containing hydrophilic segments [25], the coating of synthetic polymer surfaces by natural polymers like collagen [26], or the attachment of cell adhesion molecules onto the polymer surface [27]. A promising and recently established strategy to improve cellular acceptance of biomaterials like titanium consists in their surface functionalization using allylamine plasma polymerization under nonthermal conditions. In this surface activation method, an ultrathin and relatively stable plasma polymerized allylamine (PPAAm) layer is deposited onto the material surface changing its hydrophobic nature and providing a hydrophilic coverage for adhering cells [28]. Due to incorporated positively charged amino groups, the PPAAm layer enhances the interaction with negatively charged pericellular matrix components, for example, hyaluronan [29]. Recently, basic cell experiments impressively demonstrated that the PPAAm-activated surfaces promoted adhesion of osteoblasts not only on titanium [28] and calcium phosphate ceramics [30] but also on polymer films and fiber meshes [31]. PPAAm induced early steps in the development of intracellular adhesion components, for example, the actin cytoskeleton and paxillin [29], without disturbing the metabolic activity in living cells [32].

Due to capability of electrospinning to create not only plane geometries but also round shaped and tubular ones and due to the flexible and soft nature of electrospun devices, this technique is considered to have a promising potential in soft tissue and vascular engineering. In this study, we aimed to study efficient PPAAm-coating of poly(L-lactide-*co*-D/L-lactide) (PLA) fiber meshes with hydrophilic characteristics varying the plasma pretreatment of the PLA meshes. We furthermore investigated the initial cell adhesion of epithelial cells on PPAAm-coated PLA meshes and studied the influence of γ-sterilization as a validated sterilization process used for implant materials. Finally, we present first in vivo data on the tissue acceptance of these scaffolds.

2. Materials and Methods

2.1. Materials. A poly(L-lactide-co-D/L-lactide) 70/30 (PLA, Resomer LR 708, Boehringer Ingelheim, Germany) with M_w (weight-average molecular weight) = 1.5×10^6 g mol^{-1} (gel permeation chromatography in chloroform with polystyrene as external standard) was used for electrospinning. Allylamine (for synthesis; M = 57.09 g mol^{-1}, 99%, VWR, Darmstadt, Germany) was used as precursor for the plasma polymerization process. All other chemicals were of reagent grade.

2.2. Electrospinning. A custom designed electrospinning apparatus consisting of a high-voltage power supply (ESV-100, Ingenieurbüro Gerhard Fuhrmann, Leverkusen, Germany), an infusion pump, and a 5 mL plastic syringe connected by a 25 cm PTFE tube to a stainless-steel straight-end hollow needle (0.4 mm) was used. A mirror (20 × 20 cm) was used as a collector plate for collecting the electrospun fibers. The needle and the mirror were connected to the ESV-100. The syringe was mounted vertically against the collector, and the sample solution was fed at a constant rate through the syringe to the needle tip. The distance between the needle tip and the mirror was maintained at 18 cm. The voltage applied to the needle was adjusted to 22 kV. A solution (3 wt%) of the polymer in chloroform/methanol (3 : 1 v/v) was employed. The flow rate of the solution was controlled at 1.5 mL h^{-1}, resulting in the formation of fibers with an average diameter of about 1.67 μm.

Table 1: Fiber mesh plasma preactivation process parameters.

Method	Preactivation conditions		
	Gas composition	Flow [sccm]	Plasma impact
0	Without preactivation		
1	O_2	100	Pulsed
2	O_2/Ar	100/25	Pulsed
3	O_2/Ar	50/75	Pulsed
4	O_2/Ar	25/100	Pulsed
5	Ar	100	Pulsed
6	O_2/Ar	100/25	Continued (10 s)

2.3. Fiber Mesh Preactivation. In general, a microwave plasma reactor (500 W, 50 Pa) was used for surface activation of fiber meshes generating pulsed plasma (10 ms on/90 ms off; 50 s gross time = 5 s). Different preactivation conditions were used as given in Table 1.

2.4. PPAAm Coating Process. After the preactivation process polymer meshes were treated without breaking the vacuum in a microwave plasma reactor (V55G Plasma Finish, Schwedt, Germany) in a downstream position (9 cm from the microwave coupling window) with respect to disc-like planar plasma of about 2 cm thickness [28]. The samples were coated by using allylamine as monomer in microwave excited (2.45 GHz, 500 W), low pressure (p = 50 Pa) gas discharge plasma with an effective overall treatment duration of 480 s. Two different process regimes of preactivation have been preferred, namely, preactivation methods number 5 and number 6. For comparison, PPAAm coating was performed without preactivation. Thin layers (<50 nm) of PPAAm were deposited.

2.5. Surface Analytics. The elemental chemical surface composition and chemical binding properties of PPAAm layers on PLA fiber meshes were determined by X-ray photoelectron spectroscopy (XPS) using an AXIS ULTRA spectrometer (Kratos, Manchester, UK). The measurement conditions were described in detail previously [28]. Briefly, the monochromatic Al Kα line at 1486 eV (150 W), implemented charge neutralization, and pass energy of 80 eV were used for estimating the chemical elemental composition and an energy of 10 eV was used for estimating of the highly resolved C1s peaks. Each surface composition value represents an average over three XPS measuring steps on the surface. Primary amino groups were reacted with 4-trifluoromethylbenzaldehyde (TFBA) at 40°C for 2 h in a saturated gas phase to label them for detection [28]. The polar and disperse part of

surface free energy was calculated from measurements of contact angles with different liquids. Water, ethylene glycol, and methylene iodide contact angles were determined with the help of the contact angle measuring system OCA 30 (DataPhysics Instruments GmbH, Germany) by the sessile drop method (using software SCA20). Measurements were always performed within 30 min after sample preparation. The morphology of the meshes has been studied after gold sputtering (coater SCD 004, BAL-TEC, Balzers, Lichtenstein) using the scanning electron microscope DSM 960A (Carl Zeiss, Oberkochen, Germany).

2.6. Cell Cultivation. Human gingiva epithelial cells (Ca9-22, HSRRB, TKG 0485, NIBIO, Osaka, Japan), human uroepithelial cells (SV40-HUC-1, ATCC, CRL-9520, LGC Promochem, Wesel, Germany), and human MG-63 osteoblastic cells (cell line, ATCC, No. CRL-1427, LGC Promochem) were seeded onto untreated and PPAAm-coated (preactivated with method 6, continuous O_2/Ar plasma) fiber meshes with a density of 1×10^5 cells cm^{-2} and cultured in Dulbecco's modified Eagle medium (DMEM, Invitrogen, Carlsbad, USA) with 10% fetal calf serum (FCS Gold, PAA Laboratories, Pasching, Austria) or serum free for MG-63 cells [28] and 1% gentamicin (Ratiopharm, Ulm, Germany) at 37°C in a humidified atmosphere with 5% CO_2 for 0.5 and 24 h to analyze morphology and spreading.

2.7. Cell Spreading. Epithelial cells were trypsinized (0.05% trypsin, 0.02% EDTA, Sigma) at 37°C for 3 min, washed in PBS, and stained with the red fluorescent linker PKH26 (PKH26 General Cell Linker Kit, Sigma-Aldrich, St. Louis, MO, USA) for 5 min in suspension. The vital, membrane stained cells were then seeded onto the fiber meshes and cultured for 0.5 and 24 h. After fixation with 4% paraformaldehyde (Merck, Darmstadt, Germany), the cells were embedded with a cover slip. The microscopical examinations were performed on the inverted confocal laser scanning microscope LSM 410 (Carl Zeiss, Jena, Germany) equipped with a He-Ne laser (excitation 543 nm) and the 63x water objective (1.25/0.17, Carl Zeiss). The size of the images was 512 × 512 pixels. Spreading (cell area in μm^2) of 40 cells/specimen was measured using the software "area measurement" of the confocal microscope LSM 410.

2.8. Cell Morphology. The cell morphology on the fiber meshes was investigated using a scanning electron microscope DSM 960A (Carl Zeiss, Oberkochen, Germany). For cell analyses, cells were grown for 0.5 and 24 h, fixed with 4% glutaraldehyde (24 h), and dehydrated in a vacuum dryer (10×10^{-3} mbar, Plano, Wetzlar, Germany). Gold sputtering was performed with the coater (SCD 004, BAL-TEC, Balzers, Lichtenstein). Due to the bulging of the meshes during this drying process, the pictures were taken from different angles (up to 40°). This allowed us to visualize the interlocking of the cells and the substrate.

2.9. Sterilization Procedure. Untreated and PPAAm-coated meshes were γ-sterilized with Cobalt-60 (minimal irradiation dose 25 kGy, Synergy Health Radeberg, Germany).

2.10. In Vivo Study. The local inflammatory tissue response was examined following simultaneous implantation of pieces (size 5 × 5 mm) of untreated and PPAAm-coated electrospun PLA meshes into the neck musculature of 24 male Lewis rats (age, 100 days; mean weight, 395 ± 13 g). After 7, 14, and 56 days, tissue samples containing the PLA meshes were collected from 8 randomly selected animals, and cryosections (5 μm) were prepared with a Cryotome 2800 Frigocut N (Reichert-Jung, Nuβloch, Germany). CD68-positive total monocytes and macrophages as well as CD163-positive tissue macrophages were immunohistochemically labelled using the monoclonal antibodies ED1 and ED2, respectively (MorphoSys AbD Serotec, Duesseldorf, Germany). The alkaline phosphatase/anti-alkaline phosphatase detection system (APAAP; DakoCytomation, Hamburg, Germany) with the colorimetric phosphatase substrate New Fuchsin was used to visualize bound primary ED1 and ED2 antibodies. Morphometric evaluation was performed with ImageJ software (U.S. National Institutes of Health, Bethesda, Maryland, USA) by quantification as percentage of positively stained area.

3. Results and Discussion

Fiber meshes of biodegradable PLA were fabricated by electrospinning from chloroform/methanol solvent mixtures, and after preactivation of the fiber surface, they were covered with ultrathin PPAAm coating as schematically shown in Figure 1.

As an important task, the conditions of plasma treatment have to be carefully adjusted paying particular attention to the fragility of nanofiber meshes and their thermal sensitivity.

3.1. PLA Fiber Mesh Preactivation. Prior to PPAAm coating, the prepared PLA fiber meshes were preactivated by plasma treatment varying the gas composition and the gas flow in the plasma reactor to establish optimum conditions for the subsequent PPAAm coating.

The values of the contact angles of electrospun meshes measured after different preactivation conditions are compared in Figure 2. As expected, the untreated PLA meshes possess a hydrophobic surface. Whereas in pure argon plasma the contact angle is only slightly changed, pure oxygen plasma drops down the contact angle to 0° indicating strong hydrophilization of the surface. Mixed O_2/Ar plasma atmospheres also lead to considerably more hydrophilic surfaces. It was an important aim to perform very mild plasma activation of the PLA surface to avoid any changes or damage of the fiber meshes.

A suitable analytical method to study the surface composition and uniformity of the PLA fibers is XPS possessing an analytical depth of about 10 nm. Figure 3 shows the elemental content for untreated (PLA) and preactivated fiber meshes found by XPS measurements. It can be seen that short-term, pulsed plasma treatment (effective treatment = 5 s) under variation of the O_2/Ar flow and continuous plasma treatment (method number 6) result only in a slight change of the C/O elemental composition. Thus, the influence of

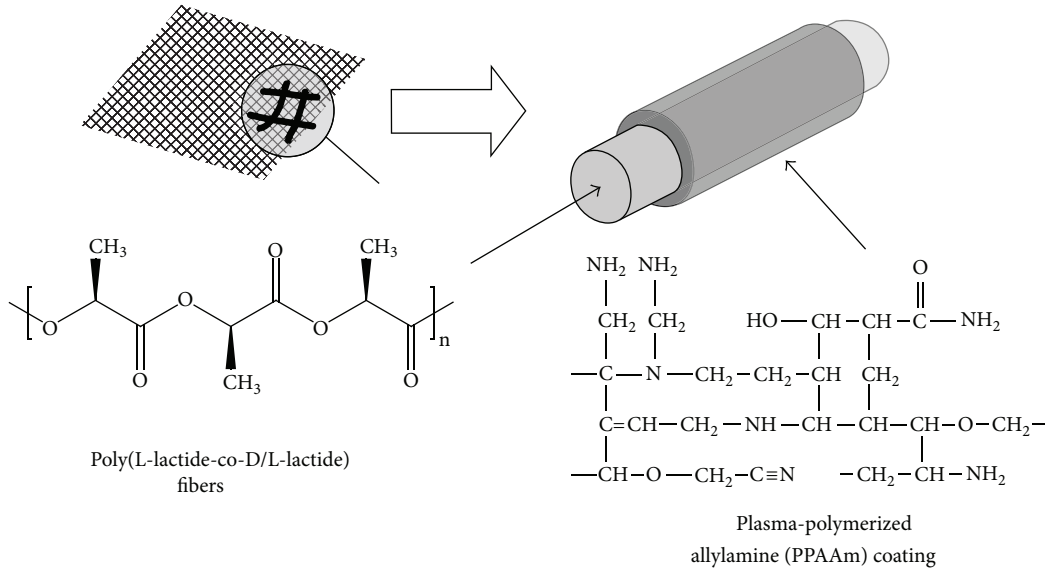

Figure 1: Schematic illustration of surface-coated fiber meshes.

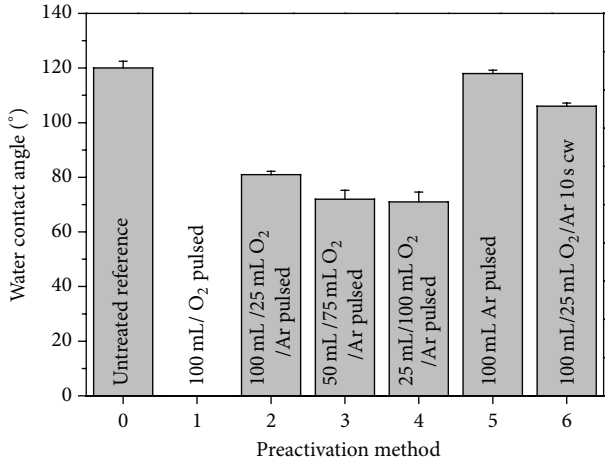

Figure 2: Water contact angles of fiber meshes measured after different preactivation conditions (for the numbering of preactivation methods, refer to Table 1).

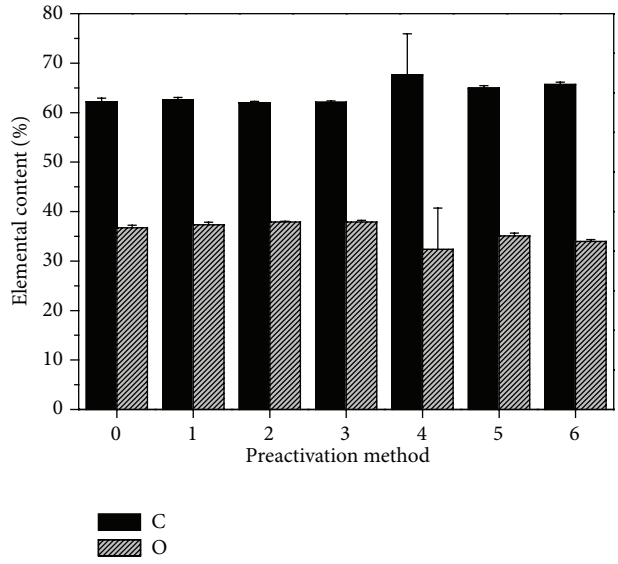

Figure 3: XPS investigations of untreated and plasma preactivated PLA fiber meshes.

the preactivation method on the surface composition is only marginal.

3.2. PPAAm Coating. Based on the results of fiber mesh preactivation, PPAAm coating with allylamine as monomer was performed in a microwave reactor without preactivation and after preactivation methods number 5 and number 6, respectively. Reaction conditions of the plasma polymerization were chosen in such a way that both homogeneous PPAAm coating on the PLA surface with a thickness of about 30 nm [28] was obtained and no surface alterations of the temperature sensitive fiber mesh could be observed.

As already shown on titanium [28] and schematically depicted in Figure 1 for PLA fibers, the deposited PPAAm coating formed a highly cross-linked polymer network containing nitrogen and oxygen functional groups, particularly primary, secondary, and tertiary amino groups.

Figure 4 (left row) shows SEM images of the fabricated porous electrospun fiber matrix with a thickness of 40 μm and a mean fiber diameter of 1.67 μm. The corresponding PPAAm surface-coated fiber meshes are exhibited in the right column of Figure 4 illustrating that the microscopic fiber structure generated by electrospinning was not changed or even damaged by plasma polymerization.

In Figures 5(a) and 5(b), the water contact angles and the surface energies of the PPAAm-coated fiber mesh surfaces obtained after preactivation methods number 5 and number

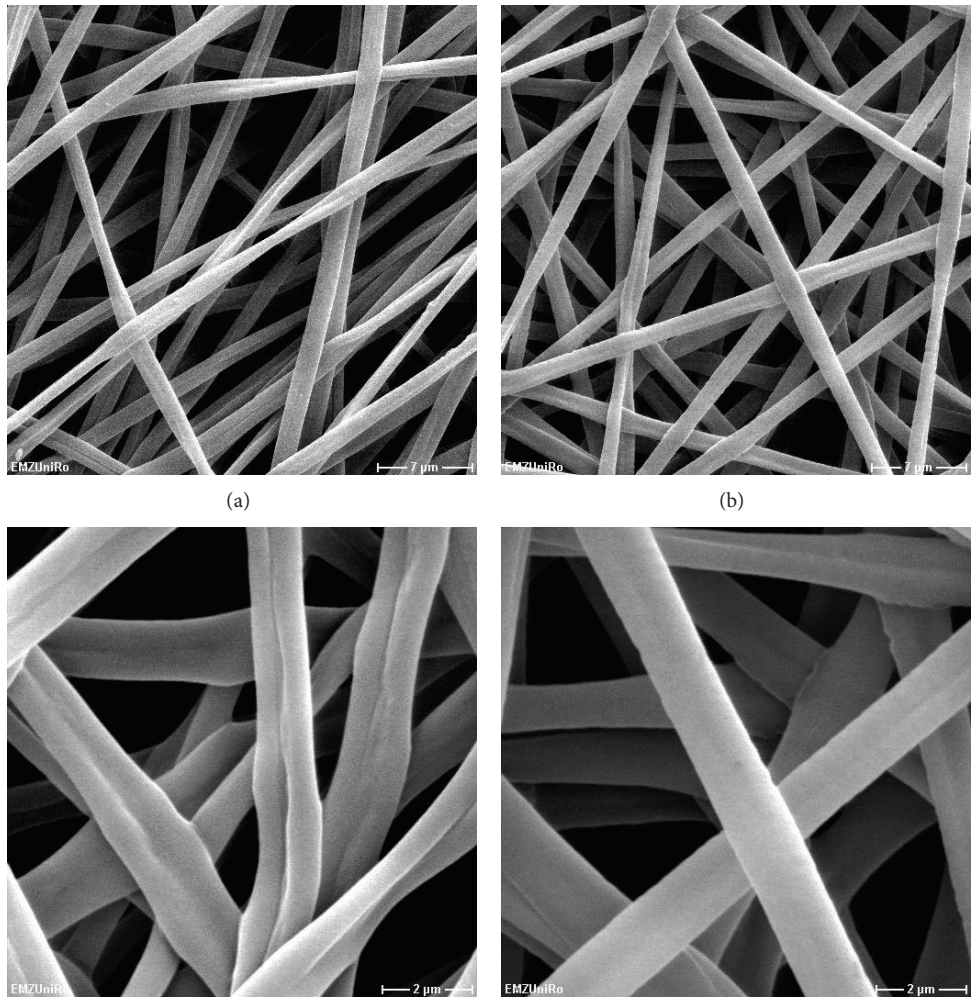

Figure 4: SEM images of untreated (left) and PPAAm-coated (right) electrospun PLA meshes (different magnification, upper row: ×3000, bar = 7 μm; lower row: ×10 000, bar = 2 μm).

6 and without preactivation, respectively, are shown. In comparison to the PPAAm-coated PLA surface without preactivation possessing a hydrophobic surface (contact angle > 100°), the PPAAm-coated fiber meshes, fabricated with mild preactivation, show the desired hydrophilic surfaces with contact angles < 50° (Figure 5(a)). A somewhat lower water contact angle was found for the PPAAm-treated mesh preactivated by a continuous plasma treatment (method number 6).

The total surface energies measured for the three PPAAm-coated fiber meshes ranged between 58 and 78 mN/m (Figure 5(b)) illustrating an increase of the polar component of the surface energy from the fiber mesh without preactivation (method number 0) to the mesh preactivated by the pulsed plasma treatment (method number 5) and continued to the mesh preactivated by method number 6 (continuous plasma treatment). It could be shown that in comparison to an untreated surface mild preactivation of the PLA surface is necessary to provide a sufficient number of positively charged polar groups on the PPAAm-coated fibers to ensure cell adhesion and proliferation.

Again, XPS was used to examine the surface composition and uniformity of the PLA fibers before and after PPAAm coating. Results are shown in Figure 6. After PPAAm coating, the PLA surface was completely covered by PPAAm characterized by the incorporation of nitrogen in all samples. It can be seen that the preactivation of the PLA fiber meshes by methods 5 and 6, respectively, leads to a decrease of the oxygen content and simultaneously to an increase of the nitrogen content (N/O ratio of 1.8% for samples without preactivation versus N/O ratio of 4-5% for preactivated samples) by the deposition of a closed and thicker PPAAm film. After TFBA derivatization of the fiber meshes, which exclusively occurs at the primary amino groups of the coated fiber surface, a higher fluorine content was found for the preactivated PPAAm-coated PLA meshes. The amino group density NH_2/C could be determined between 2% for the nonpretreated and 2.5% for the pretreated fiber meshes. Preactivation of the fiber

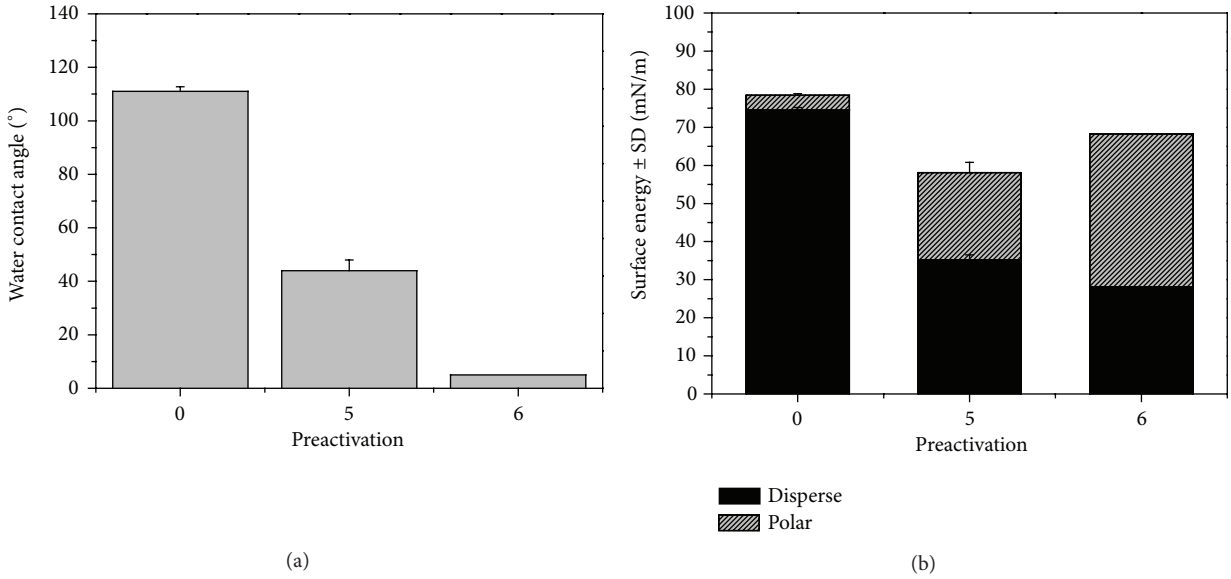

Figure 5: Water contact angles (a) and surface energies (b) of PPAAm-coated fiber meshes after fiber preactivation by methods number 5 and number 6, respectively, compared to the PPAAm-coated fiber meshes without preactivation (number 0) ($n = 5$).

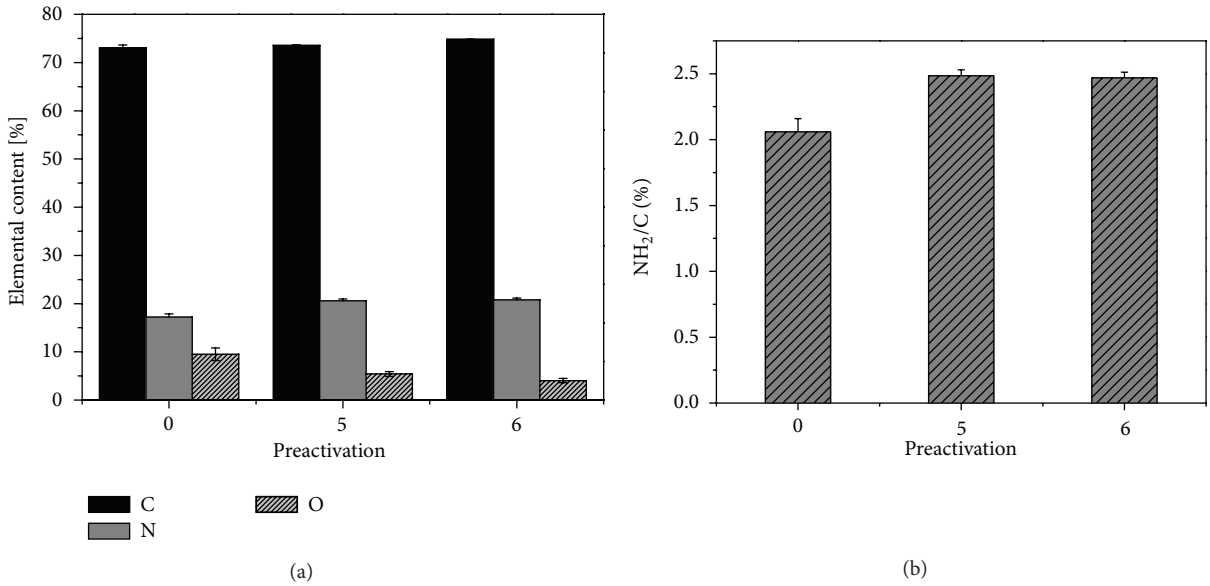

Figure 6: XPS investigations ((a) elemental composition and (b) NH_2/C ratio) of PPAAm-coated PLA fiber meshes without plasma preactivation and with plasma preactivation (methods 5 and 6), respectively.

meshes is especially necessary for a better thin film deposition by the plasma polymerization process. For all in vitro and in vivo experiments, we utilized the PPAAm functionalized PLA fiber mesh after preactivation with method number 6 (continuous O_2/Ar plasma) due to the water contact angle (see Figure 5).

3.3. Investigations on Cell Spreading. Both human gingiva epithelial cells (Ca9-22) and human uroepithelial cells (SV40-HUC-1) showed firm adhesion on PLA and PPAAm-coated fiber meshes. Time-dependent spreading is illustrated in Table 2 comparing the corresponding cell areas (in μm^2) after 0.5 and 24 h of cell seeding. As previously described for the MG-63 osteoblastic cells [31], both epithelial cell lines formed larger cell areas on PPAAm-coated PLA mesh surfaces compared to untreated PLA. For the SV40-HUC-1 cells (Figure 7), this effect was more pronounced up to 24 h, whereas in the case of Ca9-22 (Figure 8) the increase in cell areas was only visible after 0.5 h but in the same range for 24 h.

The morphology of the cells during the adhesion process has also been studied by SEM. In Figure 7, it can be impressively seen how spreading of SV40-HUC-1 uroepithelial

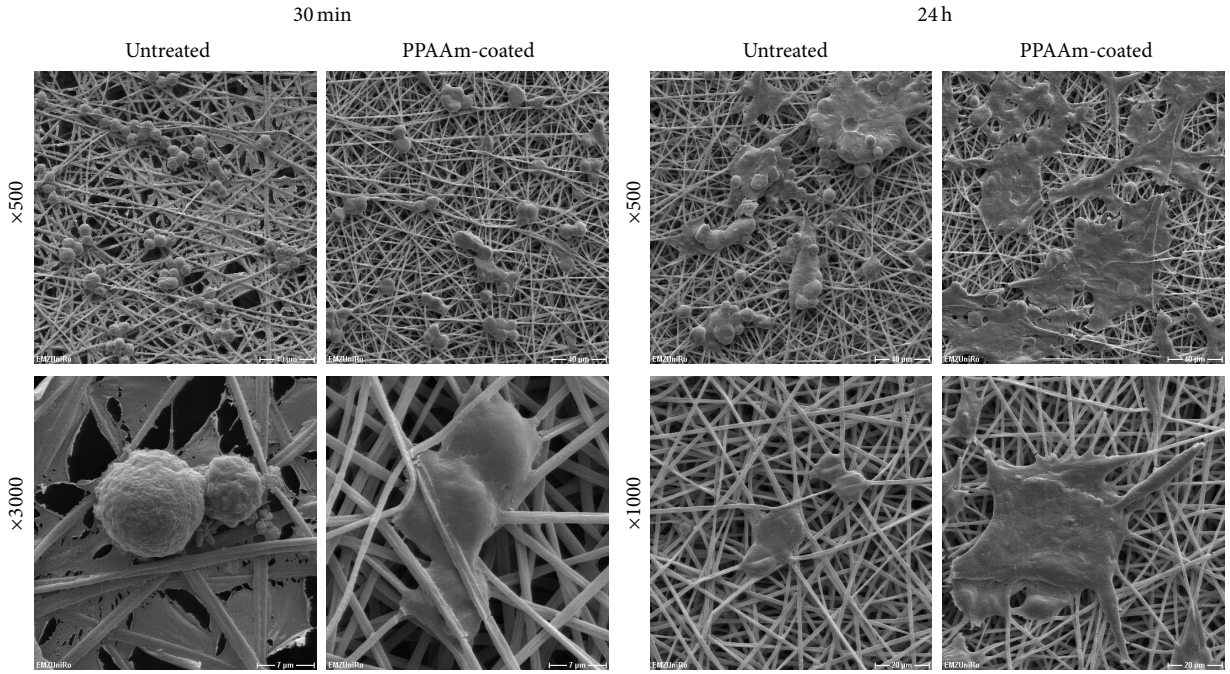

Figure 7: SEM images showing spreading of SV40-HUC-1 uroepithelial cells on untreated and PPAAm-coated PLA fiber meshes after 0.5 and 24 h (bar = 40 μm (upper row), 20 μm (lower row, right images), and 7 μm (lower row, left images)).

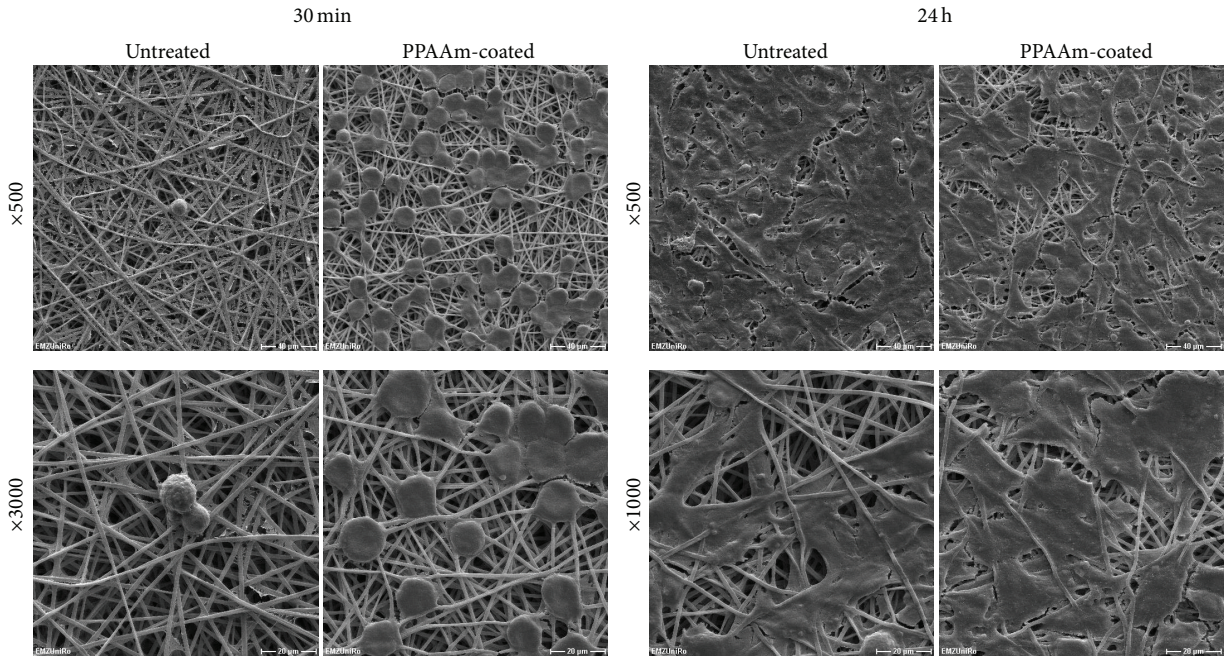

Figure 8: SEM images showing spreading of Ca9-22 human gingiva epithelial cells on untreated and PPAAm-coated PLA fiber meshes after 0.5 and 24 h (bar = 40 μm (upper row) and 20 μm (lower row)).

cells on PLA fiber mesh structure is supported by plasma treatment with PPAAm, particularly in the initial phase of cell adhesion. The same behaviour is found for Ca9-22 human gingiva epithelial cells in the first phase of occupation (Figure 8).

Overall, these preliminary cell spreading experiments confirm the adhesive capacity of PPAAm coating not only for titanium and calcium phosphate materials as previously observed [28, 30] but also for polymers in form of microfibers. Epithelial cells profit by the positively charged

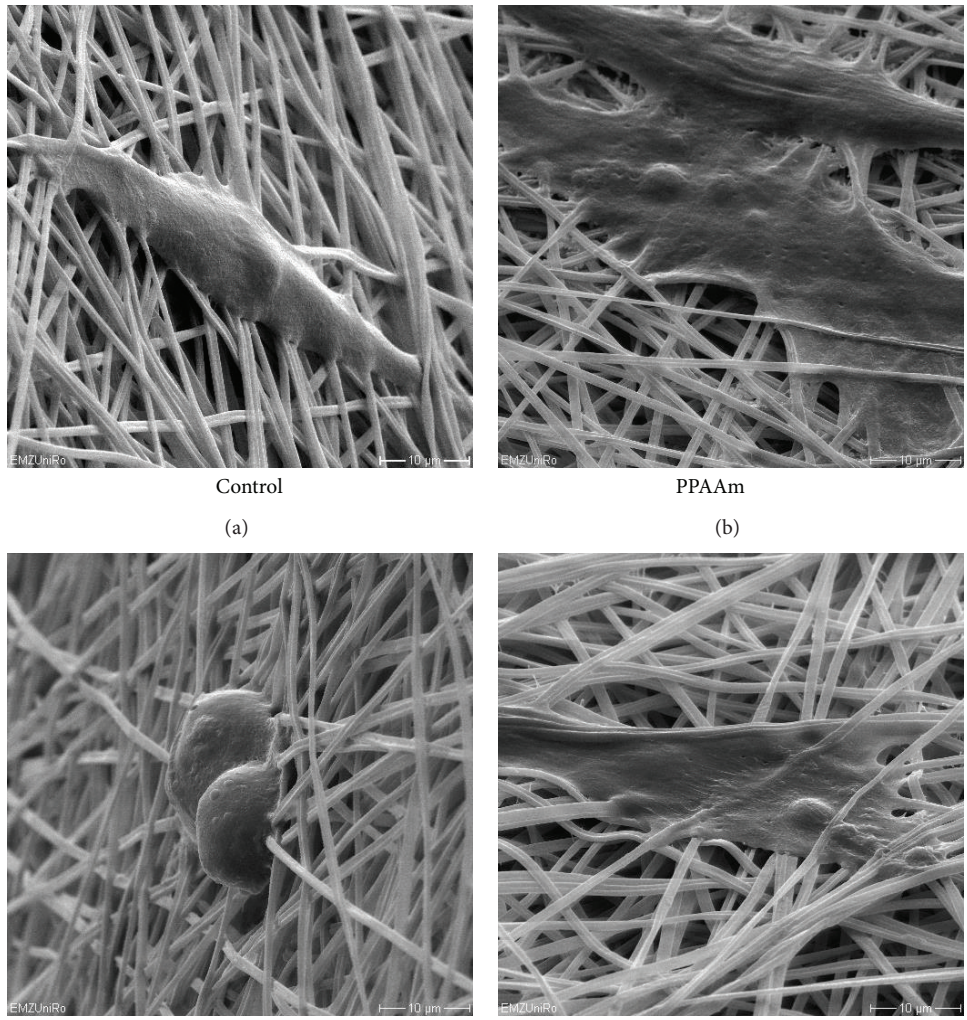

Figure 9: SEM images of test cells (MG-63) growing for 24 h on untreated and PPAAm-coated PLA meshes before (upper row) and after γ-sterilization (lower row). Note that the process of sterilization did not disturb the spreading promoting effect of PPAAm inside the mesh (right, below).

Table 2: Cell spreading of SV40-HUC-1 uroepithelial cells and Ca9-22 gingiva cells on untreated and PPAAm-coated PLA meshes after 0.5 and 24 h ($n = 40$; $^{**}P < 0.01$; $^{***}P < 0.001$; unpaired t-test).

Cell spreading (μm^2)		Untreated	PPAAm-coated
SV40-HUC-1	**30 min**	109.0 ± 30.4	137.8 ± 25.6***
	24 h	158.4 ± 31.2	186.1 ± 37.9**
Ca9-22	**30 min**	213.5 ± 46.8	288.3 ± 66.7***
	24 h	315.8 ± 86.4	315.6 ± 81.8

$^{**}P < 0.01$ versus untreated; $^{***}P < 0.001$ versus untreated (mean ± SD; $n = 40$; unpaired t-test).

surface and were qualified to rapidly accept the intrinsically hydrophobic biomaterial surface.

3.4. Investigation of Cell Spreading on Sterilized Fiber Meshes. For clinical applications of the PLA meshes, it is necessary to establish a possible sterilization process. We identified γ-sterilization as a feasible sterilization method for these PPAAm-coated PLA meshes. In Figure 9, it is demonstrated that γ-sterilization has no influence on the characteristics of the PPAAm nanolayer, which can be seen on the MG-63 cell's capability to spread out quickly on the PPAAm coating.

3.5. In Vivo Study. In a first in vivo study, both untreated electrospun PLA meshes and PPAAm-coated meshes (pre-activated by method number 6) were implanted intramuscularly into Lewis rats to investigate the local inflammatory response. The results after 7, 14, and 56 days following implantation in the peri-implant tissue and implant-infiltrating

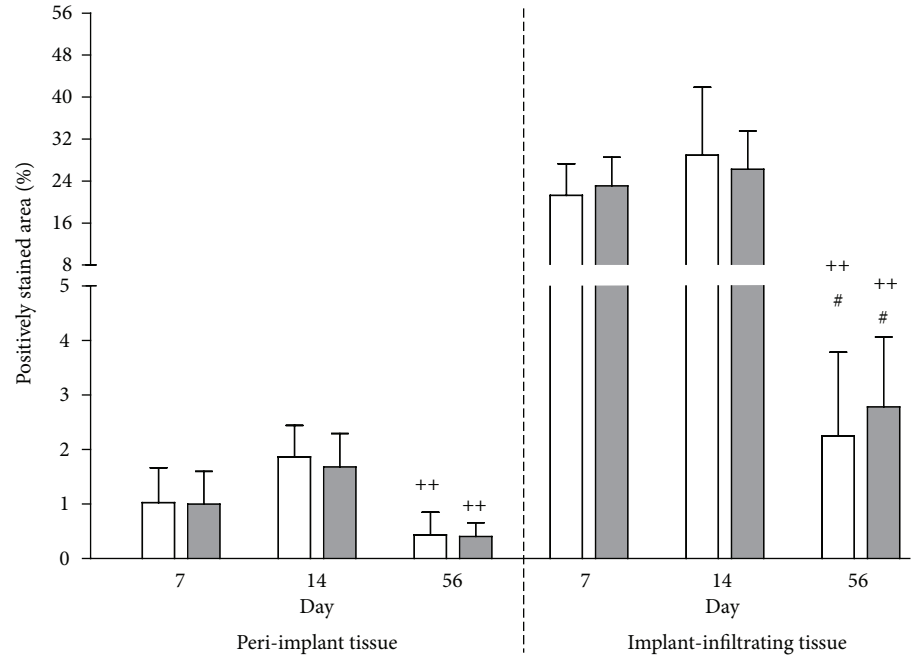

Figure 10: Local inflammatory reaction measured as tissue section area positively stained by CD68-positive total monocytes and macrophages in the peri-implant tissue and implant-infiltrating tissue following i.m. implantation of untreated electrospun PLA meshes (white columns) or PPAAm-coated meshes (gray columns) after 7, 14, and 56 days in Lewis rats. Columns represent the mean and error bars represent the standard deviation of 8 rats per experimental day. Hash symbols (#) indicate a significant difference ($P < 0.05$) versus day 7, and plus symbols (+) indicate a significant difference ($P < 0.01$) versus day 14 (Wilcoxon rank-sum test).

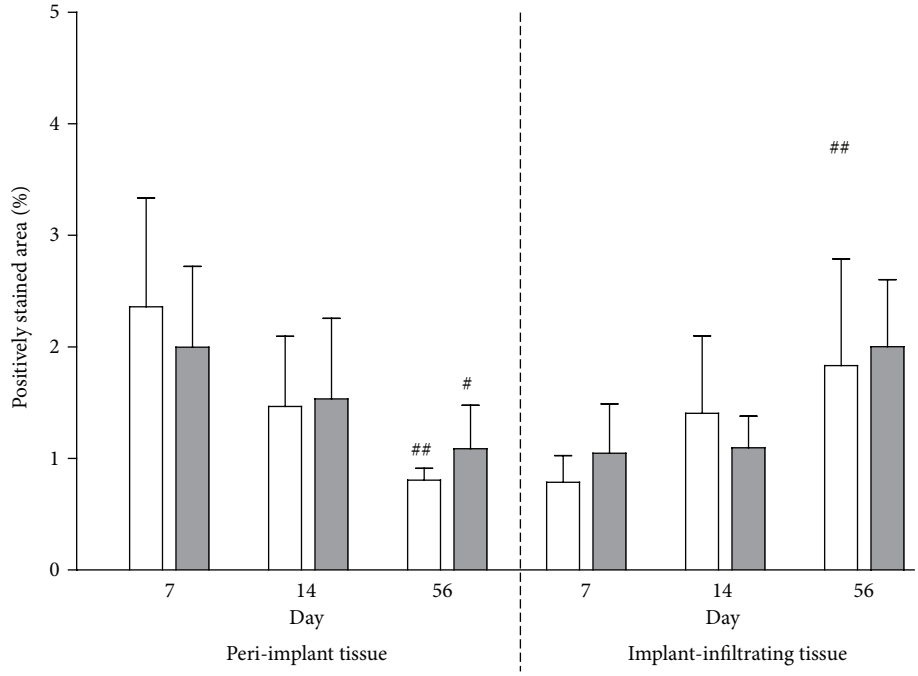

Figure 11: Local inflammatory reaction measured as tissue section area positively stained in immunohistochemistry by CD163-positive tissue macrophages in the peri-implant tissue and implant-infiltrating tissue following i.m. implantation of untreated electrospun PLA meshes (white columns) or PPAAm-coated meshes (gray columns) after 7, 14, and 56 days in Lewis rats. Columns represent the mean, and error bars represent the standard deviation of 8 rats per experimental day. Hash symbols (#) indicate a significant difference ($^{\#}P < 0.05$; $^{\#\#}P < 0.01$) versus day 7 (Wilcoxon rank-sum test).

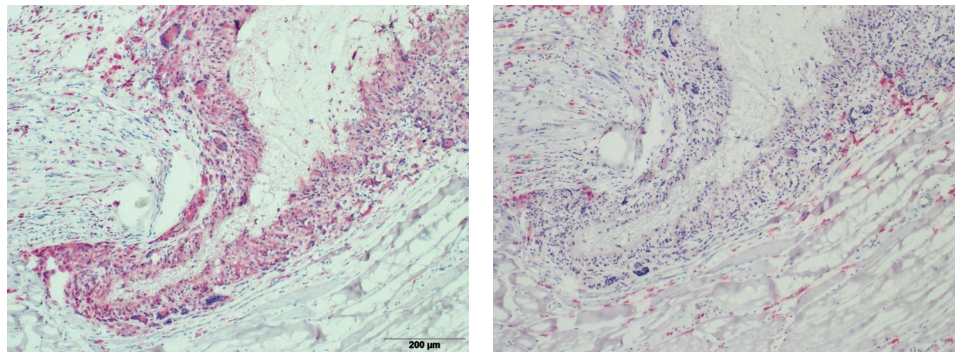

(a) (b)

Figure 12: Exemplary immunohistochemical images for staining of CD68-positive total monocytes and macrophages (ED1, left) and CD163-positive tissue macrophages (ED2, right) from experimental day 14 for an untreated PLA mesh sample.

tissue are given for the CD68-positive total monocytes and macrophages in Figure 10 and for the CD163-positive tissue macrophages in Figure 11.

The local inflammatory reaction of CD68-positive monocytes and macrophages did not differ between the untreated and the PPAAm-coated meshes on any experimental day and decreased significantly for both mesh types after day 14, consistent with a change from an acute to a chronic phase of inflammation.

Particularly on days 7 and 14 for both mesh types, the inflammatory response within the implant-infiltrating tissue was 10- to 20-fold higher than in the peri-implant tissue ($P = 0.0078$). Similar to the CD68-positive monocytes and macrophages, there was no significant difference between both mesh types on any experimental day for the CD163-positive tissue macrophages. In the peri-implant tissue, a significant decrease was observed over time (day 56 versus day 7) for both meshes, accompanied by a significant increase in the implant-infiltrating tissue for the uncoated meshes but not for the PPAAm-coated meshes. These observations are also in accordance with a shift from acute to chronic inflammation. In the peri-implant tissue, the response of CD68-positive monocytes and macrophages and CD163-positive tissue macrophages was comparable over the study course, indicating that these macrophages were predominantly tissue macrophages. In contrast, there were about 10-fold more CD68-positive monocytes and macrophages than CD163-positive tissue macrophages on days 7 and 14 in the implant-infiltrating tissue, suggesting an early influx of macrophages into this tissue area. Examples of immunohistochemical images for staining of CD68-positive total monocytes and macrophages and CD163-positive tissue macrophages from experimental day 14 for an untreated PLA mesh sample are shown in Figure 12.

Overall, the results from the histological examination demonstrate that the PPAAm-coated meshes were comparable to the untreated meshes regarding the local inflammatory tissue response. Our long-term experiments in rats up to six weeks recently revealed that this PPAAm nanolayer on titanium alloys induced bone growth and improved the bone-to-implant contact area decisively [33].

4. Conclusions

In this study, a plasma polymerization process using allylamine monomer was adapted to cover the fiber surfaces of electrospun meshes prepared from PLA. Efficient preactivation conditions for the fiber meshes before PPAAm coating have been established, and method number 6 (O_2/Ar = 100/25 mL, continuous wave 10 s) was favored for in vitro and in vivo experiments. The PPAAm coating did not affect the fragile microstructure of the fiber mesh preserving the advantageous structural properties of these materials with regard to their use in tissue engineering. The PPAAm coating providing free amino groups on the fiber surface led to a drastic change of the hydrophobic nature of PLA meshes into a hydrophilic polymer network as shown by contact angle measurements. In vitro cell experiments using human gingiva epithelial cells (Ca9-22), human uroepithelial cells (SV40-HUC-1), and MG-63 cells confirmed an improved cell spreading on positively charged, amino group-containing PPAAm surfaces already after 0.5 h of incubation. In addition, cells melt into these conditioned meshes. The γ-sterilization process did not hamper these findings. First in vivo data on the biocompatibility of PPAAm-modified polylactide meshes demonstrated that the coating has no influence on the local inflammatory reaction. For both PPAAm-coated and untreated mesh types, the time course of the examined local inflammatory reactions was generally characterized by a change from acute to chronic state as established for implantation-related inflammation. Furthermore, the response was stronger in the implant-infiltrating tissue than in the peri-implant tissue, indicating that these inflammatory processes were localized to the implant site without far-reaching effects into distant tissue areas.

Based on these results, the plasma-assisted attachment of positively charged amino groups onto biodegradable synthetic polymer mesh surfaces represents a promising

approach to improve the cellular acceptance of these materials.

Conflict of Interests

The authors declare that there is no conflict of interests regarding the publication of this paper.

Acknowledgments

Birgit Finke, Henrike Rebl, and Uwe Walschus kindly acknowledge the support of the BMBF German Pilot Program Campus PlasmaMed (Subproject PlasmaImp, 13N9775, 13N9779, 13N11188, and 13N11183). M. Schnabelrauch and R. Wyrwa (INNOVENT) thank the German Federal Ministry of Economics for financial support (INNO-KOM-Ost, MF110109). The authors appreciate technical support of U. Kellner, G. Friedrichs, U. Lindemann, R. Ihrke (INP Greifswald), K. Tornow (University of Greifswald), J. Wenzel, and J. Wetzel (University Medical Center Rostock) and the Electron Microscopy Center of the University of Rostock.

References

[1] T. J. Sill and H. A. von Recum, "Electrospinning: applications in drug delivery and tissue engineering," *Biomaterials*, vol. 29, no. 13, pp. 1989–2006, 2008.

[2] S. Agarwal, J. H. Wendorff, and A. Greiner, "Progress in the field of electrospinning for tissue engineering applications," *Advanced Materials*, vol. 21, no. 32-33, pp. 3343–3351, 2009.

[3] B. M. Baker, A. M. Handorf, L. C. Ionescu, W.-J. Li, and R. L. Mauck, "New directions in nanofibrous scaffolds for soft tissue engineering and regeneration," *Expert Review of Medical Devices*, vol. 6, no. 5, pp. 515–532, 2009.

[4] W. Liu, S. Thomopoulos, and Y. Xia, "Electrospun nanofibers for regenerative medicine," *Advanced Healthcare Materials*, vol. 1, no. 1, pp. 10–25, 2012.

[5] A. J. Meinel, O. Germershaus, T. Luhmann, H. P. Merkle, and L. Meinel, "Electrospun matrices for localized drug delivery: current technologies and selected biomedical applications," *European Journal of Pharmaceutics and Biopharmaceutics*, vol. 81, no. 1, pp. 1–13, 2012.

[6] Z.-M. Huang, Y.-Z. Zhang, M. Kotaki, and S. Ramakrishna, "A review on polymer nanofibers by electrospinning and their applications in nanocomposites," *Composites Science and Technology*, vol. 63, no. 15, pp. 2223–2253, 2003.

[7] D. H. Reneker, A. L. Yarin, E. Zussman, and H. Xu, "Electrospinning of nanofibers from polymer solutions and melts," *Advances in Applied Mechanics*, vol. 41, pp. 43–346, 2007.

[8] W.-E. Teo, W. He, and S. Ramakrishna, "Electrospun scaffold tailored for tissue-specific extracellular matrix," *Biotechnology Journal*, vol. 1, no. 9, pp. 918–929, 2006.

[9] A. Szentivanyi, T. Chakradeo, H. Zernetsch, and B. Glasmacher, "Electrospun cellular microenvironments: understanding controlled release and scaffold structure," *Advanced Drug Delivery Reviews*, vol. 63, no. 4, pp. 209–220, 2011.

[10] Z. Ma, M. Kotaki, R. Inai, and S. Ramakrishna, "Potential of nanofiber matrix as tissue-engineering scaffolds," *Tissue Engineering*, vol. 11, no. 1-2, pp. 101–109, 2005.

[11] S. P. Zhong, Y. Z. Zhang, and C. T. Lim, "Tissue scaffolds for skin wound healing and dermal reconstruction," *Wiley Interdisciplinary Reviews: Nanomedicine and Nanobiotechnology*, vol. 2, no. 5, pp. 510–525, 2010.

[12] J. A. Matthews, G. E. Wnek, D. G. Simpson, and G. L. Bowlin, "Electrospinning of collagen nanofibers," *Biomacromolecules*, vol. 3, no. 2, pp. 232–238, 2002.

[13] D. B. Khadka and D. T. Haynie, "Protein- and peptide-based electrospun nanofibers in medical biomaterials," *Nanomedicine: Nanotechnology, Biology, and Medicine*, vol. 8, no. 8, pp. 1242–1262, 2012.

[14] X. Zhang, M. R. Reagan, and D. L. Kaplan, "Electrospun silk biomaterial scaffolds for regenerative medicine," *Advanced Drug Delivery Reviews*, vol. 61, no. 12, pp. 988–1006, 2009.

[15] K. Y. Lee, L. Jeong, Y. O. Kang, S. J. Lee, and W. H. Park, "Electrospinning of polysaccharides for regenerative medicine," *Advanced Drug Delivery Reviews*, vol. 61, no. 12, pp. 1020–1032, 2009.

[16] E. Piskin, N. Bölgen, S. Egri, and I. A. Isoglu, "Electrospun matrices made of poly(α-hydroxy acids) for medical use," *Nanomedicine*, vol. 2, no. 4, pp. 441–457, 2007.

[17] Q. Su, A. Zhao, H. Peng, and S. Zhou, "Preparation and characterization of biodegradable electrospun polyanhydride nano/microfibers," *Journal of Nanoscience and Nanotechnology*, vol. 10, no. 10, pp. 6369–6375, 2010.

[18] S. A. Guelcher, "Biodegradable polyurethanes: synthesis and applications in regenerative medicine," *Tissue Engineering B: Reviews*, vol. 14, no. 1, pp. 3–17, 2008.

[19] X. Zong, H. Bien, C.-Y. Chung et al., "Electrospun fine-textured scaffolds for heart tissue constructs," *Biomaterials*, vol. 26, no. 26, pp. 5330–5338, 2005.

[20] X. M. Mo, C. Y. Xu, M. Kotaki, and S. Ramakrishna, "Electrospun P(LLA-CL) nanofiber: a biomimetic extracellular matrix for smooth muscle cell and endothelial cell proliferation," *Biomaterials*, vol. 25, no. 10, pp. 1883–1890, 2004.

[21] M. Gümüşderelioglu, S. Dalkiranoğlu, R. S. T. Aydin, and S. Çakmak, "A novel dermal substitute based on biofunctionalized electrospun PCL nanofibrous matrix," *Journal of Biomedical Materials Research A*, vol. 98, no. 3, pp. 461–472, 2011.

[22] P. J. Kluger, R. Wyrwa, J. Weisser et al., "Electrospun poly(d/l-lactide-co-l-lactide) hybrid matrix: a novel scaffold material for soft tissue engineering," *Journal of Materials Science: Materials in Medicine*, vol. 21, no. 9, pp. 2665–2671, 2010.

[23] A. S. Badami, M. R. Kreke, M. S. Thompson, J. S. Riffle, and A. S. Goldstein, "Effect of fiber diameter on spreading, proliferation, and differentiation of osteoblastic cells on electrospun poly(lactic acid) substrates," *Biomaterials*, vol. 27, no. 4, pp. 596–606, 2006.

[24] S. Wang, W. Cui, and J. Bei, "Bulk and surface modifications of polylactide," *Analytical and Bioanalytical Chemistry*, vol. 381, no. 3, pp. 547–556, 2005.

[25] D.-J. Yang, L.-F. Zhang, L. Xu, C.-D. Xiong, J. Ding, and Y.-Z. Wang, "Fabrication and characterization of hydrophilic electrospun membranes made from the block copolymer of poly(ethylene glycol-co-lactide)," *Journal of Biomedical Materials Research A*, vol. 82, no. 3, pp. 680–688, 2007.

[26] Z.-Q. Feng, H.-J. Lu, M. K. Leach et al., "The influence of type-I collagen-coated PLLA aligned nanofibers on growth of blood outgrowth endothelial cells," *Biomedical Materials*, vol. 5, no. 6, Article ID 065011, 2010.

[27] T. G. Kim and T. G. Park, "Biomimicking extracellular matrix: cell adhesive RGD peptide modified electrospun poly(D,L-lactic-co-glycolic acid) nanofiber mesh," *Tissue Engineering*, vol. 12, no. 2, pp. 221–233, 2006.

[28] B. Finke, F. Luethen, K. Schroeder et al., "The effect of positively charged plasma polymerization on initial osteoblastic focal adhesion on titanium surfaces," *Biomaterials*, vol. 28, no. 30, pp. 4521–4534, 2007.

[29] J. B. Nebe and F. Lüthen, "Integrin- and hyaluronan-mediated cell adhesion on titanium," in *Metallic Biomaterial Interactions*, J. Breme, C. J. Kirkpatrick, and R. Thull, Eds., pp. 179–182, Wiley-VCH, Weinheim, Germany, 2008.

[30] J. B. Nebe, M. Cornelsen, A. Quade et al., "Osteoblast behavior in vitro in porous calcium phosphate composite scaffolds, surface activated with a cell adhesive plasma polymer layer," *Materials Science Forum*, vol. 706-709, pp. 566–571, 2012.

[31] R. Wyrwa, B. Finke, H. Rebl et al., "Design of plasma surface-activated, electrospun polylactide non-wovens with improved cell acceptance," *Advanced Engineering Materials*, vol. 13, no. 5, pp. B165–B171, 2011.

[32] H. Rebl, B. Finke, K. Schroeder, and J. B. Nebe, "Time-dependent metabolic activity and adhesion of human osteoblast-like cells on sensor chips with a plasma polymer nanolayer," *International Journal of Artificial Organs*, vol. 33, no. 10, pp. 738–748, 2010.

[33] C. Gabler, C. Zietz, R. Göhler et al., "Evaluation of osseointegration of titanium alloyed implants modified by plasma polymerization," *International Journal of Molecular Sciences*, vol. 15, no. 2, pp. 2454–2464, 2014.

Hindawi Publishing Corporation
International Journal of Polymer Science
Volume 2014, Article ID 696045, 6 pages
http://dx.doi.org/10.1155/2014/696045

Research Article

Safety and Efficiency of Biomimetic Nanohydroxyapatite/Polyamide 66 Composite in Rabbits and Primary Use in Anterior Cervical Discectomy and Fusion

Hui Xu,[1,2] Yan Wang,[2] Xiaojing Su,[2] Xuelian Zhang,[3] and Xuesong Zhang[2]

[1] *Department of Orthopedics, Liaocheng People's Hospital, 67 Dongchang West Road, Liaocheng, Shandong 252004, China*
[2] *Department of Orthopedics, Chinese People's Liberation Army General Hospital, Beijing 100853, China*
[3] *Department of Endocrinology, China-Japan Friendship Hospital, Beijing 100029, China*

Correspondence should be addressed to Xuesong Zhang; zhangxuesong301@sina.com

Received 6 March 2014; Accepted 4 May 2014; Published 4 June 2014

Academic Editor: Xiaoming Li

This study was conducted to validate the safety and efficiency of biomimetic nanohydroxyapatite/polyamide 66 (n-HA/PA66) composite in animal model (rabbit) and report its application in anterior cervical discectomy and fusion (ACDF) for 4, 12, and 24 weeks. N-HA/PA66 composite was implanted into one-side hind femur defects and the control defects were kept empty as blank controls. A combination of macroscopic and histomorphometric studies was performed up to 24 weeks postoperatively and compared with normal healing. 60 cervical spondylosis myelopathy and radiculopathy patients who were subjected to ACDF using n-HA/PA66 and PEEK cage were involved in this study with six-month minimum follow-up. Their radiographic (cage subsidence, fusion status, and segmental sagittal alignment (SSA)) and clinical (VAS and JOA scales) data before surgery and at each follow-up were recorded and compared. Nanohydroxyapatite/polyamide 66 composite is safe and effective in animal experiment and ACDF.

1. Introduction

Generally, ideal bone graft substitute materials should have good osteogenesis, biocompatibility, and bioactivity. Furthermore, they can provide enough mechanical strength to meet the fundamental support requirements during bone healing period. Based on that concept, more attention is focused on the development of bioactive composite composed of bioactive inorganic ingredient (osteogenesis) and flexible polymer in recent years. Hydroxyapatite (HA) shows a similar composition and structure to natural bone mineral and therefore has been considered to be an ideal material to build bone repair materials due to its osteoconductivity. But its brittleness extremely limits its use in load-bearing bone repair [1–7]. Polyamide (PA) has good biocompatibility probably because of its similarity to collagen protein in chemical structure and active groups [8, 9]. PA also has excellent mechanical properties resulting from the strong hydrogen bonds between the amide groups in PA macromolecules [10, 11].

To combine advancements of the two materials, nanohydroxyapatite (n-HA)/polyamide 66 biocomposite was developed by Sichuan University [12]. This composite showed good mechanical strength similar to natural bone and good compatibility. Furthermore, cage and vertebral plate developed by this composite have been used for spine repair successfully [13–18]. The porous n-HA/PA66 composite had biological safety, good biocompatibility, osteoinduction, and osseointegration [19, 20]. However, most of the studies were conducted in one institution. The purpose of this study is to validate the safety and efficiency of biomimetic n-HA/PA66 composite in rabbits and report primary use in cervical discectomy and fusion in our department.

2. Materials and Method

2.1. Animal Experiment

2.1.1. n-HA/PA66 Characterization. The n-HA/PA66 biocomposite was prepared by thermal-press molding. The

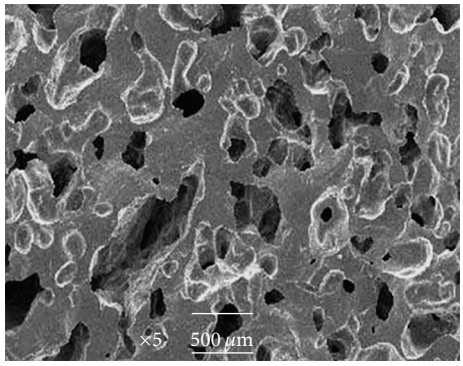

Figure 1: SEM micrographs of porous n-HA/PA66.

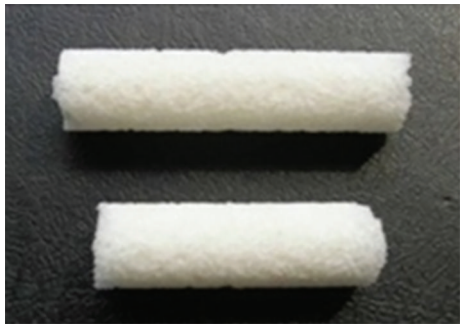

Figure 2: Columnar n-HA/PA blocks.

material presented: (1) high compressive strength which reached 13~46 MPa and (2) excellent porous structure; the average diameter of pores in the matrix was in range of 280 μm to 500 μm and porosity of 36% to 57% (Figure 1) [21]. The columnar n-HA/PA blocks (height 10 mm and diameter 5 mm) were made by Sichuan National Nano Technology Co., Ltd. (Chengdu, China) (Figure 2). The biocomposite was sterilized by gamma radiation prior to implantation.

2.1.2. n-HA/PA66 Implantation. 30 New Zealand white rabbits were involved in this experiment. After anesthesia, about 5 cm longitudinal incision was made 1 cm higher to the hind limb knee to expose the femur. Four defects (5 mm $*$ 5 mm) were drilled at low speed in the femur. Then the n-HA/PA 66 blocks were inserted into the defects in two of four bone defects and the other two defects were kept empty. Implant placement was randomized in the four defects and the wound was secured in layers. After surgery the rabbits were randomly divided into 3 groups according to sacrifice time (4, 12, and 24 weeks).

All animals were injected with 10,000 units of penicillin per day for 3 days to prevent infection. The animals were sacrificed by a lethal dose of barbiturate, respectively, at 4, 12, or 24 weeks after surgery. The femurs were removed, cleaned, and prepared for histologic testing.

2.1.3. Wound Healing and Local Inflammatory Reaction. Swelling, hematoma, infection, wound healing, and associated signs of local inflammatory reactions were observed every day in 1 week after surgery and once in 1 week up to 24 weeks postoperatively.

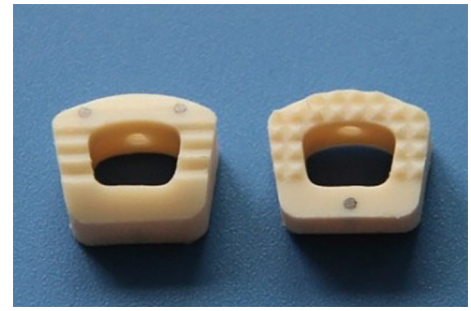

Figure 3: The n-HA/PA66 cage.

2.1.4. Macroscopic Observations and Histological Study. At the time of 4, 12, and 24 weeks after surgery, the rabbits were killed and the femurs were explored. Local bone healing was observed. 5 cm femur samples including all the defects were removed with a diamond saw. The bone samples were cleaned and were doused in 10% formalin for 7 days. After initial fixation, the bones were dehydrated in a series of alcohol until the standardization was reached. Then the samples were decalcified and embedded in epoxy resin. 5 μm cross-sections were cut by a diamond saw microtome (Leica Spa, Milan, Italy), and Masson's trichrome staining was conducted. The stained sections of each sample were observed with a light microscope (NICON E 600).

2.2. Primary Clinical Use

2.2.1. Patients and Methods. This was a prospective nonrandom compared study of patients with cervical spondylosis myelopathy or radiculopathy who underwent anterior cervical discectomy and fusion (ACDF) with cage and anterior plate. The study was approved by the Institutional Review Board and was performed at our department from January 2013 to June 2013.

During this period, 60 patients were eligible for inclusion. The inclusion criteria were (1) myelopathy or radiculopathy with failure of conservative treatment (of at least three months), (2) cervical degenerative diseases with compression of the cervical spinal cord or nerve roots, or best clinical symptoms and signs which can explain well documented radiographs, and (3) through ACDF surgery, the spinal cord or nerve roots could be adequately decompressed. The exclusion criteria were (1) cervical deformities or neoplasia, (2) severe osteoporosis, and (3) patients with psychiatric disorders. The clinical presentation and radiological findings determined the level of discectomy. The anterior fusion was performed using n-HA/PA66 cage (Sichuan National Nano Technology Co., Ltd., Chengdu, china) (see Figure 3) in 30 patients and PEEK cage (Medtronic Sofamor Danek Inc., Memphis, TN) in the other patients.

All the operations were performed by one of two senior spine surgeons. The patients were placed in the supine position with neck extension. Cervical discectomy and decompression were performed in the standard right-side anterior cervical approach. Then local autologous bone filling PEEK or n-HA/PA66 cage was implanted into the disc space. The Atlantis anterior cervical plate system (Medtronic Sofamor Danek Inc., Memphis, TN) was used in each patient for further stabilization. After surgery, all patients were requested to wear a soft cervical collar for approximately four weeks.

2.2.2. Outcomes Assessment. At three and six months after surgery, the patients had radiological follow-up. The cervical plain radiographs were taken at each follow-up examination. The following parameters were evaluated on lateral plain radiographs: preoperative and postoperative segmental sagittal alignment (SSA), cage subsidence, and fusion status. The height of the fusion segment was measured as the distance between the midpoint of the superior endplate of the upper vertebra and the midpoint of the inferior endplate of the lower vertebra. Subsidence was defined as the difference of height of the fusion segment between immediately after surgery and the later follow-up. It would be considered as severe subsidence once cage subsidence exceeded three millimeters. We defined the Cobb angle between the superior endplate of the C4 vertebra and the inferior endplate of the C7 vertebra as the SSA. The lordosis angle and the kyphosis angle were defined as positive angle and negative angle, respectively. The changes in sagittal alignment before surgery and at postoperative follow-ups were determined. When a trabecular bone across the interfaces appeared, fusion was considered complete. If the lucency between the implants and vertebral endplates surfaced, nonunion would be noted. All these radiographic parameters were measured by five independent senior spine surgeons who were not involved in the primary surgery and were unaware of the clinical results of the patients. Their average value was adopted for final analysis.

In addition, the clinical outcome of each patient was assessed by comparing the scores on a 10-point visual analogue scale (VAS) and the Japanese Orthopedic Association (JOA) scale before surgery and at six-month follow-up. Excessive operation time, blood loss, hospital stay, and surgical complications were recorded. The recovery rate (JOA) was measured by the method of Hirabayashi et al. [22]. Recovery rate (%) = post-op score − pre-op score/17 (full) − pre-op score × 100.

2.3. Statistical Analysis. In this study, SPSS 17.0 statistic software (SPSS, Chicago, IL, USA) was used for all statistical analyses. Quantitative data are presented as the mean ± standard deviation. With one-way ANOVA, the mean comparison at different time points was conducted, and with the LSD method the pairwise comparison was performed. By the Mann-Whitney test, mean comparison in two groups was analyzed. All P values were two-sided, and levels of significance reaching >95 % were accepted.

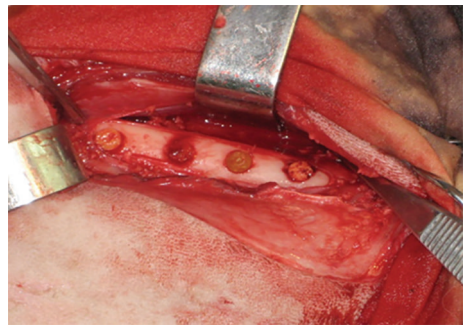

Figure 4: 4 weeks after implanting n-HA/PA66 blocks.

3. Result

3.1. Animal Experiments

3.1.1. Wound Healing and Local Inflammatory Reactions. All the rabbits survived until they were killed. Wounds healed well in all cases and sutures were removed on the tenth postoperative day. There was no swelling, fluid, or local heat during the postoperative period.

3.1.2. Macroscopic Observations. At the time of 4, 12, and 24 weeks after surgery, the femurs were exposed and were macroscopically observed. There were no obvious signs of local inflammation observed in any animal. At the fourth week, the implants were stable in the defects and the callus formation covered about 70% of the surface of implants (Figure 4); in the blank control defects, few calluses were observed. At the twelfth week, the whole surface of the implant was almost covered by callus. But in the blank control, the calluses were fewer. At twentieth week, the defects in the n-HA/PA 66 group were covered with the natural bone. In the control group, the callus was thin and the defects were still visible.

3.1.3. Histological Analyses. The defects with n-HA/PA implantation in the 4-week group were filled with newly formed bone and connective tissue. The interface between the implant and bone was filled with direct bone bonding. New osteoid tissue was observed in the pore structure, and osteoblast infiltration was seen on the surface of the implant. In the control group, loose fibrocollagen tissue filled the defects and no bone formation was observed. In the 12-week group, large amounts of new bone tissue are invading the porosity of the n-HA/PA 66 implant. Osteoid tissue was also detected in the central area of the implant. The lamellar bone transition was seen in formed bone area. In the control group, although new bone tissue was observed, fibrous tissue was more frequently observed. New bony tissue was only detected in marginal areas. 24 weeks postoperatively, part of n-HA/PA 66 also remained. But the cortex of the bone showed well-developed lamellar appearance. Mature bone trabecular was seen in no implant defects, but it was only good in marginal areas of the defects.

Figure 5: PEEK cages in a 65-year-old male postoperatively.

Figure 6: n-HA/PA66 cages in a 62-year-old male postoperatively.

3.2. Clinical Results. Of the 60 patients eligible for inclusion in this study, we obtained complete datasets (preoperative, immediately postoperative, 3 months postoperative, and 6-month follow-up data) for 57 patients (95%). It contained 37 men and 20 women with a mean age of 51.3 years (range 35–71 years). 29 patients underwent the ACDF with PEEK cage (PEEK group) (Figure 5) and the other 28 patients with n-HA/PA66 cage (n-HA/PA66 group) (Figure 6). The demographics of both groups of patients are shown in Table 1. There were no statistically significant differences in sex, age, smoking, diagnosis, or pathogenic level between these two groups (all $P > 0.05$). There were no severe complications in both groups.

3.2.1. Radiographic Analysis. There was no case of cage migration or breakage in either group at the last follow-up.

Table 1: Demographic data of cervical spondylitis.

	PEEK group ($n = 30$)	n-HA/PA66 group ($n = 30$)
M : F	18 : 12	19 : 11
One level	22	24
Two levels	8	6
C4-C5	9	10
C5-C6	18	17
C6-C7	11	9
Radiculopathy	8	9
Myelopathy	16	14
Radiculomyelography	6	7

There are no statistical differences in each item between the groups.

Table 2: Clinical outcomes.

	PEEK group ($n = 29$)	n-HA/PA66 group ($n = 28$)
VAS scores of the two groups		
Pre-op	7.1 ± 1.4	7.3 ± 1.6
Six-month follow-up	2.1 ± 1.3	2.3 ± 1.2
JOA scores of the two groups		
Pre-op	8.4 ± 2.4	8.2 ± 1.6
Six-month follow-up	15.1 ± 1.6	15.6 ± 1.2

There are no statistical differences in each item between the groups.

At three months after surgery, 24 patients' cages were fused with a fusion rate of 83% in the PEEK group that was markedly lower than the fusion rate of 93% (26 of 28) in the n-HA/PA66 group. At the six-month follow-up, the fusion rate was 100% in the two groups. There was no severe cage subsidence in the two groups. In the PEEK group, the mean SSA before surgery was 13.8°, and it significantly improved to 19.6° immediately after surgery ($P < 0.05$). While in the n-HA/PA66 group, the mean preoperative SSA was 14.1°, and it significantly improved to 19.8° immediately after surgery ($P < 0.05$). The change of SSA before and after surgery was similar in the PEEK group and n-HA/PA66 group. In later follow-ups, the mean SSA of the PEEK group and n-HA/PA66 group had no significant change.

Clinical Outcome. The six-month follow-up VAS and JOA scores of the two groups were significantly improved compared to preoperative scores. However, there is no statistical difference between the two groups over the follow-up period (Table 2).

4. Discussion

Bone grafts are widely used in orthopedics surgery and should provide support, bone conduction, and induction. Autogenous bone grafts are considered the gold standard in bone transplantation, but donor sites complications concern many surgeons. Thus biological substitutes were developed by many researchers. Developments of bone substitutes are

based on a better understanding of the biological process in the bone healing. The biological approach provides the key that plays an important role in the repair of bone defects [23, 24]. Artificial bone substitutes are clearly inferior to autogenous bone grafts in osteoinduction, but they enhance osteoconduction, provide support, and can be easily made in the required shapes. Another important point which should be considered is histocompatibility.

The n-HA/PA 66 used in this study was prepared by thermal-press molding. Compared to injection molding HA/PA [18], the pores in the materials prepared by the hot-press molding are irregular tubular, the connectivity of which is good. The shape and connectivity of the pores in the biomaterials have important effects on their biological activities in vitro and in vivo [21]. The irregular tubular biomaterial provide good interface between n-HA/PA 66 and host bone; new bone tissue can survive in the pores. The compressive strength of n-HA/PA 66 used in this study was 13~46 Mpa. N-HA/PA 66 can provide enough support during the bone healing period.

In this study, n-HA/PA 66 was well accepted and tolerated by all the rabbits, no infection, wound complications, serious inflammation, and rejection response were found in any case. The results of macroscopic and histologic analysis proved better bone reparation in the n-HA/PA 66 group than the blank controls in all groups. New bone tissue was detected around the implant and inside the pore structure 4 weeks postoperatively, which strongly demonstrated the good osteoconductivity of the bone substitute.

In our clinical study, the cage was made of n-HA/PA 66, the same material used in the animal study. Compared to the traditional PEEK cage used in ACDF, n-HA/PA 66 cages had the higher fusion rate at 3-month follow-up, but at 6-month follow-up, there was no difference. The operation time, blood loss, complications, and clinical outcome scores were similar in the two groups. The results were similar to other reports [25, 26]. However, the follow-up period was short and the probability of similar case was little. Further study is necessary.

In conclusion, the n-HA/PA 66 composite was safe and effective in repairing bone defects of rabbits. The excellent osteogenesis of the porous n-HA/PA 66 composite in this study was rationalized by not only the biomimetic composition but also the interconnecting porosity. Porous n-HA/PA 66 cage was successfully used in ACDF and had a good outcome that it can be a substitution to traditional cages.

Conflict of Interests

The authors have no conflict of interests.

References

[1] G. Wei and P. X. Ma, "Structure and properties of nano-hydroxyapatite/polymer composite scaffolds for bone tissue engineering," *Biomaterials*, vol. 25, no. 19, pp. 4749–4757, 2004.

[2] X. Li, Q. Feng, X. Liu, W. Dong, and F. Cui, "Collagen-based implants reinforced by chitin fibres in a goat shank bone defect model," *Biomaterials*, vol. 27, no. 9, pp. 1917–1923, 2006.

[3] X. Li, C. A. van Blitterswijk, Q. Feng, F. Cui, and F. Watari, "The effect of calcium phosphate microstructure on bone-related cells in vitro," *Biomaterials*, vol. 29, no. 23, pp. 3306–3316, 2008.

[4] P. X. Ma, R. Zhang, G. Xiao, and R. Franceschi, "Engineering new bone tissue in vitro on highly porous poly (alpha-hydroxyl acids)/hydroxyapatite composite scaffolds," *Journal of Biomedical Materials Research*, vol. 54, pp. 284–293, 2001.

[5] J. Wei, Y. Li, and K.-T. Lau, "Preparation and characterization of a nano apatite/polyamide6 bioactive composite," *Composites B: Engineering*, vol. 38, no. 3, pp. 301–305, 2007.

[6] R. Detsch, H. Mayr, and G. Ziegler, "Formation of osteoclast-like cells on HA and TCP ceramics," *Acta Biomaterialia*, vol. 4, no. 1, pp. 139–148, 2008.

[7] M. Motskin, D. M. Wright, K. Muller et al., "Hydroxyapatite nano and microparticles: correlation of particle properties with cytotoxicity and biostability," *Biomaterials*, vol. 30, no. 19, pp. 3307–3317, 2009.

[8] Y.-W. Wang, Q. Wu, J. Chen, and G.-Q. Chen, "Evaluation of three-dimensional scaffolds made of blends of hydroxyapatite and poly(3-hydroxybutyrate-co-3-hydroxyhexanoate) for bone reconstruction," *Biomaterials*, vol. 26, no. 8, pp. 899–904, 2005.

[9] H. H. K. Xu and C. G. Simon Jr., "Fast setting calcium phosphate-chitosan scaffold: mechanical properties and biocompatibility," *Biomaterials*, vol. 26, no. 12, pp. 1337–1348, 2005.

[10] S.-S. Kim, M. Sun Park, O. Jeon, C. Yong Choi, and B.-S. Kim, "Poly(lactide-co-glycolide)/hydroxyapatite composite scaffolds for bone tissue engineering," *Biomaterials*, vol. 27, no. 8, pp. 1399–1409, 2006.

[11] S. I. Lee and B. C. Chun, "Mechanical properties and fracture morphologies of poly(phenylene sulfide)/nylon66 blends—effect of nylon66 content and testing temperature," *Journal of Materials Science*, vol. 35, no. 5, pp. 1187–1193, 2000.

[12] X. Wang, Y. Li, J. Wei, and K. De Groot, "Development of biomimetic nano-hydroxyapatite/poly(hexamethylene adipamide) composites," *Biomaterials*, vol. 23, no. 24, pp. 4787–4791, 2002.

[13] X. Yang, Y. Song, L. Liu, H. Liu, J. Zeng, and F. Pei, "Anterior reconstruction with nano-hydroxyapatite/polyamide-66 cage after thoracic and lumbar corpectomy," *Orthopedics*, vol. 35, no. 1, pp. e66–e73, 2012.

[14] Z. Zhao, D. Jiang, Y. Ou, K. Tang, X. Luo, and Z. Quan, "A hollow cylindrical nano-hydroxyapatite/polyamide composite strut for cervical reconstruction after cervical corpectomy," *Journal of Clinical Neuroscience*, vol. 19, no. 4, pp. 536–540, 2012.

[15] M. Huang, J. Feng, J. Wang, X. Zhang, Y. Li, and Y. Yan, "Synthesis and characterization of nano-HA/PA66 composites," *Journal of Materials Science: Materials in Medicine*, vol. 14, no. 7, pp. 655–660, 2003.

[16] Q. Xu, H. Lu, J. Zhang, G. Lu, Z. Deng, and A. Mo, "Tissue engineering scaffold material of porous nanohydroxyapatite/polyamide 66," *International Journal of Nanomedicine*, vol. 5, no. 1, pp. 331–335, 2010.

[17] H. Wang, Y. Li, Y. Zuo, J. Li, S. Ma, and L. Cheng, "Biocompatibility and osteogenesis of biomimetic nano-hydroxyapatite/polyamide composite scaffolds for bone tissue engineering," *Biomaterials*, vol. 28, no. 22, pp. 3338–3348, 2007.

[18] J. C. Zhang, H. Y. Lu, G. Y. Lv, A. C. Mo, Y. G. Yan, and C. Huang, "The repair of critical-size defects with porous hydroxyapatite/polyamide nanocomposite: an experimental study in rabbit mandibles," *International Journal of Oral and Maxillofacial Surgery*, vol. 39, no. 5, pp. 469–477, 2010.

[19] X. Luo, L. Zhang, Y. Morsi et al., "Hydroxyapatite/polyamide66 porous scaffold with an ethylene vinyl acetate surface layer used for simultaneous substitute and repair of articular cartilage and underlying bone," *Applied Surface Science*, vol. 257, no. 23, pp. 9888–9894, 2011.

[20] Y. Xiong, C. Ren, B. Zhang et al., "Analyzing the behavior of a porous nano-hydroxyapatite/polyamide 66 (n-HA/PA66) composite for healing of bone defects," *International Journal of Nanomedicine*, vol. 9, pp. 485–494, 2014.

[21] H. Li, Y. Li, Y. Yan, J. Li, A. Yang, and H. Xiang, "Fabrication of porous n-HA/PA66 composite for bone repair," *Key Engineering Materials*, vol. 330-332, pp. 321–324, 2007.

[22] K. Hirabayashi, J. Miyakawa, K. Satomi, T. Maruyama, and K. Wakano, "Operative results and postoperative progression of ossification among patients with ossification of cervical posterior longitudinal ligament," *Spine*, vol. 6, no. 4, pp. 354–364, 1981.

[23] X. Li, L. Wang, Y. Fan, Q. Feng, F.-Z. Cui, and F. Watari, "Nanostructured scaffolds for bone tissue engineering," *Journal of Biomedical Materials Research A*, vol. 101, no. 8, pp. 2424–2435, 2013.

[24] X. Li, H. Liu, X. Niu et al., "The use of carbon nanotubes to induce osteogenic differentiation of human adipose-derived MSCs in vitro and ectopic bone formation in vivo," *Biomaterials*, vol. 33, no. 19, pp. 4818–4827, 2012.

[25] F. Suetsuna, T. Yokoyama, E. Kenuka, and S. Harata, "Anterior cervical fusion using porous hydroxyapatite ceramics for cervical disc herniation: a two-year follow-up," *The Spine Journal*, vol. 1, no. 5, pp. 348–357, 2001.

[26] X. Yang, Q. Chen, L. Liu et al., "Comparison of anterior cervical fusion by titanium mesh cage versus nano-hydroxyapatite/polyamide cage following single-level corpectomy," *International Orthopaedics*, vol. 37, no. 12, pp. 2421–2427, 2013.

Hindawi Publishing Corporation
International Journal of Polymer Science
Volume 2014, Article ID 805634, 14 pages
http://dx.doi.org/10.1155/2014/805634

Review Article

Polymer Composites Reinforced by Nanotubes as Scaffolds for Tissue Engineering

Wei Wang,[1] Susan Liao,[2] Ming Liu,[1] Qian Zhao,[1] and Yuhe Zhu[1]

[1] *Department of Prosthodontics, School of Stomatology, China Medical University, Nanjing North Street, Heping District, No. 117, Shenyang 110002, China*
[2] *School of Materials Science and Engineering, Nanyang Technological University, Singapore 639798*

Correspondence should be addressed to Wei Wang; yuhe740442@hotmail.com

Received 10 April 2014; Accepted 18 May 2014; Published 1 June 2014

Academic Editor: Xiaoming Li

The interest in polymer based composites for tissue engineering applications has been increasing in recent years. Nanotubes materials, including carbon nanotubes (CNTs) and noncarbonic nanotubes, with unique electrical, mechanical, and surface properties, such as high aspect ratio, have long been recognized as effective reinforced materials for enhancing the mechanical properties of polymer matrix. This review paper is an attempt to present a coherent yet concise review on the mechanical and biocompatibility properties of CNTs and noncarbonic nanotubes/polymer composites, such as Boron nitride nanotubes (BNNTs) and Tungsten disulfide nanotubes (WSNTs) reinforced polymer composites which are used as scaffolds for tissue engineering. We also introduced different preparation methods of CNTs/polymer composites, such as in situ polymerization, solution mixing, melt blending, and latex technology, each of them has its own advantages.

1. Introduction

Tissue engineering, an important emerging topic in biomedical engineering, has shown tremendous promise in creating biological alternatives for harvested tissues, implants, and prostheses [1]. Tissue engineering may be defined as the application of biological, chemical, and engineering principles toward the repair, restoration, or regeneration of living tissues using biomaterials, cells, and factors alone or in combination [2]. Scaffold is one of the key components in the tissue engineering paradigm in which it can function as a template to allow new tissue growth and also provide temporary support while serving as a delivery vehicle for cells and/or bioactive molecules structure [3, 4]. The scaffold should be porous and permeable to permit the ingress of cells and nutrients and should exhibit the appropriate surface structure and chemistry for cell attachment. Ideal scaffold should possess a suitable combination of physical properties to match those of the replaced tissue with good biocompatibility. Various synthetic alternatives such as metal, alloys, ceramics, polymers, and biocomposites have been researched as scaffold for bioapplications. Among those scaffold biomaterials, the polymers and polymers composites occupy significant position. Polymer materials are playing an increasingly important part in a diverse range of applications; polymer systems can be used for a variety of applications, such as drug delivery, diagnostics, tissue engineering and "smart" optical systems, switching surfaces and adhesives, and protective coatings that adapt to the environment, as well as biosensors, microelectromechanical systems, coatings, and textiles [5]. Nowadays, synthetic degradable polymers, such as polycaprolactone (PCL), polyglycolic acid, polyvinyl alcohol (PVA), and polylactic acid (PLA), have been evaluated extensively as scaffold biomaterials [6]. However, the results of research show that their mechanical properties and biocompatibility are unsatisfactory for the tissue engineering of load-bearing bone. Several strategies for improving the mechanical properties (compression and flexural) of polymeric scaffolds have been reported, with a focus towards developing nanomaterials reinforced polymeric composites [6].

Nanomaterials, which are materials with basic structural units, grains, particles, fibers, or other constituent components smaller than 100 nm in at least one dimension, have

evoked a great amount of attention [7]. Nanomaterials have special mechanical, electrical magnetic, optical, chemical, and other biological properties because of their high aspect ratio and surface area. Among nanomaterials, the nanotube material attracted wide attention of researchers. Nanotubes, with structures that resemble tiny drinking straws, large inner volumes can be filled with sundry chemicals and biomolecules, ranging in size from small molecules to proteins [8, 9]. After carbon nanotubes (CNTs) were discovered by lijima in 1991, noncarbonic nanotubes were manufactured by different routes: in 2000, Rothschild et al. discovered Tungsten disulfide nanotubes (WSNTs) by vapor-solid growth method; Nath et al. composited MS_2 nanotube in 2001 by vapor phase method; Kinenkamp et al. synthesised ZnS nanotube by restoring sulfurization process [10–12]. Then a variety of noncarbonic nanotubes has been synthesized, such as boron nitride nanotubes (BNNTs) [13], Bi_2S_3 nanotube [14], NbS_2 nanotube [15], $NbSe_2$ nanotube [16], AIN nanotube [17], GaN nanotube [18], InP nanotube [19], SiO_2 nanotube [20], and ZnO nanotube [21]. CNTs, one of the most concerned nanomaterials, with unique electrical, mechanical, and surface properties, such as high aspect ratio, high strength-to-weight ratio, extraordinary mechanical properties (their axial elastic modulus and tensile strength were theoretically predicted to be as high as 1-2 TPa and 200 GPa, resp.), have held great interest with respect to biomaterials, particularly those to be positioned in contact with bone such as prostheses for arthroplasty, plates or screws for fracture fixation, drug delivery systems, and scaffolding for bone regeneration, whose outstanding properties have sparked an abundance of research [22–31]. In recent years, some reports have showed that functionalized CNTs even can improve cell compatibility of matrix material, promote tissue regeneration, and inhibit the formation of glial scar and fibrous tissue [32, 33]. These results suggest that CNTs might hold great promise for synthesizing new kinds of multifunctional nanocomposites in biomedical applications and might be used as reinforcements to improve biological properties of polymer. Noncarbonic nanotubes are important members in quasi-one-dimensional family, because they have a high volume percentage of surface area, which show a high chemical activity and unique physical properties. Through modifying by physical and chemical methods, giving nanotubes new features, such as in the information element, biosensors, molecular field of ion channel machine, smart drugs, microtools, and advanced technology materials in aerospace have important applications. To noncarbonic nanotubes, their research has been focused on the discussion of their manufacturing method and properties, and few reports have investigated the application of their reinforce polymer in tissue engineering; only BNNTs and WSNTs as reinforcement factor with polymer composites have been reported.

In this paper, we will present a comprehensive review about the preparation and processing and the properties of polymer composites reinforced by carbon and noncarbonic nanotube that used or potentially could be used as scaffolds in tissue engineering.

2. Preparation of Nanotubes

CNTs were discovered in the late 1950s while the synthesis of CNTs was first reported in 1991 by Iijima [23] and Bacon [42]. Right now, there are several methods to produce CNTs including arc discharge, laser ablation, chemical vapor deposition (CVD), catalyst chemical vapor deposition (CCVD), and template-directed synthesis [43]. Although arc discharge is a common method for CNTs synthesis, it is difficult to control the morphology of CNTs, such as length, diameter, and number of layers. Compared with arc-discharge and laser-ablation methods, CVD is most widely used for its low setup cost, high production yield, and ease of scale-up. There are two main types of nanotubes existing: the single-walled nanotubes (SWNTs) which are composed by a rolled monolayered graphene sheet and the multiwalled nanotubes (MWNTs) which possess several graphitic concentric layers. In the high-temperature methods, multiwalled carbon nanotubes (MWCNTs) can be produced from the evaporation of pure carbon, but the synthesis of single-walled carbon nanotubes (SWCNTs) requires the presence of a metallic catalyst. The CVD approach requires a catalyst for both types of CNTs but also allows the production of carbon nanofibers [44].

In recent years, people from compounds of graphite, boron nitride which have layered structure synthesized nanotubes. Methods of noncarbonic nanotubes mainly are arc discharge, chemical vapor deposition, laser ablation, carbothermal reduction, carbon nanotubes as a template, pyrolysis, a ball mill, and a relatively low temperature of decomposition [13, 45–51]. Recently, the mechanism of nanotubes has a new understanding, breaking conventional wisdom that only layered materials can form nanotubes. Scientists have developed new ideas of synthesis and proposed a new mechanism of into the tube and from the nonlayered material prepared nanotubes. For example, from chalcogenide MX_2 (M = Mo, W, Nb, X = S, Se) prepared nanotubes. Methods preparing chalcogenide nanotubes are direct vulcanization MO_3 method, decomposition MX_3 method, decomposition (NH_4) MS_4 method, carbon tube template method, a hydrothermal synthesis method, and so on. In 2000, Rothschild et al. prepared nanoscale diameter of WS_2 nanotubes by vapor-solid growth method [10].

BNNTs represent V compound nanotubes that can be obtained through a variety of methods, such as arc discharge, chemical vapor deposition, laser ablation, carbothermal reduction, carbon nanotube template method, pyrolysis method, ball milling method, and hydrothermal synthesis method [13, 45–51]. In 2000, Lourie et al. synthesized BNNTs by chemical vapor deposition method [13]. Xu et al.'s team prepared BNNTs by hydrothermal synthesis method in 2003 [51]. After obtaining BNNTs, a number of groups used BNNTs, by filling heterogeneous substances into the pipe body cavity to get the nanotubes reinforced composites, hoping to obtain superior characteristics.

3. Preparation of Polymer Composites Reinforced by Nanotubes

Preparing nanotubes/polymer composites must solve two major problems: favorably dispersed of nanotubes in the

Table 1: Comparison of CNTs/polymer composites with various fabricating methods.

Method	Advantages	Disadvantages
Solution mixing	Wider applicability, better dispersion	Low stability, residual solution
Melt blending	Wide applicability, good dispersion	Poor dispersion, large residual stress, and low interfacial bonding strength
In situ polymerization	Widest applicability, best dispersion	Residual monomer, matrix strength decline, and large residual stress
Latex technology	Versatile, reproducible, and reliable	Mechanical properties of the material were not significantly improved

matrix and the interface binding with the polymer and nanotubes. Due to small diameter and high surface energy, nanotubes tend to agglomerate easily, which affect their dispersion in the polymer uniformly. Therefore, the primary problem in the preparation of nanotubes/polymer composites is to solve the uniform dispersion of nanotubes in a polymer matrix. In recent years, ultrasound treatment as an important method of dispersing nanotubes, which benefits its dispersion and activation and initiates the polymerization, can effectively solve the problem of nanotubes dispersion in the polymer [6]. In order to improve the adhesion of the interface between the polymer and the nanotubes, it is possible to introduce functional groups into the surface of nanotubes or using the plasma treatment (e.g., NH_3) [52].

The common fabricating methods of nanotubes/polymer composites are solution mixing, melt blending, latex technology, and in situ polymerization method. These methods and their features are briefly described in Table 1. Solution mixing is the most common method for the fabrication of nanotubes/polymer nanocomposites because it is amenable to small sample sizes. In solution mixing, nanotubes are generally dispersed in solvent and then mixed with polymer solution by mechanical mixing, magnetic agitation, or high energy sonication. Subsequently, the nanotubes/polymer composites can be obtained by vaporizing the solvent at a certain temperature [53–55]. Many researchers, such as Xu et al. and Lau et al., have fabricated the CNTs/epoxy composite using this method [56, 57]. For laboratory studies, the solution blending method is a simple way, often to achieve the desired results, but for insoluble polymers, this method is not applicable. It is also not suitable for large-scale industrial preparation. Because this method the process is long and complicated to operate, the consumption of solvents, and complete removal of the solvent are difficult [58]. Melt blending is a versatile and commonly used method to fabricate polymeric materials, especially for thermoplastic polymers. Melt blending uses a high temperature and a high shear force to disperse nanotubes in a polymer matrix [59–61]. The major advantage of this method is that no solvent is employed to disperse nanotubes. Its well-known disadvantage is that nanotubes can easily be damaged to a certain extent or broken in some cases [44, 62–64]. Latex technology is a relatively new approach to incorporate nanotubes into a polymer matrix. By using this technology, it is possible to disperse nanotubes in most of polymers that are produced by emulsion polymerization or that can be brought into the form of an emulsion. The advantages of this technique are obvious: the whole process is easy, versatile, reproducible, and reliable [53–55]. The solvent used for nanotubes dispersion is water; thus, the process is a safe, environmentally friendly, and low-cost. In situ polymerization is considered as a very efficient method to significantly improve the nanotubes dispersion and the interaction between nanotubes and polymer matrix. Generally, nanotubes are firstly mixed with monomers, either in the presence or absence of a solvent, and then these monomers are polymerized via addition or condensation reactions with a hardener or curing agents at an elevated temperature. One of the major advantages of this method is that covalent bonding can be formed between the functionalized nanotubes and polymer matrix, resulting in much improved mechanical properties of composites through strong interfacial bonds [65–67]. To improve the processability, electrical, magnetic, and optical properties of nanotubes, some conjugated or conducting polymers are attached to their surfaces by in situ polymerization. It enables grafting of polymer macromolecules onto the convex walls of nanotubes. This then provides a better nanotubes dispersion and formation of a strong interface between the nanotube and the polymer matrix. Epoxy-based nanocomposites comprise the majority of reports using in situ polymerization methods [68–75]. Song et al. successfully covalently grafted biocompatible poly (L-lactic acid) (PLA) onto the convex surfaces and tips of the MWNTs by one step based on in situ polycondensation of the commercially available L-lactic acid monomers [76].

4. Properties of Polymer Composites Reinforced by Nanotubes as Scaffold for Tissue Engineering

4.1. Polymer Composites Reinforced by Carbon Nanotubes. Recently, polymers have received broad attention in the field of biomedicine. However, their respective problems, such as insufficient mechanical properties and biocompatibility, can directly affect their performance in vivo. For example, although PGA and poly-L-lactic acid (PLLA) can provide a proper plasticity and controlled biodegradation, the biocompatibility is not as satisfactory as that of other biomaterials and the mechanical properties of them seem like insufficient when they are used for large bone defect repair. Conversely, natural polymers, such as collagen, chitosan, and natural extracellular matrix (ECM), exhibit excellent biocompatibility, biodegradable properties; however, their weak mechanical properties have limited their clinical applications [77]. An ideal composite with proper mechanical properties for biomedical applications must be biodegradable and biocompatible and promote cell growth and proliferation. For instance, polymers, which include natural polymer and synthesized polymer, when they are fabricated as CNTs/polymer composites, some of them demonstrate excellent biocompatibility and bioactivity due to the high aspect ratio and

surface area of nanostructure. Nanostructured surfaces of CNTs show high (bio- and cyto-) compatibility, by promoting protein adsorption and enhancing subsequent cellular adhesion and tissue growth more than on traditional biomaterials' surfaces such as ceramics, titanium alloy, and biopolymers. Many experimental results have shown that the combination of CNTs offers an attractive route to introduce new mechanical properties. The use of CNTs/polymeric biomaterial composites as scaffolds for bone engineering has recently become a subject of interest. Scaffolds for tissue regeneration require properties such as rigidity to bear external force, biodegradability and absorption, the ability to promote the adhesion and proliferation of cells, and the ability to be penetrated by blood vessels and body fluids. To date, CNTs have been used to reinforce the weak points of existing scaffold materials. In 2011, Zhang synthesized a series of poly (lactic-co-glycolic acid) (PLGA)/MWNTs composite scaffolds for tissue engineering [34]. Compared to the pure PLGA scaffold, the tensile stress of the PLGA/0.25% MWNTs scaffolds was increased by 54% (from 5.88 to 9.08 MPa), Young's modulus was increased by 8% (from 163.53 to 176.83 MPa), and the elongation at break was increased by 49% (from 27.14% to 40.39%). It is evident that even a small amount of MWNTs would significantly improve the tensile strength of the composites. Thermal characterization showed that the incorporation of MWNTs into the PLGA matrix increased the thermal stability of the composite scaffolds. After 24 hours of rat bone marrow-derived mesenchymal stem cells (BNSCs) culture, compared to the pure PLGA scaffolds, cells on the PLGA/MWNTs composites were spread more with long filopodia. In addition, cells on the PLGA/1.25% MWNTs scaffolds had started to migrate through the pores and grow inside the fiber network. The cells that came in contact with each other through filopodia integrated with the surrounding fibers to form a 3D cellular network, indicating better adhesion on the PLGA/1.25% MWNTs scaffolds. Therefore, the mechanical and biological properties of PLGA reinforced by MWNTs have improved significantly and the PLGA/MWNTs composite scaffolds fabricated by electrospinning may be potentially useful in tissue engineering applications, particularly as scaffolds for bone tissue regeneration. In 2013, Vozzi et al. microfabricated three-dimensional (3D) scaffolds by mixing PLLA and MWCNTs for bone tissue engineering [35]. In the test, their mechanical properties are measured and their biocompatibility with human fetal osteoblasts (hFOB) is studied. The 3D microfabricated PLLA/MWCNTs nanocomposite scaffolds showed higher stiffness and cell viability than the pure 3D microfabricated PLLA scaffolds. The result of nanoindentation test suggested that the presence of CNTs increased the elastic modulus. The results showed that the PLLA/MWCNTs nanocomposite structures exhibited an improvement in the mechanical properties that could be tailored through changes in the topology of the structure. Cell test showed that all of the composite films possess good cell compatibility, with a value from the viability test of higher than 75% with respect to the control (Figure 1(a)). At different times, the cell density statistically increased (Figure 1(b)), so this result suggests that the cells on the PLLA/MWCNTs scaffold were more viable. In 2013, Chen et al. synthesized Chitosan-multiwalled carbon nanotubes/hydroxyapatite nanocomposites (CHI-MWCNTs/HA) for bone tissue engineering (Figure 2). The mechanical properties of the composites were evaluated by measuring their compressive strength and elastic modulus [36]. The result showed that elastic modulus and compressive strength increased sharply from 509.9 to 1089.1 MPa and from 33.2 to 105.5 MPa with an increase of multiwalled carbon/chitosan weight ratios from 0 to 5%, respectively. Biological results suggested that no matter on the CHI-HA composites or on the CHI-MWNTs/HA composites with different MWNTs/CHI weight ratios, the cells were spread out and had some filopodia. Meanwhile, the cells presented fusiform and polygonal morphology. These results demonstrate that preosteoblast MC3T3-E1 cells attachment and adhesion on the surface of the CHI-MWNTs/HA composites are good and the CHI-MWNTs/HA composites possess noncytotoxicity. Using CCK-8 assay to quantify cell proliferation, the result showed that MC3T3-E1 cell proliferation on CHI-HA or CHI-MWNTs/HA surface at 7 days of culture is higher than that at 3 days of culture, indicating good in vitro biocompatibility of CS-HA and CHI-MWNTs/HA nanocomposites.Abarrategi et al. studied the use of MWCNTs/CHI scaffolds, with a well-defined microchannel porous structure, has been shown biocompatible and biodegradable supports for culture growth, which was suitable for biomedical applications [78]. Zawadzak et al. developed porous polyurethane foams coated with CNTs by depositing CNTs on the surfaces of polyurethane foams using electrophoretic deposition (EPD), with the overall objective of creating a new family of functional bone tissue engineering scaffolds with nanostructured surface topography shown in Figure 3. The scaffolds retained their high porosity and interconnected pore structure after CNTs coating [79]. Furthermore, the CNTs coating was thought to promote the scaffolds osteoconductivity and mineralization potential as well as provide not only a nanostructured surface but also an electric conductivity function, suggesting that the polyurethane foams with CNTs coating have the potential to be used as bioactive scaffolds in bone tissue engineering due to their high interconnected porosity, bioactivity, and nanostructured surface topography. Shi et al. [80] studied the fabrication of highly porous scaffolds made of three different materials: poly (propylene fumarate (PPF) polymer, an ultrashort single-walled carbon nanotube (US-tube) nanocomposite, and a dodecylated US-tube (F-US-tube) nanocomposite. To assess the influence of the different composition and porosity of materials on the properties of scaffolds, scanning electron microcopy, microcomputed tomography, and mercury intrusion porosimetry were used to analyze the pore structures of scaffolds. The results indicate that the good performance of the functionalized ultrashort SWCNTs nanocomposite, which is tunable porosity and mechanical properties, may be a promise candidate of the ideal materials for scaffolds applied for the bone tissue engineering applications.

4.2. Polymer Composites Reinforced by Noncarbonic Nanotubes. The first inorganic nanotubes WSNTs were discovered in 1992 by Tenne and coworkers [81]. The study

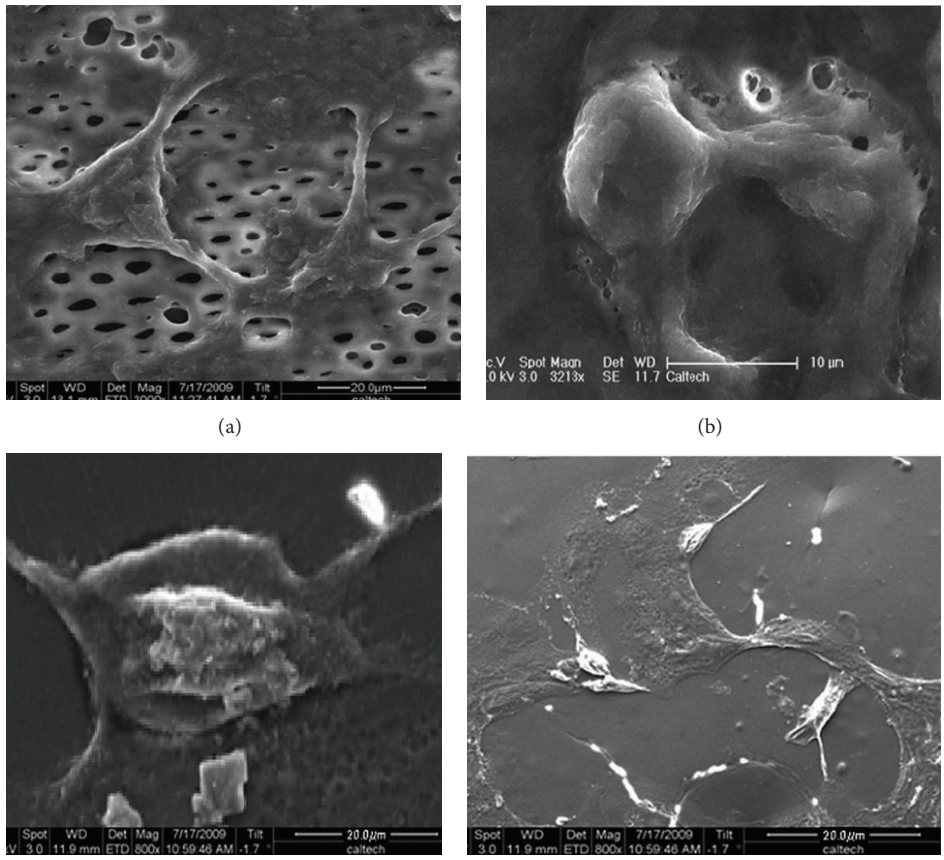

Figure 1: SEM micrographs of hFOB 1.19 cells cultured on the (a) PLLA/CNT spun film, (b) PLLA spun film, (c) PLLA/CNT 3D bonelike PAM scaffold, and (d) PLLA 3D bonelike PAM scaffold [35].

observed closed polyhedral and cylindrical crystals of tungsten disulphide semiconductor compound. WSNTs possess high mechanical properties (Young's modulus ≈150 GPa, bending modulus ≈217 GPa) [82, 83] and functional groups make it possible to disperse in organic solvents, polymers, epoxy, and resins [84]. In comparison to CNTs [85–93], few reports have investigated the mechanical properties of WSNTs-reinforced polymeric nanocomposites [39, 94]. Zohar et al. [39] evaluated the effect of embedding inorganic nanotubes (INT) of tungsten disulfide (WS_2) in an epoxy matrix, on the mechanical, thermal, and adhesion properties of the resulting nanocomposites and reported ≈49%, ≈39%, and ≈85% improvements in fracture toughness, shear strength, and peel strength of epoxy composites (compared to pristine epoxy controls) at 0.5 wt.% loading of WSNTs. Reddy et al. reported an ≈22-fold improvement in the elastic modulus and 30–35% improvements in the tensile strength and toughness of electrospun PMMA fiber composites (compared to pristine PMMA fiber controls) at 2 wt.% loading of WSNTs [40]. The study shows that the mechanical properties of polymeric nanocomposites can be significantly enhanced at very low loading concentrations of WSNTs. Lalwani et al. investigated the efficacy of WSNTs as reinforcing agents to improve the mechanical properties of PPF composites as a function of nanomaterial loading concentration (0.01–0.2 wt.%), compared with SWCNTs and MWCNTs, and crosslinked PPF composites [41]. TEM result showed that WSNTs (Figures 4(c) and 4(d)) existed as individually dispersed sharp needle-like nanotubes with mean outer diameter of ≈100 nm and a length of ≈1–15 lm. TEM was performed on 50–100 nm thick sections of crosslinked PPF nanocomposites to assess the dispersion of nanostructures in the polymer matrix (Figure 4). WSNTs were well dispersed as individual nanotubes. Mechanical testing (compression and three-point bending) shows a significant enhancement (up to 28–190%) in the mechanical properties (compressive modulus, compressive yield strength, flexural modulus, and flexural yield strength) of WSNTs-reinforced PPF nanocomposites compared to the crosslinked PPF composites. In general, WSNTs showed mechanical reinforcement better than (up to 127%) or equivalent to that of carbon nanotubes (SWCNTs and MWCNTs). Sol fraction analysis showed significant increases in the crosslinking density of PPF in the presence of WSNTs (0.01–0.2 wt.%). The results taken together indicate that PPF nanocomposites were fabricated at low loading concentrations (0.01–0.2 wt.%) of WSNTs towards the fabrication of biodegradable polymeric implants possessing improved mechanical properties. And none of

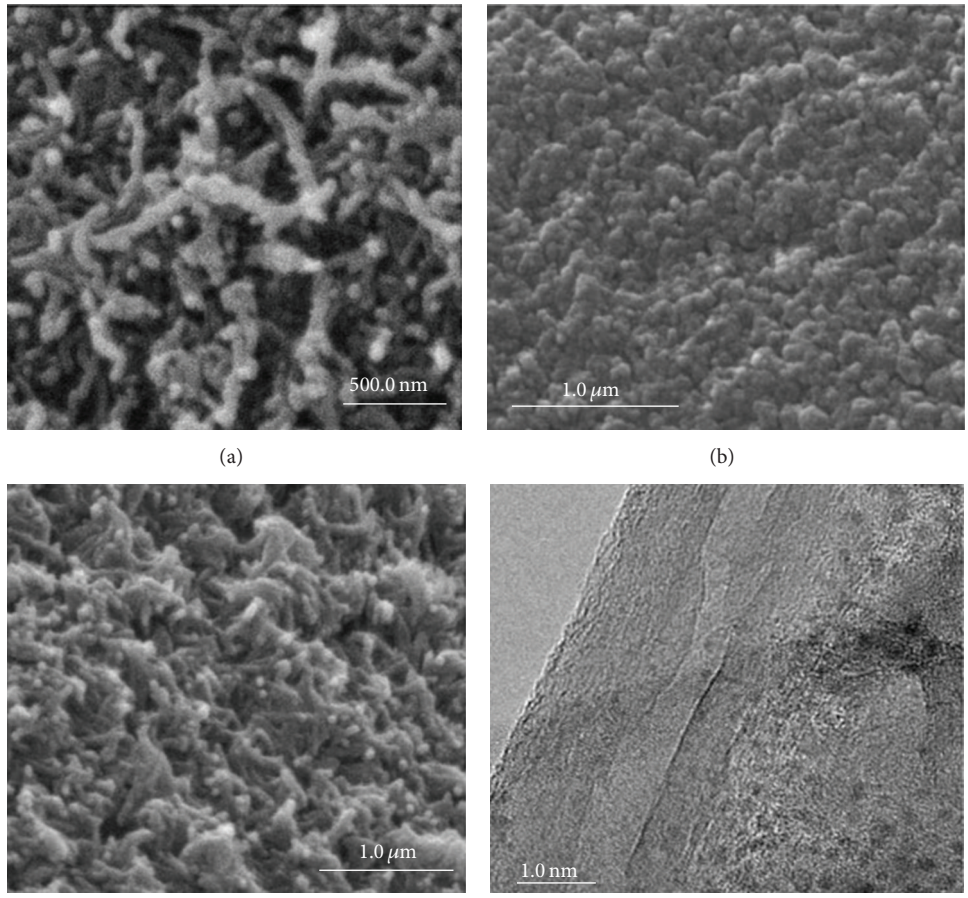

Figure 2: SEM micrographs of (a) MWNTs, (b) the CS/HA composite, (c) the CS-MWNTs/HA composite, and (d) TEM micrographs of the CS-MWNTs/HA composites [36].

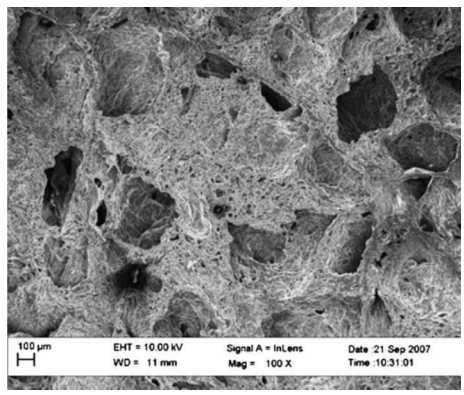

Figure 3: SEM image showing the macroscopic pore structure of a polyurethane foams coated with CNTs by EPD (deposition voltage: 20 V) [79].

these studies have focused on biomedical applications or have made direct comparisons between carbon and inorganic nanotubes as reinforcing agents.

BNNTs, other important noncarbonic nanotubes, were predicted theoretically in 1994 and they were synthesized shortly thereafter [45, 95, 96]. Boron nitride is isoelectronic to carbon and has a stable hexagonal structure analogous to that of graphite and possesses chiralities [46] (Figure 5). BNNTs have excellent elastic modulus of 1.22 TPa (similar to CNTs) and tensile strength similar to CNTs, which makes it a potential candidate as reinforcement. In addition to their structural similarity, BNNTs and CNTs have similar mechanical properties and thermal conductivity [97, 98]. However, BNNTs are distinct in several key aspects. First, BNNTs are wide band gap semiconductors whose electrical properties are independent of geometry, while CNTs may be metal or semiconducting depending on chirality and diameter. Second, BNNTs are more chemically inert and structurally stable than CNTs [99]. Hence, their reinforcement will not adversely affect the ductility of the scaffolds. BNNTs have higher chemical stability than CNTs in oxidative atmosphere, with their oxidation starting at 1223 k compared to CNTs at 773 k. The flexible and elastic nature of BNNTs and its ability to withstand heavy deformation could be helpful in preventing damage to itself during high pressure application. High temperature oxidation resistance of BNNTs is better than CNTs, which makes it more suitable for high temperature processing. BNNTs are noncytotoxic to osteoblasts and

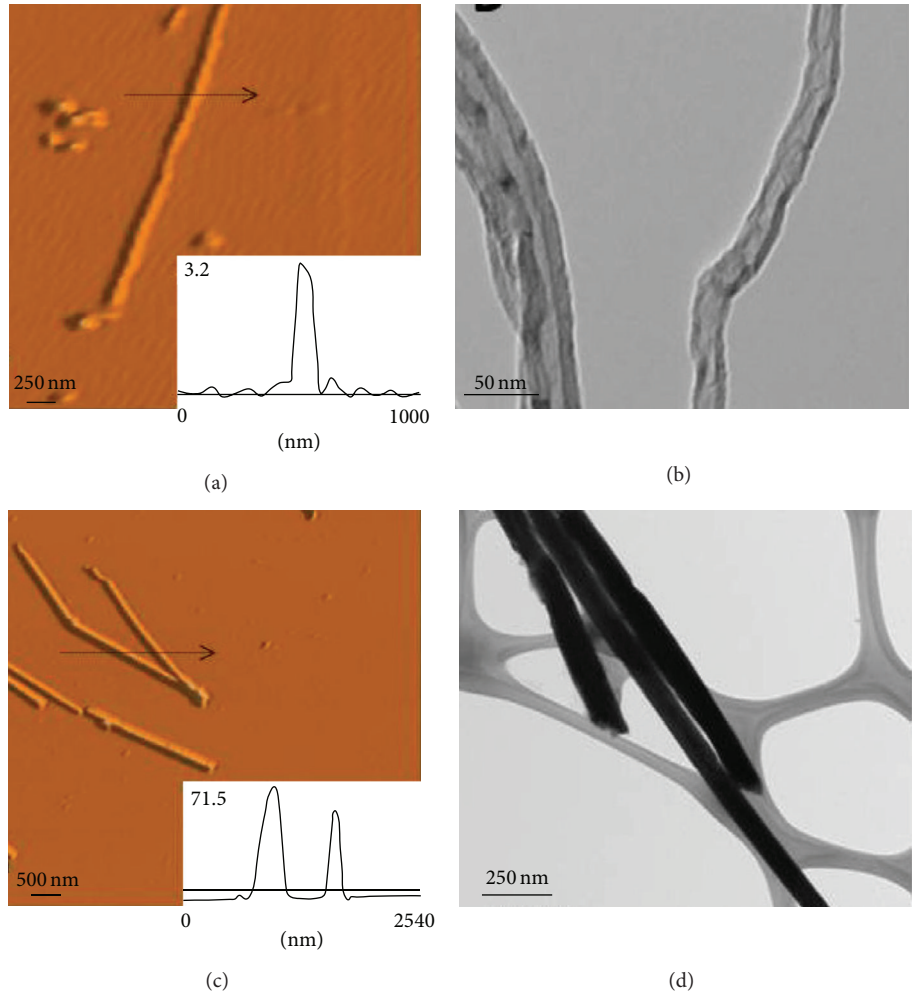

Figure 4: AFM and TEM images of MWCNTs ((a) and (b)) and WSNTs ((c) and (d)). The insets in (a) and (c) show the corresponding height (Z) profiles [41].

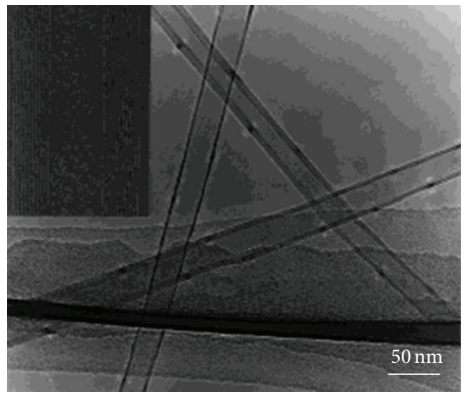

Figure 5: TEM images of BN straight cylindrical nanotubes. The inset shows the perfect ordering of BN tubular layers [46].

macrophages. BNNTs are also found to be noncytotoxic to human embryonic kidney cells and human neuroblastoma cell line. BNNTs are relatively new in the field of composites with very few studies on them being available. BNNTs-reinforced polymer composites have shown improvement in thermal, mechanical, and optical properties [37, 100–104]. In 2005, By Zhi et al. fabricated BNNTs-reinforced composites by using poly(methyl methacrylate) (PMMA), polystyrene (PS), poly(vinyl butyral) (PVB), or poly(ethylene vinyl alcohol) (PEVA) as the matrix and their thermal, electrical, and mechanical properties are evaluated by Vickers microhardness tests [105]. More than 20-fold thermal conductivity improvement in BNNTs-containing polymers is obtained, and such composites maintain good electrical insulation. The coefficient of the thermal expansion of the BNNTs-loaded polymers is dramatically reduced comparing the breakdown electric fields of neat polymers with those of their BNNTs composites including PMMA, PS, PVB, and PEVA. Only in the case of PS dose the breakdown electric field decreases, while in the other three cases, it marginally increases. In any case, all the materials remain insulating and possess a high breakdown electric field. The Vickers hardness of PEVA, PS, and PMMA was only slightly affected when they were loaded with the BNNTs. This indicated that there is no

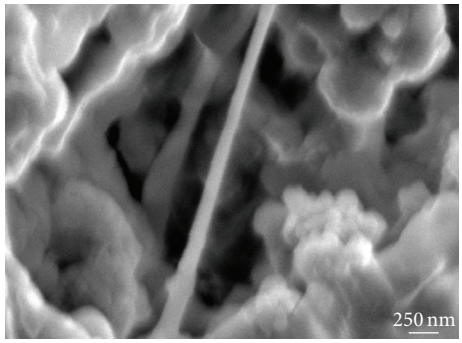

Figure 6: SEM image of the fracture surface of PLC-5BNNT composite showing polymer coated BNNTs of varying diameters [37].

obvious negative effect on the mechanical properties of the composites.

Lahiri et al. [37] studied the cytocompatibility of BNNTs reinforced polylactide-polycaprolactone (PLC) copolymer composite with osteoblasts and macrophages in vitro in 2010. The results show that the BNNTs addition to PLC enhances the tensile strength and also resulted in an increase in the expression levels of the Runx2 gene, the main regulator of osteoblast differentiation. Stress-strain behavior shows a gradual increase in the tensile strength with the addition of BNNTs from 2.67 MPa in PLC to 4.98 and 5.59 MPa for PLC-2BNNTs and PLC-5BNNTs, respectively. Tensile strength at 2.4 strain increases by 87% and 109%, with addition of 2 and 5 wt.% BNNTs, respectively. SEM images of the fracture surface of PLC-5BNNTs (Figure 6) show the BNNTs bridges within PLC matrix. Dangling BNNTs with the other end fully embedded in the polymer matrix. Cytotoxicity assay of bare BNNTs on osteoblast and macrophage cells shows that presence of BNNTs does not increase the number of dead cells and hence are biocompatible to these cells. Osteoblast cell viability study on polymer films reveals a 30% increase in live to dead cells ratio with BNNTs addition in PLC. Gene expression results indicate accelerated osteoblast differentiation and growth in the presence of BNNTs. Biodegradable PLC-BNNTs composite films, with improved mechanical properties and biocompatibility, have been successfully synthesized for their possible application in orthopedic scaffolds. In the same year, Lahiri et al. propose BNNTs reinforced hydroxyapatite (HA) as a composite material for orthopedic implant application. HA-4 wt% BNNTs composite offers excellent mechanical properties—120% increment in elastic modulus, 129% higher hardness, and 86% more fracture toughness, as compared to HA [38]. HA-BNNTs composite also showed 75% improvement in the wear resistance. Tribological behavior of HA and HA-BNNTs composite is quantified in terms of coefficient of friction (CoF) and wear volume loss. The CoF increases by ~25% with BNNTs reinforcement in HA. The presence of BNNTs decreases the wear volume loss of HA matrix by 75%. Proliferation and viability of osteoblast cells are evaluated on HA and HA-BNNTs surface after in vitro culturing for 1, 3, and 5 days. The population of the osteoblast also increases visibly from 1 to 3 days on both surfaces. This observation indicated that HA and HA-BNNTs surfaces are suitable for osteoblast cell proliferation. Population of osteoblast cells is slightly denser on HA-BNNTs surface than HA after 3 days of culture. Osteoblast proliferation and cell viability showed no adverse effect of BNNTs addition. HA-BNNTs composite is, thus, envisioned as a potential material for stronger orthopedic implants.

We summarized the properties of the polymer composites reinforced by nanotubes mentioned in this paper in Table 2.

5. Conclusion and Future Developments

In this review, we provide an overview of the research on polymer composites reinforced by CNTs and noncarbonic nanotubes. CNTs and noncarbonic nanotubes reinforced polymer composites are an emerging class of high-performance materials with unique and promising properties. CNTs and noncarbonic nanotubes reinforced polymer, in particular, aimed at taking advantage of nanotubes' superior mechanical properties as well as their high aspect ratio and surface area [106, 107]. CNTs and noncarbonic nanotubes/polymer nanocomposites have the advantage of size compatibility between their constituents. Introducing CNTs and noncarbonic nanotubes to polymer matrices modifies mechanical, electrical, thermal, and morphological properties of the produced nanocomposite. The prospect of obtaining advanced nanocomposites with multifunctional features, for example, materials used for structures and electrical conductors, has attracted the efforts of researchers in both academia and industry [108, 109]. Biomedical in particular recognizes many potential applications such as scaffolds for bone and neural tissue engineering materials [110–112].

The most commonly employed synthetic polymers for tissue engineering are biodegradable polyesters. Although they do not possess adequate mechanical stiffness to provide structural support in bone constructs, they are very easy to manufacture and process compared with biopolymers such as collagen, which are highly labile, or ceramics such as hydroxyapatite, which are difficult to melt, dissolve, or extrude. Advanced polymer-based nanocomposite materials have gained popularity for wide engineering applications which have been conducted in vitro and in vivo environments in research in the past few years. Many researches have also demonstrated the use of nanostructural materials as reinforcements to enhance the mechanical properties and thermal stability of biocompatible polymers for artificial joints and scaffolding [113–115]. To keep highly porous structure of scaffolds, which can further provide an ideal environment for the migration and proliferation of cells, they had better supply and adequate mechanical strength during the initial healing state. Moreover, it is shown that many research efforts have been directed towards producing CNTs and noncarbonic nanotubes/polymer composites for functional and structural applications [116–119].

Emergence of carbon nanotubes raises nanotube research boom, and researchers have prepared a variety of noncarbonic nanotubes. Overall, new trends appear in preparation

Table 2: Property improvements of polymer composites reinforced by nanotubes.

Reinforcement			Biocompatibility		Mechanical properties		References
Type	Content (%)	Matrix	Method	Improvement	Property	Percentage	
MWNT	>95 wt	PLGA	BMSCs cells culture	Improve cell adhesion and proliferation	Tensile stress	54	[34]
MWCNT	—	PLLA	Human fetal osteoblasts cells	Improve cell compatibility	Elastic modulus	67	[35]
MWNT	—	CHI-HA	CCK-8	Improve cells attachment and cell proliferation	Elastic modulus	53	[36]
BNNT	2 wt	PLC	Osteoblast cell	Accelerated osteoblast differentiation and growth	Tensile strength	87	[37]
BNNT	5 wt	PLC	Osteoblast cell	Accelerated osteoblast differentiation and growth	Tensile strength	109	[37]
BNNT	4 wt	HA	HA-BNNT to osteoblasts	Improve osteoblast proliferation and viability	Elastic modulus	120	[38]
WSNT	0.5 wt	Epoxy	—	—	Peel strength	85	[39]
WSNT	2 wt	PMMA	—	—	Elastic modulus	30	[40]
WSNT	0.01–0.2 wt	PPF	—	—	Compressive modulus	60	[41]

of noncarbonic nanotubes which is mainly from random growth transition to controlled growth and from disorder growth transition to order growth. Evaluation of the performance will be the main theme of research in the field of noncarbonic nanotubes and exploring the causes of the growth mechanism and the peculiar physical properties are the focus of research from now on. Contacting the noncarbon nanotubes with the next generation of nanodevices also becomes future research development direction in this area.

There are still some challenges to be confronted. It has become clear that issues of dispersion, alignment, and stress transfer are crucial and often problematic at this size scale. Dispersion is often obtained by using unentangled nanotubes, high viscosities, and high shear rates. A degree of alignment has been successfully obtained using shear and elongation as well as, to a lesser extent, magnetic and electrical fields. However, the most critical factor is the production and how to achieve efficient, fast, large, and continuous production of low-cost high purity nanotube is also a need to solve practical problems, such as the progress of research on BNNTs is still limited by the poor availability of BNNT samples for widespread investigation of their properties and applications. The lack of a simple and straightforward production process has made it extremely difficult to perform an accurate biocompatibility investigation [120, 121]. Recently, new techniques have been developed to obtain high-purity BNNTs using common furnaces exploited for CNT synthesis [122, 123]. This will allow an increment of BNNT production and a more sustained availability of good samples for future biological investigations.

In conclusion, the improvement and application of these composites will depend on how effectively we can handle the challenges. The significant progress in the understanding of these composite systems within the past few years points toward a bright future.

Conflict of Interests

The authors declare that there is no conflict of interests regarding the publication of this paper.

Acknowledgments

The authors acknowledge the financial support from the Liaoning Provincial Department of Education Sciences Research Grant for Research on Advanced Medical Technology (L2011131). The authors acknowledge the graduate students in Department of Prosthodontics, School of Stomatology, China Medical University, for their kind help.

References

[1] D. J. Mooney and A. G. Mikos, "Growing new organs," *Scientific American*, vol. 280, no. 4, pp. 60–65, 1999.

[2] C. T. Laurencin, F. K. Ko, M. D. Borden, J. A. Cooper Jr., W.-J. Li, and M. A. Attawia, "Fiber based tissue engineered scaffolds for musculoskeletal applications: in vitro cellular response," in *Biomedical Materials-Drug Delivery, Implants and Tissue Engineering*, vol. 550 of *MRS Proceedings*, pp. 127–135, December 1998.

[3] R. Langer and J. P. Vacanti, "Tissue engineering," *Science*, vol. 260, no. 5110, pp. 920–926, 1993.

[4] A. S. Mistry and A. G. Mikos, "Tissue engineering strategies for bone regeneration," *Advances in Biochemical Engineering/Biotechnology*, vol. 94, pp. 1–22, 2005.

[5] M. A. C. Stuart, W. T. S. Huck, J. Genzer et al., "Emerging applications of stimuli-responsive polymer materials," *Nature Materials*, vol. 9, no. 2, pp. 101–113, 2010.

[6] X. M. Li, R. Cui, W. Liu, L. Sun, and F. Watari, "The use of nanoscaled fibers or tubes to improve biocompatibility and bioactivity of biomedical materials," *Journal of Nanomaterials*, vol. 2013, Article ID 728130, 16 pages, 2013.

[7] R. W. Siegel and G. E. Fougere, "Mechanical properties of nanophase metals," *Nanostructured Materials*, vol. 6, no. 1–4, pp. 205–216, 1995.

[8] S. B. Lee, D. T. Mitchell, L. Trofin, T. K. Nevanen, H. Söderlund, and C. R. Martin, "Antibody-based bio-nanotube membranes for enantiomeric drug separations," *Science*, vol. 296, no. 5576, pp. 2198–2200, 2002.

[9] D. T. Mitchell, S. B. Lee, L. Trofin et al., "Smart nanotubes for bioseparations and biocatalysis," *Journal of the American Chemical Society*, vol. 124, no. 40, pp. 11864–11865, 2002.

[10] A. Rothschild, J. Sloan, and R. Tenne, "Growth of WS2 nanotubes phases," *Journal of the American Chemical Society*, vol. 122, no. 21, pp. 5169–5179, 2000.

[11] M. Nath, A. Govindaraj, and C. N. R. Rao, "Simple synthesis of MoS2 and WS2 nanotubes," *Advanced Materials*, vol. 13, no. 4, pp. 283–286, 2001.

[12] R. Kinenkamp, R. Engelhardt, K. Ernst, S. Fiechter, I. Sieber, and R. Könenkamp, "Hexagonal nanotubes of ZnS by chemical conversion of monocrystalline ZnO columns," *Applied Physics Letters*, vol. 78, p. 3687, 2001.

[13] O. R. Lourie, C. R. Jones, B. M. Bartlett, P. C. Gibbons, R. S. Ruoff, and W. E. Buhro, "CVD growth of boron nitride nanotubes," *Chemistry of Materials*, vol. 12, no. 7, pp. 1808–1810, 2000.

[14] C. Ye, G. Meng, Z. Jiang, Y. Wang, G. Wang, and L. Zhang, "Rational growth of Bi2S3 nanotubes from quasi-two-dimensional precursors," *Journal of the American Chemical Society*, vol. 124, no. 51, pp. 15180–15181, 2002.

[15] M. Nath and C. N. R. Rao, "New metal disulfide nanotubes," *Journal of the American Chemical Society*, vol. 123, no. 20, pp. 4841–4842, 2001.

[16] D. H. Galvan, J. H. Kim, M. B. Maple, M. Avalos-Borja, and E. Adem, "Formation of NbSe2 nanotubes by electron irradiation," *Fullerene Science and Technology*, vol. 8, no. 3, pp. 143–151, 2000.

[17] Q. Wu, Z. Hu, X. Wang et al., "Synthesis and characterization of faceted hexagonal aluminum nitride nanotubes," *Journal of the American Chemical Society*, vol. 125, no. 34, pp. 10176–10177, 2003.

[18] J. Goldberger, R. He, Y. Zhang et al., "Single-crystal gallium nitride nanotubes," *Nature*, vol. 422, no. 6932, pp. 599–602, 2003.

[19] E. P. A. M. Bakkers and M. A. Verheijen, "Synthesis of InP nanotubes," *Journal of the American Chemical Society*, vol. 125, no. 12, pp. 3440–3441, 2003.

[20] R. Fan, Y. Wu, D. Li, M. Yue, A. Majumdar, and P. Yang, "Fabrication of silica nanotube arrays from vertical silicon nanowire templates," *Journal of the American Chemical Society*, vol. 125, no. 18, pp. 5254–5255, 2003.

[21] X. H. Zhang, S.-Y. Xie, Z.-Y. Jiang et al., "Rational design and fabrication of ZnO nanotubes from nanowire templates in a microwave plasma system," *The Journal of Physical Chemistry B*, vol. 107, no. 37, p. 10114, 2003.

[22] X. Li, H. Liu, X. Niu et al., "The use of carbon nanotubes to induce osteogenic differentiation of human adipose-derived MSCs in vitro and ectopic bone formation in vivo," *Biomaterials*, vol. 33, no. 19, pp. 4818–4827, 2012.

[23] S. Iijima, "Helical microtubules of graphitic carbon," *Nature*, vol. 354, no. 6348, pp. 56–58, 1991.

[24] J. Cveticanin, G. Joksic, A. Leskovac, S. Petrovic, A. V. Sobot, and O. Neskovic, "Using carbon nanotubes to induce micronuclei and double strand breaks of the DNA in human cells," *Nanotechnology*, vol. 21, no. 1, Article ID 015102, 2010.

[25] D. H. Robertson, D. W. Brenner, and J. W. Mintmire, "Energetics of nanoscale graphitic tubules," *Physical Review B*, vol. 45, no. 21, pp. 12592–12595, 1992.

[26] B. I. Yakobson, C. J. Brabec, and J. Bernholc, "Nanomechanics of carbon tubes: instabilities beyond linear response," *Physical Review Letters*, vol. 76, no. 14, pp. 2511–2514, 1996.

[27] X. Li, L. Wang, Y. Fan, Q. Feng, and F.-Z. Cui, "Biocompatibility and toxicity of nanoparticles and nanotubes," *Journal of Nanomaterials*, vol. 2012, Article ID 548389, 2012.

[28] J. P. Lu, "Elastic properties of carbon nanotubes and nanoropes," *Physical Review Letters*, vol. 79, no. 7, pp. 1297–1300, 1997.

[29] E. W. Wong, P. E. Sheehan, and C. M. Lieber, "Nanobeam mechanics: elasticity, strength, and toughness of nanorods and nanotubes," *Science*, vol. 277, no. 5334, pp. 1971–1975, 1997.

[30] C. F. Cornwell and L. T. Wille, "Elastic properties of single-walled carbon nanotubes in compression," *Solid State Communications*, vol. 101, no. 8, pp. 555–558, 1997.

[31] Y. Usui, K. Aoki, N. Narita et al., "Carbon nanotubes with high bone-tissue compatibility and bone-formation acceleration effects," *Small*, vol. 4, no. 2, pp. 240–246, 2008.

[32] X. Li, X. Liu, J. Huang, Y. Fan, and F.-Z. Cui, "Biomedical investigation of CNT based coatings," *Surface and Coatings Technology*, vol. 206, no. 4, pp. 759–766, 2011.

[33] X. Li, H. Gao, M. Uo et al., "Maturation of osteoblast-like SaoS2 induced by carbon nanotubes," *Biomedical Materials*, vol. 4, no. 1, Article ID 015005, 2009.

[34] H. Zhang, "Electrospun poly (lactic-co-glycolic acid)/ multi-walled carbon nanotubes composite scaffolds for guided bone tissue regeneration," *Journal of Bioactive and Compatible Polymers*, vol. 26, no. 4, pp. 347–362, 2011.

[35] G. Vozzi, C. Corallo, and C. Daraio, "Pressure-activated microsyringe composite scaffold of poly(L -lactic acid) and carbon nanotubes for bone tissue engineering," *Journal of Applied Polymer Science*, vol. 129, no. 2, pp. 528–536, 2013.

[36] L. Chen, J. Hu, X. Shen, and H. Tong, "Synthesis and characterization of chitosan-multiwalled carbon nanotubes/hydroxyapatite nanocomposites for bone tissue engineering," *Journal of Materials Science: Materials in Medicine*, vol. 24, no. 8, pp. 1843–1851, 2013.

[37] D. Lahiri, F. Rouzaud, T. Richard et al., "Boron nitride nanotube reinforced polylactide-polycaprolactone copolymer composite: mechanical properties and cytocompatibility with osteoblasts and macrophages in vitro," *Acta Biomaterialia*, vol. 6, no. 9, pp. 3524–3533, 2010.

[38] D. Lahiri, V. Singh, A. P. Benaduce, S. Seal, L. Kos, and A. Agarwal, "Boron nitride nanotube reinforced hydroxyapatite composite: mechanical and tribological performance and in-vitro biocompatibility to osteoblasts," *Journal of the Mechanical Behavior of Biomedical Materials*, vol. 4, no. 1, pp. 44–56, 2011.

[39] E. Zohar, S. Baruch, M. Shneider et al., "The effect of WS2 nanotubes on the properties of epoxy-based nanocomposites," *Journal of Adhesion Science and Technology*, vol. 25, no. 13, pp. 1603–1617, 2011.

[40] C. S. Reddy, A. Zak, and E. Zussman, "WS2 nanotubes embedded in PMMA nanofibers as energy absorptive material," *Journal of Materials Chemistry*, vol. 21, no. 40, pp. 16086–16093, 2011.

[41] G. Lalwani, A. M. Henslee, B. Farshid et al., "Tungsten disulfide nanotubes reinforced biodegradable polymers for bone tissue engineering," *Acta Biomaterialia*, vol. 9, no. 9, pp. 8365–8373, 2013.

[42] R. Bacon, "Growth, structure, and properties of graphite whiskers," *Journal of Applied Physics*, vol. 31, no. 2, pp. 283–290, 1960.

[43] C. E. Baddour and C. Briens, "Carbon nanotube synthesis: a review," *International Journal of Chemical Reactor Engineering*, vol. 3, no. 1, 2005.

[44] M. S. P. Shaffer and J. K. W. Sandler, "Carbon nanotube/nanofibre polymer composites," in *Processing and Properties of Nanocomposites*, S. G. Advani, Ed., pp. 1–60, World Scientific, New York, NY, USA, 2006.

[45] N. G. Chopra, R. J. Luyken, K. Cherrey et al., "Boron nitride nanotubes," *Science*, vol. 269, no. 5226, pp. 966–967, 1995.

[46] R. Ma, Y. Bando, and T. Sato, "Controlled synthesis of BN nanotubes, nanobamboos, and nanocables," *Advanced Materials*, vol. 14, no. 5, pp. 366–368, 2002.

[47] T. Laude, Y. Matsui, A. Marraud, and B. Jouffrey, "Long ropes of boron nitride nanotubes grown by a continuous laser heating," *Applied Physics Letters*, vol. 76, no. 22, pp. 3239–3241, 2000.

[48] V. V. Pokropivny, V. V. Skorokhod, G. S. Oleinik et al., "Boron nitride analogs of fullerenes (the fulborenes), nanotubes, and fullerites (the fulborenites)," *Journal of Solid State Chemistry*, vol. 154, no. 1, pp. 214–222, 2000.

[49] K. B. Shelimov and M. Moskovits, "Composite nanostructures based on template-grown boron nitride nanotubules," *Chemistry of Materials*, vol. 12, no. 1, pp. 250–254, 2000.

[50] Y. Chen, J. Fitz Gerald, J. S. Williams, and S. Bulcock, "Synthesis of boron nitride nanotubes at low temperatures using reactive ball milling," *Chemical Physics Letters*, vol. 299, no. 3-4, pp. 260–264, 1999.

[51] L. Xu, Y. Peng, Z. Meng et al., "A co-pyrolysis method to boron nitride nanotubes at relative low temperature," *Chemistry of Materials*, vol. 15, no. 13, pp. 2675–2680, 2003.

[52] X. Li, L. Wang, Y. Fan, Q. Feng, F.-Z. Cui, and F. Watari, "Nanostructured scaffolds for bone tissue engineering," *Journal of Biomedical Materials Research Part A*, vol. 101, no. 8, pp. 2424–2435, 2013.

[53] M. Moniruzzaman and K. I. Winey, "Polymer nanocomposites containing carbon nanotubes," *Macromolecules*, vol. 39, no. 16, pp. 5194–5205, 2006.

[54] N. Grossiord, J. Loos, O. Regev, and C. E. Koning, "Toolbox for dispersing carbon nanotubes into polymers to get conductive nanocomposites," *Chemistry of Materials*, vol. 18, no. 5, pp. 1089–1099, 2006.

[55] J.-H. Du, J. Bai, and H.-M. Cheng, "The present status and key problems of carbon nanotube based polymer composites," *Express Polymer Letters*, vol. 1, no. 5, pp. 253–273, 2007.

[56] X. Xu, M. M. Thwe, C. Shearwood, and K. Liao, "Mechanical properties and interfacial characteristics of carbon-nanotube-reinforced epoxy thin films," *Applied Physics Letters*, vol. 81, no. 15, pp. 2833–2835, 2002.

[57] K.-T. Lau, S.-Q. Shi, and H.-M. Cheng, "Micro-mechanical properties and morphological observation on fracture surfaces of carbon nanotube composites pre-treated at different temperatures," *Composites Science and Technology*, vol. 63, no. 8, pp. 1161–1164, 2003.

[58] X. Gong, J. Liu, S. Baskaran, R. D. Voise, and J. S. Young, "Surfactant-assisted processing of carbon nanotube/polymer composites," *Chemistry of Materials*, vol. 12, no. 4, pp. 1049–1052, 2000.

[59] Q.-H. Zhang and D.-J. Chen, "Percolation threshold and morphology of composites of conducting carbon black/polypropylene/EVA," *Journal of Materials Science*, vol. 39, no. 5, pp. 1751–1757, 2004.

[60] D. E. Hill, Y. Lin, A. M. Rao, L. F. Allard, and Y.-P. Sun, "Functionalization of carbon nanotubes with polystyrene," *Macromolecules*, vol. 35, no. 25, pp. 9466–9471, 2002.

[61] J. Y. Kim and S. H. Kim, "Influence of multiwall carbon nanotube on physical properties of poly(ethylene 2,6-naphthalate) nanocomposites," *Journal of Polymer Science Part B*, vol. 44, no. 7, pp. 1062–1071, 2006.

[62] O. S. Carneiro and J. M. Maia, "Rheological behavior of (short) carbon fiber/thermoplastic composites. Part I: the influence of fiber type, processing conditions and level of incorporation," *Polymer Composites*, vol. 21, no. 6, pp. 960–969, 2000.

[63] R. Haggenmueller, H. H. Gommans, A. G. Rinzler, J. E. Fischer, and K. I. Winey, "Aligned single-wall carbon nanotubes in composites by melt processing methods," *Chemical Physics Letters*, vol. 330, no. 3-4, pp. 219–225, 2000.

[64] S. Kumar, H. Doshi, M. Srinivasarao, J. O. Park, and D. A. Schiraldi, "Fibers from polypropylene/nano carbon fiber composites," *Polymer*, vol. 43, no. 5, pp. 1701–1703, 2002.

[65] P.-C. Ma, N. A. Siddiqui, G. Marom, and J.-K. Kim, "Dispersion and functionalization of carbon nanotubes for polymer-based nanocomposites: a review," *Composites Part A*, vol. 41, no. 10, pp. 1345–1367, 2010.

[66] J.-H. Du, J. Bai, and H.-M. Cheng, "The present status and key problems of carbon nanotube based polymer composites," *Express Polymer Letters*, vol. 1, no. 5, pp. 253–273, 2007.

[67] Z. Jia, Z. Wang, C. Xu et al., "Study on poly(methyl methacrylate)/carbon nanotube composites," *Materials Science and Engineering A*, vol. 271, no. 1-2, pp. 395–400, 1999.

[68] F. H. Gojny, M. H. G. Wichmann, U. Köpke, B. Fiedler, and K. Schulte, "Carbon nanotube-reinforced epoxy-composites: enhanced stiffness and fracture toughness at low nanotube content," *Composites Science and Technology*, vol. 64, no. 15, pp. 2363–2371, 2004.

[69] A. Moisala, Q. Li, I. A. Kinloch, and A. H. Windle, "Thermal and electrical conductivity of single- and multi-walled carbon nanotube-epoxy composites," *Composites Science and Technology*, vol. 66, no. 10, pp. 1285–1288, 2006.

[70] P. C. Ma, B. Z. Tang, and J.-K. Kim, "Effect of CNT decoration with silver nanoparticles on electrical conductivity of CNT-polymer composites," *Carbon*, vol. 46, no. 11, pp. 1497–1505, 2008.

[71] T. V. Kosmidou, A. S. Vatalis, C. G. Delides, E. Logakis, P. Pissis, and G. C. Papanicolaou, "Structural, mechanical and electrical characterization of epoxy-amine/carbon black nanonocomposites," *Express Polymer Letters*, vol. 2, no. 5, pp. 364–372, 2008.

[72] P.-C. Ma, M.-Y. Liu, H. Zhang et al., "Enhanced electrical conductivity of nanocomposites containing hybrid fillers of carbon nanotubes and carbon black," *ACS Applied Materials and Interfaces*, vol. 1, no. 5, pp. 1090–1096, 2009.

[73] W. Wang, F. Watari, M. Omori et al., "Mechanical properties and biological behavior of carbon nanotube/polycarbosilane composites for implant materials," *Journal of Biomedical Materials Research Part B*, vol. 82, no. 1, pp. 223–230, 2007.

[74] W. Wang, Y. Zhu, F. Watari et al., "Carbon nanotubes/hydroxyapatite nanocomposites fabricated by spark plasma sintering for bonegraft applications," *Applied Surface Science*, vol. 262, pp. 194–199, 2012.

[75] X. Li, Y. Fan, and F. Watari, "Current investigations into carbon nanotubes for biomedical application," *Biomedical Materials*, vol. 5, no. 2, Article ID 022001, 2010.

[76] W. Song, Z. Zheng, W. Tang, and X. Wang, "A facile approach to covalently functionalized carbon nanotubes with biocompatible polymer," *Polymer*, vol. 48, no. 13, pp. 3658–3663, 2007.

[77] A. Gupta, M. D. Woods, K. D. Illingworth et al., "Single walled carbon nanotube composites for bone tissue engineering," *Journal of Orthopaedic Research*, vol. 31, no. 9, pp. 1374–1381, 2013.

[78] A. Abarrategi, M. C. Gutiérrez, C. Moreno-Vicente et al., "Multiwall carbon nanotube scaffolds for tissue engineering purposes," *Biomaterials*, vol. 29, no. 1, pp. 94–102, 2008.

[79] E. Zawadzak, M. Bil, J. Ryszkowska et al., "Polyurethane foams electrophoretically coated with carbon nanotubes for tissue engineering scaffolds," *Biomedical Materials*, vol. 4, no. 1, Article ID 015008, 2009.

[80] X. Shi, B. Sitharaman, Q. P. Pham et al., "Fabrication of porous ultra-short single-walled carbon nanotube nanocomposite scaffolds for bone tissue engineering," *Biomaterials*, vol. 28, no. 28, pp. 4078–4090, 2007.

[81] R. Tenne, L. Margulis, M. Genut, and G. Hodes, "Polyhedral and cylindrical structures of tungsten disulphide," *Nature*, vol. 360, no. 6403, pp. 444–446, 1992.

[82] I. Kaplan-Ashiri, S. R. Cohen, K. Gartsman et al., "On the mechanical behavior of WS2 nanotubes under axial tension and compression," *Proceedings of the National Academy of Sciences of the United States of America*, vol. 103, no. 3, pp. 523–528, 2006.

[83] M. S. Wang, I. Kaplan-Ashiri, X. L. Wei et al., "*In situ* TEM measurements of the mechanical properties and behavior of WS2 Nanotubes," *Nano Research*, vol. 1, no. 1, pp. 22–31, 2008.

[84] E. Zohar, S. Baruch, M. Shneider et al., "The effect of WS2 nanotubes on the properties of epoxy-based nanocomposites," *Journal of Adhesion Science and Technology*, vol. 25, no. 13, pp. 1603–1617, 2011.

[85] B. Sitharaman, X. Shi, L. A. Tran et al., "Injectable in situ cross-linkable nanocomposites of biodegradable polymers and carbon nanostructures for bone tissue engineering," *Journal of Biomaterials Science, Polymer Edition*, vol. 18, no. 6, pp. 655–671, 2007.

[86] X. Shi, B. Sitharaman, Q. P. Pham et al., "Fabrication of porous ultra-short single-walled carbon nanotube nanocomposite scaffolds for bone tissue engineering," *Biomaterials*, vol. 28, no. 28, pp. 4078–4090, 2007.

[87] X. Shi, J. L. Hudson, P. P. Spicer, J. M. Tour, R. Krishnamoorti, and A. G. Mikos, "Injectable nanocomposites of single-walled carbon nanotubes and biodegradable polymers for bone tissue engineering," *Biomacromolecules*, vol. 7, no. 7, pp. 2237–2242, 2006.

[88] G. Lalwani, A. M. Henslee, B. Farshid et al., "Two-dimensional nanostructure-reinforced biodegradable polymeric nanocomposites for bone tissue engineering," *Biomacromolecules*, vol. 14, no. 3, pp. 900–909, 2013.

[89] E. T. Thostenson, Z. Ren, and T.-W. Chou, "Advances in the science and technology of carbon nanotubes and their composites: a review," *Composites Science and Technology*, vol. 61, no. 13, pp. 1899–1912, 2001.

[90] S. Bal and S. S. Samal, "Carbon nanotube reinforced polymer composites—a state of the art," *Bulletin of Materials Science*, vol. 30, no. 4, pp. 379–386, 2007.

[91] E. T. Thostenson and T.-W. Chou, "Processing-structure-multi-functional property relationship in carbon nanotube/epoxy composites," *Carbon*, vol. 44, no. 14, pp. 3022–3029, 2006.

[92] P. Pötschke, A. R. Bhattacharyya, and A. Janke, "Carbon nanotube-filled polycarbonate composites produced by melt mixing and their use in blends with polyethylene," *Carbon*, vol. 42, no. 5-6, pp. 965–969, 2004.

[93] L. Ci, J. Suhr, V. Pushparaj, X. Zhang, and P. M. Ajayan, "Continuous carbon nanotube reinforced composites," *Nano Letters*, vol. 8, no. 9, pp. 2762–2766, 2008.

[94] C. S. Reddy, A. Zak, and E. Zussman, "WS2 nanotubes embedded in PMMA nanofibers as energy absorptive material," *Journal of Materials Chemistry*, vol. 21, no. 40, pp. 16086–16093, 2011.

[95] X. Blase, A. Rubio, S. G. Louie, and M. L. Cohen, "Stability and band gap constancy of boron nitride nanotubes?" *Europhysics Letters*, vol. 28, no. 5, p. 335, 1994.

[96] A. Rubio, J. L. Corkill, and M. L. Cohen, "Theory of graphitic boron nitride nanotubes," *Physical Review B*, vol. 49, no. 7, pp. 5081–5084, 1994.

[97] E. Hernández, C. Goze, P. Bernier, and A. Rubio, "Elastic properties of C and $B_xC_yN_z$ composite nanotubes," *Physical Review Letters*, vol. 80, no. 20, pp. 4502–4505, 1998.

[98] C. W. Chang, W.-Q. Han, and A. Zettl, "Thermal conductivity of B-C-N and BN nanotubes," *Applied Physics Letters*, vol. 86, no. 17, Article ID 173102, 3 pages, 2005.

[99] X. Chen, P. Wu, M. Rousseas et al., "Boron nitride nanotubes are noncytotoxic and can be functionalized for interaction with proteins and cells," *Journal of the American Chemical Society*, vol. 131, no. 3, pp. 890–891, 2009.

[100] C. Zhi, Y. Bando, C. Tang et al., "Characteristics of boron nitride nanotube-polyaniline composites," *Angewandte Chemie International Edition*, vol. 44, no. 48, pp. 7929–7932, 2005.

[101] C. Zhi, Y. Bando, C. Tang, S. Honda, H. Kuwahara, and D. Golberg, "Boron nitride nanotubes/polystyrene composites," *Journal of Materials Research*, vol. 21, no. 11, pp. 2794–2800, 2006.

[102] C. Zhi, Y. Bando, T. Terao, C. Tang, H. Kuwahara, and D. Golberg, "Towards thermoconductive, electrically insulating polymeric composites with boron nitride nanotubes as fillers," *Advanced Functional Materials*, vol. 19, no. 12, pp. 1857–1862, 2009.

[103] T. Terao, C. Zhi, Y. Bando, M. Mitome, C. Tang, and D. Golberg, "Alignment of boron nitride nanotubes in polymeric composite films for thermal conductivity improvement," *Journal of Physical Chemistry C*, vol. 114, no. 10, pp. 4340–4344, 2010.

[104] J. Ravichandran, A. G. Manoj, J. Liu, I. Manna, and D. L. Carroll, "A novel polymer nanotube composite for photovoltaic packaging applications," *Nanotechnology*, vol. 19, no. 8, Article ID 085712, 2008.

[105] C. Zhi, Y. Bando, C. Tang, and D. Golberg, "Immobilization of proteins on boron nitride nanotubes," *Journal of the American Chemical Society*, vol. 127, no. 49, pp. 17144–17145, 2005.

[106] W. Wang, Y. H. Zhu, S. Liao, and J. J. Li, "Carbon nanotubes reinforced composites for biomedical applications," *BioMed Research International*, vol. 2014, Article ID 518609, 14 pages, 2014.

[107] X. Li, Q. Feng, X. Liu, W. Dong, and F. Cui, "Collagen-based implants reinforced by chitin fibres in a goat shank bone defect model," *Biomaterials*, vol. 27, no. 9, pp. 1917–1923, 2006.

[108] A. Allaoui, S. Bai, H. M. Cheng, and J. B. Bai, "Mechanical and electrical properties of a MWNT/epoxy composite," *Composites Science and Technology*, vol. 62, no. 15, pp. 1993–1998, 2002.

[109] Z. Jin, K. P. Pramoda, G. Xu, and S. H. Goh, "Dynamic mechanical behavior of melt-processed multi-walled carbon nanotube/poly(methyl methacrylate) composites," *Chemical Physics Letters*, vol. 337, no. 1-3, pp. 43–47, 2001.

[110] S. Ayad, R. Boot-Handford, and M. Humphries, *The Extracellular Matrix Factsbook*, Academic Press, New York, NY, USA, 1998.

[111] X. Li, H. Gao, M. Uo et al., "Effect of carbon nanotubes on cellular functions in vitro," *Journal of Biomedical Materials Research Part A*, vol. 91, no. 1, pp. 132–139, 2009.

[112] T. J. Webster, M. C. Waid, J. L. McKenzie, R. L. Price, and J. U. Ejiofor, "Nano-biotechnology: carbon nanofibres as improved neural and orthopaedic implants," *Nanotechnology*, vol. 15, no. 1, pp. 48–54, 2004.

[113] M. Endo, S. Koyama, Y. Matsuda, T. Hayashi, and Y.-A. Kim, "Thrombogenicity and blood coagulation of a microcatheter prepared from carbon nanotube—nylon-based composite," *Nano Letters*, vol. 5, no. 1, pp. 101–105, 2005.

[114] J. Meng, H. Kong, H. Y. Xu, L. Song, C. Y. Wang, and S. S. Xie, "Improving the blood compatibility of polyurethane using carbon nanotubes as fillers and its implications to cardiovascular surgery," *Journal of Biomedical Materials Research Part A*, vol. 74, no. 2, pp. 208–214, 2005.

[115] X. Shi, J. L. Hudson, P. P. Spicer, J. M. Tour, R. Krishnamoorti, and A. G. Mikos, "Rheological behaviour and mechanical characterization of injectable poly(propylene fumarate)/single-walled carbon nanotube composites for bone tissue engineering," *Nanotechnology*, vol. 16, no. 7, pp. S531–S538, 2005.

[116] E. T. Thostenson, Z. Ren, and T.-W. Chou, "Advances in the science and technology of carbon nanotubes and their composites: a review," *Composites Science and Technology*, vol. 61, no. 13, pp. 1899–1912, 2001.

[117] X. Li, C. A. van Blitterswijk, Q. Feng, F. Cui, and F. Watari, "The effect of calcium phosphate microstructure on bone-related cells in vitro," *Biomaterials*, vol. 29, no. 23, pp. 3306–3316, 2008.

[118] P. M. Ajayan, L. S. Schadler, and P. V. Braun, *Nanocomposite Science and Technology*, Wiley-VCH, Weinheim, Germany, 2006.

[119] J. N. Coleman, U. Khan, and Y. K. Gun'ko, "Mechanical reinforcement of polymers using carbon nanotubes," *Advanced Materials*, vol. 18, no. 6, pp. 689–706, 2006.

[120] J. Wang, C. H. Lee, and Y. K. Yap, "Recent advancements in boron nitride nanotubes," *Nanoscale*, vol. 2, no. 10, pp. 2028–2034, 2010.

[121] C. Zhi, Y. Bando, C. Tang, and D. Golberg, "Boron nitride nanotubes," *Materials Science and Engineering R*, vol. 70, no. 3-6, pp. 92–111, 2010.

[122] C. H. Lee, J. Wang, V. K. Kayatsha, J. Y. Huang, and Y. K. Yap, "Effective growth of boron nitride nanotubes by thermal chemical vapor deposition," *Nanotechnology*, vol. 19, no. 45, Article ID 455605, 2008.

[123] C. H. Lee, M. Xie, V. Kayastha, J. Wang, and Y. K. Yap, "Patterned growth of boron nitride nanotubes by catalytic chemical vapor deposition," *Chemistry of Materials*, vol. 22, no. 5, pp. 1782–1787, 2010.

Hindawi Publishing Corporation
International Journal of Polymer Science
Volume 2014, Article ID 829145, 13 pages
http://dx.doi.org/10.1155/2014/829145

Review Article

3D-Printed Biopolymers for Tissue Engineering Application

Xiaoming Li,[1] Rongrong Cui,[1] Lianwen Sun,[1] Katerina E. Aifantis,[2] Yubo Fan,[1] Qingling Feng,[3] Fuzhai Cui,[3] and Fumio Watari[4]

[1] *Key Laboratory for Biomechanics and Mechanobiology of Ministry of Education, School of Biological Science and Medical Engineering, Beihang University, Beijing 100191, China*
[2] *College of Engineering, University of Arizona, Tucson, AZ 85721, USA*
[3] *State Key Laboratory of New Ceramic and Fine Processing, Tsinghua University, Beijing 100084, China*
[4] *Department of Biomedical Materials and Engineering, Graduate School of Dental Medicine, Hokkaido University, Sapporo 060-8586, Japan*

Correspondence should be addressed to Xiaoming Li; x.m.li@hotmail.com and Yubo Fan; yubofan@buaa.edu.cn

Received 21 January 2014; Accepted 18 March 2014; Published 24 April 2014

Academic Editor: Nicholas Dunne

3D printing technology has recently gained substantial interest for potential applications in tissue engineering due to the ability of making a three-dimensional object of virtually any shape from a digital model. 3D-printed biopolymers, which combine the 3D printing technology and biopolymers, have shown great potential in tissue engineering applications and are receiving significant attention, which has resulted in the development of numerous research programs regarding the material systems which are available for 3D printing. This review focuses on recent advances in the development of biopolymer materials, including natural biopolymer-based materials and synthetic biopolymer-based materials prepared using 3D printing technology, and some future challenges and applications of this technology are discussed.

1. Introduction

Tissue engineering has been an area of immense research in recent years because of its vast potential in the repair or replacement of damaged tissues and organs [1, 2]. The present review will focus on scaffolds as they are one of the three most important factors, including seed cells, growth factors, and scaffolds in tissue engineering [3].

According to Hutmacher [4] a scaffold should satisfy the following criteria: (1) it should be bioresorbable and biocompatible with a controllable degradation and resorption rate to match cell/tissue growth *in vitro/vivo*; (2) it should have suitable surface chemistry for cell attachment, proliferation, and differentiation; (3) it should be three-dimensional and highly porous with an interconnected porous network for cell growth, flow transport of nutrients, and metabolic waste; (4) it should have proper mechanical properties to match the tissues at the site of implantation [5].

Random processes such as foaming [6], emulsification [7] solvent casting, particle/salt leaching [8, 9], freeze drying [10], thermally induced phase separation [11], and electrospinning [12, 13] have been used for the manufacturing of tissue engineering scaffolds. One major drawback is the fact that porous scaffolds fabricated by random processes cannot be produced with complete control of the geometrical parameters, such as pore size, pore interconnection size, and porosity.

Moreover scaffolds with tailored porosity for specific defects are difficult to manufacture with most of these approaches. Such scaffolds can be designed and fabricated using three-dimensional printing (3DP), which is becoming popular due to the ability to directly print porous scaffolds with designed shape, controlled chemistry, and interconnected porosity [14].

3D printing proposes an effective means to assemble all of these necessary components through the use of biomaterials, printing techniques, and even cell delivery methods.

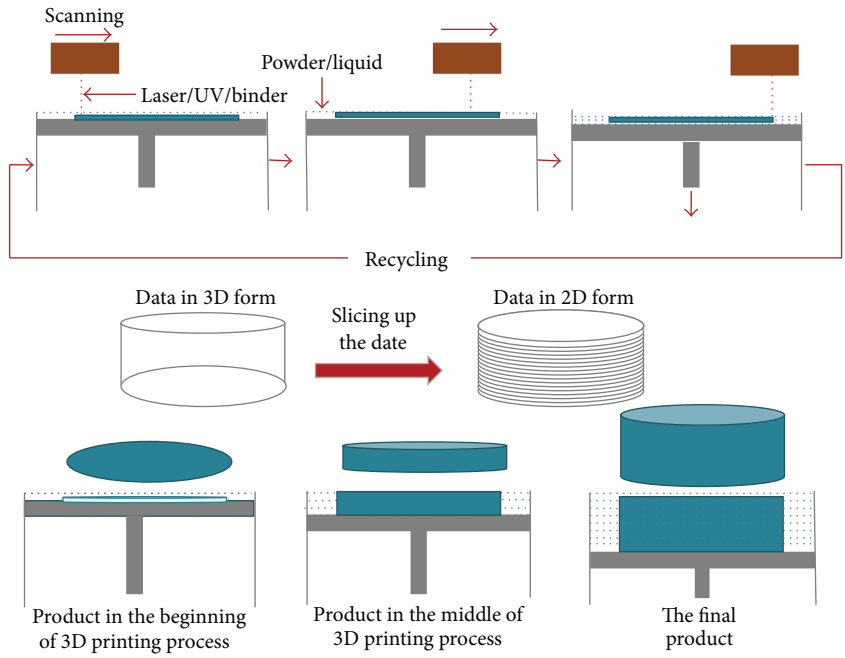

Figure 1: The principle schematic of 3D printing. The data that represents the products is sliced into two dimensions. The data, layer by layer, gets passed through the machine starting at the base of the product, and material is deposited layer by layer, infusing the newest layer of material to the old layer in an additive process.

The standard for 3D-printed tissue engineering constructs is to provide a biomimetic structural environment that facilitates tissue formation and promotes host tissue integration, including hard and soft tissues, whether through scaffold-based or scaffold-free approaches [15].

In this review, the commonly used biopolymers and basic principles of 3D printing will be introduced, as well as the development of polymers fabricated using 3D printing for tissue engineering. The development of natural polymer, synthetic polymer, and their composites is introduced, respectively, and the prospects of the 3D-printed biomaterials are discussed.

2. The Principle of 3D Printing Technology

3D printing is a process of making a three-dimensional object of virtually any shape from a digital model. 3D printing, which is additive manufacturing (AM) technology, is achieved using an additive process, where successive layers of material are laid down in different shapes. The 3D printing technology is used for both prototyping and distributed manufacturing, with applications in industrial design, automative industry, aerospace, architecture, medical industries, tissue engineering, and even food.

The first step of 3D printing is modeling. 3D printing takes virtual models from computer-aided design (CAD) or animation modeling software and "slices" them into digital cross-sections, so that the machine can successively use them as a guideline to print. Depending on the machine used, material or a binding material is deposited on the build bed or platform until the material/binder layering is complete and the final 3D model has been printed. The second step of 3D printing is printing. In this step, the machine reads the design from an stl file and lays down successive layers of liquid, powder, or some other materials to build the model from a series of cross-sections. At last, the 3D-printed object is finished according to the modeling. Some 3D printing techniques are capable of using multiple materials in the course of constructing parts and some may also utilize supports when building. Supports are removable or dissolvable upon completion of the print and the final object can be obtained. Postprocessing may be needed for some 3D-printed objects, while for others it may not be necessary. The principle schematic of 3D printing is shown in Figure 1.

A large number of additive processes including selective laser sintering (SLS), stereolithography (SLA), fused deposition modeling (FDM), and direct metal laser sintering (DMLS) are available for 3D printing. They differ among them in the materials that can be used and in the way the layers are deposited to create parts. For biopolymers, the most commonly used processes are SLS, SLA, and FDM.

In SLS, one of the many 3D printing technologies available, the slices are written by a carbon dioxide (CO_2) laser beam. The written process derives from the coalescence of particles through sinterization caused by the application of laser and thermal energy [16, 17]. The slice geometries are defined by selective sintering that follows the laser beam scanning onto the powder layers, according to the digital slices. The interaction of the laser beam with the powder raises the powder temperature to the point of melting and causes the particles to be fused together to form a solid mass.

The sintered material forms the object and the powder supports it during its manufacturing [18]. In the final stage of the SLS process the object is removed from the powder environment and it is cleaned from the remaining powder attached to its walls [17].

In SLA, thin successive layers are photocrosslinked by ultraviolet or visible light that induces photopolymerization of a reactive system according to a sliced CAD model. The technique requires a liquid photocrosslinkable resin with defined viscosity properties and, for that reason, reactive or nonreactive diluents are typically used. SLA can generate a large number of widely differing 3D structures in a reproducible way with precise control over the final microstructure and geometry [19]. In addition, nonlinear scaffold geometries can be produced.

In FDM, like other RP methods, one layer at a time is printed but typically the material is directly deposited on a surface where it is desired. Extrusion through a nozzle results in a cylindrical coiled morphology of each layer [20]. FDM uses a small temperature-controlled extruder to force out a thermoplastic filament material and deposit the semimolten polymer onto a platform in a layer by layer process. The monofilament is moved by two rollers and acts as a piston to drive the semimolten extrudate. At the end of each finished layer, the base platform is lowered and the next layer is deposited.

3. Materials Fabricated by 3D Printing for Tissue Engineering

In the search for alternatives to conventional treatment strategies for the repair or replacement of missing or malfunctioning human tissues and organs, promising solutions have been explored through tissue engineering approaches. Biomaterials-based scaffolds have played a pivotal role in this quest. At present, biomaterials have been widely used in skin [21, 22], cartilage [23], bone [24, 25], tendons [26], vessels [27, 28], nerves [29], bladder [30], and liver [31] tissue engineering. When designing a polymeric scaffold, a combination of biological and engineering requisites is considered within an application-specific manner. Material selection for tissue engineering applications is based on several important factors including biocompatibility, degradability, surface characteristics, processability, and mechanical properties [32].

Both natural and synthetic polymers have been used for biomedical applications. Natural polymers, such as collagen [33], chondroitin sulphate [34, 35], chitin [36, 37], and chitosan [38, 39], are widely used for tissue engineering and organ regeneration, since they facilitate cell attachment and maintenance of differentiation. Synthetic polymers such as poly(ε-caprolactone) (PCL), poly(lactic acid) (PLA), poly (glycolic acid) (PGA), poly(lactic-*co*-glycolic acid) (PLGA), and other synthetic polymers can provide extreme versatility regarding the control of their physicochemical properties and are generally easy to process into tissue engineering scaffolds [40–42]. Synthesis of these polymers can be tailored to yield a specific molecular weight, chemical structure, end group chemistry, and composition (homopolymers, copolymers, and polymer blends) in terms of tissue response. Furthermore, the biodegradation time of synthetic polymers makes them more attractive over natural ones [43].

Among the polymers used in tissue engineering, poly(α-hydroxy esters) (such as PLA, PGA, and PLGA) have attracted extensive attention for a variety of biomedical applications. Besides, PCL has been widely utilized as a tissue engineering scaffold. Blends and block copolymers of PCL with other poly(α-hydroxy esters) (such as poly(L-lactic acid-*co*-ε-caprolactone) (PLLACL) or poly(D,L-lactic acid-*co*-ε-caprolactone) (PDLLACL)) have been used to produce polymers with tailored properties [44–46]. In order to increase wettability, biocompatibility, or softness of bioresorbable polymers, blends and copolymers with nondegradable poly (ethylene glycol) (PEG) have been developed, such as block copolymers of PEG with poly(L-lactide) (PLLA), PLGA, and PCL [46, 47].

3.1. Natural Polymer and Its Composites Fabricated by 3D Printing Technology. Gelatin, the main component of hydrolyzed collagen, has been given much attention due to its natural origins in the extracellular matrix (ECM) and its ability to suspend cells in a gel at low temperatures [15]. Yan and others manually printed a liver tissue construct made of gelatin and chitosan mixed with hepatocytes followed by glutaraldehyde fixation [15, 48].

Research that explores natural polymers (such as starch) with water-based binders for use in direct 3D printing methods has shown promising results and can be combined with synthetic polymers for the desired biodegradable and mechanical properties. Starch-based polymers allow for increased degradation time and consequently expanded porosity as cellular integration increases, which is optimal for bone tissue engineering. A unique blend of starch-based polymer powders (cornstarch, dextran, and gelatin) was developed for the 3DP process by Lam et al. [49]. The scaffold properties were characterized by scanning electron microscopy (SEM), differential scanning calorimetry (DSC), porosity analysis, and compression tests. The analysis and tests demonstrated that porous 3D scaffolds created by a new blend of materials through 3DP were achievable. Starch and cellulose composites were shown to be biocompatible, which has been utilized in polymers designed for controlled drug delivery [50, 51] and bone cement [52, 53]. Salmoria et al. present the rapid fabrication of starch-cellulose and cellulose acetate scaffolds by SLS and the evaluation of the laser power, laser scan speed, and the polymer particle size influence on the scaffold properties [54]. The specimens with small particle sizes presented a higher degree of sintering and a significant level of closed pores, as indicated by the density measurements and mechanical tests, while the mechanical properties of specimens prepared with larger particles presented lower values of elastic modulus and tensile strength because of the low degree of sintering and limited number of unions. The results obtained showed that it is possible to fabricate biopolymer scaffold structures using starch-cellulose and cellulose acetate using SLS by process optimization based on the adjustment of laser power and scan speed. Specimens prepared with small particle size exhibit

satisfactory mechanical properties and level of porosity for the design and fabrication of scaffolds with potential use in tissue engineering and drug delivery [54].

The application of 3D printing in tissue engineering has enabled new methods for the printing of cells and matrix materials to fabricate tissue-analogous structures [55–57]. The practicality of using 3D printing to fabricate cell-laden constructs was demonstrated, where cells were localized as intended and the cell viability of the fabricated constructs was high.

Gelatin methacrylate was used to fabricate via the proposed projection stereolithography (PSL) platform, which can be used to design intricate 3D structure that can be engineered to mimic the microarchitecture of tissues, based on CAD [58]. Variation of the structure and prepolymer concentration enabled tailoring the mechanical properties of the scaffolds. A dynamic cell seeding method was utilized to improve the coverage of the scaffold throughout its thickness. The results demonstrated that the interconnectivity of pores allowed for uniform human umbilical vein endothelial cells (HUVECs) distribution and proliferation in the scaffolds, leading to high cell density and confluence at the end of the culture period. Moreover, immunohistochemistry results showed that cells seeded on the scaffold maintained their endothelial phenotype, demonstrating the biological functionality of the microfabricated GelMA scaffolds.

In 2014 Billiet et al. [59] reported the 3D printing of gelatin methacrylamide cell-laden tissue-engineered constructs with high cell viability for liver tissue engineering. They used VA-086 as a photoinitiator with enhanced biocompatibility compared to the conventional Irgacure 2959. A parametric study on the printing of gelatins was performed in order to characterize and compare construct architectures. The parameters including hydrogel building block concentration, the printing temperature, the printing pressure, the printing speed, and the cell density were analyzed in depth and optimized. The scaffolds can be designed having a 100% interconnected pore network in the gelatin concentration range of 10–20 w/v%. Control over the deposited strand dimensions can be guaranteed due to the physical properties of gelatin methacrylamide hydrogels and machine operating parameters. High viability (>97%) constructs displaying a maintained expression of liver specific functions were obtained using the VA-086 photoinitiator.

3.2. Synthetic Biopolymers and Their Composites Fabricated by 3D Printing

3.2.1. Synthetic Biopolymers Fabricated by 3D Printing. Among several tissues that are being actively researched, bone is one of the most widely studied, due to its critical functions in everyday life. When bone experiences disease or trauma, the defective portion often needs to be surgically removed [60]. Bone is able to self-regenerate; however, regeneration is limited to a distance of a few millimeters from healthy bone. Thereafter, a graft used to replace the removed portion of bone in order to restore functionality is required [61]. Autografting, which is the gold standard in filling bone defects, has known disadvantages, such as donor site morbidity, greater scar formation, and increased surgery times, as well as limited donor sites [62]. To enhance bone regeneration bone defects must be filled with an artificial porous spacer allowing the ingrowth of blood vessels and bone but restricting soft tissue ingrowth. In general, it is agreed that the porous network should consist of interconnected pores with a diameter in the range of 50–1000 μm [5]. Because of the obvious advantage of 3D printing, many researchers study the potential of 3D printing biopolymers for bone tissue engineering.

The most commonly used polymer for 3D porous scaffold is PCL, which, despite its good biocompatibility and processability, is rather hydrophobic leading to limited cell-scaffold interactions. Further, PCL is semicrystalline which together with its hydrophobicity and low water absorbing capacity, resulted in very slow degradation kinetics, which is regarded as a soft and hard tissue compatible bioresorbable material [43, 63]. Sudarmadji et al. chose PCL to fabricate 3D porous scaffolds using SLS [64]. Mathematical relations correlating scaffold porosity and compressive stiffness readings were formulated and compiled. In addition, cytotoxicity assessment was conducted to evaluate the toxicity of the fabricated PCL scaffolds [46]. The porosities, compressive stiffnesses, and yield strengths of the scaffolds varied in the ranges 40–84%, 2.74–55.95 MPa, and 0.17–5.03 MPa, respectively. This range of stiffness closely matches that of cancellous bone in the maxillofacial region. Besides, the chosen mode of fabrication for the PCL scaffolds has been proven to be feasible, as it is evident from the results of the cytotoxicity assessment. Elomaa et al. prepared and applied a photocrosslinkable PLC-based resin to build a porous scaffold using solvent-free SLA [65] (Figure 2). Photocrosslinkable macromers were prepared by methacrylating three-armed oligomers with methacrylic anhydride. Photocrosslinked networks had a high gel content, which indicates a high degree of crosslinking. Since macromers were heated above the melting temperature to obtain the suitable viscosity, no solvent was needed. No material shrinkage was observed after extraction and drying of the scaffolds due to the absence of solvent. The scaffolds accurately represented the structure modeled by computer-aided design. The average porosity was $70.5 \pm 0.8\%$, and the average pore size was 465 μm. The interconnectivity of the pores was high, indicating a great potential for these structures in cell seeding and implanting. PCL was developed as a filament modeling material to produce porous scaffolds, made of layers of directionally aligned microfilaments, using this computer-controlled extrusion and deposition process by Zein et al. in 2002 [66]. The PCL scaffolds were produced with a range of channel size 160–700 mm, filament diameter 260–370 mm, and porosity 48–77% and regular geometrical honeycomb pores, depending on the processing parameters. The scaffolds of different porosity also exhibited a pattern of compressive stress-strain behavior characteristics of porous solids under such loading. The compressive stiffness ranged from 4 to 77 MPa, yield strength from 0.4 to 3.6 MPa, and yield strain from 4% to 28%. Analysis of the measured data shows a high correlation between the scaffold porosity and

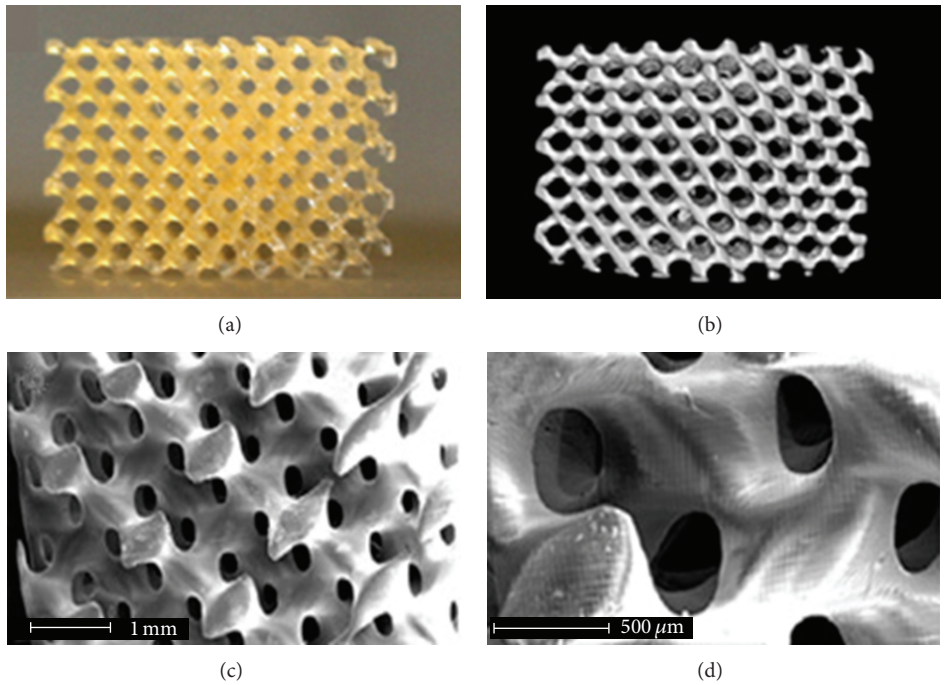

Figure 2: Photograph (a), μCT visualization (b), and SEM images ((c) and (d)) of a scaffold built by SLA using PCL macromere (the targeted theoretical molecular weights (Mn) of which was 1500 g/mol) [65].

the compressive properties based on a power-law relationship.

Cardiomyocytes are terminally differentiated cells and therefore unable to regenerate after infarction [67]. Myocardial infarction (MI) refers to necrosis or death of myocardial cells resulting from coronary occlusions. The medical condition called ventricular remodeling typically results in scar formation, heart wall thinning, and ventricular dilation [68, 69]. The major cause of progressive heart failure and death after myocardial infarction is the adverse remodeling [70] which has motivated the rapidly growing interest in developing regenerative therapies to restore the heart function and regenerate cardiomyocytes. Yeong et al. [69] present results on sintering PCL powder to fabricate a highly porous scaffold by SLS for application in cardiac tissue engineering. The tensile stiffness, mechanical property of sintered PCL struts, was characterized. C2C12 myoblasts were cultured on the scaffold in order to investigate the cellularity of the scaffold design for up to 21 days. Cell culture results were characterized using the MTS cell proliferation assay, F-actin and myosin heavy chain (MHC), and fluorescence immunostaining of the nucleus. Scaffolds produced by SLS with micropores are suitable for cell attachments and offer consistency and reproducibility in building complicated scaffolds. *In vitro* cell cultures using C2C12 cells showed the formation of multinucleated myotubes in the scaffold after 11 days of cell culture. A stable colony of cells was observed throughout 21 days of cell culture. This scaffold could potentially be used for cardiac and skeletal muscle tissue engineering.

There are some other polymers, in addition to PCL, that are used in 3D printing for tissue engineering. In 1998 Kim et al. [71] demonstrated the potential of 3DP technology when it is combined with salt leaching in the fabrication of polymeric scaffolds. The material used was copolymers of PLGA and a suitable solvent. They fabricated cylindrical scaffolds (8 mm in diameter and 7 mm in height) and managed to achieve interconnected porous channels of about 800 Am and microporosities of 45–150 Am by using salt leaching [49]. In 2001, scaffolds of varying pore sizes (38–150 Am) and void fractions (75% and 90%) were fabricated using PLLA and chloroform via the 3DP technology and salt leaching technique by Zeltinger et al. [72]. The cellular reactions to pore size and void fractions were investigated based on 3DP fabricated scaffolds. Cell proliferation was also observed on these scaffolds.

Poly(3-hydroxybutyrate) (PHB) is a natural thermoplastic polyester produced by microorganisms under imbalanced growth conditions and has attracted attention for applications in biomedical areas, such as in the production of scaffolds for tissue engineering due to its biocompatibility and biodegradability [17]. PHB processing by 3D printing can be made without the incorporation of additives such as plasticizers unlike the traditional methods. Oliveira et al. [73] successfully produced PHB porous structures with a height around 2.5 mm and pores with the size of 1 mm. Pereira et al. successfully produced PHB three-dimensional structures using 3D printing technology. The physical models showed dimensional features and geometries very close to the digital model. It was also demonstrated that the PHB powder was not altered after being submitted to 32.5 hours of SLS processing. The thermal properties of the physical model obtained with unprocessed PHB and PHB powder, which

underwent printing sets, did not show a significant difference between them. This corroborated the powder analysis, which indicated that the reuse of remaining material from a 32.15 hours-SLS did not affect the reproducibility of the process [17].

Recently, a functionalized aliphatic polyester based on PCL, namely, poly(hydroxymethylglycolide-*co*-ε-caprolactone) (PHMGCL) which possesses significantly higher hydrophilicity due to its hydroxyl groups attached to the backbone, resulting in a significant increase in human mesenchymal stem cell adhesion, proliferation, and differentiation as compared to PCL, was developed [74]. To evaluate the *in vivo* biodegradation and biocompatibility of 3D-printed scaffolds based on PHMGCL, which has enhanced hydrophilicity, increased degradation rate, and improved cell-material interactions as compared to its counterpart PCL, 3D scaffolds based on this polymer were prepared by means of fiber deposition (melt plotting) [75]. The biodegradation and tissue biocompatibility of PHMGCL and PCL scaffolds after subcutaneous implantation in Balb/c mice were investigated. The *in vitro* enzymatic degradation of these scaffolds was also investigated in lipase solutions. It was shown that PHMGCL 3D scaffolds lost more than 60% of their weight within 3 months of implantation while PCL scaffolds showed no weight loss in this time frame. The molecular weight (Mw) of PHMGCL decreased significantly after 3 months of implantation, while the molecular weight of PCL was unchanged in this period. *In vitro* enzymatic degradation showed that PHMGCL scaffolds were degraded within 50 h, while the degradation time for PCL scaffolds of similar structure was longer. A normal foreign body response to both scaffold types characterized by the presence of macrophages, lymphocytes, and fibrosis was observed with a more rapid onset in PHMGCL scaffolds. The extent of tissue-scaffold interactions as well as vascularization was shown to be higher for PHMGCL scaffolds compared to PCL ones. Therefore, the fast degradable PHMGCL which showed good biocompatibility is a promising biomaterial for bone and cartilage tissue engineering [75].

3.2.2. Synthetic Biopolymer-Based Composites Fabricated by 3D Printing. Griffith and others bound a mixed biodegradable polymer powder of 25% PLLA and 75% PLGA using chloroform as a binder to print a branched liver construct with internal architecture [76]. This design took host implantation into consideration by creating an artery- and vein-like inlet and outlet [15]. Organogenesis of liver tissue using 3D-printed PLLA/PLGA scaffolds has been investigated *in vitro* [14]. It was shown that culturing a mixture of hepatocytes and endothelial cells on a channeled biodegradable scaffold results in the desired tissue structure intrinsically.

Pati et al. [77] successfully printed 3D cell-laden constructs using the principle of hybrid structure fabrication, using PEG and PCL as materials. They printed an ear-shaped construct with a complex porous structure using the process described above. The use of sacrificial layer technology allowed the stacking of complicated structures regardless of geometrical shape. To fabricate the ear-shaped construct, a CAD model was generated from a computerized tomography (CT) scanned image of an ear; both the main framework and sacrificial parts were designed. A code generation process was then carried out via a motion program generator developed in house. In particular, two different hydrogels were printed into the framework, because native human ears consist of both cartilage and fat tissues.

Two photocrosslinkable hydrogel biopolymers, poly (ethylene glycol) dimethacrylate (PEG-DMA, MW 1000) and poly(ethylene glycol) diacrylate (PEG-DA, MW 3400), were used as the primary scaffold materials to prepare multimaterials [78]. Multimaterial scaffolds were fabricated by including controlled concentrations of fluorescently labeled dextran, fluorescently labeled bioactive PEG, or bioactive PEG in different regions of the scaffold. The presence of the fluorescent component in specific regions of the scaffold was analyzed with fluorescent microscopy, while human dermal fibroblast cells were seeded on top of the fabricated scaffolds with selective bioactivity and phase contrast microscopy images were used to show specific localization of cells in the regions patterned with bioactive PEG. Multimaterial spatial control was successfully demonstrated. In addition, the equilibrium swelling behavior of the two biopolymers after SL fabrication was determined and used to design constructs with the specified dimensions at the swollen state. The use of multimaterial SL and the relative ease of conjugating different bioactive ligands or growth factors to PEG allow for the fabrication of tailored three-dimensional constructs with specified spatially controlled bioactivity.

The majority of current protocols utilize water-insoluble photoinitiators that are incompatible with live cell-fabrication and ultraviolet (UV) light that is damaging to the cellular DNA. Various studies have reported the use of water-soluble dimethacrylatedpoly(ethyleneglycol)(PEG-DMA) to create structured, cell-containing hydrogels by stereolithography [79]. Dhariwala et al. were the first to successfully encapsulate (Chinese hamster ovary) cells in PEG-DMA hydrogels, using SLA [80]. Later, PEG-DMA constructs containing encapsulated human dermal fibroblasts [36] and PEG-diacrylate gel structures containing marrow stromal cells [81] were reported. In these cases, large numbers of cells could be capsulated at high densities (several millions of cells per mL) [82]. Lin et al. [79] reported the development of a visible light-based PSL system (VL-PSL), using lithium phenyl-2,4,6-trimethylbenzoylphosphinate (LAP) as the initiator and polyethylene glycol diacrylate (PEGDA) as the monomer, to produce hydrogel scaffolds with specific shapes and internal architectures. Furthermore, live human adipose-derived stem cells (hADSCs) were suspended in PEGDA/LAP solution during the PSL process and were successfully incorporated within the fabricated hydrogel scaffolds. hADSCs in PEG scaffolds showed high viability (>90%) for up to 7 days after fabrication as revealed by live/dead staining. Scaffolds with porous internal architecture retained higher cell viability and activity than solid scaffolds, likely because of the increased oxygen and nutrients exchange into the interior of the scaffolds. The VLPSL can be applicable as an efficient and effective tissue engineering technology for point-of-care tissue repair in the clinic. Three-dimensional biodegradable PEG/PDLLA hydrogel structures

were prepared by Seck et al. using SLA at high resolutions [83]. The porous hydrogel structures had a well-defined pore network architecture, with a narrow pore size distribution and high interconnectivity of the pores. The resin and the built structures were compatible with cells. Upon seeding, human mesenchymal stem cells attached to the surfaces of the hydrogel structures and showed a spread morphology. After five days in culture, proliferation of the cells was observed. These hydrogel structures could therefore be used in tissue engineering, drug delivery, cell transplantation, and other biomedical applications.

ABS is not widely used in medical devices in comparison to materials such as PCL and PLA which offer greater native biocompatibility [20]. Applications involving biological systems require materials that can minimize protein and any other biomolecule adhesion during flow. It is therefore of great interest to chemically modify the surface of ABS to engineer hydrophilicity and enable biocompatibility. Surface modification, specifically by the grafting of PEG, has long been shown to be a promising strategy to increase the biocompatibility of materials [20, 84]. McCullough and Yadavalli [20] examined the use of ABS as a core material for the construction of microdevices. A method to fabricate water-tight microfluidic devices using chemical dissolution via acetone is shown to render a porous FDM ABS device impervious to water flow between layers, while preserving the structural fidelity of printed microstructures down to 250 μm. A strategy is then presented that can enable the formation of a stable, biocompatible surface of ABS by the photoinduced grafting of PEG groups that improves the biocompatibility of the ABS by reducing the biofouling behavior. Surface characterization and protein adhesion studies are presented that demonstrate that this modified ABS represents a versatile material that can be used in fused deposition modeling to form microfluidic channels resistant to biofouling, thereby broadening the range of possible uses for ABS based FDM in microdevice and lab-on-a-chip type applications. The grafting caused the contact angle of the surface to be lowered from 77.58° for native ABS samples to below 40° for ABS-g-PEG and reduced the adhesion of the protein BSA. The results clearly indicate that sealing an FDM ABS surface with an acetone treatment can be achieved with minimal effect on the device and the grafting of PEGMA onto ABS is a viable method to increase surface hydrophilicity and biocompatibility.

Currently, composites of polymers and bioactive inorganic materials are being developed with the aim of increasing the mechanical scaffold stability and improving tissue interaction. By combining biodegradable polymers and bioactive ceramics, such as hydroxyapatite (HA) and tricalcium phosphate (TCP), calcium phosphate (CaP) composite scaffolds were made by 3D printing. Nanosized osteoconductive calcium phosphates (Ca-Ps), including HA, tricalcium phosphate (TCP), and substituted HA and TCP, have gained much recognition in biomaterials development due to their small size, high surface area to volume ratio, and biomimetic similarity to natural bone structure when combined with biopolymers such as collagen, PLLA, and chitosan [17, 85, 86].

Hydroxyapatite ($Ca_{10}(PO4)_6(OH)_2$) has attracted much interest due to its chemical similarity to the calcium phosphate mineral present in biological hard tissues [87, 88]. HA has been used for a variety of biomedical applications, such as a matrix for controlled drug release and a carrier material in bone tissue engineering [89]. Recently, nanosized hydroxyapatite (nHA) has been highlighted due to its advantageous features over conventional microsized materials. nHA has the potential to act as a carrier of therapeutic agents, enabling controlled drug release extracellularly or intracellularly, and at the same time it has high absorbability in the body for the regeneration of hard tissue [90, 91].

PCL/HA composite has attracted a great interest for the bone tissue engineering application. Wiria et al. researched the use of biocomposite materials, consisting of PCL and HA, to fabricate tissue engineering scaffolds via the SLS technology in 2007 [92]. Simulated body fluid (SBF) samples show the formation of hydroxy carbonate apatite, as a result of soaking HA in a SBF environment. Cell culture experiments showed that Saos-2 cells were able to live and replicate on the fabricated scaffolds. The results show the favorable potential of PCL/HA biocomposites as tissue engineering scaffolds that are fabricated via SLS. Eosoly et al. [93] studied PCL/HA composite scaffolds in the same year. In their study HA and PCL, which were considered suitable for hard tissue engineering purposes, were used in a weight ratio of 30 : 70. Four parameters, namely, laser fill power, outline laser power, scan spacing, and part orientation, were investigated according to a central composite design. A model of the effects of these parameters on the accuracy and mechanical properties of the fabricated parts was developed. The compressive modulus and yield strength of the fabricated microstructures with a designed relative density of 0.33 varied between 0.6 and 2.3, 0.1 and 0.6 MPa, respectively. The mechanical behavior was strongly dependent on the manufacturing direction. Eshraghi and Das [94] studied the experimental characterization of the compressive mechanical properties of PCL-HA composite scaffolds prepared by SLS technology for bone tissue engineering. In their study, they further establish the ability of SLS to manufacture PCL-HA composite scaffolds with near-full density in designed solid regions for bone tissue engineering. The mechanical properties of the PCL-HA composites showed improvement over that of pure PCL. They also demonstrate that the mechanical properties of these scaffolds can be predicted before manufacturing with high accuracy. A direct extension of being able to predict the mechanical properties of composite materials at any filler loading in combination with a direct fabrication method with the capability to produce complex anatomic parts is the ability to custom design both the material properties and the anatomical shape of tissue-engineered constructs for both patient and site-specific recovery strategies.

A poly(D,L-lactide)/nanosized hydroxyapatite (PDLLA/nHA) composite resin was prepared and used to fabricate composite films and computer designed porous scaffolds by Ronca et al. [95] using SLA, mixing varying quantities of nHA powder and a liquid photoinitiator into a photocrosslinkable PDLLA-diacrylate resin. The influence of nHA on the rheological and photochemical properties of the resins was

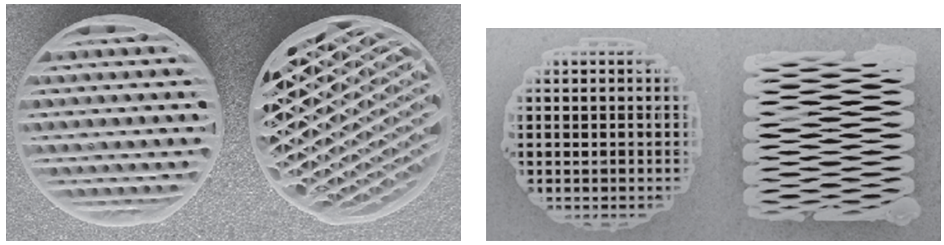

(a) (b)

Figure 3: Three dimensionally interconnected controlled porosity PP-TCP composite scaffolds with different internal architecture using FDM process [101].

investigated, with the materials being characterized with respect to their mechanical, thermal, and morphological properties after postpreparation curing. In the cured composites stiffness was observed to increase with increasing concentration of nanoparticles. With increasing ceramic component the resins became more viscous, and NMP was added as a nonreactive diluent to decrease the viscosity and allow processing by stereolithography. SEM images showed exposed ceramic particles on the pore surface, allowing interaction between the bone-forming nHA and cells.

Calcium phosphate ceramics have the ability to induce osteogenic differentiation of human adipose-derived stem cells by osteoinduction [96–99]. Three-dimensional na-nocomposite scaffolds based on calcium phosphate (Ca-P)/poly(hydroxybutyrate-co-hydroxyvalerate) (PHBV) and carbonated hydroxyapatite (CHAp)/PLLA nanocomposite microspheres were successfully fabricated by Duan et al. [100] using SLS. The optimized scaffolds had controlled material microstructure, totally interconnected porous structure, and high porosity. The morphology and mechanical properties of Ca-P/PHBV and CHAp/PLLA nanocomposite scaffolds as well as PHBV and PLLA polymer scaffolds were studied. Biological evaluation showed that SaOS-2 cells had high cell viability and normal morphology and phenotype after 3- and 7-day culture on all scaffolds. The incorporation of Ca-P nanoparticles significantly improved cell proliferation and alkaline phosphatase activity for Ca-P/PHBV scaffolds, whereas CHAp/PLLA nanocomposite scaffolds exhibited a similar level of cell response compared with PLLA polymer scaffolds. The three-dimensional nanocomposite scaffolds provide a biomimetic environment for osteoblastic cell attachment, proliferation, and differentiation and have great potential for bone tissue engineering applications. Particulate-reinforced polymer-ceramic composites were developed by high shear mixing of polypropylene (PP) polymer and tricalcium phosphate (TCP) ceramic [101] (Figure 3). Processing aids were used to improve plasticity and processability to the composites. Controlled porosity scaffolds were fabricated via the FDM. These porous scaffolds were characterized for their use as bone grafts in terms of physical, mechanical, and biological properties. Hg porosimetry was performed to determine pore size and their distribution. Scaffolds with different complex internal architectures were also fabricated using this composite material. Tensile properties of neat PP, PP with processing aids (without TCP), and PP-TCP composite (with processing aids) were evaluated and compared using standard dog bone samples. Uniaxial compression tests were performed on cylindrical porous samples with an average pore size of 160 Am and varying vol.% porosity (36%, 48%, and 52%). Samples with 36 vol.% porosity showed the best compressive strength of 12.7 MPa. Cytotoxicity and cell proliferation studies were conducted with a modified human osteoblast cell line (HOB). Results showed that these samples were nontoxic with excellent cell growth during the first two weeks of *in vitro* testing.

Bioactive glass is known to benefit cell interactions of polymeric tissue engineering scaffolds [102, 103]. Most likely, the best response is obtained when the glass is on the scaffold surface without a cover. Miller and others recently developed a 3D fiber drawing system to fabricate perfusable carbohydrate glass lattices coated with a thin layer of poly(d-lactide-*co*-glycolide), resembling patterned vascular networks [104]. Elomaa et al. [105] combined a photocrosslinkable PCL resin with bioactive glass and fabricated the composite scaffold. Bioactive glass was homogeneously distributed through the highly porous scaffolds and their surface. The presence of calcium phosphate deposits on the surface of the composite scaffolds indicated *in vitro* bioactivity. The bioactive glass increased the metabolic activity of fibroblasts. The research showed that SLA technology enables the fabrication of well-defined composite scaffolds in which the bioactive glass is homogeneously distributed on the surface and readily available for rapid ion release and cell interactions. By SLA, an unwanted polymer layer covering the BG particles on the scaffold surface can be successfully avoided. The study suggested that photocrosslinked composite scaffolds of BG and PCL prepared by SLA technology had great potential as bioactive and biodegradable supports for cells in regenerative medicine.

Serra et al. combined PEG and CaP glass particles with the PLA matrix to fabricate 3D biodegradable porous composite scaffolds [106]. The 3D printing technique permitted the fabrication of highly porous scaffolds with mechanical properties considerably higher than other methods commonly used to fabricate 3D polymer scaffolds. The addition of the soluble CaP glass particles (and PEG) to the PLA matrix changed both the morphology and the physicochemical properties of the surface of the materials which affected

cell behavior. Surface properties were also assessed, showing that the incorporation of glass particles increased both the roughness and the hydrophilicity of the scaffolds. Mechanical tests indicated that compression strength is dependent on the scaffold geometry and the presence of glass. Preliminary cell response was studied with primary mesenchymal stem cells (MSC) and revealed that CaP glass improved cell adhesion. Overall, the results showed the suitability of the technique/materials combination to develop 3D porous scaffolds and their initial biocompatibility, with both being valuable characteristics for tissue engineering applications.

4. Prospects and Conclusions

By the year of 2014, 3D printing technology has been studied by biotechnology firms and academia for possible use in tissue engineering applications in which organs and body parts are built using inkjet techniques. One of the main advantages of 3D printing is that it allows the manufacturing of objects having complex geometries and intricate internal structure, which can be designed according to the needs of individual patients using their 3D medical scan data. A great prospect for biomedical applications, especially for tissue engineering applications, has been shown. Both natural and synthetic polymers have been developed for tissue engineering via the 3D printing technology, and numerous additional materials are being developed. Fibers and particles have been combined with polymers to fabricate materials with better bioactivity and biocompatibility, as well as physical and chemical properties.

For a wider application of 3D printing, the moral problem related to the 3D-printed organ for medical application should be further studied, the cost of 3D printers should be less, and more materials systems which are available for 3D printing should be developed. A further study on the mechanism of cell attachment, differentiation, and growth within the 3D-printed materials should be carried on as well.

With the development of nanotechnology, materials such as nanotubes [107–110], nano-structured particles [111], nanofibers [112, 113], and other nanosized materials [114–116] have been fabricated. Nanomaterials have special mechanical, electrical, magnetic, optical, chemical, and other biological properties due to their high aspect ratio and surface area [117–119]. Many nanomaterial surfaces exemplify high (bio- and cyto-) compatibility, by promoting protein adsorption and enhancing subsequent cellular adhesion and tissue growth more than on conventional flat implant surfaces such as titanium, ceramics, and biopolymers [114]. Nanocomposites attract more attention because of their potential combination of properties from both the nanomaterials and the host materials matrix [108, 120–122]. It is promising to incorporate nanomaterials in 3D printing. The nanomaterials can be introduced into 3D printing in the following way: (1) premixing the nanomaterials into the host matrix before 3D printing and (2) introducing the nanomaterials at the intermittent stoppages of the 3D-printed host matrix [123]. All in all, 3D printing will help to expand the application of nanomaterials for tissue engineering.

Conflict of Interests

The authors declare that there is no conflict of interests regarding the publication of this paper.

Acknowledgments

The authors acknowledge the financial support from the National Basic Research Program of China (973 Program, no. 2011CB710901), the National Natural Science Foundation of China (no. 31370959), Fok Ying Tong Education Foundation (no. 141039), Beijing Natural Science Foundation (no. 7142094), the Beijing Nova Program (no. 2010B011), Program for New Century Excellent Talents (NCET) in University from Ministry of Education of China, State Key Laboratory of New Ceramic and Fine Processing (Tsinghua University), International Joint Research Center of Aerospace Biotechnology and Medical Engineering, Ministry of Science and Technology of China, and the 111 Project (no. B13003).

References

[1] X. M. Li, Y. Huang, L. S. Zheng et al., "Effect of substrate stiffness on the functions of rat bone marrow and adipose tissue derived mesenchymal stem cells in vitro," *Journal of Biomedical Materials Research A*, vol. 102A, pp. 1092–1101, 2014.

[2] X. Li, Y. Fan, and F. Watari, "Current investigations into carbon nanotubes for biomedical application," *Biomedical Materials*, vol. 5, no. 2, Article ID 022001, 2010.

[3] S. P. Nukavarapu and D. L. Dorcemus, "Osteochondral tissue engineering: current strategies and challenges," *Biotechnology Advances*, vol. 31, pp. 706–721, 2013.

[4] D. W. Hutmacher, "Scaffolds in tissue engineering bone and cartilage," *Biomaterials*, vol. 21, no. 24, pp. 2529–2543, 2000.

[5] A. Butscher, M. Bohner, S. Hofmann, L. Gauckler, and R. Müller, "Structural and material approaches to bone tissue engineering in powder-based three-dimensional printing," *Acta Biomaterialia*, vol. 7, no. 3, pp. 907–920, 2011.

[6] L. M. Mathieu, T. L. Mueller, P.-E. Bourban, D. P. Pioletti, R. Müller, and J.-A. E. Månson, "Architecture and properties of anisotropic polymer composite scaffolds for bone tissue engineering," *Biomaterials*, vol. 27, no. 6, pp. 905–916, 2006.

[7] M. Bohner, G. H. Van Lenthe, S. Grünenfelder, W. Hirsiger, R. Evison, and R. Müller, "Synthesis and characterization of porous β-tricalcium phosphate blocks," *Biomaterials*, vol. 26, no. 31, pp. 6099–6105, 2005.

[8] M. Stoppato, S. Vahabzadeh, and A. Bandyopadhyay, "Bone tissue engineering using 3D printing," *Bioactive and Compatible Polymers*, vol. 28, pp. 16–32, 2013.

[9] H. Cao and N. Kuboyama, "A biodegradable porous composite scaffold of PGA/β-TCP for bone tissue engineering," *Bone*, vol. 46, no. 2, pp. 386–395, 2010.

[10] X. Li and Q. Feng, "Porous poly-L-lactic acid scaffold reinforced by chitin fibers," *Polymer Bulletin*, vol. 54, no. 1-2, pp. 47–55, 2005.

[11] H. D. Kim, E. H. Bae, I. C. Kwon, R. R. Pal, J. D. Nam, and D. S. Lee, "Effect of PEG-PLLA diblock copolymer on macroporous PLLA scaffolds by thermally induced phase separation," *Biomaterials*, vol. 25, no. 12, pp. 2319–2329, 2004.

[12] C. P. Grey, S. T. Newton, G. L. Bowlin et al., "Gradient fiber electrospinning of layered scaffolds using controlled transitions in fiber diameter," *Biomaterials*, vol. 34, pp. 4993–5006, 2013.

[13] Y. Jun Lee, J.-H. Lee, H.-J. Cho et al., "Electrospun fibers immobilized with bone forming peptide-1 derived from BMP7 for guided bone regeneration," *Biomaterials*, vol. 34, pp. 5059–5069, 2013.

[14] S. Bose, S. Vahabzadeh, and A. Bandyopadhyay, "Bone tissue engineering using 3D printing," *Materials Today*, vol. 16, pp. 496–504, 2013.

[15] D. Jack Richards, Y. Tan, J. Jia et al., "3D printing for tissue engineering," *Israel Journal of Chemistry*, vol. 53, pp. 805–814, 2013.

[16] A. Sachdeva, S. Singh, and V. S. Sharma, "Investigating surface roughness of parts produced by SLS process," *International Journal of Advanced Manufacturing Technology*, vol. 64, pp. 1505–1516, 2012.

[17] T. F. Pereira, M. F. Oliveira, I. A. Maia et al., "3D printing of poly(3-hydroxybutyrate) porous structures using selective laser sintering," *Macromolecular Symposia*, vol. 319, pp. 64–73, 2012.

[18] K. Senthilkumaran, P. M. Pandey, and P. V. M. Rao, "Influence of building strategies on the accuracy of parts in selective laser sintering," *Materials and Design*, vol. 30, no. 8, pp. 2946–2954, 2009.

[19] B. Wendel, D. Rietzel, F. Kühnlein, R. Feulner, G. Hülder, and E. Schmachtenberg, "Additive processing of polymers," *Macromolecular Materials and Engineering*, vol. 293, pp. 799–809, 2008.

[20] E. J. McCullough and V. K. Yadavalli, "Surface modification of fused deposition modeling ABS to enable rapid prototyping of biomedical microdevices," *Journal of Materials Processing Technology*, vol. 213, pp. 947–954, 2013.

[21] S. Gautam, C.-F. Chou, A. K. Dinda et al., "Surface modification of nanofibrouspolycaprolactone/gelatin composite scaffold by collagen type I grafting for skin tissue engineering," *Materials Science and Engineering C*, vol. 34, pp. 402–409, 2014.

[22] F. Groeber, M. Holeiter, M. Hampel, S. Hinderer, and K. Schenke-Layland, "Skin tissue engineering—in vivo and in vitro applications," *Advanced Drug Delivery Reviews*, vol. 63, no. 4, pp. 352–366, 2011.

[23] W.-J. Li, R. Tuli, C. Okafor et al., "A three-dimensional nanofibrous scaffold for cartilage tissue engineering using human mesenchymal stem cells," *Biomaterials*, vol. 26, no. 6, pp. 599–609, 2005.

[24] A. I. Rodrigues, M. E. Gomes, I. B. Leonor et al., "Bioactive starch-based scaffolds and human adipose stem cells are a good combination for bone tissue engineering," *Acta Biomaterialia*, vol. 8, pp. 3765–3776, 2012.

[25] X. Li, Q. Feng, W. Wang, and F. Cui, "Chemical characteristics and cytocompatibility of collagen-based scaffold reinforced by chitin fibers for bone tissue engineering," *Journal of Biomedical Materials Research B: Applied Biomaterials*, vol. 77, no. 2, pp. 219–226, 2006.

[26] S. Sahoo, L.-T. Ang, J. Cho-Hong Goh, and S.-L. Toh, "Bioactive nanofibers for fibroblastic differentiation of mesenchymal precursor cells for ligament/tendon tissue engineering applications," *Differentiation*, vol. 79, no. 2, pp. 102–110, 2010.

[27] J. Hu, X. Sun, H. Ma, C. Xie, Y. E. Chen, and P. X. Ma, "Porous nanofibrous PLLA scaffolds for vascular tissue engineering," *Biomaterials*, vol. 31, no. 31, pp. 7971–7977, 2010.

[28] A. Hasan, A. Memic, N. Annabi et al., "Electrospun scaffolds for tissue engineering of vascular graft," *Acta Biomaterial*, vol. 10, pp. 11–25, 2014.

[29] L. Ghasemi-Mobarakeh, M. P. Prabhakaran, M. Morshed, M.-H. Nasr-Esfahani, and S. Ramakrishna, "Electrospun poly(ε-caprolactone)/gelatin nanofibrous scaffolds for nerve tissue engineering," *Biomaterials*, vol. 29, no. 34, pp. 4532–4539, 2008.

[30] M. A. Pattison, S. Wurster, T. J. Webster, and K. M. Haberstroh, "Three-dimensional, nano-structured PLGA scaffolds for bladder tissue replacement applications," *Biomaterials*, vol. 26, no. 15, pp. 2491–2500, 2005.

[31] F. Chen, M. Tian, D. Zhang et al., "Preparation and characterization of oxidized alginate covalently cross-linked galactosylated chitosan scaffold for liver tissue engineering," *Materials Science and Engineering C*, vol. 32, no. 2, pp. 310–320, 2012.

[32] B.-S. Kim, I.-K. Park, T. Hoshiba et al., "Design of artificial extracellular matrices for tissue engineering," *Progress in Polymer Science (Oxford)*, vol. 36, no. 2, pp. 238–268, 2011.

[33] X. Li, Q. Feng, X. Liu, W. Dong, and F. Cui, "Collagen-based implants reinforced by chitin fibres in a goat shank bone defect model," *Biomaterials*, vol. 27, no. 9, pp. 1917–1923, 2006.

[34] M. C. Serrano, S. Nardecchia, C. García-Rama et al., "Chondroitin sulphate-based 3D scaffolds containing MWCNTs for nervous tissue repair," *Biomaterials*, vol. 35, pp. 1543–1551, 2014.

[35] L. Zhao, H.-J. Gwon, Y.-M. Lim et al., "Hyaluronic acid/chondroitin sulfate-based hydrogel prepared bygamma irradiation technique," *Carbohydrate Polymers*, vol. 102, pp. 598–605, 2014.

[36] X. Li, X. Liu, W. Dong et al., "In vitro evaluation of porous poly(L-lactic acid) scaffold reinforced by chitin fibers," *Journal of Biomedical Materials Research B: Applied Biomaterials*, vol. 90, no. 2, pp. 503–509, 2009.

[37] H. Tamura, T. Furuike, S. V. Nair, and R. Jayakumar, "Biomedical applications of chitin hydrogel membranes and scaffolds," *Carbohydrate Polymers*, vol. 84, no. 2, pp. 820–824, 2011.

[38] A. Islam, T. Yasin, and I. Ur Rehman, "Synthesis of hybrid polymer networks of irradiated chitosan/poly(vinyl acohol) for biomedical applications," *Physics and Chemistry*, vol. 96, pp. 115–119, 2014.

[39] X. Li, Q. Feng, Y. Jiao, and F. Cui, "Collagen-based scaffolds reinforced by chitosan fibres for bone tissue engineering," *Polymer International*, vol. 54, no. 7, pp. 1034–1040, 2005.

[40] I. Sousa, A. Mendes, and P. J. Bártolo, "PCL scaffolds with collagen bioactivator for applications in Tissue Engineering," *Procedia Engineering*, vol. 59, pp. 279–284, 2013.

[41] G. Chen, J. Tanaka, and T. Tateishi, "Osteochondral tissue engineering using a PLGA-collagen hybrid mesh," *Materials Science and Engineering C*, vol. 26, no. 1, pp. 124–129, 2006.

[42] C. Zhang, N. Sangaj, Y. Hwang, A. Phadke, C.-W. Chang, and S. Varghese, "Oligo(trimethylene carbonate)-poly(ethylene glycol)-oligo(trimethylene carbonate) triblock-based hydrogels for cartilage tissue engineering," *Acta Biomaterialia*, vol. 7, no. 9, pp. 3362–3369, 2011.

[43] H. Sun, L. Mei, C. Song, X. Cui, and P. Wang, "The in vivo degradation, absorption and excretion of PCL-based implant," *Biomaterials*, vol. 27, no. 9, pp. 1735–1740, 2006.

[44] E. D. Boland, B. D. Coleman, C. P. Barnes, D. G. Simpson, G. E. Wnek, and G. L. Bowlin, "Electrospinning polydioxanone for biomedical applications," *Acta Biomaterialia*, vol. 1, no. 1, pp. 115–123, 2005.

[45] M. J. Smith, M. J. McClure, S. A. Sell et al., "Suture-reinforced electrospun polydioxanone-elastin small-diameter tubes for use in vascular tissue engineering: a feasibility study," *Acta Biomaterialia*, vol. 4, no. 1, pp. 58–66, 2008.

[46] M. Singh, F. Kurtis Kasper, and A. G. Mikos, CHAPTER II.6.3 tissue engineering scaffolds. SECTION II.6 Applications of biomaterials in functional tissue engineering 1138–1159.

[47] B. Baroli, "Hydrogels for tissue engineering and delivery of tissue-inducing substances," *Journal of Pharmaceutical Sciences*, vol. 96, no. 9, pp. 2197–2223, 2007.

[48] Y. Yan, X. Wang, Y. Pan et al., "Fabrication of viable tissue-engineered constructs with 3D cell-assembly technique," *Biomaterials*, vol. 26, no. 29, pp. 5864–5871, 2005.

[49] C. X. F. Lam, X. M. Mo, S. H. Teoh, and D. W. Hutmacher, "Scaffold development using 3D printing with a starch-based polymer," *Materials Science and Engineering C*, vol. 20, no. 1-2, pp. 49–56, 2002.

[50] M. G. Duarte, D. Brunnel, M. H. Gil, and E. Schacht, "Microcapsules prepared from starch derivatives," *Journal of Materials Science: Materials in Medicine*, vol. 8, no. 5, pp. 321–323, 1997.

[51] C. Elvira, J. F. Mano, J. San Román, and R. L. Reis, "Starch-based biodegradable hydrogels with potential biomedical applications as drug delivery systems," *Biomaterials*, vol. 23, no. 9, pp. 1955–1966, 2002.

[52] I. R. Matthew, R. M. Browne, J. W. Frame, and B. G. Millar, "Subperiosteal behaviour of alginate and cellulose wound dressing materials," *Biomaterials*, vol. 16, no. 4, pp. 275–278, 1995.

[53] I. Espigares, C. Elvira, J. F. Mano, B. Vázquez, J. San Román, and R. L. Reis, "New partially degradable and bioactive acrylic bone cements based on starch blends and ceramic fillers," *Biomaterials*, vol. 23, no. 8, pp. 1883–1895, 2002.

[54] G. V. Salmoria, P. Klauss, R. A. Paggi, L. A. Kanis, and A. Lago, "Structure and mechanical properties of cellulose based scaffolds fabricated by selective laser sintering," *Polymer Testing*, vol. 28, no. 6, pp. 648–652, 2009.

[55] K. Jakab, C. Norotte, F. Marga, K. Murphy, G. Vunjak-Novakovic, and G. Forgacs, "Tissue engineering by self-assembly and bio-printing of living cells," *Biofabrication*, vol. 2, Article ID 022001, 2010.

[56] F. Marga, K. Jakab, C. Khatiwala et al., "Toward engineering functional organ modules by additive manufacturing," *Biofabrication*, vol. 4, Article ID 022001, 2012.

[57] C. Norotte, F. S. Marga, L. E. Niklason, and G. Forgacs, "Scaffold-free vascular tissue engineering using bioprinting," *Biomaterials*, vol. 30, no. 30, pp. 5910–5917, 2009.

[58] R. Gauvin, Y.-C. Chen, J. W. Lee et al., "Microfabrication of complex porous tissue engineering scaffolds using 3D projection stereolithography," *Biomaterials*, vol. 33, no. 15, pp. 3824–3834, 2012.

[59] T. Billiet, E. Gevaert, and T. De Schryver, "The 3D printing of gelatin methacrylamide cell-laden tissue-engineered constructs with high cell viability," *Biomaterials*, vol. 35, pp. 49–62, 2014.

[60] X. M. Li, X. H. Liu, G. P. Zhang et al., "Repairing 25mm bone defect using fibres reinforced scaffolds as well as autograft bone," *Bone*, vol. 43, article S94, 2008.

[61] J. Christophe Fricain, S. Schlaubitz, C. Le Visage et al., "Ananohydroxyapatite—pullulan/dexran polysaccharide composite macroporous materials for bone tissue engineering," *Biomaterials*, vol. 34, pp. 2947–2959, 2013.

[62] X. M. Li, L. Wang, Y. B. Fan, Q. L. Feng, and F. Z. Cui, "Biocompatibility and toxicity of nanoparticles and nanotubes," *Journal of Nanomaterials*, vol. 2012, Article ID 548389, 19 pages, 2012.

[63] H. L. Khor, K. W. Ng, J. T. Schantz et al., "Poly (ε-caprolactone) films as a potential substrate for tissue engineering an epidermal equivalent," *Materials Science and Engineering C*, vol. 20, no. 1-2, pp. 71–75, 2002.

[64] N. Sudarmadji, J. Y. Tan, K. F. Leong, C. K. Chua, and Y. T. Loh, "Investigation of the mechanical properties and porosity relationships in selective laser-sintered polyhedral for functionally graded scaffolds," *Acta Biomaterialia*, vol. 7, no. 2, pp. 530–537, 2011.

[65] L. Elomaa, S. Teixeira, R. Hakala, H. Korhonen, D. W. Grijpma, and J. V. Seppälä, "Preparation of poly(ε-caprolactone)-based tissue engineering scaffolds by stereolithography," *Acta Biomaterialia*, vol. 7, no. 11, pp. 3850–3856, 2011.

[66] I. Zein, D. W. Hutmacher, K. C. Tan, and S. H. Teoh, "Fused deposition modeling of novel scaffold architectures for tissue engineering applications," *Biomaterials*, vol. 23, no. 4, pp. 1169–1185, 2002.

[67] M. Shin, O. Ishii, T. Sueda, and J. P. Vacanti, "Contractile cardiac grafts using a novel nanofibrous mesh," *Biomaterials*, vol. 25, no. 17, pp. 3717–3723, 2004.

[68] M. A. Laflamme and C. E. Murry, "Regenerating the heart," *Nature Biotechnology*, vol. 23, no. 7, pp. 845–856, 2005.

[69] W. Y. Yeong, N. Sudarmadji, H. Y. Yu et al., "Porous polycaprolactone scaffold for cardiac tissue engineering fabricated by selective laser sintering," *Acta Biomaterialia*, vol. 6, no. 6, pp. 2028–2034, 2010.

[70] A. A. Kocher, M. D. Schuster, M. J. Szabolcs et al., "Neovascularization of ischemic myocardium by human bone-marrow-derived angioblasts prevents cardiomyocyte apoptosis, reduces remodeling and improves cardiac function," *Nature Medicine*, vol. 7, no. 4, pp. 430–436, 2001.

[71] S. S. Kim, H. Utsunomiya, J. A. Koski et al., "Survival and function of hepatocytes on a novel three-dimensional synthetic biodegradable polymer scaffold with an intrinsic network of channels," *Annals of Surgery*, vol. 228, no. 1, pp. 8–13, 1998.

[72] J. Zeltinger, J. K. Sherwood, D. A. Graham, R. Müeller, and L. G. Griffith, "Effect of pore size and void fraction on cellular adhesion, proliferation, and matrix deposition," *Tissue Engineering*, vol. 7, no. 5, pp. 557–572, 2001.

[73] M. F. Oliveira, I. A. Maia, P. Y. Noritomi et al., "Building tissue engineering Scaffolds utilizing rapid prototyping," *Revista Materia*, vol. 12, p. 373, 2007.

[74] H. Seyednejad, T. Vermonden, N. E. Fedorovich et al., "Synthesis and characterization of hydroxyl-functionalized caprolactone copolymers and their effect on adhesion, proliferation, and differentiation of human mesenchymal stem cells," *Biomacromolecules*, vol. 10, no. 11, pp. 3048–3054, 2009.

[75] H. Seyednejad, D. Gawlitta, R. V. Kuiper et al., "In vivo biocompatibility and biodegradation of 3D-printed porous scaffolds based on a hydroxyl-functionalized poly(ε-caprolactone)," *Biomaterials*, vol. 33, no. 17, pp. 4309–4318, 2012.

[76] L. G. Griffith, B. Wu, M. J. Cima, M. J. Powers, B. Chaignaud, and J. P. Vacanti, "In vitro organogenesis of liver tissue," *Annals of the New York Academy of Sciences*, vol. 831, pp. 382–397, 1997.

[77] F. Pati, J.-H. Shim, J.-S. Lee et al., "3D printing of cell-laden constructs for heterogeneous tissue regeneration," *Manufacturing Letters*, vol. 1, pp. 49–53, 2013.

[78] K. Arcaute, B. Mann, and R. Wicker, "Stereolithography of spatially controlled multi-material bioactive poly(ethylene glycol) scaffolds," *Acta Biomaterialia*, vol. 6, no. 3, pp. 1047–1054, 2010.

[79] H. Lin, D. Zhang, P. G. Alexander et al., "Application of visible light-based projection stereolithography for live cell-scaffold fabrication with designed architecture," *Biomaterials*, vol. 34, pp. 331–339, 2013.

[80] B. Dhariwala, E. Hunt, and T. Boland, "Rapid prototyping of tissue-engineering constructs, using photopolymerizable hydrogels and stereolithography," *Tissue Engineering*, vol. 10, no. 9-10, pp. 1316–1322, 2004.

[81] Y. Lu, G. Mapili, G. Suhali et al., "Adigitalmicro-mirrordevice-based system for the microfabrication of complex, spatially patterned tissue engineering scaffolds," *Journal of Biomedical Materials Research Part A*, vol. 77A, no. 2, pp. 396–405, 2006.

[82] F. P. W. Melchels, J. Feijen, and D. W. Grijpma, "A review on stereolithography and its applications in biomedical engineering," *Biomaterials*, vol. 31, no. 24, pp. 6121–6130, 2010.

[83] T. M. Seck, F. P. W. Melchels, J. Feijen, and D. W. Grijpma, "Designed biodegradable hydrogel structures prepared by stereolithography using poly(ethylene glycol)/poly(d,l-lactide)-based resins," *Journal of Controlled Release*, vol. 148, no. 1, pp. 34–41, 2010.

[84] D. L. Elbert and J. A. Hubbell, "Surface treatments of polymers for biocompatibility," *Annual Review of Materials Science*, vol. 26, no. 1, pp. 365–394, 1996.

[85] C. Liu, Z. Han, and J. T. Czernuszka, "Gradient collagen/nanohydroxyapatite composite scaffold: development and characterization," *Acta Biomaterialia*, vol. 5, no. 2, pp. 661–669, 2009.

[86] C. Xianmiao, L. Yubao, Z. Yi, Z. Li, L. Jidong, and W. Huanan, "Properties and in vitro biological evaluation of nanohydroxyapatite/chitosan membranes for bone guided regeneration," *Materials Science and Engineering C*, vol. 29, no. 1, pp. 29–35, 2009.

[87] J. Christophe Fricain, S. Schlaubitz, C. Le Visage et al., "A nanohydroxyapatite e Pullulan/dextran polysaccharide composite macroporous material for bone tissue engineering," *Biomaterials*, vol. 34, pp. 2947–2959, 2013.

[88] Y. Deng, H. Wang, L. Zhang et al., "In situ synthesis and in vitro biocompatibility of needle-like nano-hydroxyapatiteinagar-gelatinco-hydrogel," *Materials Letters*, vol. 104, pp. 8–12, 2013.

[89] M. N. Salimi and A. Anuar, "Characterizations of biocompatible and bioactive hydroxyapatite particles," *Procedia Engineering*, vol. 53, pp. 192–196, 2013.

[90] M. Suto, E. Nemoto, S. Kanay et al., "Nanohydroxyapatite increases BMP-2 expression via a p38 MAP kinase dependent pathway in periodontal ligament cells," *Archives of Oral Biology*, vol. 58, no. 8, pp. 1021–1028, 2013.

[91] H. Wang, Y. Li, Y. Zuo, J. Li, S. Ma, and L. Cheng, "Biocompatibility and osteogenesis of biomimetic nano-hydroxyapatite/polyamide composite scaffolds for bone tissue engineering," *Biomaterials*, vol. 28, no. 22, pp. 3338–3348, 2007.

[92] F. E. Wiria, K. F. Leong, C. K. Chua, and Y. Liu, "Poly-ε-caprolactone/hydroxyapatite for tissue engineering scaffold fabrication via selective laser sintering," *Acta Biomaterialia*, vol. 3, no. 1, pp. 1–12, 2007.

[93] S. Eosoly, D. Brabazon, S. Lohfeld, and L. Looney, "Selective laser sintering of hydroxyapatite/poly-ε-caprolactone scaffolds," *Acta Biomaterialia*, vol. 6, no. 7, pp. 2511–2517, 2010.

[94] S. Eshraghi and S. Das, "Micromechanical finite-element modeling and experimental characterization of the compressive mechanical properties of polycaprolactone-hydroxyapatite composite scaffolds prepared by selective laser sintering for bone tissue engineering," *Acta Biomaterialia*, vol. 8, no. 8, pp. 3138–3143, 2012.

[95] A. Ronca, L. Ambrosio, and D. W. Grijpma, "Preparation of designed poly(D, L-lactide)/nanosized hydroxyapatite composite structures by stereolithography," *Acta Biomaterialia*, vol. 9, pp. 5989–5996, 2013.

[96] X. Li, H. Liu, X. Niu et al., "Osteogenic differentiation of human adipose-derived stem cells induced by osteoinductive calcium phosphate ceramics," *Journal of Biomedical Materials Research B: Applied Biomaterials*, vol. 97, no. 1, pp. 10–19, 2011.

[97] X. M. Li, X. H. Liu, M. Uo, Q. L. Feng, F. Z. Cui, and F. Watari, "Investigation on the mechanism of the osteoinduction for calcium phosphate," *Bone*, vol. 43, pp. S111–S112, 2008.

[98] R. A. Surmenev, M. A. Surmeneva, and A. A. Ivanova, "Significance of calcium phosphate coatings for the enhancement of new bone osteogenesis—a review," *Acta Biomaterialia*, vol. 10, pp. 557–579, 2014.

[99] X. Li, C. A. van Blitterswijk, Q. Feng, F. Cui, and F. Watari, "The effect of calcium phosphate microstructure on bone-related cells in vitro," *Biomaterials*, vol. 29, no. 23, pp. 3306–3316, 2008.

[100] B. Duan, M. Wang, W. Y. Zhou, W. L. Cheung, Z. Y. Li, and W. W. Lu, "Three-dimensional nanocomposite scaffolds fabricated via selective laser sintering for bone tissue engineering," *Acta Biomaterialia*, vol. 6, no. 12, pp. 4495–4505, 2010.

[101] S. J. Kalita, S. Bose, H. L. Hosick, and A. Bandyopadhyay, "Development of controlled porosity polymer-ceramic composite scaffolds via fused deposition modeling," *Materials Science and Engineering C*, vol. 23, no. 5, pp. 611–620, 2003.

[102] D. Xynos, A. J. Edgar, L. D. K. Buttery, L. L. Hench, and J. M. Polak, "Gene-expression profiling of human osteoblasts following treatment with the ionic products of Bioglass 45S5 dissolution," *Biomedical Materials Research*, vol. 55, pp. 151–157, 2001.

[103] G. Jell and M. M. Stevens, "Gene activation by bioactive glasses," *Journal of Materials Science: Materials in Medicine*, vol. 17, no. 11, pp. 997–1002, 2006.

[104] J. S. Miller, K. R. Stevens, M. T. Yang et al., "Rapid casting of patterned vascular network for perfusable engineered three-dimensional tissues," *Nature Materials*, vol. 11, pp. 768–774, 2012.

[105] L. Elomaa, A. Kokkari, T. Närhi et al., "Porous 3D modeled scaffolds of bioactive glass and photocrosslinkable poly(e-caprolactone) by stereolithography," *Composites Science and Technology*, vol. 74, pp. 99–106, 2013.

[106] T. Serra, J. A. Planell, and M. Navarro, "High-resolution PLA-based composite scaffolds via 3-D printing technology," *Acta Biomaterialia*, vol. 9, pp. 5521–5530, 2013.

[107] X. Li, H. Liu, X. Niu et al., "The use of carbon nanotubes to induce osteogenic differentiation of human adipose-derived MSCs in vitro and ectopic bone formation in vivo," *Biomaterials*, vol. 33, no. 19, pp. 4818–4827, 2012.

[108] G. Ciofani, S. Del Turco, G. Graziana Genchia et al., "Transferrin-conjugated boron nitride nanotubes: protein grafting, characterization, and interaction with human endothelial cells," *International Journal of Pharmaceutics*, vol. 436, pp. 444–453, 2012.

[109] X. Li, H. Gao, M. Uo et al., "Maturation of osteoblast-like SaoS2 induced by carbon nanotubes," *Biomedical Materials*, vol. 4, Article ID 015005, 2009.

[110] Y. Yang, Q. He, L. Duan, Y. Cui, and J. Li, "Assembled alginate/chitosan nanotubes for biological application," *Biomaterials*, vol. 28, no. 20, pp. 3083–3090, 2007.

[111] G. E. Poinern, R. K. Brundavanam, N. Mondinos, and Z.-T. Jiang, "Synthesis and characterisation of nanohydroxyapatite using an ultrasound assisted method," *Ultrasonics Sonochemistry*, vol. 16, no. 4, pp. 469–474, 2009.

[112] V. Vamvakaki, K. Tsagaraki, and N. Chaniotakis, "Carbon nanofiber-based glucose biosensor," *Analytical Chemistry*, vol. 78, no. 15, pp. 5538–5542, 2006.

[113] L. Wu, J. Lei, X. Zhang, and H. Ju, "Biofunctional nanocomposite of carbon nanofiber with water-soluble porphyrin for highly sensitive ethanol biosensing," *Biosensors and Bioelectronics*, vol. 24, no. 4, pp. 644–649, 2008.

[114] X. M. Li, R. R. Cui, W. Liu et al., "The use of nano-scaled fibers or tubes to improve biocompatibility and bioactivity of biomedical materials," *Journal of Nanomaterials*, vol. 2013, Article ID 728130, 16 pages, 2013.

[115] X. M. Li and Q. L. Feng, "Dynamic rheological behaviors of the bone scaffold reinforced by chitin fibres," *Materials Science Forum*, vol. 475–479, pp. 2387–2390, 2005.

[116] S. Zhang, L. Chen, Y. Jiang et al., "Bi-layer collagen/microporouselectrospunnanofiber scaffold improves the osteochondral regeneration," *Acta Biomaterialia*, vol. 9, pp. 7236–7247, 2013.

[117] X. Li, H. Gao, M. Uo et al., "Effect of carbon nanotubes on cellular functions in vitro," *Journal of Biomedical Materials Research A*, vol. 91, no. 1, pp. 132–139, 2009.

[118] X. Li, X. Liu, J. Huang, Y. Fan, and F.-Z. Cui, "Biomedical investigation of CNT based coatings," *Surface and Coatings Technology*, vol. 206, no. 4, pp. 759–766, 2011.

[119] X. M. Li, L. Wang, Y. B. Fan, Q. L. Feng, F. Z. Cui, and F. Watari, "Nanostructured scaffolds for bone tissue engineering," *Journal of Biomedical Materials Research Part A*, vol. 101A, pp. 2424–2435, 2013.

[120] S.-H. Hsu, H.-J. Tseng, and Y.-C. Lin, "The biocompatibility and antibacterial properties of waterborne polyurethane-silver nanocomposites," *Biomaterials*, vol. 31, no. 26, pp. 6796–6808, 2010.

[121] W. Wang, Y. Zhu, F. Watari et al., "Carbon nanotubeshydroxyapatite nanocomposites fabricated by spark plasma sintering for bonegraft applications," *Applied Surface Science*, vol. 262, pp. 194–199, 2012.

[122] X. M. Li, Y. Yang, Y. B. Fan, Q. L. Feng, F. Z. Cui, and F. Watari, "Biocomposites reinforced by fibers or tubes, as scaffolds for tissue engineering or regenerative medicine," *Journal of Biomedical Materials Research Part A*, vol. 102A, pp. 1580–1594, 2014.

[123] T. A. Campbell and S. O. Ivanova, "3D printing of multifunctional nanocomposites," *Nano Today*, vol. 8, pp. 119–120, 2013.

Hindawi Publishing Corporation
International Journal of Polymer Science
Volume 2014, Article ID 654597, 9 pages
http://dx.doi.org/10.1155/2014/654597

Research Article

The Application of Polysaccharide Biocomposites to Repair Cartilage Defects

Feng Zhao,[1] Wei He,[2] Yueling Yan,[1] Hongjuan Zhang,[2] Guoping Zhang,[1] Dehu Tian,[2] and Hongyang Gao[1]

[1] *Department of Orthopedics, The First Hospital of Hebei Medical University, Shijiazhuang 050031, China*
[2] *Department of Hand Surgery, The Third Hospital of Hebei Medical University, Shijiazhuang 050051, China*

Correspondence should be addressed to Hongyang Gao; ghy0618@126.com

Received 21 January 2014; Accepted 17 March 2014; Published 17 April 2014

Academic Editor: Xiaoming Li

Owing to own nature of articular cartilage, it almost has no self-healing ability once damaged. Despite lots of restore technologies having been raised in the past decades, no repair technology has smoothly substituted for damaged cartilage using regenerated cartilage tissue. The approach of tissue engineering opens a door to successfully repairing articular cartilage defects. For instance, grafting of isolated chondrocytes has huge clinical potential for restoration of cartilage tissue and cure of chondral injury. In this paper, SD rats are used as subjects in the experiments, and they are classified into three groups: natural repair (group A), hyaluronic acid repair (group B), and polysaccharide biocomposites repair (hyaluronic acid hydrogel containing chondrocytes, group C). Through the observation of effects of repairing articular cartilage defects, we concluded that cartilage repair effect of polysaccharide biocomposites was the best at every time point, and then the second best was hyaluronic acid repair; both of them were better than natural repair. Polysaccharide biocomposites have good biodegradability and high histocompatibility and promote chondrocytes survival, reproduction, and spliting. Moreover, polysaccharide biocomposites could not only provide the porous network structure but also carry chondrocytes. Consequently hyaluronic acid-based polysaccharide biocomposites are considered to be an ideal biological material for repairing articular cartilage.

1. Introduction

Articular cartilage plays a vital role in the function of joint action. Complete articular cartilage is the foundation of the normal function of the joint to exercise. Articular cartilage is a single tissue without supply of blood and lymphatic. As the cartilage cells divide very slowly, its ability to repair itself is low and it usually cannot be repaired. Therefore articular cartilage defects are a significant problem in orthopedic surgery. For the reason of primary osteoarthritis or from trauma, it will cause the felling of joint pain. Owing to lack of ability of self-repairing, cartilage injuries are kept for years and can result in further degeneration [1]. With the rapid development of tissue engineering, techniques to restore articular cartilage defects have also made tremendous progress [2], but these are still unsatisfactory for the effect of repairing articular cartilage defect. For decades, lots of researches have been conducted on articular cartilage, we had a better understanding of the biological repair process, and it has recently been shown that articular cartilage has a spontaneous repair reaction in the case of full-thickness cartilage defects [3]. However, the extent of this repair response is finite. By contrast, few useful elaborations with respect to repair processes in terms of partial-thickness lesions restricted the cartilage itself [4].

Despite the fact that lots of methods have been employed to repair cartilage damages, they work ineffectively, such as chondrectomy [5], drilling [6], cartilage scraping [7], arthroplasty [8], grafting of autogenic or allogenic chondrocytes [9, 10], and periosteum [11] as well as cartilage and bone flap being the most commonly applied [12]. Although the bone repair could be induced [13], it will remain to be a great challenge in terms of repairing large defects of articular cartilage [14].

Rebuilding cartilage makes it possible to repair cartilage defects with the rapid development of tissue engineering.

The primary method is to repair cartilage defects by the use of seeding cells and scaffolds [15]. Scaffolds are generally employed to restore cartilage defects mainly because of their three-dimensional surroundings needed for regeneration of cartilaginous tissues [16]. Both synthetic [17–20], natural [21–25] scaffolding materials and other composites containing fillers biomaterials [26] have been used for cell conveying in special cell regeneration.

Synthetic scaffolds are artificial option for biological repairing. In comparison with natural scaffolds, their advantage lies in the ability to stand weight-bearing forces by means of regulating their mechanical performance. Also, it has been reported for the successful use of different synthetic polymers in repairing the cartilage defects. However, synthetic materials have the following disadvantages: first, acidic byproducts will be created and accumulated in the use of scaffolds; second, they take on a poor biocompatibility; last, the underlying toxicity of byproducts in the course of these materials' degradation may give rise to an inflammatory reaction [27].

In all natural materials, chitosan [28, 29], collagen [30, 31], atelocollagen gel [32, 33], fibrin [34], alginate [35], and agarose [36] have been employed as effective scaffolds for cartilage repairing, and the repair effect of all above natural materials are relatively satisfactory natural materials. De Franceschi et al. demonstrated that implanting chondrocytes via the carrier of an atelocollagen gel could boost the repair of the articular cartilage in the knee [30]; especially when the scaffold exhibits nanostructure, the effect of repair will be more clear and effective [37].

For the existing form of polyanion, hyaluronic acid with linear high molecular mass polysaccharide is generally known as hyaluronan; also α-1,4-D-glucuronic acid and β-1,3-N-acetyl-D-glucosamine are component unit of hyaluronic acid. Generally speaking, the molecular weight of hyaluronic acid lies in the range of 103 to 107 [38]. Hyaluronic acid is the component not only existing inthe ECM of various connective tissues, but also interacting with binding proteins. Proteoglycans which function as lubricant safeguarding the surface of articular cartilage help in the control of water balance. Additionally, hyaluronic acid plays a role of selecting and protecting around the cell membrane; what is more, special cell receiverswhich control inflammation, cell behavior, angiogenesis, and healing processes could be easily identified by hyaluronic acid [37]. Umbilical cord, synovial fluid, rooster comb, and vitreous humor are major source for commercially available hyaluronic acid [39, 40]; however, hyaluronic acid could be also obtained by means of massive microbial fermentation, avoiding the danger of animal-derived pathogens [40], and sometimes natural materials like hyaluronic acid could be guided by other specific materials [41].

As a result of excellent biocompatibility and viscoelastic performances, hyaluronic acid has been broadly studied and employed in the biomedical area for cell encapsulation, carrier systems, and tissue engineering. It is just because of its nonimmunogenic performances, extensive use, and simple operating of chain size that hyaluronic acid is especially suitable for tissue engineering applications. What is more, by means of interaction with cell-surface receptors, it immediately imposes an influence on tissue organization, which advances the transfer of ECM remodeling and special cell. Hyaluronic acid is well known to interact with chondrocytes by means of every exterior receptor related to signaling pathway, which enable chondrocytes to keep their original phenotype. Additionally, hyaluronic acid could activate collagen II and aggrecan along with cell proliferation. What is more, by means of integrating alginate, chitosan, and fibrin gel matrices, hyaluronic acid possesses the ability to offer artificial ECM surroundings. So hyaluronic acid scaffold is a very promising biomaterial to repair articular cartilage defects. In this study, polysaccharide biocomposites (hyaluronic acid hydrogel containing chondrocytes) were used to repair full-thickness articular cartilage defects in rats. According to the evaluation of histological and biochemical criteria, the repair effect of restoration materials will provide a basis for its application.

2. Materials and Methods

2.1. Grouping. In this experiment, we selected 120 250 ± 20 g clean-grade SD rats (The Animal Experimental Center of Hebei Medical University) and classified them into three groups randomly: natural repair (group A), hyaluronic acid repair (group B), and polysaccharide biocomposites repair (hyaluronic acid hydrogel containing chondrocytes, group C). Each group has 36 rats. The remaining 12 rats are used to get chondrocytes.

2.2. Obtaining Chondrocytes. Cut rats' xiphoid cartilage under sterile conditions, and shear cartilage into pieces. Then, digest cartilage pieces by 0.25% trypsin (GIBCO Company, France) at 37°C for 3 minutes, drain the supernatant, and after that digest treated cartilage pieces by 0.25% trypsin (GIBCO Company, France) again at 37°C for 1 hour; then digest them by 0.2% collagenase II (Baiao Biotechnology Company) at 37°C for 2 hours. Get the supernatant and centrifuge at 800 rpm for 10 minutes for collecting chondrocytes. Via Toluidine blue staining, we made an identification of chondrocytes. By means of Trypan blue staining, the fact that the viability of acquired cells was greater than 90% was detected. Few medium was added into collected cells, and cells density was adjusted at 1×10^5/mL and mixed evenly by vortex shaker to reserve.

2.3. Preparation of Polysaccharide Biocomposites. The achieved chondrocytes were added into 1% hyaluronic acid hydrogel (The Experimental Center of The First Hospital of Hebei Medical University; pH: 6.8~7.8, osmotic pressure ratio: 1.0~1.2). The cell density was adjusted to 5×10^4/mL and mixed evenly by vortex shaker to reserve.

2.4. Surgical Methods

2.4.1. Preparation of Cartilage Damage Model. Animals were banned food and water 12 hours before surgery and injected with anesthetic (ketamine 1%, 10 mg/kg, diazepam 1 mg/kg)

in the upper left thigh. The experimental animals that had been anaesthetized were put on the sterile surgical drapes with both their legs' extension position fixed in a supine position. The surgical area in right leg was disinfected by 2% iodine, 75% alcohol. Skin was slit in longitudinal orientation from the 2 mm on the pole of patella to the 2 mm under the lower pole of patella on its right knee. Medial support belt and joint capsule were slit in level at 1 mm inside the inner edge of the patella. The patella was dislocated to the outside. Femoral trochlear appeared in flexion at 90°. In order to form full-thickness cartilage defects, use a hollow drill (with a diameter of 2.5 mm) to drill several 3 mm holes in the middle of trochlea humeri. After ful hemostasis, medial retinaculum, joint capsule, and the skin were sutured in turn. After surgery, 0.1 mL of hyaluronic acid hydrogel was injected into articular cavity of group B. Also 0.1 mL of polysaccharide biocomposites (hyaluronic acid hydrogel containing chondrocytes) was injected into articular cavity of group C; the rats of group A would be naturally repaired. All surgeries were performed by experimenter under the help of same assistants.

2.4.2. Postoperative Treatment. The operative incision was disinfected by 75% alcohol once a day and surgical suture was removed after 7 days.

2.5. The Experimental Details of Some Steps

2.5.1. HE Staining. Prepare the tissue slice and dewax in the xylene for 5–10 min; then remove slice into the mixture of xylene and absolute ethanol (1 : 1). Soak the slice in the 100%, 90%, and 85% ethyl alcohol in sequence each for 2–5 min; at last, after dealing with the distilled water, transfer it to dye liquor; stain the slice with hematoxylin dyeing for 5–15 min, wash redundant dye off the slide with water, and separate color using 0.5–1% hydrochloric acid alcohol for a moment; perform a microscopy control until the nucleus and chromatin are clear. Flush with running water for 15–30 minutes, and then the nuclei will turn blue. Then wash the slice with distilled water for a short time, and stain with 0.1–0.5% eosin dye for 1–5 min, dehydrate with 85%, 90%, and 100% ethyl alcohol in sequence each for 2-3 min. Treat sample with xylene twice for about 10 min totally. In the end, wipe the excess xylene around the section, and drop proper amount of neutral gum rapidly; then seal the slice with coverslip.

2.5.2. Masson Staining. Fix the tissue with neutral formaldehyde liquid, prepare paraffin section, and dewax to water routinely. Then, stain section with Masson compound staining liquid for about 5 min, and wash with 0.2% acetic acid aqueous solution for a short time. Treat section with 5% phosphotungstic acid for 5–10 min, and then embathe section with 0.2% acetic acid aqueous solution twice; then stain with aniline blue for 5 min and wash with 0.2% acetic acid aqueous solution for a moment. Finally, dehydrate section with absolute alcohol and treat using xylene; seal slice with neutral balsam.

2.5.3. Scanning Electron Microscope Observation. Select 4 rats randomly in each group 40 days after cartilage damage repair operation; cut open along original operative incision immediately after rabbits' execution. Obtain materials regularly according to electron microscope specimen. Cut and acquire a tissue block (with the size of $2.5 \times 2.5 \times 1.0\,mm^3$) in the local damage cartilage rapidly, fix the tissue block with 4% glutaraldehyde fixation fluid, observe the scanning electron microscope, and take pictures.

2.5.4. Immunohistochemistry. Fix the tissue, prepare paraffin section and dewax routinely. Conduct a digestion using enzyme and then carry out rehydration. Wash section using PBS (0.01 mol/L, pH: 7.2–7.4) for 5 min, dry with cold wind, and put into the wet box. Drop diluted fluorescent antibody at temperature of 37°C for 30–60 minutes. Wash sections with PBS twice and distilled water once, respectively, in sequence. Eventually, seal slices with 50% glycerol buffer, examine the section under fluorescence microscope, and then conduct control staining.

2.5.5. Measuring the Contents of Type II Collagen. In the experiment, the content of type II collagen was calculated via determination of content of hydroxyproline. Specifically, the average content of hydroxyproline in collagen is 13.4%, and the content of type II collagen accounts for 80% in articular cartilage collagen; as a consequence, as long as we make a determination of content of hydroxyproline in articular cartilage, we will figure out the content of type II collagen.

Determination of content of hydroxyproline: cut and acquire a tissue block (with the size of $2.5 \times 2.5 \times 1.0\,mm^3$) in the local damage cartilage, and the block weighs about 60–80 mg. Then dehydrate the tissue block with 1 mL anhydrous ethanol for 1 h after physiological saline flushing, discard the supernatant, and degrease the tissue block 2 times with 1.6 mL mixture of acetone and ethyl ether, each time of degreasing operation stays overnight. Take out and dry out the tissue block; then put it into oven (at temperature of 110°C) and dry to constant weight, weigh 5 mg cartilage samples accurately, and put into a test tube; then add 0.7 mL muriatic acids (at concentration of 6 mol/L) into tube and hydrolyze in the oven (at temperature of 105°C) for 24 h; adjust the solution to pH 6 with 6 mol/L sodium hydroxide. Then, adjust the volume to 5 mL accurately, centrifuge at the rate of 2500~3000 rpm for 10 min, and gain 0.6 mL supernatant for determining content of hydroxyproline.

2.6. Statistical Analysis. Data were analyzed with SAS software, and expressed as mean ± SD. The difference between the two groups was compared with Student's t-test. A value of $P < 0.05$ was considered statistically significant.

3. Results

In the observation of electron microscope observation, specimen staining revealed that the bottom of restoration area in group A appeared to be a small amount of red granulation tissue whose surface was covered by pale, relatively

smooth, and transparent membrane after 10 days of operation (Figure 1(a)). The restoration area of groups B and C was filled with regenerated tissue which was white and soft and also had an uneven surface and clear boundary (Figures 1(b) and 1(c)). After 20 days of surgery, repair tissue of restoration area in group A was white and slightly hard and had uneven surface and clear boundary (Figure 1(d)); repair tissue of restoration area in groups B and C was milky white and tough and also had a flat surface and clear boundary (Figures 1(e) and 1(f)). After 40 days of surgery, the bottom of restoration area group A was filled with granulation tissue (Figure 1(g)). Restoration area in group B was filled with repair tissue which was yellowish white and had a relatively clear boundary, tough quality, and uneven surface (Figure 1(h)). The repair tissue of group C without clear boundary with normal cartilage (Figure 1(i)) was tough and translucent. After 10 days of surgery, the case of inflammatory cell (most were lymphocytes) infiltration was found in repair tissue. 20 days later, inflammatory cell infiltration went clearer. after 40 days of operation, lymphocytes cell infiltration reduced. For groups A and B, slight lymphocytes cell infiltration appeared in the repair tissue of both groups after 10 days of operation; lymphocytes cell infiltration got a little more after 20 days of operation, but obviously less than group C; lymphocytes cell infiltration reduced obviously after 40 days of operation. According to the specimen staining, group C (Figure 2(a)) performed best in the synthesis of collagen in repair area. The second best is group B (Figure 2(b)) and both group C and group B outperformed group A (Figure 2(c)).

By the observation of scanning electron microscopy, collagen fibers in parallel with articular surface arranged regularly as with group C (Figure 3(c)) in the restoration area, and the boundary of collagen fibers in the restoration area is not clear with normal cartilage after 40 days of operation. In case of group B (Figure 3(b)), the arrangement of collagen fibers was relatively regular; also fibers were relatively thinner and partially fractured or sunken. For group A (Figure 3(a)), collagen fibers in the restoration area were in disorder and thick; just like group B, collagen fibers in group A were partially fractured too. In the results of immunohistochemical detection, brown and yellow positive reaction product was found in every cell cytolymph in the restoration area. The amount of group C (Figure 4(a)) was the most and well dispersed; the second was group B (Figure 4(b)) and the reaction product dispersed uniformly, and just few positive reaction products were found in group A (Figure 4(c)).

In Table 1, We can obviously see that the content of type II collagen was the highest in group C in the tissue of repair area; then the second highest was group B; the last is group A after 10, 20, and 40 days of operation.

In a word, at every time point, through the evaluation of histology and biochemistry, cartilage repair effect of group C is the best; the second best is group B; both of them were better than group A.

4. Discussions

Articular cartilage is hyaline cartilage, whose tissue's metabolic activity is low, without blood supply and lymphatic drainage, and cartilage cells divide very slowly, so its ability to repair itself is low; usually it cannot be repaired [42–44]. Therefore, how to promote the repair of damaged cartilage is one of the key research points to scholars for a long time. With the development of tissue engineering technology, cartilage injury repair has made some progress [45–48]. Currently, cartilage tissue engineering research's main content focused on seed cells, the carrier material, and the interaction of seed cells and carrier [49]. In the process of tissue engineering materials application, there is no generally accepted ideal implant because of the compatibility of the seed cells; the carrier's adhesion and degradation should be considered [50–52]. Ideal carrier material whose extracellular matrix components are as close as to the nature chondrocytes should have good tissue compatibility and biodegradability [53]. Currently there are two categories: natural materials and synthetic materials. Synthetic materials include polylactic acid, polyglycolic acid copolymer, hydroxyapatite, and calcium phosphate [54, 55]. Owing to lack of binding sites which cells can recognize, so synthetic material has no biological activity and its degradation products may be toxic. Natural materials are mainly collagen, fibrin gel, hyaluronic acid, and so on. Its biocompatible and biodegradable properties are better than synthetic materials'. But its different resources make obviously different structure and performance [56–59].

Hyaluronic acid is a nonsulfated polysaccharide-based natural cartilage matrix, whose three-dimensional structure has high porosity and surface and space area are bigger, which is benefit for growth of cell adhesion, extracellular matrix deposition, the take-up of gases and nutrients, and metabolic product discharge, and offers a good interface of material-cell function. Hyaluronic acid can improve adhesion between cells and extracellular matrix burial and play an important role in cartilage nutrition, maintaining cartilage characteristics and joint lubrication [60–62]. Hyaluronic acid also can maintain normal growth of cartilage cells and promote the integration of transplanted chondrocytes and damaged cartilage [63–66]. Certainly, along with other natural materials, such as chitosan [67, 68] and collagen [69], the hyaluronic acid could be used as biomaterials scaffolds for repairing articular cartilage. The purity of hyaluronic acid is higher, the immunogenicity is lower, and the biocompatibility is better. Hyaluronic acid's degradation products can promote wound healing [70–73]. Hyaluronic acid as a treatment for osteoarthritis medication has been in clinical use for many years [74]. Its efficacy is satisfactory with fewer side effects. And its operation is simple as an injectable material. So in this study hyaluronic acid is selected as a carrier material. Experimental results indicate that the repair effect of group B is better than that of group A in terms of tissue science and biochemical evaluation, which fully proved that hyaluronic acid can promote cartilage repair.

In this experiment, inflammatory cells, mainly lymphocytes, are in infiltration in each group restoration area at early stage after surgery under light microscope and Group C is the most obvious. With time going, inflammatory cells' quantity becomes less. 10 days after the injection of repair materials, infiltration of inflammatory cells can be seen in restoration area for identification of phagocytic cells. Groups A and B have the same level of infiltration of inflammatory

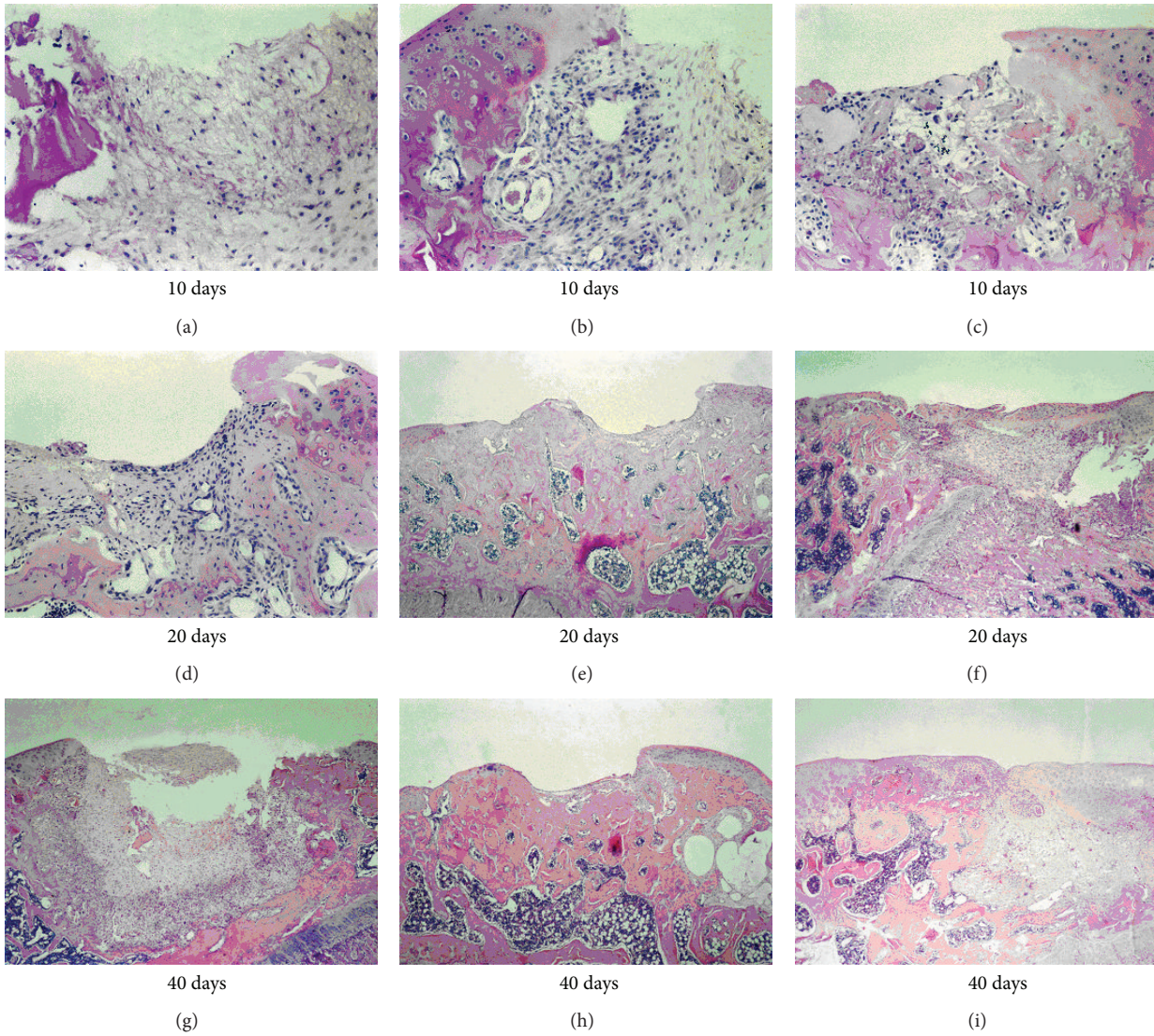

Figure 1: The results of specimen HE staining in restoration area; magnification times of all pictures in Figure 1 are 200. Pictures (a), (d), and (g) belong to group A; pictures (b), (e), and (h) belong to group B; pictures (c), (f), and (i) belong to group C.

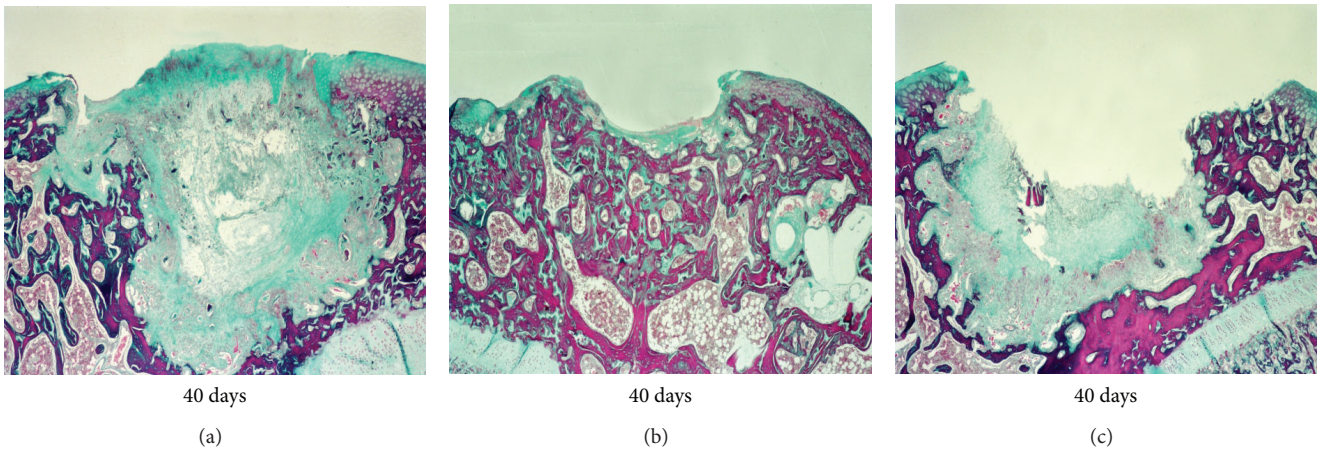

Figure 2: The results of specimen Masson staining in restoration area; magnification times of all pictures in Figure 2 are 200. Pictures (a), (b), and (c) belong to groups A, B, and C, respectively.

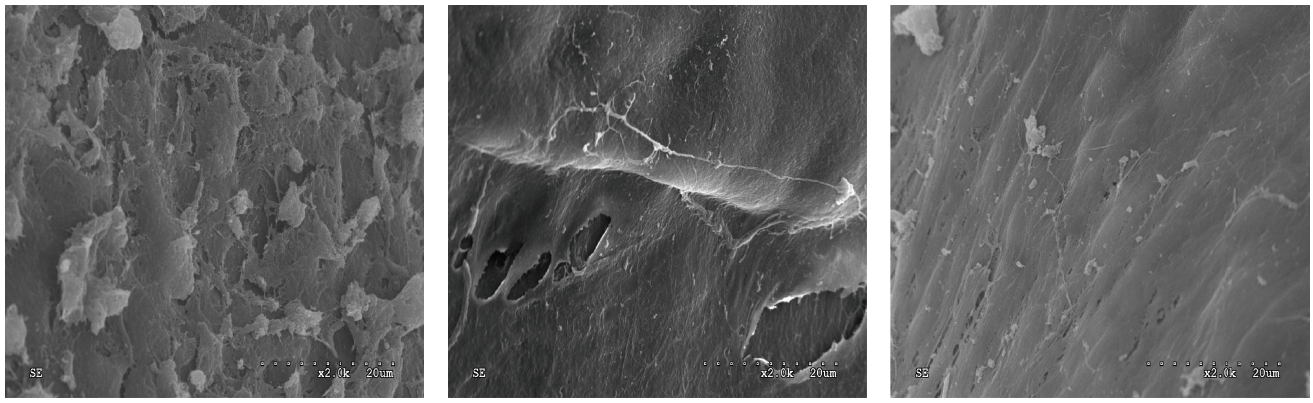

40 days (a) 40 days (b) 40 days (c)

Figure 3: The scanning electron microscopy images of collagen fibers in repair area; magnification times of all pictures in Figure 3 are 2000. Pictures (a), (b), and (c) belong to groups A, B, and C, respectively.

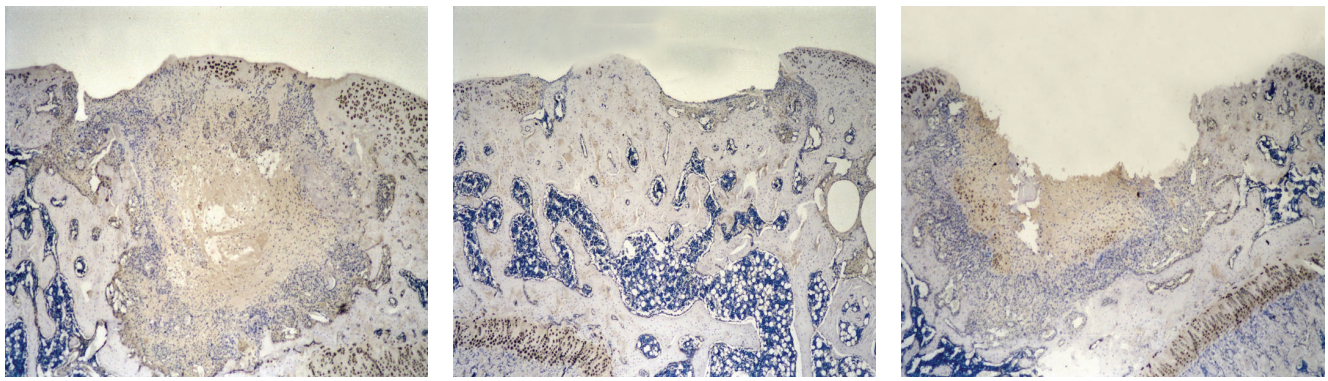

40 days (a) 40 days (b) 40 days (c)

Figure 4: The results of immunohistochemical detection in restoration area; magnification times of all pictures in Figure 4 are 200. Pictures (a), (b), and (c) belong to groups A, B, and C, respectively.

cells, which indicates that hyaluronic acid as a carrier material has good biocompatibility. The level of infiltration of inflammatory cells at each time point is the best, which indicates that resource of immune resource is major histocompatibility antigens on cartilage cell's surface. The result of immunohistochemistry shows that positive reaction product of Group A restoration area is the least, which indicates that its ability of proteoglycan synthesis was significantly reduced; positive reaction product of group C restoration area is the most in the all 3 groups, which indicated that hyaluronic porous network structure is conducive to the growth of cartilage cells and extracellular matrix is proteoglycan-rich both of which can slow down the degradation of type II collagen synthesis of chondrocytes. The sign of the maturity level of cartilage is collagen because the structural basis of cartilage is collagen. Masson staining indicates that a large number of collagen fibers can be seen in group C restoration area, which is more than groups A and B. As with hydroxyproline content, group C contained the most; then the second is group B; the last is group A. Three groups' difference is statistically significant. All can prove that this repair material can effectively promote cartilage repair. Through the experiment, compared to natural repair, the overall repair effect of hyaluronic acid performed better. This fact fully demonstrated that hyaluronic acid played a catalytic role for cartilage repair. When compared with hyaluronic acid, the repair effect of polysaccharide biocomposites (hyaluronic acid hydrogel containing chondrocytes) was better, which fully illustrated that the combined action of hyaluronic acid and chondrocytes was advantageous to the growth of cartilage cells and collagen and proteoglycan synthesis. Of course, its porous network structure also played a driving role in repairing cartilage defects. These polysaccharide biocomposites, which were obtained easily and prepared simply, are a relatively ideal biomaterial for cartilage repair and could be made into injection.

Because clinical cartilage damage is mostly closed, selection of repair material tends from solid to liquid and the method of transplantation tends from open graft with large injury to simple, minimally invasive intra-articular

Table 1: The content of type II collagen in the repair area at different time points (μg/mg).

Groups	10 days (μg/mg)	20 days (μg/mg)	40 days (μg/mg)
Natural repair	80.83 ± 4.91	81.03 ± 5.01	80.94 ± 5.35
Hyaluronic acid	90.35 ± 9.59*	88.39 ± 7.96**	89.17 ± 8.52**
Composites	99.78 ± 7.56*	105.55 ± 7.49*	101.97 ± 7.34*

*$P < 0.01$; **$P < 0.05$.

injection. In this experiment, polysaccharide biocomposites (hyaluronic acid containing chondrocytes) were applied in intra-articular injection to repair cartilage defects, whose result indicates that this method is feasible, satisfactory, and provides a theoretical basis for clinical application. However, due to the separation and culture of chondrocytes being directly related to repair effect, the isolation and culture techniques of chondrocytes are needed to further improve.

5. Conclusion

Transplantation of isolated chondrocytes which belongs to the category of tissue engineering has tremendous potential for treatment of cartilage injury and regeneration of articular cartilage tissue. As to transplantation of isolated chondrocytes and formation of cartilage tissue, the determining factor of success lays in particular cell-carrier materials. In terms of restoring articular cartilage, hyaluronic acid biomaterials outperformed natural repair obviously; of course, polysaccharide biocomposites performed best in effect of restoration. Polysaccharide biocomposites could offer the porous network structure which could promote chondrocytes proliferation, and it could also carry chondrocytes effectively. The porous network structure has high histocompatibility with the surrounding and good biodegradability, and it also favors chondrocytes survival, reproduction, and splitting. So the polysaccharide biocomposites is an appropriate specific cell-carrier material. Consequently hyaluronic acid-based polysaccharide hydrogels biocomposites are considered to be an ideal biological material for repairing articular cartilage.

Conflict of Interests

The authors declare that there is no conflict of interests regarding the publication of this paper.

Authors' Contribution

Feng Zhao and Wei He contributed equally to this work.

References

[1] J. A. Buckwalter and H. J. Mankin, "Articular cartilage: degeneration and osteoarthritis, repair, regeneration, and transplantation," *Instructional Course Lectures*, vol. 47, pp. 487–504, 1998.

[2] X. Li, X. Liu, J. Huang, Y. Fan, and F.-Z. Cui, "Biomedical investigation of CNT based coatings," *Surface and Coatings Technology*, vol. 206, no. 4, pp. 759–766, 2011.

[3] F. Shapiro, S. Koide, and M. J. Glimcher, "Cell origin and differentiation in the repair of full-thickness defects of articular cartilage," *Journal of Bone and Joint Surgery A*, vol. 75, no. 4, pp. 532–553, 1993.

[4] E. B. Hunziker and L. C. Rosenberg, "Repair of partial-thickness defects in articular cartilage: cell recruitment from the synovial membrane," *Journal of Bone and Joint Surgery A*, vol. 78, no. 5, pp. 721–733, 1996.

[5] J. A. Buckwalter, "Articular cartilage: injuries and potential for healing," *Journal of Orthopaedic and Sports Physical Therapy*, vol. 28, no. 4, pp. 192–202, 1998.

[6] J. R. Steadman, B. S. Miller, S. G. Karas, T. F. Schlegel, K. K. Briggs, and R. J. Hawkins, "The microfracture technique in the treatment of full-thickness chondral lesions of the knee in National Football League players," *Journal of Knee Surgery*, vol. 16, no. 2, pp. 83–86, 2003.

[7] S. W. Holmes Jr., "Articular cartilage injuries in the athlete's knee: current concepts in diagnosis and treatment," *Southern Medical Journal*, vol. 97, no. 8, pp. 742–747, 2004.

[8] I. Martin, S. Miot, A. Barbero, M. Jakob, and D. Wendt, "Osteochondral tissue engineering," *Journal of Biomechanics*, vol. 40, no. 4, pp. 750–765, 2007.

[9] M. Sittinger, C. Perka, O. Schultz, T. Häupl, and G.-R. Burmester, "Joint cartilage regeneration by tissue engineering," *Zeitschrift fur Rheumatologie*, vol. 58, no. 3, pp. 130–135, 1999.

[10] V. J. Sammarco, R. Gorab, R. Miller, and P. J. Brooks, "Human articular cartilage storage in cell culture medium: guidelines for storage of fresh osteochondral allografts," *Orthopedics*, vol. 20, no. 6, pp. 497–499, 1997.

[11] M. Brittberg, "Autologous chondrocyte implantation—technique and long-term follow-up," *Injury*, vol. 39, no. 1, pp. 40–49, 2008.

[12] H. K. Outerbridge, R. E. Outerbridge, and D. E. Smith, "Osteochondral defects in the knee: a treatment using lateral patella autografts," *Clinical Orthopaedics and Related Research*, no. 377, pp. 145–151, 2000.

[13] X. Li, H. Gao, M. Uo et al., "Maturation of osteoblast-like SaoS2 induced by carbon nanotubes," *Biomedical Materials*, vol. 4, no. 1, Article ID 015005, 2009.

[14] X. Guo, C. Wang, Y. Zhang et al., "Repair of large articular cartilage defects with implants of autologous mesenchymal stem cells seeded into β-tricalcium phosphate in a sheep model," *Tissue Engineering*, vol. 10, no. 11-12, pp. 1818–1829, 2004.

[15] X. M. Li, Y. Yang, Y. B. Fan, Q. L. Feng, F. Z. Cui, and F. Watari, "Biocomposites reinforced by fibers or tubes, as scaffolds for tissue engineering or regenerative medicine," *Journal of Biomedical Materials Research A*, 2013.

[16] C. Chung and J. A. Burdick, "Engineering cartilage tissue," *Advanced Drug Delivery Reviews*, vol. 60, no. 2, pp. 243–262, 2008.

[17] T.-K. Kim, B. Sharma, C. G. Williams et al., "Experimental model for cartilage tissue engineering to regenerate the zonal organization of articular cartilage," *Osteoarthritis and Cartilage*, vol. 11, no. 9, pp. 653–664, 2003.

[18] X. Li, X. Liu, W. Dong et al., "In vitro evaluation of porous poly(L-lactic acid) scaffold reinforced by chitin fibers," *Journal of Biomedical Materials Research B*, vol. 90, no. 2, pp. 503–509, 2009.

[19] W.-J. Li, K. G. Danielson, P. G. Alexander, and R. S. Tuan, "Biological response of chondrocytes cultured in three-dimensional nanofibrous poly(ε-caprolactone) scaffolds," *Journal of Biomedical Materials Research A*, vol. 67, no. 4, pp. 1105–1114, 2003.

[20] H. J. Lee, J.-S. Lee, T. Chansakul, C. Yu, J. H. Elisseeff, and S. M. Yu, "Collagen mimetic peptide-conjugated photopolymerizable PEG hydrogel," *Biomaterials*, vol. 27, no. 30, pp. 5268–5276, 2006.

[21] X. Li, Q. Feng, X. Liu, W. Dong, and F. Cui, "Collagen-based implants reinforced by chitin fibres in a goat shank bone defect model," *Biomaterials*, vol. 27, no. 9, pp. 1917–1923, 2006.

[22] C. R. Lee, S. Grad, K. Gorna, S. Gogolewski, A. Goessl, and M. Alini, "Fibrin-polyurethane composites for articular cartilage tissue engineering: a preliminary analysis," *Tissue Engineering*, vol. 11, no. 9-10, pp. 1562–1573, 2005.

[23] C. R. Lee, A. J. Grodzinsky, and M. Spector, "Biosynthetic response of passaged chondrocytes in a type II collagen scaffold to mechanical compression," *Journal of Biomedical Materials Research A*, vol. 64, no. 3, pp. 560–569, 2003.

[24] X. Li, Q. Feng, W. Wang, and F. Cui, "Chemical characteristics and cytocompatibility of collagen-based scaffold reinforced by chitin fibers for bone tissue engineering," *Journal of Biomedical Materials Research B*, vol. 77, no. 2, pp. 219–226, 2006.

[25] P. Buma, J. S. Pieper, T. van Tienen et al., "Cross-linked type I and type II collagenous matrices for the repair of full-thickness articular cartilage defects—a study in rabbits," *Biomaterials*, vol. 24, no. 19, pp. 3255–3263, 2003.

[26] X. M. Li, Y. Huang, L. S. Zheng et al., "Effect of substrate stiffness on the functions of rat bone marrow and adipose tissue derived mesenchymal stem cells in vitro," *Journal of Biomedical Materials Research A*, vol. 102, pp. 1092–1101, 2014.

[27] J. Bujia, D. Reitzel, and M. Sittinger, "In-vitro engineering of cartilage tissue: influence of L(+)-lactic acid and glycolic acid on cultured human chondrocytes," *Laryngo-Rhino-Otologie*, vol. 74, no. 3, pp. 183–187, 1995.

[28] D. L. Nettles, S. H. Elder, and J. A. Gilbert, "Potential use of chitosan as a cell scaffold material for cartilage tissue engineering," *Tissue Engineering*, vol. 8, no. 6, pp. 1009–1016, 2002.

[29] Y.-C. Kuo and C.-Y. Lin, "Effect of genipin-crosslinked chitin-chitosan scaffolds with hydroxyapatite modifications on the cultivation of bovine knee chondrocytes," *Biotechnology and Bioengineering*, vol. 95, no. 1, pp. 132–144, 2006.

[30] L. de Franceschi, B. Grigolo, L. Roseti et al., "Transplantation of chondrocytes seeded on collagen-based scaffold in cartilage defects in rabbits," *Journal of Biomedical Materials Research A*, vol. 75, no. 3, pp. 612–622, 2005.

[31] X. Li, Q. Feng, and F. Cui, "In vitro degradation of porous nano-hydroxyapatite/collagen/PLLA scaffold reinforced by chitin fibres," *Materials Science and Engineering C*, vol. 26, no. 4, pp. 716–720, 2006.

[32] M. Ochi, Y. Uchio, K. Kawasaki, S. Wakitani, and J. Iwasa, "Transplantation of cartilage-like tissue made by tissue engineering in the treatment of cartilage defects of the knee," *Journal of Bone and Joint Surgery B*, vol. 84, no. 4, pp. 571–578, 2002.

[33] Y. Ito, M. Ochi, N. Adachi et al., "Repair of osteochondral defect with tissue-engineered chondral plug in a rabbit model," *Arthroscopy*, vol. 21, no. 10, pp. 1155–1163, 2005.

[34] V. Ting, C. Derek Sims, L. E. Brecht et al., "In vitro prefabrication of human cartilage shapes using fibrin glue and human chondrocytes," *Annals of Plastic Surgery*, vol. 40, no. 4, pp. 413–421, 1998.

[35] Y. Park, M. Sugimoto, A. Watrin, M. Chiquet, and E. B. Hunziker, "BMP-2 induces the expression of chondrocyte-specific genes in bovine synovium-derived progenitor cells cultured in three-dimensional alginate hydrogel," *Osteoarthritis and Cartilage*, vol. 13, no. 6, pp. 527–536, 2005.

[36] R. L. Mauck, X. Yuan, and R. S. Tuan, "Chondrogenic differentiation and functional maturation of bovine mesenchymal stem cells in long-term agarose culture," *Osteoarthritis and Cartilage*, vol. 14, no. 2, pp. 179–189, 2006.

[37] X. M. Li, L. Wang, Y. B. Fan, Q. L. Feng, F. Z. Cui, and F. Watari, "Nanostructured scaffolds for bone tissue engineering," *Journal of Biomedical Materials Research A*, vol. 101, pp. 2424–2435, 2013.

[38] T. C. Laurent, U. B. G. Laurent, and J. R. Fraser, "Functions of hyaluronan," *Annals of the Rheumatic Diseases*, vol. 54, no. 5, pp. 429–432, 1995.

[39] T. C. Laurent, "Biochemistry of hyaluronan," *Acta Oto-Laryngologica*, vol. 104, no. 442, pp. 7–24, 1987.

[40] P. B. Malafaya, G. A. Silva, and R. L. Reis, "Natural-origin polymers as carriers and scaffolds for biomolecules and cell delivery in tissue engineering applications," *Advanced Drug Delivery Reviews*, vol. 59, no. 4-5, pp. 207–233, 2007.

[41] X. Li, H. Gao, M. Uo et al., "Effect of carbon nanotubes on cellular functions in vitro," *Journal of Biomedical Materials Research A*, vol. 91, no. 1, pp. 132–139, 2009.

[42] L. Hangody, G. Vásárhelyi, L. R. Hangody et al., "Autologous osteochondral grafting—technique and long-term results," *Injury*, vol. 39, no. 1, pp. 32–39, 2008.

[43] B. J. Cole, C. Pascual-Garrido, and R. C. Grumet, "Surgical management of articular cartilage defects in the knee," *Journal of Bone and Joint Surgery A*, vol. 91, no. 7, pp. 1778–1790, 2009.

[44] A. M. Haleem and C. R. Chu, "Advances in tissue engineering techniques for articular cartilage repair," *Operative Techniques in Orthopaedics*, vol. 20, no. 2, pp. 76–89, 2010.

[45] X. Li, Y. Fan, and F. Watari, "Current investigations into carbon nanotubes for biomedical application," *Biomedical Materials*, vol. 5, no. 2, Article ID 022001, 2010.

[46] C.-C. Jiang, H. Chiang, C.-J. Liao et al., "Repair of porcine articular cartilage defect with a biphasic osteochondral composite," *Journal of Orthopaedic Research*, vol. 25, no. 10, pp. 1277–1290, 2007.

[47] H. Chiang and C.-C. Jiang, "Repair of articular cartilage dafects: review and perspectives," *Journal of the Formosan Medical Association*, vol. 108, no. 2, pp. 87–101, 2009.

[48] X. Liu, X. Li, Y. Fan et al., "Repairing goat tibia segmental bone defect using scaffold cultured with mesenchymal stem cells," *Journal of Biomedical Materials Research B*, vol. 94, no. 1, pp. 44–52, 2010.

[49] F. B. Stillaert, C. di Bartolo, J. A. Hunt et al., "Human clinical experience with adipose precursor cells seeded on hyaluronic acid-based spongy scaffolds," *Biomaterials*, vol. 29, no. 29, pp. 3953–3959, 2008.

[50] J. S. Temenoff and A. G. Mikos, "Review: tissue engineering for regeneration of articular cartilage," *Biomaterials*, vol. 21, no. 5, pp. 431–440, 2000.

[51] X. Li, H. Liu, X. Niu et al., "The use of carbon nanotubes to induce osteogenic differentiation of human adipose-derived MSCs in vitro and ectopic bone formation in vivo," *Biomaterials*, vol. 33, no. 19, pp. 4818–4827, 2012.

[52] J. F. Mano and R. L. Reis, "Osteochondral defects: present situation and tissue engineering approaches," *Journal of Tissue Engineering and Regenerative Medicine*, vol. 1, no. 4, pp. 261–273, 2007.

[53] D. F. Williams, "On the mechanisms of biocompatibility," *Biomaterials*, vol. 29, no. 20, pp. 2941–2953, 2008.

[54] X. Li, H. Liu, X. Niu et al., "Osteogenic differentiation of human adipose-derived stem cells induced by osteoinductive calcium phosphate ceramics," *Journal of Biomedical Materials Research B*, vol. 97, no. 1, pp. 10–19, 2011.

[55] X. Li, C. A. van Blitterswijk, Q. Feng, F. Cui, and F. Watari, "The effect of calcium phosphate microstructure on bone-related cells in vitro," *Biomaterials*, vol. 29, no. 23, pp. 3306–3316, 2008.

[56] I. E. Erickson, S. R. Kestle, K. H. Zellars, G. R. Dodge, J. A. Burdick, and R. L. Mauck, "Improved cartilage repair via in vitro pre-maturation of MSC-seeded hyaluronic acid hydrogels," *Biomedical Materials*, vol. 7, no. 2, Article ID 024110, 2012.

[57] F. M. D. Henson, A. M. J. Getgood, D. M. Caborn, C. W. Wayne McIlwraith, and N. Rushton, "Effect of a solution of hyaluronic acid-chondroitin sulfate-N-acetyl glucosamine on the repair response of cartilage to single-impact load damage," *American Journal of Veterinary Research*, vol. 73, no. 2, pp. 306–312, 2012.

[58] A. Podškubka, C. Povýšil, R. Kubeš, J. Šprindrich, and R. Sedláček, "Treatment of deep cartilage defects of the knee with autologous chondrocyte transplantation on a hyaluronic acid ester scaffolds (Hyalograft C)," *Acta Chirurgiae Orthopaedicae et Traumatologiae Cechoslovaca*, vol. 73, no. 4, pp. 251–262, 2006.

[59] M. Kayakabe, S. Tsutsumi, H. Watanabe, Y. Kato, and K. Takagishi, "Transplantation of autologous rabbit BM-derived mesenchymal stromal cells embedded in hyaluronic acid gel sponge into osteochondral defects of the knee," *Cytotherapy*, vol. 8, no. 4, pp. 343–353, 2006.

[60] M. N. Collins and C. Birkinshaw, "Hyaluronic acid based scaffolds for tissue engineering—a review," *Carbohydrate Polymers*, vol. 92, pp. 1262–1279, 2013.

[61] J. Y. Kang, C. W. Chung, J.-H. Sung et al., "Novel porous matrix of hyaluronic acid for the three-dimensional culture of chondrocytes," *International Journal of Pharmaceutics*, vol. 369, no. 1-2, pp. 114–120, 2009.

[62] I. L. Kim, R. L. Mauck, and J. A. Burdick, "Hydrogel design for cartilage tissue engineering: a case study with hyaluronic acid," *Biomaterials*, vol. 32, no. 34, pp. 8771–8782, 2011.

[63] S. M. Julovi, H. Ito, K. Nishitani, C. J. Jackson, and T. Nakamura, "Hyaluronan inhibits matrix metalloproteinase-13 in human arthritic chondrocytes via CD44 and P38," *Journal of Orthopaedic Research*, vol. 29, no. 2, pp. 258–264, 2011.

[64] H. Laroui, L. Grossin, M. Léonard et al., "Hyaluronate-covered nanoparticles for the therapeutic targeting of cartilage," *Biomacromolecules*, vol. 8, no. 12, pp. 3879–3885, 2007.

[65] A. H. Gomoll, "Serum levels of hyaluronic acid and chondroitin sulfate as a non-invasive method to evaluate healing after cartilage repair procedures," *Arthritis Research & Therapy*, vol. 11, no. 4, article 118, 2009.

[66] S. A. Unterman, M. Gibson, J. H. Lee et al., "Hyaluronic acid-binding scaffold for articular cartilage repair," *Tissue Engineering A*, vol. 18, no. 23-24, pp. 2497–2506, 2012.

[67] C. R. Correia, L. S. Moreira-Teixeira, L. Moroni et al., "Chitosan scaffolds containing hyaluronic acid for cartilage tissue engineering," *Tissue Engineering C*, vol. 17, no. 7, pp. 717–730, 2011.

[68] H. Park, B. Choi, J. Hu, and M. Lee, "Injectable chitosan hyaluronic acid hydrogels for cartilage tissue engineering," *Acta Biomaterialia*, vol. 9, pp. 4779–4786, 2013.

[69] A. Matsiko, T. J. Levingstone, F. J. O'Brien, and J. P. Gleeson, "Addition of hyaluronic acid improves cellular infiltration and promotes early-stage chondrogenesis in a collagen-based scaffold for cartilage tissue engineering," *Journal of the Mechanical Behavior of Biomedical Materials*, vol. 11, pp. 41–52, 2012.

[70] S. S. Kim, M. S. Kang, K. Y. Lee et al., "Therapeutic effects of mesenchymal stem cells and hyaluronic Acid injection on osteochondral defects in rabbits' knees," *Knee Surgery & Related Research*, vol. 24, no. 3, pp. 164–172, 2012.

[71] R. Jin, L. S. M. Teixeira, A. Krouwels et al., "Synthesis and characterization of hyaluronic acid-poly(ethylene glycol) hydrogels via Michael addition: an injectable biomaterial for cartilage repair," *Acta Biomaterialia*, vol. 6, no. 6, pp. 1968–1977, 2010.

[72] J. Chang, J. J. Rasamny, and S. S. Park, "Injectable tissue-engineered cartilage using a fibrin sealant," *Archives of Facial Plastic Surgery*, vol. 9, no. 3, pp. 161–166, 2007.

[73] K. B. Lee, V. T. Wang, Y. H. Chan et al., "A novel, minimally-invasive technique of cartilage repair in the human knee using arthroscopic microfracture and injections of mesenchymal stem cells and hyaluronic Acid-a prospective comparative study on safety and short-term efficacy," *Annals of the Academy of Medicine, Singapore*, vol. 41, no. 11, pp. 511–517, 2012.

[74] J. A. Burdick and G. D. Prestwich, "Hyaluronic acid hydrogels for biomedical applications," *Advanced Materials*, vol. 23, no. 12, pp. H41–H56, 2011.

Hindawi Publishing Corporation
International Journal of Polymer Science
Volume 2014, Article ID 238247, 9 pages
http://dx.doi.org/10.1155/2014/238247

Research Article

The Experimental Study on Promoting the Ilizarov Distraction Osteogenesis by the Injection of Liquid Alg/nHAC Biocomposites

Xinhui Liu,[1] Di Yu,[1] Jieyan Xu,[1] Chao Zhu,[1] Qingling Feng,[2] Chuanyong Hou,[1] Hua Wang,[1] Yelin Yang,[1] and Guoping Guan[1]

[1] *Orthopaedics, The Affiliated Jiangning Hospital of Nanjing Medical University, Nanjing 211100, China*
[2] *State Key Laboratory of New Ceramic and Fine Processing, Tsinghua University, Beijing 100084, China*

Correspondence should be addressed to Xinhui Liu; professorlxh2008@163.com

Received 7 February 2014; Accepted 7 March 2014; Published 14 April 2014

Academic Editor: Xiaoming Li

Limb lengthening is frequently utilized in treating limb length inequalities, angulation deformities, nonunions, complex fractures, and deficiencies after tumor resection in more recent year. The procedure of limb lengthening pioneered by Ilizarov is now a widely accepted method for correcting limb length inequality and short stature as well as for bridging large defects in long bones. In order to promote bone healing during distraction osteogenesis and reduce the complications caused by limb lengthening pioneered, an alginate/nanohydroxyapatite/collagen (Alg/nHAC) composite was fabricated. General observation, histologically morphological observations, X-ray examination, biomechanical test, bone density, and the percentage area of bone trabecula were used to assay the ability of Alg/nHAC composite to promote bone healing. The present study demonstrates that the injection of liquid Alg/nHAC composites can significantly promote distraction osteogenesis. Alg/nHAC composite is promising for clinical application, solving the healing problem of backbone osteotomy and the fixing problem of metaphyseal backbone.

1. Introduction

Corrective limb lengthening is frequently utilized in treating limb length inequalities, angulation deformities, nonunions, complex fractures, deficiencies after tumor resection, and, in more recent years, persons of short stature. During the last two decades, many developments were achieved in the field of limb lengthening surgery, in which the main goal was to increase patients' acceptance and comfort during lengthening [1]. Among them, the adaptation of bone during distraction osteogenesis (DO) is reliable and predictable [2], which is a surgical procedure used to promote tissue regeneration in long bones. It is used to lengthen limbs, repair major bone defects caused by infections or tumours, and correct congenital or acquired craniofacial defects [3, 4].

The procedure of limb lengthening pioneered by Ilizarov is now an accepted method for correcting limb length inequality and short stature as well as for bridging large defects in long bones. Limb lengthening is associated with numerous complications: infections [5, 6], stiff joints [6, 7], pseudarthrosis [6–8], early union [7, 8], and neurological sequela [7–9]. The bone healing problems associated with the other methods of limb lengthening have largely been resolved. Even though external systems have been improved over the years, problems with soft tissue transfixation, neurovascular injuries, pin track infections, malalignment, joint stiffness, pain, and poor cosmetic results are still frequent [10, 11]. A further study about lengthening is necessary.

Along with the development of tissue engineering, bone tissue engineering was applied to treat bone defect. Large amounts of material systems have been developed to mimic the natural extracellular matrix (ECM) and induce bone formation [12–15]. Researches had demonstrated that nHA had ability to promote ossification and bone regeneration [16–19] and collagen was a natural polymer with excellent biocompatibility and bioactivity [20–24]. The combination of bone tissue engineering and DO technology is promising. In this research, a liquid Alg/nHAC composite was injected into

the extension area of rabbits' tibia to study the effect on bone healing.

2. Materials and Methods

2.1. Materials. Acid-soluble type I collagen gel (solid content: 1%) was produced by Beihua Fine Chemicals Co., Ltd., Beijing. Sodium phosphate and calcium sulfate were produced by Yili Fine Chemicals Co., Ltd., Beijing. Sodium alginate was produced by Guoyao Chemical Reagent Co., Ltd. Calcium carbonate was produced by Beijing Modern Oriental Fine Chemicals Co., Ltd. Kirschner wire (12 mm) was produced by Jinlu Medical Equipment Company, Jiangsu. The New Zealand rabbits were obtained from laboratory animal center of Hebei Medical University.

2.2. Equipment. Philips 500mAX film machine (Germany), IPP (Image-Pro Plus IPP) Mediaplayer (USA), DEXAUNIT-2000 dual-energy X-ray absorptiometry instrument (Beijing, China), USS biomechanical testing machine (Shenyang, China), automatic dehydrator TP1020 (Germany), slicer 2125 (Germany), automatic paraffin embedding machine TKY-BM (Hubei, China), roast machine HI1220 (Germany), pushing machine HI1210 (Germany), Olympus camera binocular microscope CX31 (Japan), and image analysis system (Beijing, China) were used in this research.

2.3. Methods

2.3.1. Preparation of Alg/nHAC. A small amount of sodium alginate was mixed with sodium alginate ($Na_3PO_4{\cdot}12H_2O$) and dissolved in deionized water. After stirring for 20 minutes, a pale yellow aqueous solution of completely dissolved alginate was obtained. Calcium sulfate and deionized water were mixed in a beaker according to the setting proportion to obtain a slurry of calcium sulphate. The slurry was stirred until no significant particles can be seen and then kept more than 24 h to remove static. A certain amount of bone meal (nHAC) which was prepared according to the research of Li et al. [25] was dissolved in water and stirred to obtain sufficient bone paste. Then, the bone paste was mixed with the aqueous solution of sodium alginate and stirred to produce an intermixture. Next, the slurry of calcium sulphate was mixed with the intermixture and stirred to obtain a new intermixture. The new obtained intermixture was kept alone for about 15 min. The solid bone repair materials were got after the internal situ crosslinking reaction. Finally, the materials were sterilized with Co60 irradiation (2.5 Mrad) for the next experiments.

2.3.2. Manufacture of External Fixation Devices. In the experiment, we made use of self-made and improved Ilizarov full-ring external fixation with an outer diameter of 90 mm, an insider diameter of 60 mm, thickness of 4 mm, and 14 holes through the ring. The diameter of each is 6.5 mm. The diameter of each screw rod is 6 mm and the length is 105 mm. The screw pitch is 1 mm/lap, so 1 mm extension length can be achieved by extending one lap of the screw rod. The fixed needle is medical Klinefelter needle with diameter of 1.2 mm and 1.0 mm, respectively.

2.3.3. The Preparation of Animal Model of Rabbit Tibia Limbs' Elongation. We selected big-ear white New Zealand rabbits (2–2.5 Kg) as the experimental animal. The rabbits were banned from food intake before operation and their left hind shins were reserved. Then we anaesthetized the rabbits by intravenous injection of 1% pentobarbital sodium after that disinfected the bed sheets and put the rabbit back on the rabbit platform. We drilled two 1.2 mm Kirschner wires across in the location 1.0 cm above tubercles of tibia. A ring of preassembled external fixation was installed and the Kirschner wire would be fixed on the steel ring. Two 1.0 mm Kirschner wires were drilled across in the distal of tubercles of tibia in order to correspond with proximal Kirschner wire, and the steel needle would be fixed on the steel ring using screw bolt meanwhile. Adjust external fixation to be firm and parallel. Under aseptic conditions, we made anterior lateral tibial longitudinal incision which was as deep as periosteum between the upper and lower two sets of needles. Moreover, the incision was peeled in the periosteum and the upper tibial appeared. Pry the lower end of the fibula into two parts and truncate tibia fully in tubercles of tibia by fretsaw. Adjust external fixation to make two ends of the fracture close and keep the anatomical paraposition. Then tighten all the nuts in order to avoid any accidental. Wash the wound and close the incision after the suture of periosteum. To prevent infection, making penicillin 400000 U intramuscular injection for 5 days is necessary after operation. We should make an Anerdian wet compress on the blade and needle tract at the same time. It started to extend at the speed of 1 mm/day after 5 days of operation. Finally, it would extend 20 mm by 2 times in 20 days. It should be kept fixed for 9 weeks after lengthening. Raise the rabbits under the same conditions, and the rabbits are free to move in the cage. Rabbits were executed at particular period and the specimens were obtained. The animal model of rabbit tibia elongation was shown in Figure 1.

2.3.4. Animal Grouping. 60 New Zealand rabbits (2–2.5 Kg) were classified into two groups equally, namely, group A and group B. After the end of the extension, liquid Alg/nHAC was injected into rabbits of group A in the region of elongation. Rabbits of group B were not given any treatment as control. Groups A and B were molded and raised under the same conditions and the rabbits are free to move in the cage. Rabbits were executed at particular period and obtained the specimen.

2.4. Observations and Tests

2.4.1. General Observation. The general observation should include the following contents: the conditions of postoperative wound healing, daily activities of rabbits, and general bone formation of specimens in the extension area and whether the needle track was infected.

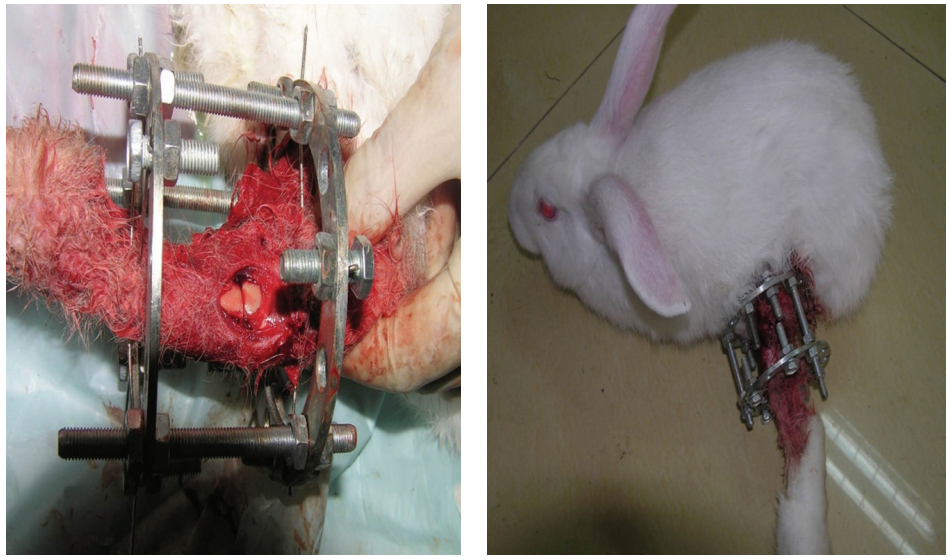

(a) (b)

Figure 1: The animal model of rabbit tibia elongation ((a) osteotomy in the tibia and (b) the situation of rabbit after the osteotomy surgery).

2.4.2. Histological Observation. We executed rabbits and acquired specimens at the following periods: medium term of bone elongation, termination of bone elongation at 2, 4, and 8 weeks after termination of bone elongation, respectively. The acquired specimens were fixed by 10% formaldehyde, and ossified specimens were decalcified for 2 weeks. Then we embedded sections by paraffin, conducted HE staining, and made an observation under light microscope after fixing sections.

2.4.3. X-Ray Observation. We took photos of bone elongation at three periods, respectively: after operation, termination of bone elongation, and 2, 4, and 8 weeks after termination of bone elongation. By means of these photos in different periods, we could observe the condition of bone formation of extended position and formation of poroma. The camera model was Philips 500mAX, and conditions of exposure were 50 KV, 4 ms.

2.4.4. Measurement of the Percentage Area of Bone Trabecula. We observed the tissue slices under the microscope and acquired images and measured the percentage area of trabecular bone using IPP (Image-Pro Plus IPP) Mediaplayer measurement software.

2.4.5. Bone Density Test. Five rabbits were killed in each group for obtaining the samples after 8 weeks, five rabbits were killed in each group to obtain the samples of termination of bone elongation. We determined the bone density using dual-energy X-ray bone densometer.

2.4.6. Biomechanical Test. Three-point bending experiment was conducted in elongation area of rabbit tibia at 2, 4, and 8 weeks, respectively. Five specimens in each group (groups A and B) were prepared at each period and 5 specimens from normal contralateral tibia were obtained and set as control group. For the specimens, intermediate point was support point and both ends were fixed with a span of 30 mm. Then a loading was imposed slowly at the constant speed of 0.5 mm/min until specimens fractured. The average stress value was taken and compared with the maximum stress value of each group.

2.4.7. Statistical Methods. All acquired data were statistically analyzed by statistical software SPSS10.0.

3. Results

3.1. General Observation. The rabbits had regular diet and normal activities after operation. Affected limbs were slightly swelled, the swelling would be reduced in 1-2 weeks, and all the incisions would also be healed normally. In the course of experiment, 15 rabbits died because of diarrhea and 2 rabbits fractured in the Kirschner wire fixation. Except the rabbits mentioned above, which were excluded in this experiment, all the other rabbits survived. External fixation was fixed so reliably that it made no adverse effects to animals. We acquired 3 specimens after termination of bone elongation. Via the observation of elongation region, dense fibrous connective tissue was found in the region of elongation, and the material quality was soft and tough without the appearance of ossification.

Five rabbits of each group were executed, and a total of 10 rabbits were put to death for obtaining specimens after 2 weeks of termination of bone elongation. Most of the elongation region in group A was ossified, and it was difficult to cut poroma using operating knife blade. As to group B, elongation region was ossified slightly; however, a majority of fibrous connective tissue still existed.

Five rabbits of each group were executed, and a total of 10 rabbits were put to death for obtaining specimens after

Figure 2: Compared with uninjured lateral tibia (right), operation side lateral tibia (left) extended 2 cm.

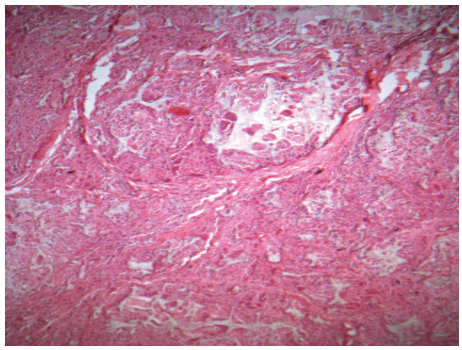

Figure 3: Histologically morphological observations of the extension area in medium item. The extension area was filled with dense fibrous connective tissue and no osteogenesis can be seen.

4 weeks of termination of bone elongation. For group A, elongation region was totally ossified, but the intensity of elongation region was weaker than the uninjured side and it could be broken easily. As to group B, elongation region was ossified basically, and the intensity of callus was not high and it was practicable to cut using operating knife blade.

Five rabbits of each group were executed, and a total of 10 rabbits were put to death for obtaining specimens after 8 weeks of termination of bone elongation. The elongation regions of groups A and B were ossified entirely. The appearance of group A was similar to normal bone and it was very hard to fracture, while group B was prone to fracture. Compared with uninjured lateral tibia, operation side lateral tibia extended 2 cm (Figure 2).

3.2. Histologically Morphological Observations. Five rabbits were killed at each medium term and termination of elongation, respectively, and a total of 10 rabbits were killed for obtaining specimens. The elongation region was filled with dense fibrous connective tissue, and bone tissues were not found (Figure 3).

Five rabbits of each group were executed and a total of 10 rabbits were put to death for obtaining specimens after 2 weeks of termination of bone elongation. The material implanted into group A was separated by fibrous connective tissue; fibrous connective tissue and blood vessel grew into the transplanted material. Osteoid formation mainly comprised of fibrous callus could be seen in most of the material, but a few osseous calluses appeared around separated materials (Figure 4).

Five rabbits were executed and a total of 10 rabbits were put to death for obtaining specimens after 4 weeks of termination of bone elongation. For group A, most mature bone could be seen, bone lacuna and the amount of endoskeleton cells increased obviously, and transplanted materials decreased obviously (Figure 5(a)). For group B, lots of osteoid appeared, woven bone was formed, and trabecular bone got mature gradually; part of osteoblast grew into osteocyte gradually, trabecular bone increased compared to 2 weeks of termination of bone elongation, and immature trabecular bones were still in the the major (Figure 5(b)).

Five rabbits of each group were executed and a total of 10 rabbits were put to death for obtaining specimens after 8 weeks of termination of bone elongation. As to group A, injected material disappeared basically, only very small amount of material existed in the center, and massive mature bony callus was formed (Figure 6(a)). As to group B, generous fibrous callus and bony callus accounted for the bulk, and a few mature bone lacuna and osteocyte emerged (Figure 6(b)).

3.3. X-Ray Examination. The X-ray examination after the surgery showed that the tibial osteotomy is complete, the fibula is also disconnected, and the site and lines of the osteotomy are well matched (Figure 7(a)). The X-ray examination done at 10 days after surgery showed that the tibial osteotomy had been apart and the line of osteotomy matched well (Figure 7(b)). The X-ray examination done after lengthening showed that a range about 2 cm existed and the line of osteotomy matched well. The extended area was of low density development and no calcification could be observed (Figure 7(c)). Besides, the Alg/NHAC used in group A, which is a liquid injection, is also of low density development (Figure 7(d)).

At 2 weeks after lengthening, large amounts of high density development formed and filled in the extension area in group A (Figure 8(a)). A small amount of high density development could be observed, namely, a few of new bones formed in group B (Figure 8(b)). At 4 weeks after the lengthening, the high density development in extension area of group A obviously increased (Figure 8(c)). The callus volume of group B increased when compared to group B at two weeks but less than group A at the same period (Figure 8(d)). At 8 weeks after lengthening, X-ray examination showed that the imaging performance of group A had been close to normal bone, with a connected marrow and similar bone density between cortical bone of extension area and normal bone upper and lower (Figure 8(e)). The elongation areas were all ossification in group B, but the bone mineral densities were lower and bone masses were less (Figure 8(f)).

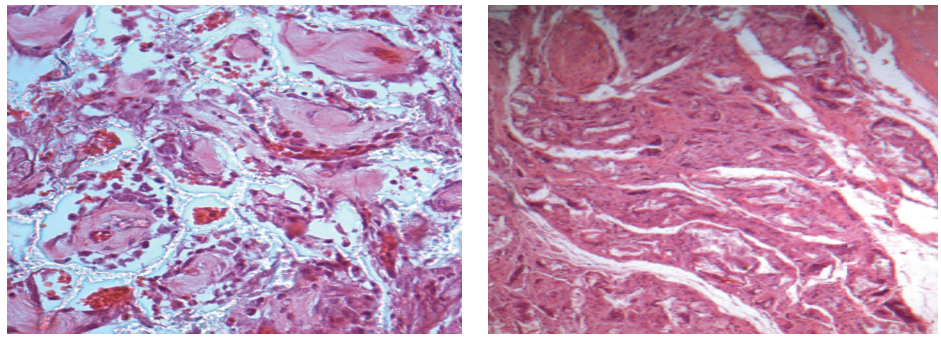

(a) (b)

Figure 4: In the first two weeks after the end of the extension, in group A, osteoid based on fibrous callus can be seen in most of the materials (a); in group B, large amounts of fibrous connective tissue can be seen and there is a small amount of osteoid formation (b).

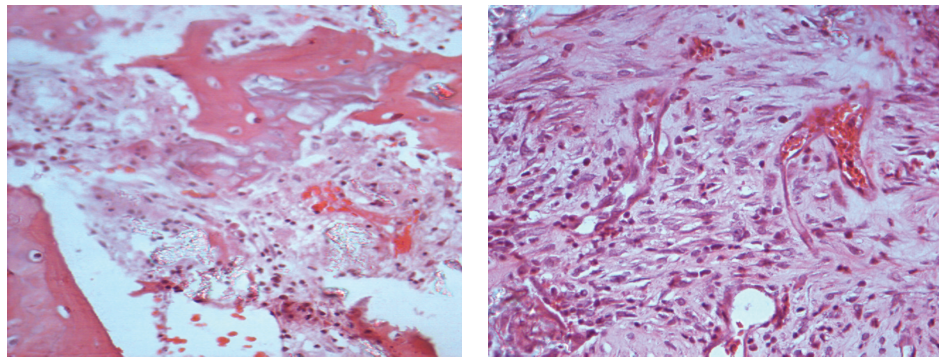

(a) (b)

Figure 5: In the first four weeks after the end of the extension: (a) the histologically morphological observations of the extension area of group A and (b) the histologically morphological observations of the extension area of group B.

3.4. Measurement of the Percentage Area of Trabecular Bone. 30 specimens were obtained by three times, of which, 10 specimens (group A: 5, group B: 5) were obtained at week 2, 8 specimens (group A: 5, group B: 5) were obtained at week 4, and the last 10 specimens (group A: 5, group B: 5) were obtained at week 8.

The statistical analysis showed that the percentage areas of the two groups were significantly different in 2, 4, and 8 weeks, $P < 0.05$. The percentage area of trabecular bone in group A was significantly higher than in group B, as shown in Table 1.

3.5. Measurement of the Bone Density. In this study, 13 specimens were obtained: (group A: 6, group B: 7) at week 8. The contralateral normal tibial bone was set as group C and measured.

BMD of groups A, B, and C was (0.1240 ± 0.0069), (0.0873 ± 0.0042), and (0.1771 ± 0.0078) separately. The BMD of group A is higher than group B, and a significant difference existed ($P < 0.01$) at week 8.

The bone density in group A was to recover to 70.29 percent when compared to normal bone, while that of group B was to recover to 49.29%. There was a significant difference ($P < 0.01$) between the two groups.

Table 1: Percentage area of trabecular bone in two groups at 2, 4, and 8 weeks ($\overline{x} \pm s$).

	2 w	4 w	8 w
Group A	4.51 ± 1.83	18.68 ± 3.77	33.11 ± 4.11
Group B	11.2 ± 2.01	32.42 ± 2.88	51.49 ± 9.28

3.6. Biomechanical Test. In this test, 13 specimens were obtained: (group A: 6, group B: 7) at week 8. Five contralateral normal tibial bones were set as group C and measured.

The maximum bending stress in groups A, B, and C was (273.524 ± 50.680) N, (132.471 ± 37.010) N, and (396.570 ± 45.121) N separately.

The maximum bending stress of group A is higher than that of group B at week 8, and a significant difference ($P < 0.01$) existed. The biomechanical property of group A was to recover 68.94%, while that of group B was to recover 33.33%. There was a significant difference ($P < 0.01$) between the two groups.

4. Discussion

Although the Ilizarov method is regarded as a revolution in the history of orthopedic therapeutics, the bone healing

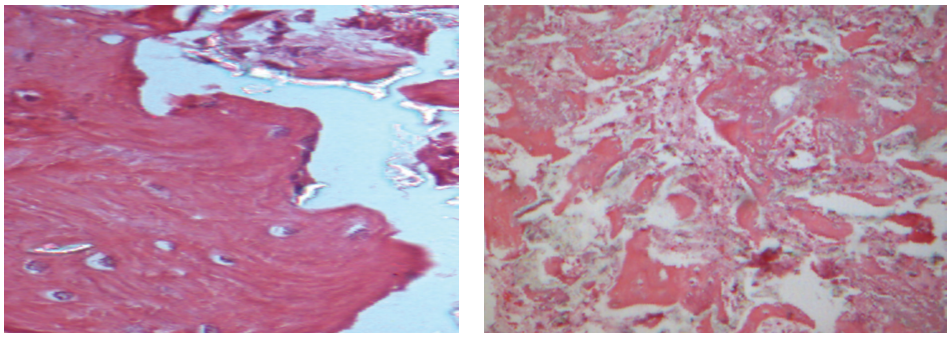

(a) (b)

Figure 6: In the first eight weeks after the end of the extension: (a) the histologically morphological observations of the extension area of group A and (b) the histologically morphological observations of the extension area of group B.

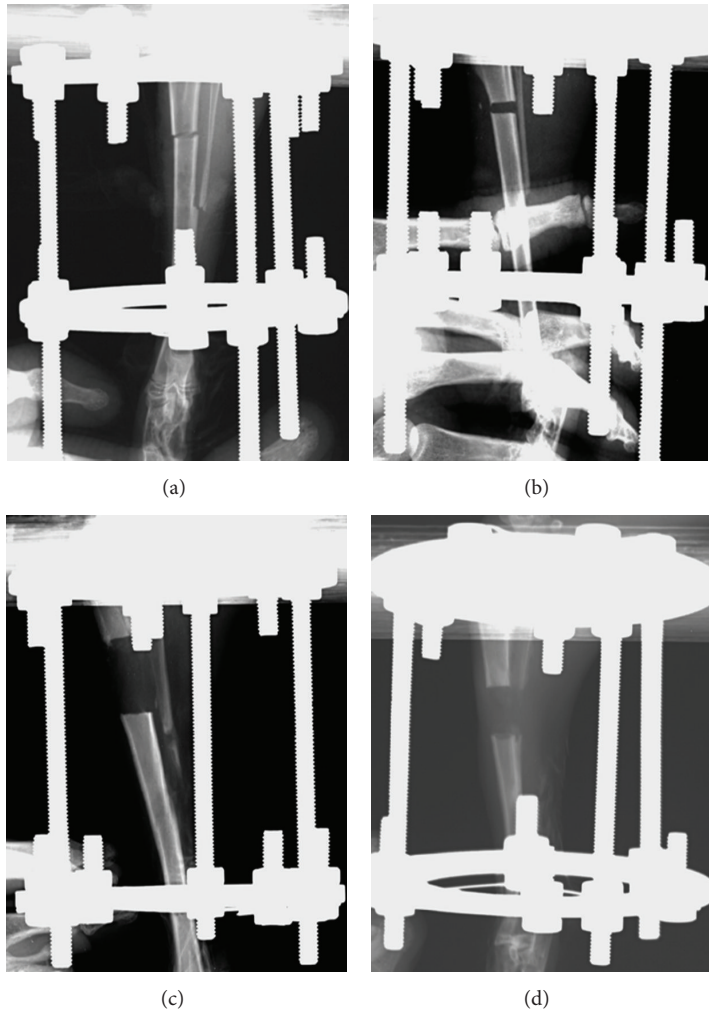

(a) (b)

(c) (d)

Figure 7: The X-ray image of rabbit tibia of different group immediately taken after the surgery.

is relatively slow and there are more complications existing. Besides, the pull speed can just be 1.0 mm a day, considering the bone healing time of extended area, and each extension of 1.0 mm needs about one or two months [26]. Therefore, many scholars have explored the mechanism and method to promote bone healing. The biological mechanism of limb lengthening was regarded as osteotylus lengthening. Ilizarov [27] has described the biological characteristics of broken ends of fractured bone in the traction state. It was discovered that the connection of the collagen fibers in bone gap and

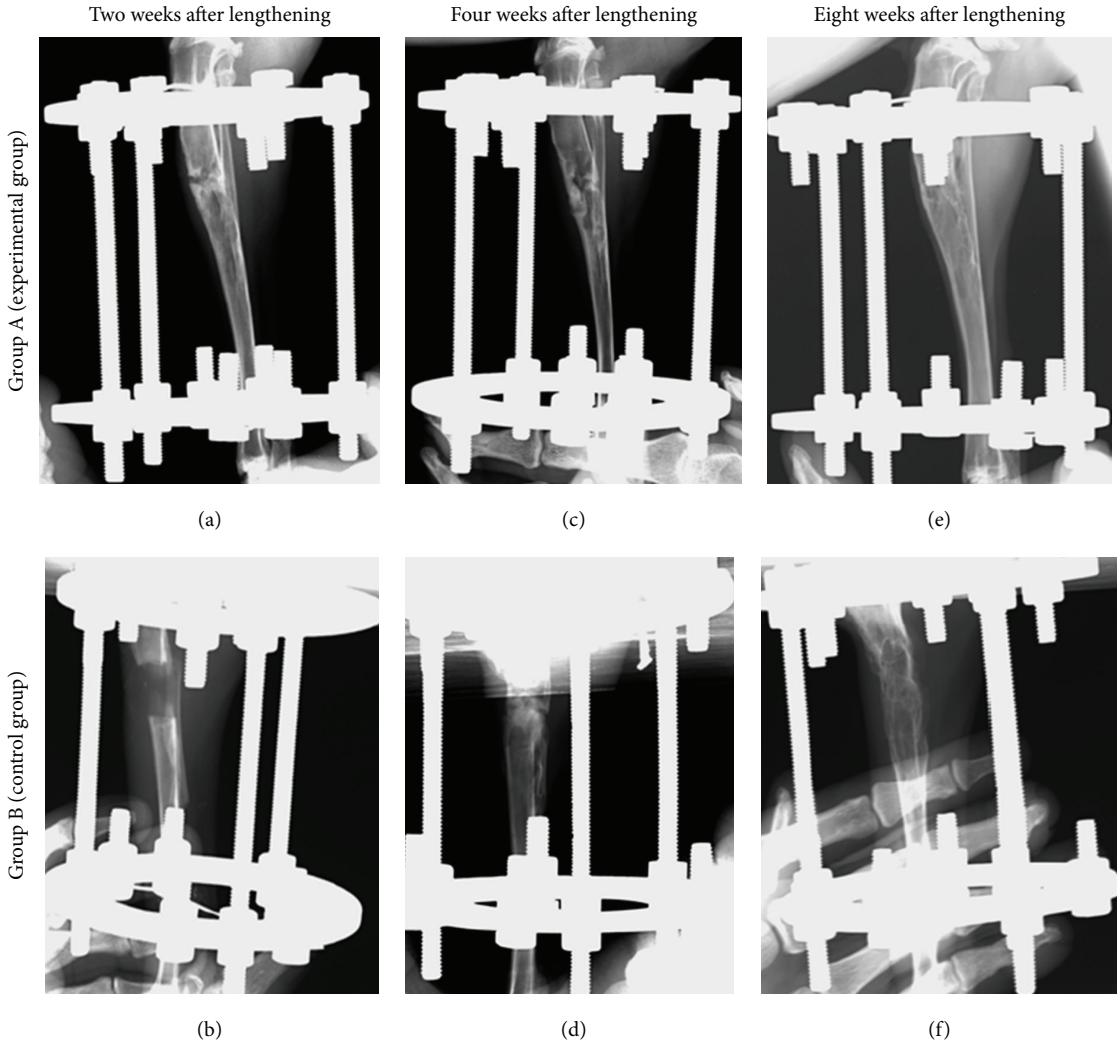

Figure 8: The X-ray image of rabbit tibia in different group at different time after lengthening.

the fusion of the trabecular of new bone were an ongoing repair process which contained new bone formation and the translation of matrix to matrix. In the extension of the human tibia, cancellous bone and bundle bone were clearly observed and finally turned to osteocyte, which was a process that looked like fetal growth and development. The discovery of tumor-related gene c-fos and c-jun in the early stages of limb lengthening, which was related to the fetal development, further proved the theory that distraction osteogenesis can make some process that usually took place in the stage of fatal development repeat in adult tissue.

The biological theory of distraction-traction osteogenesis (DO) offered the theory support for limb lengthening and changed the biological mechanism of limb lengthening. The application of DO concept significantly improved the quality of bone growth and reduced incidence of nonunion complications. Limb lengthening was not just a simple extension of bone length, but the interaction of bone, soft tissue, joint, and systemic factors in the overall. Polo and domestic scholars [28, 29] have shown that nerves, blood vessels, and muscle tissue have the same adaptation and regeneration potential just like the osteocyte. Striated muscle cells which have stopped regenerating and splitting in adult tissue, differentiated into muscle stem cells along with the proliferation of stellate cells, and finally formed the new muscle tissue in the slow pulling process. The research has shown that slow pulling process can also induce the regeneration of new nerve tissue [30]. Thus, limb lengthening is a combination of modern histology, biochemistry, and other systemic factors which influence each other. Its meaning based on the concept DO has a new extension, which should be the regeneration and rebuilding of limb composite tissue under a slow pulling process, namely, distraction histogenesis (DH).

In limb lengthening surgery, the speed and time of lengthening process, the site and method of osteotomy, patient age, and other factors will affect the bone healing process. First, the extension rate is one of the most important factors which influence bone healing process [31]. A large number of clinical and animal experiments confirmed that 1.0 mm/d is the most reasonable and beneficial extension rate to the healing of bone and soft tissue adaptation. Second, the osteotomy site is also one of the most important factors

which affect bone healing process. Due to the ability of blood supply and bone formation, different osteotomy sites have different bone osteotomy healing rate. In metaphyseal extension, the bone formation is faster because of the rich blood supply, while the fixture is easy to lose, which have serious impact on joint function and even cause permanent barriers. Backbone osteotomy is far away from the joint, which has light effect on the joint in the lengthening process, and the function of joint can be restored through the exercise. Because of the poor blood circulation here and the smaller diameter of bone, the healing time and fixing time should be increased. In comparison, the backbone of the bone ends is the ideal osteotomy site. Due to the osteotomy line which is farther away from the joint and has light effect on the joint, the change of the joint function in the lengthening process can be restored through exercise after surgery. Besides, the blood circulation here is closed to the bone end and the osteogenesis rate is faster than that of the backbone. Third, osteotomy method also affects bone healing of extension area. Frierson et al. [32] compared different osteotomy method and found that the simple cortex osteotomy has no significant differences with the common osteotomy. Fourth, bone healing can be affected when the delay extension or immediate extension method is used. Yasui et al. [33] have proved that the delay extension method is superior to immediate extension because the blood can be rebuilt and the soft tissue damaged after osteotomy surgery can be restored in the delay extension process.

The Alg/nHAC composite actually promotes the Ilizarov distraction osteogenesis and there maybe two reasons as follows. On one hand, nHAC composite can promote bone healing according to the research done before [25]. The microstructure of nHA may increase surface areas of implant. The microstructured calcium phosphate materials could concentrate more proteins, which may influence the attachment, proliferation, and differentiation of cells. These proteins may include bone-inducing proteins, which could differentiate inducible cells to osteogenic cells that form inductive bone. On another hand, the introduction of algorithm which stabilizes collagen as a cross-linker and preserves its helical structure creates a favorable microenvironment for the regeneration of tissue.

In order to promote bone healing, great amounts of researches had been done [34–38]. By the development of the modern medical technology, minimally invasive technology has aroused people's attention. The combination of clinical treatment and minimally invasive technology is promising. All in all, a further study about DO is rather necessary.

5. Conclusion

In this study, the liquid Alg/nHAC was injected into the extension area of tibia. The group which was injected into the liquid composite has more regenerated calluses than the control group through general observation and histological observation. The X-ray observation showed that the high density area in the experimental group is superior to the control group in different period. The results of bone density test and biomechanical test also demonstrated that the degree of bone healing and the strength of bone are much more better than the control group. Alg/nHAC was an ideal material for limb lengthening. The present study demonstrates that the injection of liquid calcium alginate/nHAC composites can significantly promote distraction osteogenesis. Alginate/nHAC is promising to be used for clinical application to solve the healing problem of backbone osteotomy and the fixing problem of metaphyseal backbone which has bad effect on the closed joint and causes complication.

Conflict of Interests

The authors declare that there is no conflict of interests regarding the publication of this paper.

References

[1] M. Kenawey, C. Krettek, E. Liodakis, U. Wiebking, and S. Hankemeier, "Leg lengthening using intramedullay skeletal kinetic distractor: results of 57 consecutive applications," *Injury*, vol. 42, no. 2, pp. 150–155, 2011.

[2] R. M. Olabisi, T. M. Best, C. Hurschler, R. Vanderby, and K. J. Noonan, "The biomechanical effects of limb lengthening and botulinum toxin type A on rabbit tendon," *Journal of Biomechanics*, vol. 43, no. 16, pp. 3177–3182, 2010.

[3] A. Hernandez-Fernandez, R. Vélez, F. Soldado et al., "Effect of administration of platelet-rich plasma in early phases of distraction osteogenesis: an experimental study in an ovine femur model," *Injury: International Journal of the Care of the Injured*, vol. 44, no. 7, pp. 901–907, 2013.

[4] A. M. Tuzuner-Oncul and R. S. Kisnisci, "Response of ramus following vertical lengthening with distraction osteogenesis," *Journal of Cranio-Maxillofacial Surgery*, vol. 39, no. 6, pp. 420–424, 2011.

[5] A. H. Simpson and J. Kenwright, "Fracture after distraction osteogenesis," *Journal of Bone and Joint Surgery B*, vol. 82, no. 5, pp. 659–665, 2000.

[6] D. Zarzycki, M. Tesiorowski, M. Zarzycka, W. Kacki, and B. Jasiewicz, "Long-term results of lower limb lengthening by the Wagner method," *Journal of Pediatric Orthopaedics*, vol. 22, no. 3, pp. 371–374, 2002.

[7] V. Antoci, C. M. Ono, V. Antoci Jr., and E. M. Raney, "Bone lengthening in children: how to predict the complications rate and complexity?" *Journal of Pediatric Orthopaedics*, vol. 26, no. 5, pp. 634–640, 2006.

[8] D. Paley, "Problems, obstacles, and complications of limb lengthening by the Ilizarov technique," *Clinical Orthopaedics and Related Research*, no. 250, pp. 81–104, 1990.

[9] F. Launay, R. Younsi, M. Pithioux et al., "Fracture following lower limb lengthening in children: a series of 58 patients," *Orthopaedics & Traumatology: Surgery & Research*, vol. 99, no. 1, pp. 72–79, 2013.

[10] P. H. Thaller, J. Fürmetz, F. Wolf et al., "Limb lengthening with fully implantable magnetically actuated mechanical nails (PHENIX1)-Preliminary results," *Injury: International Journal of the Care of the Injured*, vol. 45S, pp. S60–S65, 2014.

[11] L. Yang, G. Cai, L. Coulton, and M. Saleh, "Knee joint reaction force during tibial diaphyseal lengthening: a study on a rabbit model," *Journal of Biomechanics*, vol. 37, no. 7, pp. 1053–1059, 2004.

[12] X. M. Li, C. A. Van Blitterswijk, Q. L. Feng, F. Z. Cui, and F. Watari, "The effect of calcium phosphate microstructure on bone-related cells in vitro," *Biomaterials*, vol. 29, no. 23, pp. 3306–3316, 2008.

[13] A. I. Rodrigues, M. E. Gomes, I. B. Leonor et al., "Bioactive starch-based scaffolds and human adipose stem cells are a good combination for bone tissue engineering," *Acta Biomaterialia*, vol. 8, no. 10, pp. 3765–3776, 2012.

[14] Y. Liu, J. Lim, S.-H. Teoh et al., "Review: development of clinically relevant scaffolds for vascularised bone tissue engineering," *Biotechnology Advances*, vol. 31, no. 5, pp. 688–705, 2013.

[15] X. M. Li, X. H. Liu, W. Dong et al., "In vitro evaluation of porous poly(L-lactic acid) scaffold reinforced by chitin fibers," *Journal of Biomedical Materials Research B Applied Biomaterials*, vol. 90, no. 2, pp. 503–509, 2009.

[16] Y. Deng, H. Wang, L. Zhang et al., "In situ synthesis and in vitro biocompatibility of needle-like nano-hydroxyapatiteinagar-gelatinco-hydrogel," *Materials Letters*, vol. 104, pp. 8–12, 2013.

[17] X. M. Li, H. F. Liu, X. F. Niu et al., "Osteogenic differentiation of human adipose-derived stem cells induced by osteoinductive calcium phosphate ceramics," *Journal of Biomedical Materials Research B Applied Biomaterials*, vol. 97, no. 1, pp. 10–19, 2011.

[18] M. N. Salimi and A. Anuar, "Characterizations of biocompatible and bioactive hydroxyapatite particles," *Procedia Engineering*, vol. 53, pp. 192–196, 2013.

[19] X. M. Li, X. H. Liu, M. Uo, Q. L. Feng, F. Z. Cui, and F. Watari, "Investigation on the mechanism of the osteoinduction for calcium phosphate," *Bone*, vol. 43, supplement 1, pp. S111–S112, 2008.

[20] X. M. Li, Q. L. Feng, W. J. Wang, and F. Z. Cui, "Chemical characteristics and cytocompatibility of collagen-based scaffold reinforced by chitin fibers for bone tissue engineering," *Journal of Biomedical Materials Research B Applied Biomaterials*, vol. 77, no. 2, pp. 219–226, 2006.

[21] X. M. Li, Q. L. Feng, X. H. Liu, W. Dong, and F. Cui, "Collagen-based implants reinforced by chitin fibres in a goat shank bone defect model," *Biomaterials*, vol. 27, no. 9, pp. 1917–1923, 2006.

[22] Y.-C. Chiu, M.-H. Cheng, S. Uriel, and E. M. Brey, "Materials for engineering vascularized adipose tissue," *Journal of Tissue Viability*, vol. 20, no. 2, pp. 37–48, 2011.

[23] X. M. Li, Q. L. Feng, Y. F. Jiao, and F. Z. Cui, "Collagen-based scaffolds reinforced by chitosan fibres for bone tissue engineering," *Polymer International*, vol. 54, no. 7, pp. 1034–1040, 2005.

[24] G. Chen, J. Tanaka, and T. Tateishi, "Osteochondral tissue engineering using a PLGA-collagen hybrid mesh," *Materials Science and Engineering C*, vol. 26, no. 1, pp. 124–129, 2006.

[25] X. M. Li, Q. L. Feng, and F. Z. Cui, "In vitro degradation of porous nano-hydroxyapatite/collagen/PLLA scaffold reinforced by chitin fibres," *Materials Science and Engineering C*, vol. 26, no. 4, pp. 716–720, 2006.

[26] A. D. Kanellopoulos and P. N. Soucacos, "Management of nonunion with distraction osteogenesis," *Injury*, vol. 37, supplement 1, pp. S51–S55, 2006.

[27] G. A. Ilizarov, "Clinical application of the tension-stress effect for limb lengthening," *Clinical Orthopaedics and Related Research*, no. 250, pp. 8–26, 1990.

[28] A. Polo, R. Aldegheri, A. Zambito et al., "Lower-limb lengthening in short stature. An electrophysiological and clinical assessment of peripheral nerve function," *Journal of Bone and Joint Surgery B*, vol. 79, no. 6, pp. 1014–1018, 1997.

[29] K. Huang, Y. Zeng, H. Xia, and C. Liu, "Alterations in the biorheological features of some soft tissues after limb lengthening," *Biorheology*, vol. 35, no. 4-5, pp. 355–363, 1998.

[30] G. A. Ilizarov, *Transosseous Osteosynthesis: Theoretical and Clinical Aspects of Regeneration and Growth of Tissue*, vol. 1, Springer, Berlin, Germany, 1992.

[31] S. H. White and J. Kenwright, "The importance of delay in distraction of osteotomises," *Orthopedic Clinics of North America*, vol. 569, no. 4, pp. 569–579, 1991.

[32] M. Frierson, K. Ibrahim, M. Boles, H. Bote, and T. Ganey, "Distraction osteogenesis: a comparison of corticotomy techniques," *Clinical Orthopaedics and Related Research*, no. 301, pp. 19–24, 1994.

[33] N. Yasui, H. Kojimoto, K. Sasaki, A. Kitada, H. Shimizu, and Y. Shimomura, "Factors affecting callus distraction in limb lengthening," *Clinical Orthopaedics and Related Research*, no. 293, pp. 55–60, 1993.

[34] B. Kassis, C. Glorion, W. Tabib, O. Blanchard, and J. Pouliquen, "Callus response to micromovement after elongation in the rabbit," *Journal of Pediatric Orthopaedics*, vol. 16, no. 4, pp. 480–485, 1996.

[35] K. S. Eyres, M. Saleh, and J. A. Kanis, "Effect of pulsed electromagnetic fields on bone formation and bone loss during limb lengthening," *Bone*, vol. 18, no. 6, pp. 505–509, 1996.

[36] X. M. Li, H. F. Liu, X. F. Niu et al., "The use of carbon nanotubes to induce osteogenic differentiation of human adipose-derived MSCs in vitro and ectopic bone formation in vivo," *Biomaterials*, vol. 33, no. 19, pp. 4818–4827, 2012.

[37] P. M. Van Roermound, B. M. Ter Haar Romeny, and T. Sakou, "Bone growth and remodeling," *Journal of Bone and Mineral Research*, vol. 19, no. 6, pp. 84–88, 1997.

[38] X. M. Li, L. Wang, Y. B. Fan, Q. L. Feng, F. Z. Cui, and F. Watari, "Nanostructured scaffolds for bone tissue engineering," *Journal of Biomedical Materials Research A*, vol. 101A, no. 8, pp. 2424–2435, 2013.

Hindawi Publishing Corporation
International Journal of Polymer Science
Volume 2014, Article ID 236259, 6 pages
http://dx.doi.org/10.1155/2014/236259

Research Article

Enhancement of VEGF on Axial Vascularization of Nano-HA/Collagen/PLA Composites: A Histomorphometric Study on Rabbits

Xiao Chang,[1] Hai Wang,[1] Zhihong Wu,[1] Xiaojie Lian,[2] Fuzhai Cui,[2] Xisheng Weng,[1] Bo Yang,[1] Guixing Qiu,[1] and Baozhong Zhang[1]

[1] *Department of Orthopaedic Surgery, Peking Union Medical College Hospital, No. 1, Shuaifuyuan Hutong, Beijing 100730, China*
[2] *Department of Materials Science & Engineering, Tsinghua University, Beijing 100084, China*

Correspondence should be addressed to Baozhong Zhang; zbz9639@sina.com

Received 28 January 2014; Accepted 6 March 2014; Published 31 March 2014

Academic Editor: Xiaoming Li

The aim of this study was to investigate whether the nanohydroxyapatite/collagen/poly(L-lactic acid) (nHAC/PLA) composite is suitable to be compounded with VEGF to enhance the axial vascularization in vivo. Thirty rabbits were divided into 2 groups of 15 animals each. In control group, a nHAC/PLA scaffold slice was vascularized axially by an inserted ligated femoral arteriovenous (AV) bundle in the animal. In experimental group, a slice compounded with VEGF gel was applied. The rabbits were sacrificed at 2 weeks, 6 weeks, and 10 weeks after surgery; the specimens of scaffold slices underwent histomorphometric examination; analysis of the microvessel density (MVD) of both groups was done. The combination with VEGF (Group B) did not enhance the vascularization in early phase (2 and 6 weeks, $P > 0.05$) but worked in later phase (10 weeks, $P < 0.05$). The data of the experiment demonstrated the suitability of the nHAC/PLA composite as carrier for the growth factor VEGF, enabling its sustained release in bioactive form with enough binding efficacy.

1. Introduction

Critical-sized bone defect due to serious trauma, infection, malignant tumor resection, or congenital deformity is not rare in clinic and remains a major challenge for surgeons. Tissue engineered bone (TEB) represents a promising method to resolve these problems. In the future, TEB might become the most popular choice for surgeons when they repair segmental bone defects [1]. Significant progress has been made to develop several bone substitute materials which mimics natural bone matrix in both composition and microstructure [2–4]. Some kinds of seed cells and bioactive factors have been composited with scaffolds by many tissue engineering methods [5]. However, repair of bone defects over 30 mm using TEB still is a difficult problem [6], because seed cells and bioactive factors will survive only with oxygen and nutrition supplied by blood flow in limited scale. The osteoinduction and osteogenesis of large tissue-engineered scaffold will not function because of absence of vascularization in the scaffold.

Vascularization plays a very important role in skeletal development and repair [7]. To repair large bone defect, it is critical to vascularize the whole scaffold; there is more new bone formation where the matrix is vascularized more adequately [8]. There are two methods to promote the angiogenesis of matrix of TEM. First, through microsurgical procedure, a major vessel is implanted in the scaffold to enhance angiogenesis around the vessel which is called axial vascularization. Second, angiogenic factors are composited with the scaffold to induce vessels formation. In the factors the vascular endothelial growth factor (VEGF) and bone morphogenetic protein (BMP) are the most commonly used [9].

Nanohydroxyapatite/collagen/poly(L-lactic acid) (nHAC/PLA) composite is a new type bone substitute scaffold; it is similar to the natural bone in main composition and in

hierarchical microstructure [9–12]. In previous studies we have revealed that the nHAC/PLA composites can be axial vascularized by femoral arteriovenous bundle of rabbits [13]. The purpose of this study was to investigate whether VEGF can be loaded on nHAC/PLA composites to promote the axial vascularization of the scaffold in vivo.

2. Materials and Methods

2.1. Materials. Process of synthesis of nHAC/PLA has been previously described [9–13]. After ultrasonication, the material was fabricated into cylindrical slices (Φ10 mm × 10 mm) with a hole of 1.5 mm diameter in the center.

2.2. Experimental Design. The whole experiment was approved by the Animal Ethic Committee of Peking Union Medical College Hospital (PUMCH), and the procedures were conducted in accordance with the guidelines for the care and maintenance of animals. Thirty-three-month-old New Zealand rabbits (Experimental Animal Center of PUMCH, Beijing, China) weighing 2.5 to 3.0 kg were divided randomly into group A and group B ($n = 15$). All operations were performed under sterile conditions by one surgeon. In group A (control group), a nHAC/PLA composite slice was directly implanted into the intramuscular gap with an arteriovenous (AV) bundle in the left groin of a rabbit. In group B (experimental group), the nHAC/PLA composite slice was coated with VEGF165 gel and then implanted into the animal with the same procedure as group A. Histological examinations were performed at 2, 6, and 10 weeks after implantation.

2.3. Experimental Steps

2.3.1. Compositing of VEGF. In clean bench, 10 cylindrical slices were dripped into 50 mL fibrinogen solution at 50 mg/mL; the same volume of VEGF165 solution at 5 ng/mL was added in. Then the mixture of VEGF165 and fibrinogen infiltrated into the micropores of nHAC/PLA through vacuum suction for 30 minutes. The 100 mL thrombin solution at 250 U/ml was added in and the vacuum suction was repeated for 30 minutes. The thrombin transferred fibrinogen to gel which contained VEGF165. After being removed from the solution and air-dried, the slices were kept in sterile and 4°C environment until operation.

2.3.2. Surgical Protocol. With an intravenous injection of 3% pentobarbital sodium (1 mL/kg body weight, Sigma, USA), the animals were anesthetized. Before procedures, 800,000 IU penicillin sodium (North China Pharmaceutical Group Corporation, China) was injected intramuscularly in order to prevent perioperative infection. The animals were placed on the table in supine position. After shaving, sterilizing, and draping, through a skin incision from the left groin midpoint to the left knee, the femoral neurovascular bundle was exposed, and the nerve was protected. The left femoral artery and vein were surgically dissociated and then were transversely cut and ligated at 2 to 3 cm under the femoral artery furcation for an AV bundle. In group A, the AV bundle was placed in the hole of a nHAC/PLA composite slice, and the slice was placed into the intramuscular gap. In group B, the nHAC/PLA composite slice coated with VEGF165 gel was applied to place AV bundle in. Femoral muscle and skin were sutured with 3–0 silk sutures. Postoperatively, 800,000 IU penicillin sodium and 0.15 mg buprenorphine (Tianjing Institute of Pharmaceutical Research, China) were separately administered intramuscularly every 12 hours for 3 days.

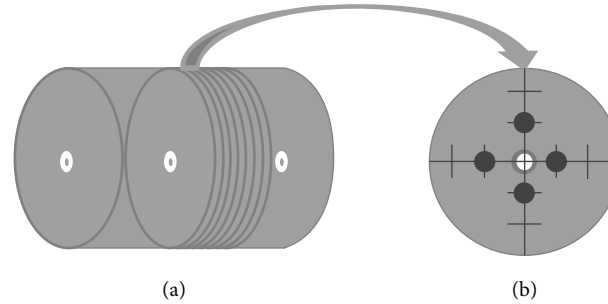

Figure 1: Stick drawing demonstrating the section process of histological examinations: (a) 8 cross-sections were obtained perpendicular to the AV bundle in the middle; (b) 4 microphotographs of interest in the inner 1/3 radius at 3, 6, 9, and 12 o'clock at 400x magnification were evaluated for MVD (dark black points) [13].

2.4. Histological Examinations. The animals were sacrificed after 2, 6, and 10 weeks ($n = 5$, resp.). The slices were removed and fixed in 10% buffered formalin for 24 hours. After washing, they were decalcified by 14% ethylenediaminetetraacetic acid (EDTA) solution for 4–6 weeks. Then, they were dehydrated in graded ethanol and embedded in paraffin. Eight cross-sections (5 μm) were obtained from each specimen, perpendicular to the AV bundle in the middle (Figure 1(a)), using a Leica microtome (Leica Microsystems, Wetzlar, Germany). For histomorphometric analysis, four sections were randomly selected for haematoxylin and eosin (H&E) staining and microphotographs were taken using a microscope and a digital camera (Leica Microsystems); see Figure 5. On each section, four microphotographs of interest in the inner 1/3 radius at 3, 6, 9, and 12 o'clock at 400x magnification were evaluated, and the number of vessels in high power field (HPF) was counted by two independent and blinded pathologists (Figure 1(b)). Microvessel density (MVD) was calculated for each group and each time point. One of the other sections was chosen randomly for CD31 immunohistochemical staining for qualitative assessment.

2.5. Statistics Analysis. The MVDs were given as means ± standard deviation (X ± SD, vessels/HPF). Statistical analysis was performed using the paired samples Student's t-test with SPSS 16.0. The critical level of statistical significance was set at $P < 0.05$.

3. Result

3.1. Surgery and Macroscopic Appearance. 27 rabbits tolerated the surgical procedure and survived well. One rabbit in group

Table 1: Quantification of MVD (X ± SD, vessels/HPE) between group A and group B, analyzed by histomorphometrics. P values < 0.05 were marked (∗).

	Group A (controlled group without VEGF)	Group B (experimental group with VEGF)	P value
2 weeks	9.35 ± 1.58	9.02 ± 1.60	0.897
6 weeks	15.60 ± 3.20	16.04 ± 2.89	0.917
10 weeks	17.35 ± 2.64	20.92 ± 3.91	0.048*

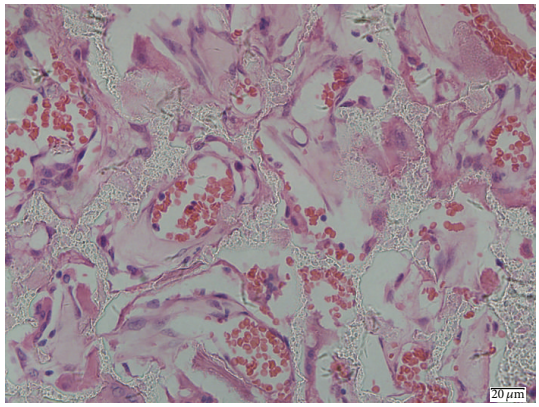

Figure 2: Hematoxylin and eosin (HE) staining of specimens 10 weeks after implantation (magnification ×400) showed the tube architecture of the newly formed vessels.

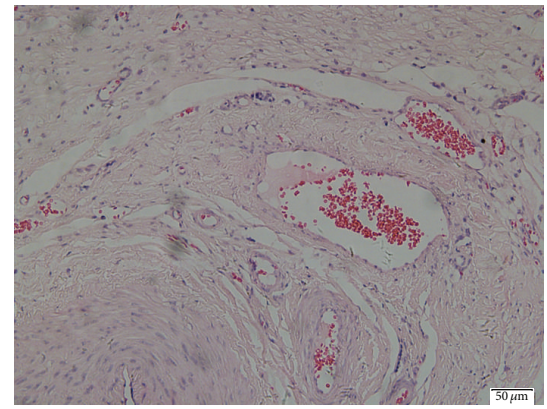

Figure 3: HE staining of specimens 10 weeks after implantation (magnification ×200) showed arteriogenesis: new collateral vessels formed around ligation AV bundle.

A and one in group B died of diarrhea in two weeks after procedures; one in group A was complicated with incision infection. Above-mentioned three animals were excluded from the experiment and 3 new animals were selected to replace the excluded. No extrusion of the implanted slices occurred over the observation period. The slices were surrounded by neighboring tissue when removal was performed; vessel-like tissues were observed on the surface of the implanted slices of both groups.

3.2. Histological Examinations. Microscopic angiogenesis was identified in both groups of any time point. At low magnification, the vision was full of connective tissue and granulation tissue composed of inflammatory cells, blood cells, fibroblasts, and blood vessels; at high magnification, vascular endothelial cells could be identified (Figure 2). Around the ligation AV bundle there were new vessels formed which indicated arteriogenesis (Figure 3). The new vessels formed in the slices could be identified through CD31 immunohistochemical staining; the endothelial cells of vessel wall showed significant light brown (Figure 4). Along with the time extension, there were fewer inflammatory cells and more fibroblasts and vessels. By 10 weeks, more vessels even arteriole-like ones were observed in both groups.

A trend towards an increase in MVD was observed in each group over time, and MVD of group B gradually showed its significance more than that of group A. At 2 and 6 weeks after implantation, MVD of groups A and B had no significant differences ($P = 0.897$ and $P = 0.917$); at the last time point of 10 weeks, the MVD of group B was significant more than group A ($P = 0.048$) (Table 1).

4. Discussion

Angiogenesis is a prerequisite for bone formation. The newly formed vessel net supplies the site of bone formation with nutrients, oxygen, and soluble factors [14]. Vascularization also seems particularly to be important for the healing process following the implantation of bone substitute materials [1, 15]. The establishment of a dense vascular network is essential for bone formation, osseointegration, and the subsequent material replacement by newly formed bone [16].

In previous studies, we have established animal models for axial vascularization of the nHAC/PLA composite and improved the scaffold to be applicable to axial vascularization of vessel bundle [13].

The distal ligation arteriovenous (AV) bundle is one of axial vascular carriers. Compared with the other two methods, shunt loop and flow-through type AV bundle, the distal ligation AV bundle is easy to construct and can be used as the pedicle vessels if transposition repair is necessary. The distal ligation AV bundle has been used clinically as vascular carriers [17, 18]. The vascularization of AV bundle is based on arteriogenesis. Upon occlusion of an artery, the blood flow is redirected into preexisting arteriolar anastomoses that experience increased mechanical forces such as shear stress and circumferential wall stress. The endothelium of the arteriolar connections is then activated, resulting in an increased release of monocyte-attracting proteins as well as an upregulation of adhesion molecules [19]. Upon adherence and extravasation, monocytes promote arteriogenesis by supplying growth factors and cytokines that bind to receptors that are expressed on vascular cells within a limited

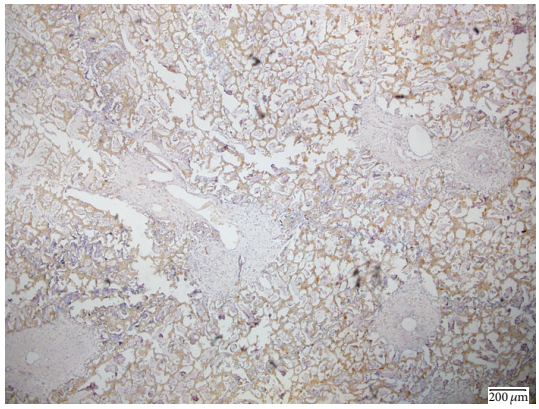

(a)

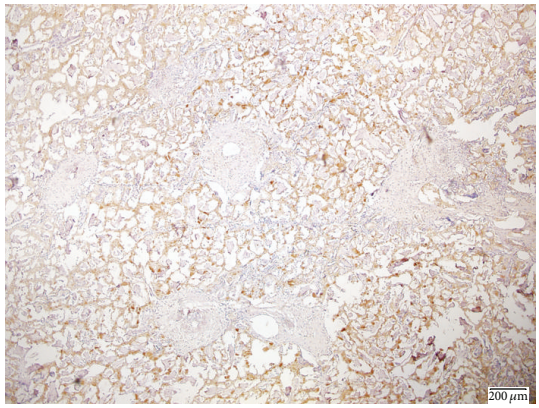

(b)

Figure 4: CD31 immunohistochemical staining of specimens 10 weeks after implantation (magnification ×20): the arteriole-like vessels can be seen, (a) from group A, (b) from group B.

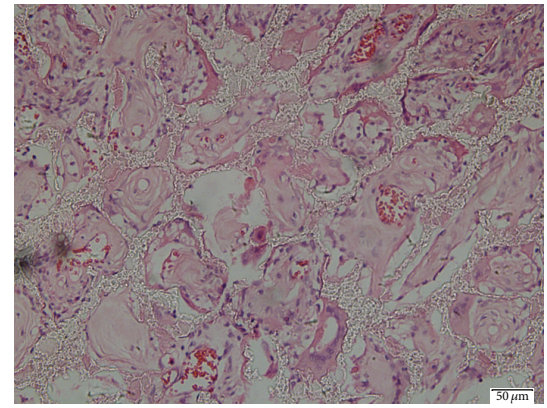

(a)

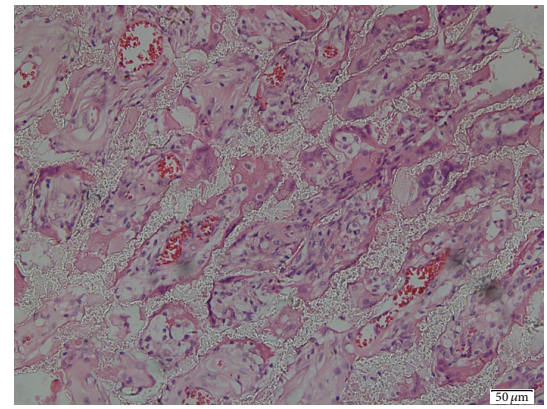

(b)

Figure 5: HE staining of specimens (magnification ×100): the vascular walls and red blood cells can be seen in both groups 10 weeks after implantation: (a) from group A; (b) from group B.

time frame [20]. There is ischemic zone around AV bundle secondary to surgical trauma and ligation of vessels. The ischemia and hypoxia cause new collateral vessels formation through cell proliferation and vessel budding [21].

The results of histological examinations showed good biocompatibility and property for angiogenesis of nHAC/PLA composite. In early period of implantation, there was inflammatory cells in the scaffold which indicated foreign body reaction; in late period, the connective tissue replaced the inflammatory tissue and new vessels formed. The count of microvessels showed that the AV bundle promotes the vascularization of the scaffold. Though it is difficult to repair critical-sized bone defect for the nHAC/PLA composite, it is a promising scaffold material to construct TEB to repair larger bone defects in the future [22].

To upload the bioactive factors with the scaffold is another method to promote vascularization of the scaffold and VEGF is used most commonly. More recently, VEGF has gained increasing attention because it has been demonstrated to be mostly capable of stimulating angiogenesis in bone grafts. VEGF is highly specific for vascular endothelial cells and its bioactivity in angiogenesis is stronger than any of the other known proangiogenic factors; any proangiogenic factor promotes vessel formation through VEGF directly or indirectly. In vivo, VEGF induces angiogenesis and permeabilization of blood vessels. VEGF165 is the most active member of the family; by binding receptors in the endothelial cells, it can stimulate endothelial cells to divide and proliferate; it also can be the chemokine to push the EPCs to migrate from bone marrow to get involved in angiogenesis [23].

In the experiment, VEGF165 was loaded on the scaffold and released slowly in animals. Because of the short half-life in vivo, VEGF165 degrades into inactive fragments quickly. To prevent it from degradation, different methods were applied to keep the activity of VEGF165 and release the activity gradually [24, 25]. The method in the study was similar to that introduced by Lode A [26, 27]. The mixed solution of VEGF165 and fibrinogen adhered to the scaffold by vacuum suction, and the mixture transferred to gel when thrombin was added in. The activity of VEGF165 was kept in the gel and released to function slowly.

The effect of angiogenesis by VEGF released from the nHAC/PLA composite was not significant until 10 weeks after implantation. In early time points, the histological examination showed new vessel formation in the scaffolds of

both groups, but there was no significant difference in MVDs by statistic analysis. It was most likely due to lack of cells and tissues as the targets of VEGF in early time after implantation. With time, especially when inflammatory reaction was over, the pores of scaffold were full of living tissue, and there were enough target-cells of VEGF to activate. As a result, the MVD of the experimental group was significantly higher than that of the controlled group in 10 weeks.

There are still problems to resolve for VEGF in promotion of angiogenesis of the substitute bone materials. The safety of VEGF in vivo is unknown because VEGF is closely related to the development and progression of tumors. The procedure of compounding VEGF and the scaffold is the lack of standardization. The concentration and release speed vary due to different microstructure of the scaffolds. There still is a lot of research work to do to bridge the laboratory experimentation to practical clinical settings.

5. Conclusions

The data of the experiment demonstrated the suitability of the nHAC/PLA composite as carrier for the growth factor VEGF, enabling its sustained release in bioactive form with enough binding efficacy. The microstructure of this kind of scaffold not only fits new born tissue growing after axial vascularization, but also fits coating of growth factor such as VEGF. The nHAC/PLA composite is proved to be a promising scaffold material to construct the TEB in the future.

Conflict of Interests

The authors declare that there is no conflict of interests regarding the publication of this paper.

Acknowledgment

This paper is sponsored by the National Natural Science Foundation of China under Contract Grant no. 81000802. Xiao Chang and Hai Wang are co-first authors.

References

[1] X. Li, L. Wang, Y. Fan, Q. Feng, F. Z. Cui, and F. Watari, "Nanostructured scaffolds for bone tissue engineering.," *Journal of Biomedical Materials Research A*, vol. 101, no. 8, pp. 2424–2435, 2013.

[2] X. Li, C. A. van Blitterswijk, Q. Feng, F. Cui, and F. Watari, "The effect of calcium phosphate microstructure on bone-related cells in vitro," *Biomaterials*, vol. 29, no. 23, pp. 3306–3316, 2008.

[3] G. Zhou, Y. Hou, L. Liu et al., "Preparation and characterization of NiW-nHA composite catalyst for hydrocracking," *Nanoscale*, vol. 4, no. 24, pp. 7698–7703., 2012.

[4] G. Zhou, Z. Wu, Y. Hou et al., "Research on the structure of fish collagen nanofibers influenced cell growth," *Journal of Nanomaterials*, vol. 2013, Article ID 764239, 6 pages, 2013.

[5] X. Li, H. Liu, X. Niu et al., "The use of carbon nanotubes to induce osteogenic differentiation of human adipose-derived MSCs in vitro and ectopic bone formation in vivo," *Biomaterials*, vol. 33, no. 19, pp. 4818–4827, 2012.

[6] X. Li, Q. Feng, X. Liu, W. Dong, and F. Cui, "Collagen-based implants reinforced by chitin fibres in a goat shank bone defect model," *Biomaterials*, vol. 27, no. 9, pp. 1917–1923, 2006.

[7] L. L. Ren, D. Y. Ma, X. Feng, T. Q. Mao, Y. P. Liu, and Y. Ding, "A novel strategy for prefabrication of large and axially vascularized tissue engineered bone by using an arteriovenous loop," *Medical Hypotheses*, vol. 71, no. 5, pp. 737–740, 2008.

[8] J. DELEU and J. TRUETA, "Vascularisation of bone grafts in the anterior chamber of the eye," *The Journal of Bone and Joint Surgery*, vol. 47, pp. 319–329, 1965.

[9] J. Li, J. Hong, Q. Zheng et al., "Repair of rat cranial bone defects with nHAC/PLLA and BMP-2-related peptide or rhBMP-2," *Journal of Orthopaedic Research*, vol. 29, no. 11, pp. 1745–1752, 2011.

[10] S. S. Liao, F. Z. Cui, W. Zhang, and Q. L. Feng, "Hierarchically biomimetic bone scaffold materials: nano-HA/collagen/PLA composite," *Journal of Biomedical Materials Research B: Applied Biomaterials*, vol. 69, no. 2, pp. 158–165, 2004.

[11] C. Du, F. Z. Cui, W. Zhang, Q. L. Feng, X. D. Zhu, and K. de Groot, "Formation of calcium phosphate/collagen composites through mineralization of collagen matrix," *Journal of Biomedical Materials Research*, vol. 50, no. 4, pp. 518–527, 2000.

[12] C. Du, F. Z. Cui, X. D. Zhu, and K. de Groot, "Three-dimensional nano-HAp/collagen matrix loading with osteogenic cells in organ culture," *Journal of Biomedical Materials Research*, vol. 44, no. 4, pp. 407–415, 1999.

[13] H. Wang, X. Chang, G. Qiu et al., "Axial vascularization of Nano-HA/Collagen/PLA composites by arteriovenous bundle," *Journal of Nanomaterials*, vol. 2013, Article ID 391832, 6 pages, 2013.

[14] J. Harper and M. Klagsbrun, "Cartilage to bone—angiogenesis leads the way," *Nature Medicine*, vol. 5, no. 6, pp. 617–618, 1999.

[15] J. M. Kanczler and R. O. C. Oreffo, "Osteogenesis and angiogenesis: the potential for engineering bone," *European Cells and Materials*, vol. 15, pp. 100–114, 2008.

[16] E. Wernike, M.-O. Montjovent, Y. Liu et al., "Vegf incorporated into calcium phosphate ceramics promotes vascularisation and bone formation in vivo," *European Cells and Materials*, vol. 19, pp. 30–40, 2010.

[17] J. J. Pribaz, P. K. M. Maitz, and N. A. Fine, "Flap prefabrication using the "vascular crane" principle: an experimental study and clinical application," *British Journal of Plastic Surgery*, vol. 47, no. 4, pp. 250–256, 1994.

[18] K. C. Tark, R. K. Khouri, K. S. Shin, and W. W. Shaw, "The fasciovascular pedicle for revascularization of other tissues," *Annals of Plastic Surgery*, vol. 26, no. 2, pp. 149–155, 1991.

[19] E. Deindl and W. Schaper, "The art of arteriogenesis," *Cell Biochemistry and Biophysics*, vol. 43, no. 1, pp. 1–15, 2005.

[20] K. Kosaki, J. Ando, R. Korenaga, T. Kurokawa, and A. Kamiya, "Fluid shear stress increases the production of granulocyte-macrophage colony-stimulating factor by endothelial cells via mRNA stabilization," *Circulation Research*, vol. 82, no. 7, pp. 794–802, 1998.

[21] A. Arkudas, G. Pryymachuk, J. P. Beier et al., "Combination of extrinsic and intrinsic pathways significantly accelerates axial vascularization of bioartificial tissues," *Plastic and Reconstructive Surgery*, vol. 129, no. 1, pp. 55e–65e, 2012.

[22] X.] Li, Y. Yang, Y. Fan, Q. Feng, F. Z. Cui, and F. Watari, "Biocomposites reinforced by fibers or tubes as scaffolds for tissue engineering or regenerative medicine," *Journal of Biomedical Materials Research A*, 2013.

[23] E. Boscolo, J. B. Mulliken, and J. Bischoff, "VEGFR-1 mediates endothelial differentiation and formation of blood vessels in a murine model of infantile hemangioma," *The American Journal of Pathology*, vol. 179, no. 5, pp. 2266–2277, 2011.

[24] Q. Tan, H. Tang, J. Hu et al., "Controlled release of chitosan/heparin nanoparticle-delivered VEGF enhances regeneration of decellularized tissue-engineered scaffolds," *International journal of nanomedicine*, vol. 6, pp. 929–942, 2011.

[25] P. Yang, C. Wang, Z. Shi et al., "Prefabrication of vascularized porous three-dimensional scaffold induced from rhVEGF165: a preliminary study in rats," *Cells Tissues Organs*, vol. 189, no. 5, pp. 327–337, 2009.

[26] A. Lode, A. Reinstorf, A. Bernhardt, C. Wolf-Brandstetter, U. König, and M. Gelinsky, "Heparin modification of calcium phosphate bone cements for VEGF functionalization," *Journal of Biomedical Materials Research A*, vol. 86, no. 3, pp. 749–759, 2008.

[27] A. Lode, C. Wolf-Brandstetter, A. Reinstorf et al., "Calcium phosphate bone cements, functionalized with VEGF: release kinetics and biological activity," *Journal of Biomedical Materials Research A*, vol. 81, no. 2, pp. 474–483, 2007.

Hindawi Publishing Corporation
International Journal of Polymer Science
Volume 2014, Article ID 153453, 5 pages
http://dx.doi.org/10.1155/2014/153453

Research Article

Vascularization of Nanohydroxyapatite/Collagen/Poly(L-lactic acid) Composites by Implanting Intramuscularly In Vivo

Hai Wang,[1] Xiao Chang,[1] Guixing Qiu,[1] Fuzhai Cui,[2] Xisheng Weng,[1] Baozhong Zhang,[1] Xiaojie Lian,[2] and Zhihong Wu[1]

[1] *Department of Orthopaedics, Peking Union Medical College Hospital, No. 1 Shuaifuyuan Hutong, Beijing 100730, China*
[2] *Biomaterials Laboratory, Department of Material Science & Engineering, Tsinghua University, Beijing 100084, China*

Correspondence should be addressed to Zhihong Wu; wuzh3000@126.com

Received 23 January 2014; Accepted 10 February 2014; Published 10 March 2014

Academic Editor: Xiaoming Li

It still remains a major challenge to repair large bone defects in the orthopaedic surgery. In previous studies, a nanohydroxyapatite/collagen/poly(L-lactic acid) (nHAC/PLA) composite, similar to natural bone in both composition and structure, has been prepared. It could repair small sized bone defects, but they were restricted to repair a large defect due to the lack of oxygen and nutrition supply for cell survival without vascularization. The aim of the present study was to investigate whether nHAC/PLA composites could be vascularized in vivo. Composites were implanted intramuscularly in the groins of rabbits for 2, 6, or 10 weeks ($n = 5 \times 3$). After removing, the macroscopic results showed that there were lots of rich blood supply tissues embracing the composites, and the volumes of tissue were increasing as time goes on. In microscopic views, blood vessels and vascular sprouts could be observed, and microvessel density (MVD) of the composites trended to increase over time. It suggested that nHAC/PLA composites could be well vascularized by implanting in vivo. In the future, it would be possible to generate vascular pedicle bone substitutes with nHAC/PLA composites for grafting.

1. Introduction

In the past, autograft, allograft, xenograft, and synthetic bone graft substitute materials have been available for repairing bone defects [1]. Although autologous bone grafting is still the gold standard for osteogenic bone replacement, its inherent shortcomings, including limited availability of bone for harvest and significant donor-site morbidity, restrict its application [2]. Allogenic and xenogenic bone grafts are alternatives, but they are used with reservation because of the risk of disease transmission [3]. Synthetic bone substitute has become technically feasible to repair small sized bone defects in clinical practice, but it is difficult to repair large one [4], because blood supply is restricted in its exterior portion, and cells are the lack of reliable oxygen and nutrient supply. Vascularization plays a very important role in bone repair [5]. It is crucial for tissue-engineered bone (TEB) to establish a vascular network that temporally precedes the formation of new bone [6]. A new bone scaffold material, a nanohydroxyapatite/collagen/poly(L-lactic acid) (nHAC/PLA) composite, had been developed by biomimetic synthesis before [7–9]. It mimiced the microstructure of cancellous bone. The purpose of this study was to evaluate whether nHAC/PLA composites could be vascularized in vivo.

2. Materials and Methods

nHAC/PLA composites were synthesised according to the previous method described before [7–10]. The solution of Type I collagen (0.67 g/L) (CELLON Company, Strassen, Luxembourg) was diluted with deionized (DI) water. Solutions of $CaCl_2$ and H_3PO_4 were then separately added by drops according to the ratio of Ca and P (Ca/P = 1.66). The solution was adjusted with sodium hydroxide solution to pH 7.4 at room temperature. After 48 hours, it was centrifugated and freeze-dried. Then, the nHAC deposition was harvested. The nHAC powder was distributed in the PLA matrix (MW = 1.0×10^5 Da; Shandong Medical Appliance Factory,

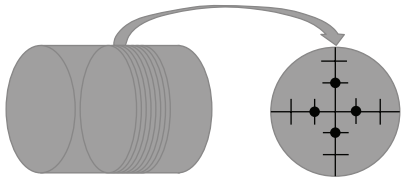

Figure 1: Schematic drawing demonstrating the approach to histological examinations: (a) 8 cross sections were obtained perpendicular to the long axis in the middle; (b) 4 microphotographs of interest in the inner 1/3 radius at 3, 6, 9, and 12 o'clock at 400x magnification were evaluated for MVD (dark black points).

Figure 2: Macroscopic views of nHAC/PLA composites.

Liaocheng, China) at a 1 : 1 weight ratio (nHAC/PLA). The mixture was frozen at −20°C overnight and lyophilized for removing dioxane. After ultrasonication, a cylindrical material was fabricated. The diameter was 10 mm and the height was 10 mm.

The study was approved by the animal ethic committee of Peking Union Medical College Hospital (PUMCH). All the procedures were conducted in accordance with the guidelines for the care and maintenance of animals. Fifteen three-month-old New Zealand rabbits (Experimental Animal Center of PUMCH, Beijing, China) weighing 2.5 to 3.0 kg were used. All operations were performed under sterile conditions by the same surgeon. An nHAC/PLA composite was directly implanted into the intramuscular gap in the groin. Histological examinations were performed at 2, 6, and 10 weeks after implantation.

3% pentobarbital sodium (1 mL/kg body weight, Sigma, USA) was used for the anesthesia of the animals. 800,000 IU penicillin sodium (North China Pharmaceutical Group Corporation, China) was prophylactically injected before the operation. All the animals were treated as follows. A 2 cm skin incision from the groin midpoint to the knee was taken, and the myolemma was longitudinally split. A composite was directly placed into the intramuscular gap. The femoral muscle and skin were sutured with 3-0 silk sutures. Postoperatively, 800,000 IU penicillin sodium and 0.15 mg buprenorphine (Tianjing Institute of Pharmaceutical Research, China) were separately administered intramuscularly every 12 hours for 3 days.

The animals were, respectively, sacrificed after 2, 6, and 10 weeks ($n = 5 \times 3$). The composites were removed and fixed in 10% buffered formalin for 24 hours. After washing, they were decalcified by 14% ethylenediaminetetraacetic acid (EDTA) solution for 6 weeks. Then, they were dehydrated in graded ethanol and embedded in paraffin. Eight cross sections (5 μm) were obtained from each specimen, perpendicular to the long axis in the middle (Figure 1(a)), using a leica microtome (Leica Microsystems, Wetzlar, Germany). For histomorphometric analysis, four sections were randomly selected for haematoxylin and eosin (H & E) staining and microphotographs were taken using a microscope and a digital camera (Leica Microsystems). On each section, four microphotographs of interest in the inner 1/3 radius at 3, 6, 9, and 12 o'clock at 400x magnification were evaluated, and the number of vessels in high power field (HPF) was counted by two independent and blinded pathologists (Figure 1(b)). Microvessel density (MVD) was calculated for each sample. The results were given as means ± standard deviation (x ± SD, vessels/HPF). Sections of each implant were evaluated for endothelial cell structures by immunofluorescence staining against CD31. The primary antibody was rabbit anti-PECAM-1 (Beijing Biosynthesis Biotechnology Corporation, China), and the second antibody was goat anti-rabbit IgG/FITC (Beijing Biosynthesis Biotechnology Corporation, China).

3. Results

All rabbits tolerated the surgical procedure and survived well. No perioperative complication, including infection, hematomas, and wound dehiscence, was found. After removing, the implants were surrounded by rich blood supply tissue (Figure 2). As time goes on, the volume of tissue adhering to the implant was also increasing.

Figure 3 showed that there were a lot of inflammatory cells, fibroblasts, blood vessels, and vascular sprouts in the middle of the composites. Along with the time extension, there were fewer inflammatory cells and more fibroblasts and vessels. MVD of the implants was significantly increased (Figure 4, 2 weeks: 6.23 ± 1.55 vessels/HPF, 6 weeks: 10.58 ± 2.60 vessels/HPF, and 10 weeks: 12.96 ± 2.60 vessels/HPF). The vascular walls of new vessels and red blood cells in the composites were both emphasized as light green fluorescence by CD31 immunofluorescence histochemical staining (Figure 5).

4. Discussion

As early as 1763, the importance of blood vessels in bone formation was noted: "the origin of bone is the artery carrying the blood and in it the mineral elements" [11]. Blood vessels are key contributors to the process of osteogenesis, both in development and during repair. Since oxygen and nutrition supply by diffusion are restricted to a maximum range of 200 μm into a given matrix [12] and suboptimal initial

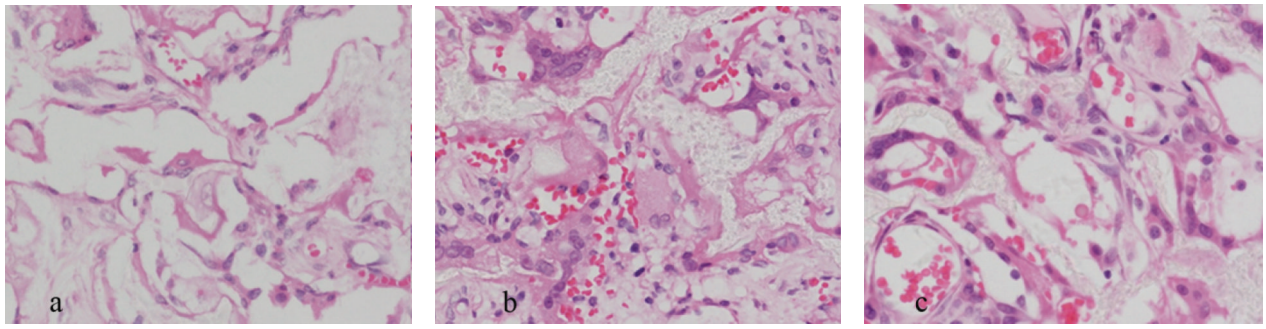

(a) (b) (c)

Figure 3: Hematoxylin and eosin (H & E) staining of specimens (magnification ×400): (a) 2 weeks, (b) 6 weeks, and (c) 10 weeks.

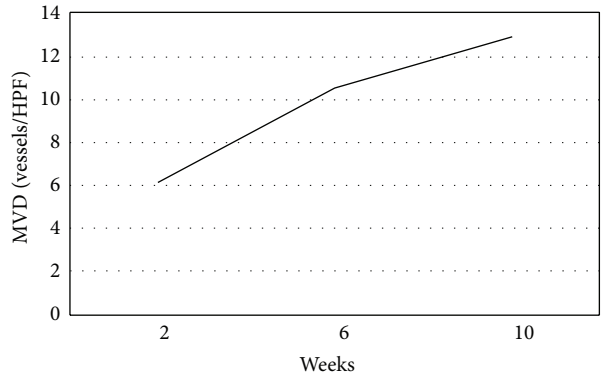

Figure 4: Microvessel density (MVD) of the composites.

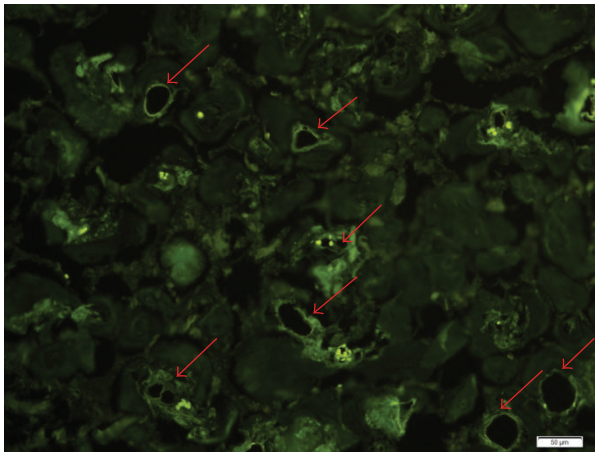

Figure 5: CD31 immunofluorescence histochemical staining of specimens by 10 weeks after implantation (magnification ×200): the vascular walls and red blood cells display remarkable light green fluorescence.

vascularization often limits survival of cells in the center of large constructs [13], therefore, the vascularization of TEB has drawn scholars' interests recently. It includes the progresses of angiogenesis (the sprouting of capillaries from preexisting blood vessels) and vasculogenesis (the assembly of capillaries in situ from undifferentiated endothelial cells) [14]. Angiogenesis is involved in the initiation and promotion of endochondral and intramembranous ossification in bone growth and remodeling [15].

Nowadays, the technology of constructing a blood vessel system has still many difficult issues that cannot be resolved by the development of tissue engineering alone. Surgical angiogenesis is the unique promising method to establish a functional vascular network. It utilizes the preexisting blood vessels as a vascular carrier to regenerate nutrient vessels by incorporating artificial materials and cells into them.

The most frequent method of neovascularization in tissue engineering is that the neovascular bed originates from the periphery of the construct implanted into a site of high vascularization potential (subcutaneous [16], intramuscular [17], and intraperitoneal [13]). Vascularization occurs via an endogenous response to the surgical implantation, which creates an inflammatory wound-healing response [14]. Endogenous angiogenic growth factors are expressed because of the hypoxia of the implant. Exogenous angiogenic growth factors can be incorporated into the implant to enhance the vascularization. Warnke et al. reported that they had successfully used intramuscularly as in vivo bioreactor for prefabrication of a large mandible replacement in a clinical practice [18].

Tissue engineering is promising therapeutic strategies for the repairment of diseased or injured tissues and organs [19]. There are three elements in tissue engineering, including

scaffolds, seeding cells, and cytokines. Scaffolds play an essential role, because they not only supported and regulated the growth of cells, but also guided the ingrowth of periphery tissue [20–22]. The osteogenesis and angiogenesis abilities of scaffolds have been significantly developed [21]. The advantage of biocompatibility and osteoinduction of microstructured calcium phosphate materials has been shown before [23, 24]. Similar to the natural cancellous bone in main composition and in hierarchical microstructure, a new bionic porous scaffold, nHAC/PLA composite, has been fabricated before [9]. Its pore size was about 100–300 μm, and its porosity was about 80%. Cellular activities were affected by chemical composition, conformation, porosity, and hydrophobicity of matrix [25]. The osteogenesis ability of nHAC/PLA composites were confirmed by osteoblasts culture and animal model tests [9]. But its vascularization ability did not have been estimated before. This might decide its availability for repairing large bone defects. In this study, we first demonstrated that it could guide vessels' ingrowth in vivo to achieve its vascularization.

In conclusion, the ability of nHAC/PLA composites was shown to generate new vascular networks for prefabrication of large bone substitutes by implanting intramuscularly. A vascularized large bone flap for transplanting could be prefabricated using a nHAC/PLA composite as a scaffold in the future.

Conflict of Interests

The authors have declared that there is no conflict of interests.

Authors' Contribution

Hai Wang and Xiao Chang are cofirst authors.

Acknowledgment

This work was supported by National Natural Science Foundation of China (NSFC no. 81000802).

References

[1] T. W. Bauer and G. F. Muschler, "Bone graft materials: an overview of the basic science," *Clinical Orthopaedics and Related Research*, no. 371, pp. 10–27, 2000.

[2] J. P. Beier, R. E. Horch, A. Hess et al., "Axial vascularization of a large volume calcium phosphate ceramic bone substitute in the sheep AV loop model," *Journal of Tissue Engineering and Regenerative Medicine*, vol. 4, no. 3, pp. 216–223, 2010.

[3] A. J. Aho, T. Ekfors, P. B. Dean, H. T. Aro, A. Ahonen, and V. Nikkanen, "Incorporation and clinical results of large allografts of the extremities and pelvis," *Clinical Orthopaedics and Related Research*, no. 307, pp. 200–213, 1994.

[4] C. A. Vacanti, L. J. Bonassar, M. P. Vacanti, and J. Shufflebarger, "Replacement of an avulsed phalanx with tissue-engineered bone," *The New England Journal of Medicine*, vol. 344, no. 20, pp. 1511–1514, 2001.

[5] L.-L. Ren, D.-Y. Ma, X. Feng, T.-Q. Mao, Y.-P. Liu, and Y. Ding, "A novel strategy for prefabrication of large and axially vascularized tissue engineered bone by using an arteriovenous loop," *Medical Hypotheses*, vol. 71, no. 5, pp. 737–740, 2008.

[6] H. Yu, P. J. VandeVord, L. Mao, H. W. Matthew, P. H. Wooley, and S.-Y. Yang, "Improved tissue-engineered bone regeneration by endothelial cell mediated vascularization," *Biomaterials*, vol. 30, no. 4, pp. 508–517, 2009.

[7] C. Du, F. Z. Cui, W. Zhang, Q. L. Feng, X. D. Zhu, and K. de Groot, "Formation of calcium phosphate/collagen composites through mineralization of collagen matrix," *Journal of Biomedical Materials Research*, vol. 50, no. 4, pp. 518–527, 2000.

[8] C. Du, F. Z. Cui, X. D. Zhu, and K. de Groot, "Three-dimensional nano-HAp/collagen matrix loading with osteogenic cells in organ culture," *Journal of Biomedical Materials Research*, vol. 44, no. 4, pp. 407–415, 1999.

[9] S. S. Liao, F. Z. Cui, W. Zhang, and Q. L. Feng, "Hierarchically biomimetic bone scaffold materials: nano-HA/collagen/PLA composite," *Journal of Biomedical Materials Research Part B*, vol. 69, no. 2, pp. 158–165, 2004.

[10] J. Li, J. Hong, Q. Zheng et al., "Repair of rat cranial bone defects with nHAC/PLLA and BMP-2-related peptide or rhBMP-2," *Journal of Orthopaedic Research*, vol. 29, no. 11, pp. 1745–1752, 2011.

[11] R. A. D. Carano and E. H. Filvaroff, "Angiogenesis and bone repair," *Drug Discovery Today*, vol. 8, no. 21, pp. 980–989, 2003.

[12] A. S. Goldstein, T. M. Juarez, C. D. Helmke, M. C. Gustin, and A. G. Mikos, "Effect of convection on osteoblastic cell growth and function in biodegradable polymer foam scaffolds," *Biomaterials*, vol. 22, no. 11, pp. 1279–1288, 2001.

[13] U. Kneser, P. M. Kaufmann, H. C. Fiegel et al., "Long-term differentiated function of heterotopically transplanted hepatocytes on three-dimensional polymer matrices," *Journal of Biomedical Materials Research*, vol. 47, no. 4, pp. 494–503, 1999.

[14] O. C. S. Cassell, S. O. P. Hofer, W. A. Morrison, and K. R. Knight, "Vascularization of tissue-engineered grafts: the regulation of angiogenesis in reconstructive surgery and in disease states," *British Journal of Plastic Surgery*, vol. 55, no. 8, pp. 603–610, 2002.

[15] J. M. Kanczler and R. O. C. Oreffo, "Osteogenesis and angiogenesis: the potential for engineering bone," *European Cells and Materials*, vol. 15, pp. 100–114, 2008.

[16] U. Kneser, A. Voogd, J. Ohnolz et al., "Fibrin gel-immobilized primary osteoblasts in calcium phosphate bone cement: in vivo evaluation with regard to application as injectable biological bone substitute," *Cells Tissues Organs*, vol. 179, no. 4, pp. 158–169, 2005.

[17] J. P. Beier, U. Kneser, J. Stern-Sträter, G. B. Stark, and A. D. Bach, "Y chromosome detection of three-dimensional tissue-engineered skeletal muscle constructs in a syngeneic rat animal model," *Cell Transplantation*, vol. 13, no. 1, pp. 45–53, 2004.

[18] P. Warnke, I. Springer, P. J. Wiltfang et al., "Growth and transplantation of a custom vascularised bone graft in a man," *The Lancet*, vol. 364, no. 9436, pp. 766–770, 2004.

[19] X. Li, Y. Yang, Y. Fan, Q. Feng, F. Z. Cui, and F. Watari, "Biocomposites reinforced by fibers or tubes as scaffolds for tissue engineering or regenerative medicine," *Journal of Biomedical Materials Research Part A*, 2013.

[20] R. Murugan and S. Ramakrishna, "Nano-featured scaffolds for tissue engineering: a review of spinning methodologies," *Tissue Engineering*, vol. 12, no. 3, pp. 435–447, 2006.

[21] X. Li, H. Gao, M. Uo et al., "Effect of carbon nanotubes on cellular functions in vitro," *Journal of Biomedical Materials Research Part A*, vol. 91, no. 1, pp. 132–139, 2009.

[22] X. Li, H. Liu, X. Niu et al., "The use of carbon nanotubes to induce osteogenic differentiation of human adipose-derived MSCs in vitro and ectopic bone formation in vivo," *Biomaterials*, vol. 33, no. 19, pp. 4818–4827, 2012.

[23] X. Li, L. Wang, Y. Fan, Q. Feng, F. Z. Cui, and F. Watari, "Nanostructured scaffolds for bone tissue engineering," *Journal of Biomedical Materials Research Part A*, vol. 101, no. 8, pp. 2424–2435, 2013.

[24] G. Zhou, Y. Hou, L. Liu et al., "Preparation and characterization of NiW-nHA composite catalyst for hydrocracking," *Nanoscale*, vol. 4, no. 24, pp. 7698–7703, 2012.

[25] G. Zhou, G. Zhang, Z. Wu et al., "Research on the structure of fish collagen nanofibers influenced cell growth," *Journal of Nanomaterials*, vol. 2013, Article ID 764239, 6 pages, 2013.